1176

TRANSPORTATION RESEARCH RECORD

Research on Noise and Environmental Issues

TRANSPORTATION RESEARCH BOARD
NATIONAL RESEARCH COUNCIL
WASHINGTON, D.C. 1988

Transportation Research Record 1176
Price: $13.00
Editor: Ruth Sochard Pitt
Production: Lucinda Reeder

modes
1 highway transportation
4 air transportation

subject area
17 energy and environment

Transportation Research Board publications are available by ordering directly from TRB. They may also be obtained on a regular basis through organizational or individual affiliation with TRB; affiliates or library subscribers are eligible for substantial discounts. For further information, write to the Transportation Research Board, National Research Council, 2101 Constitution Avenue, N.W., Washington, D.C. 20418.

Printed in the United States of America

Library of Congress Cataloging-in-Publication Data
National Research Council. Transportation Research Board.

Research on noise and environmental issues
p. cm.—(Transportation research record, ISSN 0361-1981 ; 1176)
ISBN 0-309-04715-3
1. Transportation—Environmental aspects. 2. Noise pollution.
3. Air—Pollution. I. National Research Council (U.S.).
Transportation Research Board. II. Series.
TE7.H5 no. 1176
[TD195.T7]
380.5 s—dc20 89-9364
[363.7'41] CIP

Sponsorship of Transportation Research Record 1176

GROUP 1—TRANSPORTATION SYSTEMS PLANNING AND ADMINISTRATION

Environmental Quality and the Conservation of Resources Section
Chairman: Carmen Difiglio, U.S. Department of Energy

Committee on Transportation and Air Quality
Chairman: Susanne Pelly Spitzer, Minnesota Pollution Control Agency
Salvatore J. Bellomo, Paul E. Benson, David L. Calkins, Norman L. Cooper, John D. Dunlap III, Alan Eschenroeder, Gary Hawthorn, Howard A. Jongedyk, Carlton Thomas Nash, Marilyn Skolnick, N. Thomas Stephens, John H. Suhrbier

Committee on Transportation-Related Noise and Vibration
Chairman: Mas Hatano, California Department of Transportation
Secretary: Win M. Lindeman, Florida Department of Transportation
Grant S. Anderson, Robert E. Armstrong, Domenick J. Billera, William Bowlby, Clifford R. Bragdon, Peter C. L. Conlon, Richard G. Dyer, C. Michael Hogan, M. Ashraf Jan, Harvey S. Knauer, Claude Andre Lamure, Bernard G. Lenzen, Christopher W. Menge, James Tuman Nelson, James R. O'Connor, Soren Pedersen, Kenneth D. Polcak, Joseph B. Pulaski, Karen L. Robertson, Simon Slutsky, Michael A. Staiano, Eric Stusnick, Dale K. Vander Schaaf

William Campbell Graeub, Transportation Research Board staff

Sponsorship is indicated by a footnote at the end of each paper. The organizational units, officers, and members are as of December 31, 1987.

Transportation Research Record 1176

Contents

Foreword

Because government research programs generally reflect policy positions of agencies, environmental concerns in transportation have not been foremost in research agenda for some time. Recently, however, some decision makers are again calling for increased work in these fields. The 12 papers in this Record show that there is considerable ongoing research into transportation-related noise and other environmental factors.

The first nine papers cover research on highway noise and noise abatement measures. The first paper, by Weiss, is a summary of highway noise barrier construction in the United States. At the end of 1986, the United States had 450 mi of completed noise barriers. About one third were constructed along existing highways, and the others were constructed as part of new or improved highway alignments. On average, the barriers are 12 ft high and built from a wide range of materials; there is no indication that use of any given material predominates.

Three papers deal directly with noise barriers. Creasey and Agent report on an effectiveness evaluation study of traffic noise barriers. In this work, insertion loss values predicted by the STAMINA 2.0 model were compared with actual field measurements and found to be very close.

Increasingly, barriers must be constructed to protect homes on both sides of roadways, but parallel barrier configurations create additional problems because of diffraction of sound waves and other complex ground reflections. In the paper by Lee et al., the results of the first application of the Tilted Parallel Barrier Program to a highway project are presented and an attempt is made to verify aspects of the model.

In the next paper, Diehl describes the formulation of a quantitative assessment of the noise environment adjacent to a new segment of I-78, before, during, and after construction. He found that the highest level of noise occurred during the initial phases of construction. After construction, with noise barriers in place, seven sites experienced no impacts from traffic noise, but three sites showed increased impacts.

Noise prediction models have been in use for over a decade. Jung and Blaney describe a simplified version of the STAMINA mainframe program that they developed for the Ontario Ministry of Transportation to predict highway traffic noise by microcomputer.

The next two papers report on noise control and abatement activities in New Jersey. The first paper, by Seigel, discusses the procedures for a community involvement process for highway projects in which construction of noise abatement has been recommended. In the second paper, Cebrick details NJDOT's noise mitigation program.

Acoustical insulation of existing buildings is another way to mitigate noise impacts. The last paper on noise, by Hogan and George, describes procedures that were used to retrofit 12 residences and 2 schools located near the San Francisco International Airport.

The last three papers in this Record are on air quality issues. Benson describes the California Line Source Dispersion Model and demonstrates how the model can be used to predict air pollutant concentrations near roadways and at intersections. In his second paper, Benson presents the development of a model to correct hot and cold start vehicle fractions for input to conventional emission factor models. In the third paper on air quality, a study of dispersion characteristics of flows in street canyons is described. Authors Hoydysh and Dabberdt found that the dispersion patterns are strongly dependent on canyon asymmetry but less dependent on the canyon's orientation toward the prevailing flow.

Summary of Highway Noise Barrier Construction in the United States

MARTIN WEISS

More than 450 mi of noise barriers have been constructed in the United States at a cost of more than $300 million (in 1986 dollars). About one third of these were constructed after the highway had originally been built, and about one third are adjacent to Interstate highways. The average barrier is ~12 ft high and costs about $12/ft^2 in 1986 dollars. More than 30 percent of all highway noise barriers are in California, and about ~10 percent are in Minnesota. It is reasonable to expect that in the future, noise barrier construction will be of the order of tens of miles annually.

Estimates of past highway noise barrier construction in the United States have been found to be useful to both governmental and nongovernmental institutions and individuals. This paper is the third such estimate and the second by FHWA (*1*, *2*). The estimate is based on physical data that are current through 1986 and on price adjustment. The bulletin *Price Trends for Federal-Aid Highway Construction* (*3*) was used to convert actual construction costs to 1986 dollars. The estimate includes noise barriers constructed with highway funds, according to data from state highway agencies (SHAs).

SUMMARY

By the end of 1986, more than 450 mi (aggregate) of noise barriers had been built in the United States at a cost of more than $300 million in 1986 dollars. About one third of all barriers, by length, were constructed along existing highways. (Henceforth these will be called Type II barriers.) About one third of all barriers, by length, were adjacent to highways other than Interstates. The average barrier is ~12 ft high. Block, concrete, earth, metal, wood, and combinations of these materials have all been used in barrier construction, and there is no indication that any given material dominates the market.

DATA UNIFORMITY

The word "estimate" has been used intentionally in the preceding material. It is important that the meaning of this word be clearly understood. The data are not uniform because they were gathered by individual SHAs. Each of these agencies had nearly full discretion in choosing what would be defined as a barrier and what would be counted as barrier costs. The following are examples of potential nonuniformity:

- Some states consider certain safety barriers to be noise barriers, whereas others do not.
- A long, continuous barrier of variable height and material may be considered to be a single barrier in one state. In another state, however, it may be considered to be two, three, or more individual barriers.
- A short barrier over a structure that is made of a different material than the adjacent barriers on each side may be considered a separate barrier in some states. Other states may consider the entire system to be a single barrier.
- A barrier that is built over the course of three construction seasons in conjunction with other highway work may be considered to have been constructed in the first year in one state or in the third year in another state. About 1 percent of barriers (by length) could not be identified by any year.
- The height of many barriers is variable. In a number of cases, barriers were tabulated under the assumption that the average height was the mean of the maximum and minimum heights.
- In some states, noise barrier costs may represent little more than the cost of barrier material. In other states, costs may include ground preparation of the entire area from the shoulder to the edge of the right of way, drainage of this same area, engineering, and administration. Still other states may have no line item in the bidding papers for the noise barrier and thus may have no way to estimate the cost. A cost could not be assigned to ~3 percent of the barriers (by length). This nonuniformity is both regrettable and unavoidable. The data on barrier length are much less affected by nonuniformity than are the data on barrier cost. Although the cost data are not uniform, they are useful for determining trends and approximate costs.

TRENDS

Of special interest to those performing, reviewing, or implementing highway traffic noise analysis or highway noise barrier design are estimates of

- trends in quantity and cost of barriers,
- construction adjacent to Interstate highways versus adjacent to non-Interstate highways,
- construction of Type I projects (new location, significant realignment, or through lane addition) versus construction of Type II projects, and
- noise barrier material and height.

Table 1 presents the overall trends in quantity and cost for total barrier construction. As can be determined from the table, 5.5 mi of barrier could not be assigned either a year of

Noise and Air Analysis Division, Office of Environmental Policy, HEV 30, FHWA, 400 7th St., S.W., Washington, D.C. 20590.

TABLE 1 NOISE BARRIER CONSTRUCTION BY YEAR

Year Constructed	Noise Barriers (linear mi)	Cost (1986 $ millions)
Unknown	5.5	Unknown
Pre-1974	3.8	2.3
1974	15.2	10.0
1975	20.2	9.8
1976	5.4	2.3
1977	14.4	11.9
1978	59.8	40.4
1979	58.2	33.1
1980	44.4	23.5
1981	38.4	29.4
1982	24.6	19.9
1983	39.3	35.2
1984	50.8	43.6
1985	41.1	34.7
1986	46.0	42.7
Total	467.1	338.8

NOTE: Costs are approximate.

construction or a cost. In addition, ~8.9 mi was assigned a year but could not be assigned a cost. Finally, one state that had substantial barrier construction was unable to provide data for barriers constructed after 1983.

In Table 2, noise barrier construction is disaggregated by Type I and Type II construction and by location adjacent to an

TABLE 2 PERCENT OF NOISE BARRIER LENGTH BY TYPE AND FACILITY LOCATION

Year	Type I (%)	Type II (%)	Interstate (%)	Other (%)
Unknown	100	0	100	0
Pre-1974	61	39	84	16
1974	41	59	57	43
1975	70	30	66	34
1976	94	6	44	56
1977	25	75	91	9
1978	62	38	71	29
1979	60	36	66	34
1980	79	21	63	37
1981	46	54	66	34
1982	72	25	74	26
1983	71	23	66	34
1984	72	28	74	26
1985	65	35	69	31
1986	74	26	67	33
Overall	65	34	70	30

Interstate versus location along other highways. The Type I and Type II percentages do not always add to 100 percent because some records indicate that barriers were built by SHAs without federal funds or by tollway authorities, or because the SHA was unable to identify the barriers as Type I or Type II. It can be observed that there are almost 2 mi of Type I barrier for every mile of Type II barrier, and there are more than 2 mi of barrier adjacent to an Interstate for every mile of barrier adjacent to another highway. The data also indicate that in the previous 9 yr, the percentage of constructed barriers located adjacent to Interstate highways has remained more or less steady. The percentage of Type I barriers has remained more or less steady for ~5 yr.

In Table 3, the total noise barrier construction is disaggregated for the SHAs that have the largest investment in barriers. As can be observed in both Table 3 and Table 1, more than 75 percent of noise barrier construction (in miles and in dollars)

TABLE 3 NOISE BARRIER CONSTRUCTION BY STATE

Construction by Length		Construction by Cost	
State	Length (linear mi)	State	Cost (1986 $ millions)
California	148.1	California	116.5
Minnesota	47.6	Minnesota	41.6
Colorado	31.2	Virginia	26.6
Virginia	26.1	New Jersey	21.5
Oregon	20.8	Michigan	16.3
Michigan	18.6	Tennessee	13.2
Arizona	17.1	New York	13.0
New York	17.1	Illinois	10.1
New Jersey	15.8	Pennsylvania	8.9
Washington	14.5	Oregon	8.7
10-state total	356.9	10-state total	276.4

NOTE: Costs are approximate. Virginia and Oregon costs are understated. Virginia totals do not count direct federal construction.

was within the 10 leading states. Total costs for Virginia and Oregon are understated because more than 5 mi of Virginia and 6 mi of Oregon barriers could not be assigned a cost. Furthermore, an additional few miles and million dollars are not counted in Table 3, even though these barriers are physically located in Virginia. This is because they are on federal land and were built directly with federal funds.

In all, 15 states have constructed Type II noise barriers. Table 4 presents these states, along with the length of constructed barriers. From Table 3 and Table 4, it can be seen that three states (California, Minnesota, and Colorado) each have more than 50 percent of their barriers classified as Type II. Colorado has ~30 percent of its barriers so classified. All other states have, at most, a modest Type II program.

TABLE 4 TYPE II NOISE BARRIER CONSTRUCTION

State	Total Barrier Length (mi)
California	94.9
Minnesota	26.5
Colorado	11.8
Michigan	11.5
Connecticut	3.1
New York	2.7
New Jersey	1.3
Wisconsin	1.0
Louisiana	1.0
Iowa	0.7
Maryland	0.7
Oregon	0.6
Georgia	0.6
Massachusetts	0.5
Washington	0.3
Total	157.0

NOTE: Maryland total is through 1983; others through 1986.

Like other highway projects, Type II noise barrier programs have periods of activity and inactivity that vary by state. For example, Colorado's previous Type II barrier was completed in 1984, and Minnesota's was completed in 1980. On the other hand, Wisconsin's first Type II barrier was completed in 1984, Massachusetts' in 1985, and New York's in 1986.

Tables 5 and 6 illustrate the trend in barrier height and the ranges of barrier heights, respectively. As can be observed in Table 5, average noise barrier heights have changed little. Before 1977, however, they were a bit lower than they have been since. Table 6 indicates that barrier height is more or less Gaussian in distribution. In general, barriers adjacent to Interstates tended to be a bit higher than other barriers (12.4 ft versus 11.2 ft), and Type II barriers were a bit higher than Type I barriers (12.4 ft versus 11.7 ft). As noted previously, the barrier height data sometimes represent an adjustment from the raw data provided by the data sources and are probably less accurate than the data on barrier length (although more accurate than those on barrier cost).

TABLE 5 AVERAGE BARRIER HEIGHT

Year	Average Height (ft)
Unknown	14.9
Pre-1974	9.1
1974	10.8
1975	11.7
1976	10.4
1977	13.3
1978	12.6
1979	11.9
1980	12.6
1981	11.1
1982	12.7
1983	12.5
1984	11.4
1985	11.9
1986	11.8
Average	12.0

TABLE 6 NOISE BARRIER LENGTH BY HEIGHT

Height Range (ft)	Miles
Under 5	4.7
5–8	76.2
9–12	194.5
13–16	139.5
17–20	41.8
21–24	6.5
24+	4.0

Tables 7 and 8 provide information on materials used for barrier construction and on trends in the use of material. Because of the nonuniformity in the cost data and the potential for misuse, only barrier lengths are provided in these tables. The totals in Table 8 are not equal to those in Table 7 because of the length of certain barriers, most of which were concrete or metal, that could not be assigned to a specific year.

Table 8 does not indicate that any specific material is clearly preferred on a national basis. There are, however, some preferences on a statewide basis. California, for example, uses block for more than 75 percent of its barrier length. This factor, in combination with the large number of barriers in California, accounts for the large national total for block barrier length. Minnesota and Colorado use wood for more than 50 percent of their combined barrier length. Of the combined barrier length for Arizona and Washington, more than 66 percent is made up of simple berms, and much of that consists of excess highway excavation material. Oregon uses a combination berm and concrete wall for ~33 percent of its barrier length. The only obvious national trend is a decreasing use of berms as a single material.

TABLE 7 TOTAL NOISE BARRIER LENGTH BY MATERIAL TYPE

Single-Material Barriers		Combination Barriers	
Material	Length (mi)	Material	Length (mi)
Block	144.2	Berm/concrete	18.0
Concrete (precast)	63.8	Wood/concrete	15.7
Berm only	47.4	Berm/wood	9.8
Wood (unspecified)	32.2	Concrete/brick	7.3
Concrete (unspecified)	27.4	Wood/metal	6.7
Wood (post & plank)	23.8	Berm/block	6.5
Metal (unspecified)	22.6	Metal/concrete	4.8
Wood (glue laminated)	12.9	Berm/metal	3.5
Brick	3.9	Wood/block	2.5
Other	2.2	Other	12.1
Total	380.4	Total	86.9

TABLE 8 TRENDS IN GENERAL MATERIALS USED IN NOISE BARRIERS

Length (mi)	Pre-1977	1977–1981	Post-1981
Combination	8.4	45.0	32.6
Block	4.5	69.7	70.1
Concrete	6.3	37.0	45.2
Berm	7.9	27.4	12.2
Metal	0.5	11.1	9.1
Wood	16.8	22.9	29.1
Other	0.2	2.2	3.6

Barrier unit cost (dollars per square foot) is one of the more important but less easily inferred values. Its importance is the result of the need, during location and design, to judge the reasonableness of an expenditure for noise abatement. The difficulty in inferring a value is caused, in part, by the previously described nonuniformities in determining total barrier cost and average barrier height. In addition, Leo Defrain of the Michigan Department of Transportation recently noted that (*4*) "noise walls of similar design, material, topographic and soil environment, and height can vary by a factor of 2 in cost per square foot due solely to unanticipatable local wages/work load/union conditions."

As an example of the problem with inferring unit costs, Table 9 provides a disaggregation by height of unit costs of berms. The square footage of a berm is calculated as if the berm were a wall of equal height. These costs were computed from those barriers whose costs were known. To say that these values violate intuition would be an understatement. No doubt this deviation is partially due to the existence of a relatively small number of berms. A special case in one barrier can thus have substantial influence. For this reason, Tables 10 and 11,

TABLE 9 UNIT COST OF BERMS BY BERM HEIGHT

Height Range (ft)	Cost (1986 $/ft^2)
Under 5	16.2
5–8	3.3
9–12	2.9
13–16	5.0
16+	2.0

which provide additional information on barrier unit costs, are not finely disaggregated.

The first row in the body of Table 10 indicates that more than 15 percent of barriers with assigned costs were no more than $5/ft^2. Of these, about 7 mi of barriers were constructed for essentially no cost (or even negative cost) because they were made of excess excavation material. The second column of Table 11 demonstrates the effect of inflation on noise barrier unit costs. The last column indicates that even without inflation, noise barrier costs appear to be increasing.

Barriers along Interstates tended to have higher unit costs than those along other highways ($12.4/ft^2 versus $10.1/ft^2, 1986 dollars). Also, as expected, Type II barriers tended to have higher unit costs than Type I barriers ($13.5/ft^2 versus $10.7/ft^2, 1986 dollars).

FUTURE NOISE BARRIER CONSTRUCTION

FHWA regulations provide a good deal of flexibility to SHAs in the administration of their own highway programs. Given this flexibility, SHAs can and do change emphasis and priorities from one year to the next. The previously noted differences in the amount of barrier construction from one state to another and from one year to another are manifestations of this flexibility. Thus it is difficult to predict the extent of future noise barrier construction.

TABLE 10 NOISE BARRIER LENGTH BY UNIT COST

Cost (1986 $/ft^2)	Length (mi)
Up to 5	79.5
5+–10	140.9
10+–15	110.6
15+–20	60.1
20+–25	40.0
25+–30	11.3
30+	10.2

TABLE 11 TREND IN UNIT COSTS

Years	Actual Cost ($/ft^2)	Relative Cost (1986 $/ft^2)
Pre-1977	5.3	9.6
1977–1981	8.3	10.1
Post-1981	13.2	14.0
Total (barriers with assigned costs)		12.0

FHWA does biennially update an estimate of the cost to complete the Interstate system on the basis of data provided by SHAs (*5*). Included in the estimate are noise barrier costs. The 1987 Interstate cost estimate for noise barriers was approximately $142 million (1986 dollars). This estimate is only for those barriers built as part of construction projects that close gaps in the Interstate system or add lanes with Interstate construction funding. Other construction projects on the Interstate system that use primary funds (i.e., funds for improvement of the primary system), 4R funds (funds for reconstruction), and so on are excluded, as is all construction on non-Interstate projects.

If past history is considered, a reasonable assumption is that the future will be somewhat like the past. This means that for the immediate future, annual noise barrier construction will be of the order of tens of miles. Annual expenditures will be of the order of tens of millions of dollars.

REFERENCES

1. Appendix A. In *A National Field Review of the Highway Traffic Noise Impact Identification and Mitigation Decisionmaking Processes.* Report. FHWA, U.S. Department of Transportation, June 8, 1982.
2. Appendix D. In *A National Field Review Report on the Management of the Highway Traffic Noise Program.* Report. FHWA, U.S. Department of Transportation, March 15, 1985.
3. *Price Trends for Federal-Aid Highway Construction.* Office of Engineering, Federal Aid Division, FHWA, U.S. Department of Transportation, 1st quarter 1987.
4. M. Weiss. *Trip Report.* FHWA, U.S. Department of Transportation, May 28, 1987.
5. *Interstate Cost Estimate: Cost Remaining as of Dec. 31, 1985.* Committee Print 100-4. Interstate Management Branch, FHWA, U.S. Department of Transportation, for the Committee on Public Works, U.S. Congress, 1987.

Publication of this paper sponsored by Committee on Transportation-Related Noise and Vibrations.

Effectiveness of Traffic Noise Barrier on I-471 in Campbell County, Kentucky

F. THOMAS CREASEY AND KENNETH R. AGENT

The objective of this study was to evaluate the effectiveness of a traffic noise barrier on Interstate 471 in Campbell County, Kentucky. Because construction of the barrier coincided with construction on I-471, it was necessary to predict noise levels that would exist if no barrier were present by using the FHWA STAMINA 2.0 computer model. The model results were compared to actual noise level measurements at the barrier site to determine the barrier insertion loss. After calibration of the STAMINA 2.0 model, noise measurements were made at 39 receiver locations during peak and off-peak traffic periods. The noise barrier reduced the noise level at adjacent residences substantially. After barrier construction, 15 homes (14 percent of the total study sample) experienced a peak period L_{eq} insertion loss of 10 dBA or more, and another 58 residences (54 percent) were observed to have a peak period insertion loss of 5.0 to 9.9 dBA. Comparison of insertion loss between values predicted by STAMINA 2.0 and actual field measurements was very close. Analyses indicated that insertion loss values predicted by the STAMINA 2.0 model will be achieved by the noise barrier. A survey of community perception of the noise barrier was also performed. Of 103 questionnaires mailed, 66 (64 percent) were returned. Community perception of the barrier was favorable: 64 percent of the respondents generally liked the noise barrier, and 95 percent felt it was effective in reducing traffic noise.

Traffic noise at locations near major highways can reach such excessive levels that noise abatement measures are necessary. One frequently used U.S. noise abatement measure involves erecting a noise barrier along the highway. These barriers are vertical walls made of wood, metal, concrete, or earth berms. They are designed to reduce noise levels at sensitive receivers adjacent to the highway and to break the line of sight between vehicles on the highway and receivers.

Currently, only one noise barrier has been constructed in Kentucky, on Interstate 471 in Campbell County (Figure 1). The 15-ft-high, 2,550-ft-long metal barrier is located adjacent to the shoulder of the interstate. Construction of the barrier in 1981 coincided with the construction of I-471. The total cost of the barrier was $392,277.

The noise barrier was designed to shield a residential neighborhood adjacent to I-471 from traffic noise. The objective of this study is to determine whether noise reduction estimates are being achieved. Because this barrier is the first to be constructed in Kentucky, determination of its effectiveness at this location will aid in future decisions about when and how additional noise barriers should be constructed. The construction of noise barriers is expensive, which means that the most efficient design must be used to minimize the barrier area required while achieving the needed noise reduction. Any improvement in design would result in reduced construction costs, as well as reductions in noise levels for the affected receivers.

F. T. Creasey, Texas Transportation Institute, Texas A&M University, College Station, Tex. 77843. K. R. Agent, Kentucky Transportation Research Program, College of Engineering, University of Kentucky, Lexington, Ky. 40506.

FIGURE 1 Noise barrier, Interstate 471, Campbell County, Kentucky.

Because the noise barrier was part of the construction of I-471, before and after data could not be obtained. This report describes the procedure that was used to determine the barrier field insertion loss. Modeling of the site is detailed along with the calibration procedure, and results of field measurements are presented. A survey developed to determine community perception of the noise barrier is also covered, and the results are documented.

INSERTION LOSS PROCEDURE

Because construction of the noise barrier coincided with construction of I-471, before and after noise measurements could not be obtained. In addition, there was no similar site along the highway without a noise barrier that could be used for comparison. A decision was made to use the procedure described in Section 5.5 of FHWA report FHWA-DP-45-1R (*1*). That procedure uses the FHWA STAMINA 2.0 model to determine insertion loss by comparing actual after sound level measurements to predicted before levels. The STAMINA 2.0 model considers highway traffic noise in relation to a roadway source, which is approximated by a series of straight line

segments, and estimates the acoustic intensity from the roadway source at a receiver location. Source characteristics are defined by speed-dependent noise emission levels and by traffic density by vehicle type. Site geography is described by a three-dimensional coordinate system. Source-receiver path characteristics are then considered, taking into account effects of noise barriers, topography, vegetation, and atmospheric absorption.

Two locations behind the noise barrier were selected, and measurements were taken to calibrate the model. In all, 39 locations were used in the data collection procedure. Once the calibration process was completed, the before sound levels were predicted by the model. The insertion loss was determined by taking the difference between the calculated before and measured after noise levels.

DEVELOPMENT AND CALIBRATION OF THE STAMINA 2.0 MODEL

The first step in the model calibration process was the physical modeling of the study site. In this process, the physical characteristics of the microphone or receiver locations, vehicles, roadway, and the barrier were quantified. Locations for the two microphones (study site and reference microphones) were selected by using maps, an aerial photograph, and a preliminary field inspection.

To select a location for the study site microphone, it was necessary first to establish a baseline perpendicular to the centerline of the near traffic lane, passing through the study site microphone location. The study site microphone had to be on the receiver side of the barrier (i.e., the barrier had to stand between the microphone and roadway), at least 10 ft from any vertical reflective surface. The geometry between the microphone and roadway was to be as simple as possible.

The reference microphone was to be located on the baseline in such a way that the noise barrier had no effect on it. This microphone required an unobstructed "view" of the roadway through a subtended arc of at least 160 degrees. Because the noise barrier was so close to the edge of the roadway, the only way to satisfy requirements for locating the reference microphone was to place it behind the noise barrier along the baseline and elevate it so that the barrier would have no effect (Figure 2). The reference microphone had to have a perpendicular clearance of 5 ft from a line that started at the near edge of the pavement and passed through the top front edge of the noise barrier. It was necessary to raise the microphone 28 ft on a tripod made of 1-in.-diameter galvanized pipe to get the required perpendicular clearance (Figure 3). Locations of the microphones were expressed in terms of X, Y, and Z coordinates, with the Z coordinate indicating the elevation of the microphone.

Vehicle types were grouped into four categories: automobiles (autos), light trucks (LT), medium trucks (MT), and heavy trucks (HT). In terms of noise emission levels, all passenger automobiles, pickup trucks, and 12- or 15-passenger vans were grouped into the automobile category. The light truck category consisted of delivery-type trucks larger than a van plus pickup trucks with two axles and four tires. Single-unit trucks with two axles and six tires were considered to be

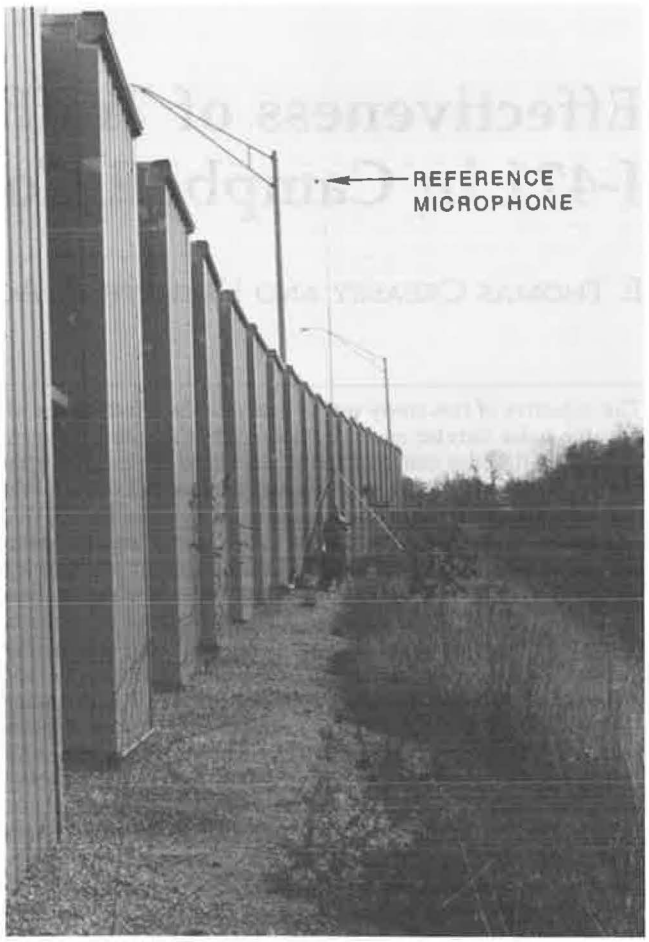

FIGURE 2 Elevated reference microphone.

medium trucks, as were buses. Motorcycles were included in this category as well because they had similar noise emission levels. Single-unit trucks with three or more axles and all combination trucks were grouped into the heavy truck category. Corresponding source heights of 0.0, 0.0, 2.3 and 8.0 ft, respectively, were assigned to the categories and input into the Stamina 2.0 model.

Although the Stamina 2.0 model includes noise emission levels for cars, medium trucks, and heavy trucks that were derived from the results of nationwide studies, the researchers decided to use noise emission levels collected for different types of Kentucky vehicles in an earlier study (*2*). It was believed that use of emission levels from Kentucky vehicles would result in a more accurate model. Thus parameters for Kentucky automobiles, light trucks, medium trucks, and heavy trucks were input into the model. Traffic flow conditions for vehicle type, volume, and speed were also input into the model. The STAMINA 2.0 user's manual (*1*) did not specify what speeds were to be used in the calibration process, so a decision was made to use the 85th-percentile speed obtained from spot speed data collected at the site.

The roadway was modeled by using a three-dimensional coordinate system to describe a sequential string of straight line segments. For each direction (northbound and southbound) the roadway model consisted of three sections: the ramp, the main-lane section upstream from the ramp, and the

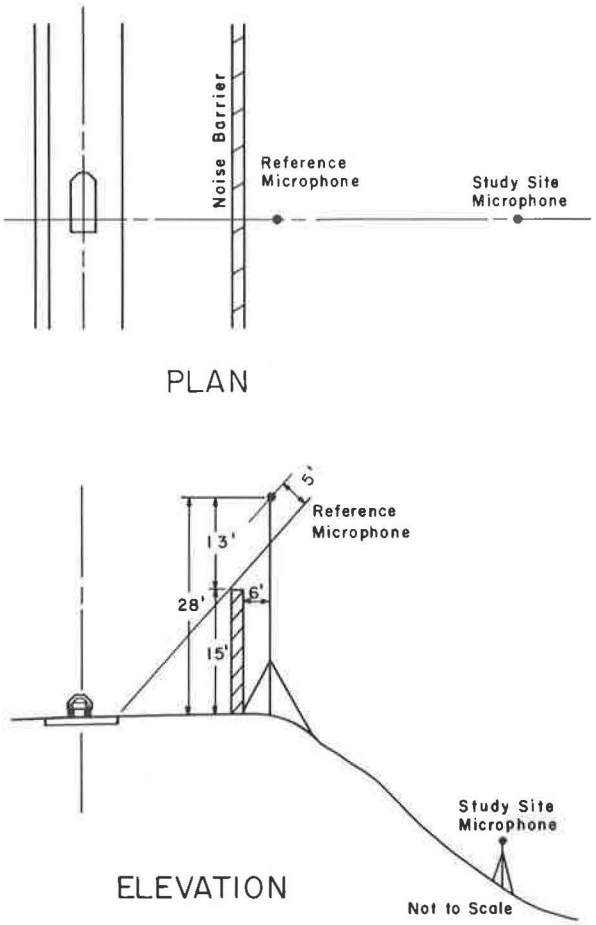

FIGURE 3 Reference microphone positioning.

main-lane section downstream from the ramp. Traffic volume data were obtained by manual counts for each of the roadway sections and input into the model.

STAMINA 2.0 allows the user to adjust the emission levels for heavy trucks moving up grades. A grade adjustment factor can be included in the roadway model and was used in the prediction process for the upgrade southbound lanes.

The noise barrier was modeled physically in the same manner as the roadway, by using a three-dimensional coordinate system to describe the barrier as a string of sequentially connected straight line segments. The height of the top of the barrier was input into the model, along with its elevation at ground level. The barrier coordinates were inserted into the model during the calibration process so that the present conditions could be predicted and then the predicted noise levels could be compared to those actually measured. After calibration of the model, the noise barrier coordinates were removed so that the conditions that would exist if the barrier were not present could be modeled.

A decision was made to model an existing concrete median barrier as a small noise barrier. Although this structure is not intended to be used as a noise barrier and its effect would be minimal, the decision was made to include it in the model so that the actual site could be approximated as closely as possible. For the same reason, three hills in the study site that were considered to be large enough to provide a significant amount of protection from traffic noise for some of the residences were also included in the model. STAMINA 2.0 recognizes three types of barriers: absorptive, reflective, and structural. The noise barrier wall and the concrete median barrier were considered to be reflective barriers, whereas the three hills were modeled as absorptive earth barriers.

Other factors recognized by STAMINA 2.0 in the modeling process are alpha factors, which concern the effect of hard or soft ground on the noise propagation rate between the source and receiver, and shielding factors, which account for the additional attenuation of noise due to shielding by buildings, rows of houses, trees, or other terrain features. The hillside behind the noise barrier was covered thickly with vegetation, leading to the use of the 4.5 dB per distance doubling propagation rate for soft ground between the roadway and the study site microphone. A propagation rate of 3 dB per distance doubling was used for the hard pavement surface between the roadway and the reference microphone. There were no shielding factors between the roadway and reference and study site microphones to cause additional noise attenuation in the model calibration process.

Noise measurements were taken at the reference microphone location by placing a microphone atop the 28-ft tripod described previously and connecting it via cable to a B&K Model 4426 Noise Level Analyzer. The microphone at the study site was supported on a smaller, 5-ft tripod and was connected to another analyzer. Wind screens were used with the microphones to minimize wind noise.

The final step in the calibration process was to obtain noise measurements at the selected microphone reference and study site locations. During this period, traffic volumes and speeds were recorded. The STAMINA 2.0 program used this information to predict noise levels at the two receiver locations. Those levels were then compared to the actual recorded levels at the receiver locations for the same periods so that the validity of the model was tested.

MODEL CALIBRATION RESULTS

As part of the model calibration, noise level measurements were obtained and corresponding traffic volumes and speeds were recorded for the reference location and the initial study site location. Data were collected during seven 10-min intervals, giving seven separate runs. The traffic volumes and speeds for each run were entered into the STAMINA 2.0 model. The model then used those volumes and speeds to predict the noise level, which was compared to measured traffic noise levels. The model was assumed to be calibrated properly if the difference between measured and predicted noise levels was less than the allowable difference.

The allowable difference in L_{eq} (the equivalent steady state sound level that contains the same acoustic energy over a particular period as the time-varying sound level during that same period) was 1.0 dBA for the reference microphone location and 2.0 dBA for the study site microphone location. The allowable difference at both of these locations was exceeded in the first calibration attempt. It was assumed that the physical characteristics of the site were not modeled precisely enough, so additional data on topography and other physical aspects of the site were collected.

Additional calibration runs were made. For seven runs, the average difference in L_{eq} at the reference microphone was determined to be 0.8 dBA, with the difference ranging from 0.2 to 1.6 dBA. The average was less than the allowable difference of 1.0 dBA. The allowable difference in L_{eq} for the study site microphone location was 2.0 dBA. For seven runs, the average difference was 0.9 dBA, which also was acceptable. The difference ranged from 0.2 to 2.0 dBA. It was therefore assumed that the STAMINA 2.0 model of the noise barrier site was calibrated properly and could be used to predict traffic noise levels for the situation in which no noise barrier existed.

MEASUREMENT OF INSERTION LOSS

After calibration of the STAMINA 2.0 model, noise data were collected for peak and off-peak traffic conditions to estimate the barrier insertion loss. Study site locations were selected throughout the neighborhood, and the after noise level measurements were obtained. Measurements for peak traffic conditions were made between 4:00 p.m. and 6:00 p.m., and off-peak data were collected between 10:30 a.m. and 3:00 p.m. Peak noise data were collected on 13 days, and off-peak data were collected on 10 days. Noise level measurements were made during 10-min intervals, and corresponding traffic volumes were recorded.

To obtain the before noise levels, the X, Y, and Z coordinates of the receiver locations were input into the STAMINA 2.0 model, as described previously in the model calibration section. Traffic noise data were collected at 39 receiver locations, as illustrated in Figure 4. The receivers were located within an area adjacent to I-471 that was determined to be affected by the noise barrier. Included in this area were 108 residences.

Coordinates of the noise barrier were excluded from the model to simulate the situation that would exist if no barrier were present. Corresponding traffic volumes and speeds were input into the model, and the STAMINA 2.0 program was run to predict the noise levels that would exist for the study site receiver locations without the noise barrier. Appropriate alpha and shielding factors were also input. The barrier insertion loss for each receiver location was calculated to be the difference between the before and after noise levels.

RESULTS

Results of insertion loss measurements are expressed in terms of L_{eq}. Experience demonstrates that L_{eq} is approximately 3 dBA less than L_{10}, which is the sound level for that period that is exceeded 10 percent of the time (*3*).

Peak Conditions

Predicted and measured average L_{eq} noise levels for peak traffic conditions are presented in Table 1. Total peak traffic volumes during the data collection period averaged 4,592 autos/hr, 2 LT/hr, 68 MT/hr, and 35 HT/hr.

The effect of the barrier on traffic noise reaching homes during the peak traffic period is presented in Table 2. For noise levels predicted by the STAMINA 2.0 model, 46 of 108 residences (43 percent) under the no-barrier condition had predicted peak L_{eq} levels of 60.0 dBA or more, whereas no residences were determined to have peak L_{eq} levels of 60.0 dBA or more with the barrier present.

Peak insertion loss estimates for study site residences are presented in Table 3. In all, 15 residences (14 percent) had an L_{eq} insertion loss of 10.0 dBA or more, and an additional 58 residences (54 percent) experienced a peak L_{eq} insertion loss of 5.0 to 9.9 dBA.

Off-Peak Conditions

Predicted and measured average L_{eq} noise levels and insertion loss estimates for off-peak traffic conditions are presented in Table 1. During the data collection period, total off-peak

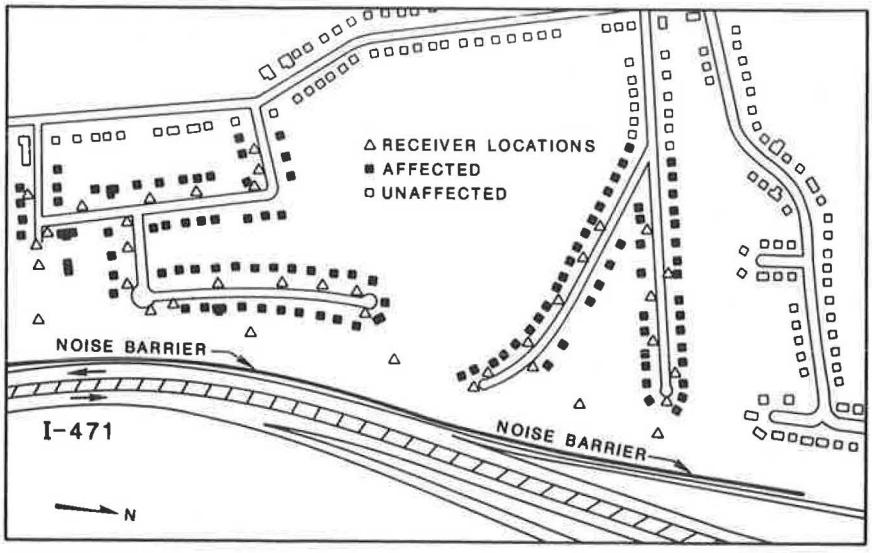

FIGURE 4 Field measurement receiver locations.

TABLE 1 INSERTION LOSS MEASUREMENTS

RECEIVER LOCATION NUMBER	AVERAGE Leq NOISE LEVEL (dBA)					
	MEASURED		PREDICTED		INSERTION LOSS	
	PEAK	OFF-PEAK	PEAK	OFF-PEAK	PEAK	OFF-PEAK
002	61.2	59.4	52.4	49.2	8.8	10.2
003	58.6	56.1	53.9	50.2	4.7	5.9
004	52.8	51.2	47.9	45.4	4.9	5.8
005	68.5	65.9	55.0	53.6	13.5	12.3
006	63.9	61.5	54.7	50.5	9.2	11.0
007	57.8	55.0	54.0	50.0	3.8	5.0
008	54.5	51.8	48.5	47.5	6.0	4.3
009	62.6	60.4	53.0	50.9	9.6	9.5
010	62.3	60.8	54.2	53.6	8.1	7.2
011	63.3	60.9	56.6	52.7	6.7	8.2
012	67.4	65.0	59.3	54.8	8.1	10.2
013	59.2	57.4	54.9	51.2	4.3	6.2
014	62.4	61.5	56.4	53.5	6.0	8.0
015	54.5	53.2	50.8	47.1	3.7	6.1
016	59.5	57.4	54.4	52.2	5.1	5.2
017	48.1	46.0	47.5	46.0	0.6	0.0
018	48.4	46.4	46.2	45.9	2.2	0.5
019	55.3	53.2	49.5	47.1	5.8	6.1
020	57.7	55.5	51.0	47.9	6.7	7.6
100	61.0	59.5	55.7	51.1	5.3	8.4
101	62.1	60.5	55.8	52.8	6.3	7.7
102	66.9	63.9	58.4	53.6	8.5	10.3
103	65.8	63.6	57.8	53.8	8.0	9.8
104	59.3	57.2	51.3	51.0	8.0	6.2
105	49.8	49.3	47.1	45.1	2.7	4.2
106	48.5	46.4	44.9	43.5	3.6	2.9
107	51.6	49.5	48.8	47.7	2.8	1.8
108	62.3	59.7	52.6	49.2	9.7	10.5
109	66.6	63.7	54.8	52.2	11.8	11.5
110	51.4	48.7	49.8	47.4	1.6	1.3
111	53.3	52.5	49.8	46.5	3.5	6.0
112	58.9	57.4	53.2	49.0	5.7	8.4
113	61.6	60.6	55.0	56.0	6.6	4.6
114	65.1	62.4	58.3	54.5	6.8	7.9
115	68.6	65.3	55.8	53.0	12.8	12.3
116	69.9	67.1	58.4	57.0	11.5	10.1
117	70.4	68.1	59.4	57.2	11.0	10.9
118	64.0	62.1	61.1	57.1	2.9	5.0
119	66.5	64.2	54.3	53.4	12.2	10.8

TABLE 2 NOISE BARRIER EFFECT ON TRAFFIC NOISE REACHING RESIDENTS

	PREDICTED (NO BARRIER)		MEASURED (BARRIER PRESENT)	
PEAK Leq NOISE LEVEL (dBA)	NUMBER RESIDENCES	PERCENT	NUMBER RESIDENCES	PERCENT
65.0 - 70.0	17	16	0	0
60.0 - 64.9	29	27	0	0
55.0 - 59.9	27	25	32	30
50.0 - 54.9	16	15	36	33
Less than 50.0	19	17	40	37

	PREDICTED (NO BARRIER)		MEASURED (BARRIER PRESENT)	
OFF-PEAK Leq NOISE LEVEL (dBA)	NUMBER RESIDENCES	PERCENT	NUMBER RESIDENCES	PERCENT
65.0 - 70.0	10	9	0	0
60.0 - 64.9	26	24	0	0
55.0 - 59.9	27	25	10	9
50.0 - 54.9	22	21	42	39
Less than 50.0	23	21	56	52

TABLE 3 NUMBER OF RESIDENCES RECEIVING GIVEN L_{eq} INSERTION LOSS

Average Insertion Loss (dBA)	Peak		Off-Peak	
	Number Residences	Percent	Number Residences	Percent
10 or above	15	14	20	18
5.0–9.9	58	54	57	53
Less than 5.0	35	32	31	29

volumes averaged 2,052 autos/hr, 7 LT/hr, 84 MT/hr, and 64 HT/hr.

The effect of the noise barrier on traffic noise reaching residences during off-peak conditions is presented in Table 2. For the situation with no noise barrier, 36 of 108 residences (36 percent) were predicted to experience an L_{eq} noise level of 60.0 dBA or more. With the barrier in place, no residences were found to experience L_{eq} noise levels of 60.0 dBA or more.

Insertion loss estimates for residences throughout the study site for off-peak traffic conditions are presented in Table 3. In all, 20 residences (18 percent) were predicted to have an L_{eq} insertion loss of 10.0 dBA or more, and an 57 additional residences (53 percent) were predicted to experience an L_{eq} insertion loss between 5.0 and 9.9 dBA.

Measured Versus Predicted Insertion Loss

One objective of this study was to determine whether computer estimates of insertion loss were being achieved. The field measurements were used to check the accuracy of the predicted insertion losses. The STAMINA 2.0 model was used to predict the noise level with the noise barrier in place.

In Table 4, a summary of insertion loss estimates using both field measurements and noise levels predicted by STAMINA 2.0 is presented. The comparisons for average insertion loss estimates in the study area are given for both peak and off-peak traffic conditions. The differences between measured and predicted insertion loss values were less than 1.0 dBA for both peak and off-peak traffic conditions. This suggests that insertion loss values predicted by the STAMINA 2.0 computer program will be achieved by the noise barrier.

TABLE 4 MEASURED VERSUS PREDICTED INSERTION LOSS

	Average L_{eq} Insertion Loss (dBA)	
	Peak	Off-Peak
Measured	6.6	7.1
Predicted	7.2	6.4
Difference	0.6	0.7

SURVEY OF COMMUNITY PERCEPTION

A survey of community perception of the noise barrier was conducted among the residents of the homes included in the analysis. A questionnaire and accompanying cover letter explaining the purpose of the survey, along with a postage-paid return envelope, were mailed to these residents. The homes included in the survey were selected subjectively on the basis of a field inspection of the area adjacent to the barrier.

The questionnaire consisted of questions commonly asked of residents in similar noise barrier evaluation projects (*4–9*). Questionnaire topics included awareness of the barrier,

TABLE 5 SUMMARY OF COMMUNITY PERCEPTION SURVEY

Questionnaire Item	Percent Responding "Yes"
1. Perception of neighborhood as quiet or very quiet:	
Before construction of barrier and roadway	96
After construction of barrier and roadway	34
2. Effect of barrier on highway-related problems:	
Overall improvement in highway noise	78
Improved privacy	71
Reduced highway dust and dirt accumulation	56
Reduced headlight glare	54
Reduced road vibrations	52
Reduced road fumes	48
3. Effect on activities:	
Relaxing outdoors less difficult	57
Conversation outdoors less difficult	56
Sleeping less difficult	48
Conversation indoors less difficult	46
Relaxing indoors less difficult	44
Telephone conversation less difficult	42
4. Disadvantages associated with barrier:	
Barrier limits or restricts view	33
Barrier unsightly	17
Barrier creates closed-in feeling	15
Perceived detrimental effect on environment	15
5. Overall opinion of noise barrier:	
Effective in reducing traffic noise	95
Appearance acceptable	78
Generally like barrier	64
No effect on property value	57

highway-related problems with the barrier, activities affected by the barrier, and the general effectiveness of the noise barrier as perceived by residents of the neighborhood. Answers to the survey questions are summarized in Table 5.

Five of the 108 residences within the study site area were either new homes under construction or were unoccupied at the time of the study. Survey questionnaires were mailed to the remaining 103 homes. Of the 103 questionnaires mailed, 66 (64 percent) were returned. Of these, 49 (48 percent) were returned initially, and an additional 17 of 54 follow-up questionnaires (31 percent) were returned by residents who did not respond initially.

Responses indicated that the affected homes were in an old and established neighborhood. The average length of residence was 18 years, with an average population of three persons per home. Among the respondents, 98 percent owned their homes.

In their answers, 96 percent of the respondents described the neighborhood as quiet or very quiet before the roadway and barrier were built, whereas 34 percent felt it to be quiet or very quiet after construction of the roadway and barrier. Ninety-eight percent of the respondents were aware that the barrier existed; of these, 63 percent learned about the barrier by observing its construction and 19 percent learned of the barrier from the newspaper.

In answer to questions about the effect of the noise barrier on highway-related problems, 78 percent of the respondents believed that the barrier made an overall improvement in reducing highway noise, and 71 percent believed that the barrier improved their privacy. In addition, 56 percent believed that the barrier reduced highway dust and dirt accumulation and litter from vehicles, 54 percent believed that it reduced headlight glare, 52 percent believed that it reduced road vibrations, and 48 percent believed that it reduced road fumes.

When questioned about various activities, 57 percent thought that relaxing outdoors was less difficult due to the presence of the barrier, and 56 percent believed that conversation outdoors was less difficult. Also, 48 percent thought that sleeping was less difficult, 46 percent thought that conversation indoors was less difficult, 44 percent thought that relaxing indoors was less difficult, and 42 percent thought that telephone conversation was less difficult. Additionally, 57 percent stated the barrier did not affect the amount that they used their yards, but 40 percent believed that they would have used their yards less if the barrier had not been built.

The respondents were questioned about the effect of the barrier on their environment. In their answers, 33 percent of them believed that the barrier limited or restricted their view, 17 percent thought the barrier was unsightly, 15 percent believed that it created a closed-in feeling, and 15 percent believed that it had a detrimental effect on the environment. It should be noted that many of the respondents appeared to have difficulty discriminating the benefits of the noise barrier from the effect of the roadway because the construction of both was coincidental. Thus many of the negative answers and comments directed toward the noise barrier were actually directed toward construction of the roadway.

In answer to questions about the barrier's appearance, 78 percent of the residents who responded to the survey considered the barrier to be acceptable and 12 percent thought it was unsightly, whereas 10 percent thought it was attractive. Compared to having no noise barrier at all, 50 percent believed that the barrier was very effective in reducing traffic noise, and 45 percent thought it was somewhat effective. In relation to property value, 57 percent believed that the barrier had no effect, 27 percent believed that their property value had decreased, and 16 percent believed that it had increased. Overall, 64 percent of those responding generally liked the noise barrier, 13 percent disliked it, and 23 percent had no opinion.

SUMMARY

The STAMINA 2.0 computer program was calibrated with a model of the study site so that the program could be used to predict noise levels by assuming that the traffic noise barrier was not present. Noise measurements were then obtained at 39 receiver locations during both peak and off-peak traffic periods so that insertion loss estimates could be made.

The noise barrier substantially reduced noise levels reaching the adjacent residences. For example, 15 homes (14 percent of the total in the study area) experienced a peak L_{eq} insertion loss of 10 dBA or more, and another 58 residences (54 percent) were estimated to receive an L_{eq} insertion loss of 5.0 to 9.9 dBA. Also, the STAMINA 2.0 model predicted that, with no barrier present, 17 residences (16 percent) would experience peak L_{eq} noise levels from 65.0 to 70.0 dBA, and another 29 homes (27 percent) would experience levels from 60.0 to 64.9 dBA. Measurements indicated that no residences

had peak L_{eq} levels more than 70.0 dBA with the barrier in place.

As an additional check, noise levels with the barrier in place were predicted by using the STAMINA 2.0 model. Comparison of insertion loss values calculated by using both predicted and measured noise levels with the barrier present were close. The analysis indicated that insertion loss values predicted by the STAMINA 2.0 computer program are being achieved by the noise barrier.

Of 103 questionnaires mailed to residents to determine their perception of the barrier, 66 (64 percent) were returned. The neighborhood perception of the barrier was favorable. Overall, 64 percent of those responding generally liked the noise barrier, 13 percent disliked it, and 23 percent had no opinion. Also, 50 percent believed that in comparison to having no noise barrier, the barrier was very effective in reducing traffic noise, and 45 percent thought it was somewhat effective.

IMPLEMENTATION

The traffic noise measurements and data analyses summarized in this report indicate that the I-471 noise barrier has caused a substantial reduction in traffic noise for the affected homes. The success of this noise barrier in providing its predicted insertion loss proves that such barriers provide an effective traffic noise abatement alternative. The construction of additional barriers should be considered in the future as a viable noise abatement measure. The results of this study can be used in future public hearings to illustrate the potential effectiveness of proposed noise barriers.

ACKNOWLEDGMENTS

This research was sponsored by the Kentucky Transportation Cabinet in conjunction with the FHWA, U.S. Department of Transportation. The study contract monitor was Ron George.

REFERENCES

1. W. Bowlby, J. Higgins, and J. Reagan. Noise Barrier Cost Reduction Procedure. In *STAMINA 2.0/OPTIMA: User's Manual.* Report FHWA-DP-58-1. FHWA, U.S. Department of Transportation, April 1982.
2. K. R. Agent. *Vehicle Noise Emission Levels in Kentucky.* Report UKTRP-81-13. Transportation Research Program, University of Kentucky, Lexington, July 1981.
3. *Federal-Aid Highway Program Manual.* Transmittal 348. FHWA, U.S. Department of Transportation, April 1982.
4. M. A. Perfater. *Community Perception of Noise Barriers,* Vol. 1. Report VHTRC 80-R14. Virginia Highway and Transportation Research Council, Richmond, September 1979.
5. F. L. Hall. Attitudes Toward Noise Barriers Before and After Construction. In *Transportation Research Record 740,* TRB, National Research Council, Washington, D.C., 1980.
6. A. N. Barass and L. F. Cohn. Noise Abatement and Public Policy Decisions: A Case Study — I-440 in Nashville. In *Transportation Research Record 789,* TRB, National Research Council, Washington, D.C., 1981.
7. L. F. Cohn. *NCHRP Report 87: Highway Noise Barriers.* TRB, National Research Council, Washington, D.C., December 1981.
8. *An Iowa Noise Barrier: Sound Levels, Air Quality and Public Acceptance.* Office of Project Planning, Planning and Research Division, Iowa Department of Transportation, Des Moines, February 1983.
9. *A Determination of Noise Barrier Effectiveness along I-285 in Atlanta, Georgia.* Office of Environmental Analysis, Georgia Department of Transportation, Atlanta, 1983.

Publication of this paper sponsored by Committee on Transportation-Related Noise and Vibration.

Analysis and Programs for Assessment of Absorptive and Tilted Parallel Barriers

SIMON SLUTSKY AND HENRY L. BERTONI

An analysis and a computer program were prepared for use in connection with a FHWA test program. As part of this procedure, a model based on ray theory was developed for the prediction of highway traffic noise in the presence of tilted, absorptive barriers that are parallel to the roadway. The model was programmed for use on a personal computer or other DOS-compatible small computer. The program, called BarrierX, uses impedance of the barrier surface as input to compute the barrier reflection coefficients, which are therefore angle dependent. The program accounts for the modification of barrier reflection due to diffraction at discontinuities of the barrier surface impedance and at the discontinuity at the upper edges. Effects of atmospheric absorption, terrain absorption, and the pavement-wayside impedance discontinuity are taken into consideration. The highway and barriers are assumed to be straight and the wayside flat, but otherwise the program inputs permit considerable flexibility. Preliminary computations made with the program are in agreement with other recent studies, which conclude that parallel reflective barriers can severely reduce the anticipated single-barrier insertion loss and that absorptive wall treatment can be very beneficial. A result of considerable interest is that in roadway geometries of interest, relatively small angles of tilt can restore almost all of the single-barrier insertion loss.

This work was motivated by the need for a convenient method to predict the effect of tilt angle and absorptive treatment on the degradation of barrier insertion loss observed with parallel barriers. This degradation of barrier performance is a consequence of the reverberant reflection of vehicle-generated sound by the barrier surfaces.

The occurrence of such degradation is well documented in the literature. The recent work by Bowlby et al. (*1, 2*) contains comprehensive summaries of papers reporting predictions and measurements of degradation (*3, 4*). Hajek's predictions note the possibility of parallel barrier degradation of as much as 12 dB, depending on the barrier-source-receiver geometry (*4*). Such high degradation possibilities were also noted by Pejaver and Shadley (*5*). Bowlby et al. also called attention to Legillon's scale model measurements (*6*), in which the usefulness of tilting the barrier is noted and compared with absorptive treatment. The work of Bowlby and Cohn (*2, 7*) reflects the need for a modification of the STAMINA program (*8*) to include parallel barrier effects in a systematic way instead of by manipulation to create virtual highways. Bowlby and Cohn's computer program does not include the effect of barrier tilt; is based on a geometric acoustics approach so that it does not consider the fields reflected by the barrier discontinuities; and for the purpose of degradation, treats excess attenuation due to soft ground at the wayside as a constant. They report good comparison with data available to them.

The intent of this project is to account for the effect of barrier tilt and the diffraction phenomena that occur in the fields reflected by the barrier because of discontinuities of the reflective properties of the barrier, as well as to incorporate available improvements in the treatment of ground interaction at the wayside. Consideration of diffraction at reflective discontinuities demanded a departure from the use of the usual angle-averaged reflection coefficients in favor of the normal impedance to define the barrier surface materials. The reflection coefficient computed from the impedance is then angle dependent.

FHWA interest in dividing the barrier facing into several reflective zones (up to three) and the existence of a strong discontinuity at the top of the barrier made it necessary to treat diffractive effects at reflective discontinuities. Although a specific solution to this problem was not found in the literature, an approximate approach (strictly valid for only one reflection) was worked out on the basis of the Fresnel-Kirchhoff diffraction formula (*9, 10*). This impedance-based treatment of reflection was incorporated into a computer program called BarrierX.

As a stepping stone to BarrierX, a simpler program called Barrier was created first. This early program, like the one mentioned previously (*2*), was based on simple (geometric acoustic) ray theory, used angle averaged reflection coefficients as input, and did not include the effect of reflective discontinuities.

The treatment of excess attenuation caused by wayside absorption has been the subject of many works in the literature (*11–17*). The field is still very active, and there is much concern over the relative merits of the local soil reaction model (*11–15*) versus the extended reaction model (*16*). The latter assumes that the soil sustains wave propagation both vertically and horizontally, whereas the former assumes only a local surface interaction with no lateral interaction. The papers by Chien and Soroka (*14, 15*) have been widely referenced and used. The convenient expressions developed for computing and coding in their model are the basis of the subroutine module used in the current programs. Some versions of the extended reaction model, such as that developed by Attenborough et al. [(*16*); note also their corrections in that work to equations by Rasmussen (*17, 18*)], are not much more complicated to code. However, Rasmussen (*17, 18*) and Habault and

Polytechnic Institute of New York, 333 Jay St., Brooklyn, N.Y. 11201.

Corsain (*19*) have noted that for most soils and frequencies, there is not much difference in predictions made with the alternative models.

Another important area of investigation is the identification of the soil parameters that describe the acoustic character of the soil. A relationship between the characteristic impedance of an isotropic porous medium and the flow resistance is discussed by Morse (*20*). Delaney and Bazley (*21*) carried out extensive measurements and concluded that the normal impedance at the soil surface, as well as the soil/air sound speed ratio, could be predicted well by the air flow resistance. Other models are considered in the literature (*21*). Habault and Corsain (*19*) describe a general procedure for identifying the soil impedance by using a least squares curve fit to measurements from several (five or six) points on the ground. Nevertheless, because the Delaney-Bazley model is generally considered effective, it is used in the present programs. A convenient table of flow resistance for various soil types can be found in the work of Embleton (*24*).

Without exception, all theories that consider reflection of spherical or cylindrical waves from an impedance surface predict eventual attenuation of the field at the rate of 6 dB per doubling of distance in excess of the free field falloff rate. The distance at which that asymptotic decay rate is achieved depends primarily on the soil impedance, the frequency, and the angle of incidence of the specular ray. At smaller distances the theories may predict values of excess attenuation per doubling that may be either larger than or smaller than 1.5 dB/dd . For example, Attenborough (*23*) used several impedance models to compute the excess attenuation from a line of vehicles consisting of a mix of automobiles and trucks with typical emission spectra. His calculations included a variety of soil types for distances up to 72.8 m. Depending on the soil type and receiver height, Attenborough found values of excess attenuation per double distance that were sometimes much less than 1.5 and sometimes exceeded 3.0. His conclusion was that current schemes for predicting the attenuation of highway noise should be modified to include real impedance effects.

Rasmussen (*17, 25*) reported measured values of excess attenuation between pairs of points alongside a roadway that were as high as 8 dB/dd at some frequencies (notably 500 Hz). He also found that the influence of the pavement-wayside impedance discontinuity needed to be taken into account in some cases to get good agreement between measurements and predictions.

Atmospheric absorption is included in the current computer program by means of a table of attenuation in decibels per thousand feet versus humidity and frequency at a temperature of 68°F. This table is appended to the input template. Data are currently available for more general temperature conditions (*26, 27*) and can be incorporated into the program if desired. No account is taken here of wind gradients, temperature gradients, turbulence, and so on.

Input parameters used to define the roadway, the barriers, and the wayside, as well as the vehicular traffic volumes, types, and sound characteristics, are listed later in the paper in the section on the program treatment. Outputs are printed to the screen and echoed to the printer if desired. They consist of eight unweighted octave band levels from 63 to 8000 Hz, eight *A*-weight octave band levels, and the overall *A*-weighted SPL. This set of outputs is printed for each receiver.

ACOUSTIC PATH FIELDS

In this section, the various ray paths by which the fields radiated by a source can reach a receiver are summarized. If no barrier is present, these paths consist of the direct ray from the source to the receiver and the ray reflected from the ground. The presence of a single barrier complicates these paths by diffraction over the top of the barrier, and the presence of two barriers gives rise to additional ray paths because of the multiple reflections between the barriers.

Diffraction by a Single Barrier

The ray paths for a single tilted barrier between the source and receiver are shown in Figure 1. Rays reaching the top of the barrier can come directly from the source *S* or by reflection from the pavement. Subsequently, the diffracted rays from the barrier edge *E* reach the receiver *R* either directly or after reflection from the wayside, so that the total number of ray paths is four.

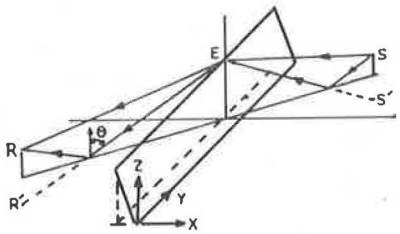

FIGURE 1 Diffracted path geometry.

Pavement Reflection

Reflection at the pavement may be treated by means of an image source at *S'*, whose strength is that of the actual source multiplied by the pavement reflection coefficient Γ. For an elevated barrier edge, the ray *SP* is never near glancing incidence, so the plane wave reflection coefficient may be used. Thus

$$\Gamma(\theta) = \frac{Z\cos(\theta) - 1}{Z\cos(\theta) + 1} \quad (1)$$

where Z is the pavement impedance normalized to that of the standard atmosphere and θ is the angle of incidence as measured from the normal to the pavement.

Barrier Diffraction

In treating diffraction at the barrier edge, the FHWA (Kurtze-Anderson) model has been adopted to facilitate comparison with other approaches and because of the speed of the resulting algorithm. This model introduces an insertion loss given in decibels by

$$\Delta = 0 \quad N \leq -0.1916$$

$$\Delta = 5.0 + 20 \log [NN/\tan (NN)] \quad -0.1916 \leq N \leq 0.0$$

$$\Delta = 5.0 + 20 \log [NN/\text{htan} (NN)] \quad 0.0 \leq N \leq 5.03$$

$$\Delta = 20.0 \quad 5.03 \leq N \tag{2}$$

where

$$NN = \sqrt{2 \Pi |N|}$$

$$N = 2\delta/\lambda \tag{3}$$

Here, N is the Fresnel number, δ is the path length difference (which can be negative for uninterrupted paths), and λ is the acoustic wavelength. Δ is the insertion loss for the path due to diffraction.

Wayside Reflection: Homogeneous Ground

The problem of reflection of a point source by a plane surface has been investigated extensively since the beginning of this century. A long list of references and summary of results may be found in a review paper by Piercy et al. (*28*). Most of the discussion of this subject is concerned with the acoustic behavior of the ground, as well as with interpretation of the solutions. In particular, the question of local versus extended reaction of the ground has received much attention. K. B. Rasmussen discusses these matters in a useful series of papers and concludes that the local reaction model is quite similar to the extended model for typical values of surface impedance (*17, 18*).

The accepted model for including the effect of ground reflection, which is employed here, is to add the contributions of the direct path field reaching R from E in Figure 1 and the field that would reach the image receiver R' multiplied by the spherical wave reflection coefficient:

$$Q = \Gamma(\theta) + [1 - \Gamma(\theta)] * E(P_e) \tag{4}$$

where θ is the angle between the ray ER' and the normal to the ground, and $\Gamma(\theta)$ is as given in Equation 1. The function $E(P_e)$ is related to the complementary error function via

$$E(P_e) = 1 + i\sqrt{\pi} P_e \exp(-P_e^2) \operatorname{erfc}(-iP_e) \tag{5}$$

and the argument is

$$P_e = \sqrt{\pi i k r_2/2}\ (1/Z + \cos\theta) \tag{6}$$

where r_2 is ER', the slant distance from the point of diffraction at the barrier edge to the image receiver. In this program the wayside and pavement may have different elevations but are assumed to be parallel to each other, so that even when S and R are not opposite to each other across the barrier, all rays between S and R lie in the same (vertical) plane.

Delaney and Bazley (*21*) have developed a widely used semi-empirical relationship for the effective normalized acoustic impedance, Z, of porous soils that depends on the flow resistance, σ, of the soil and the frequency, f:

$$Z = 1 + 9.08 (f_n)^{-0.75} + i\ 11.9 (f_n)^{-0.73} \tag{7}$$

$$f_n = 1{,}000\, f/\sigma \tag{8}$$

This expression was found to give good agreement for a large number of soils and porous media. It is used as the basis for the current formulation of ground impedance.

Wayside Reflection: Impedance Discontinuity

Although the computer program is designed to deal with the effect of barriers, in some cases the barrier is of finite extent or is not present, so that propagation paths from some sources do not involve barrier diffraction. In these cases an impedance discontinuity exists between the pavement and the wayside.

In general, the effective reflection coefficient for this case will vary between the values determined by the two surface impedances, depending on what fraction of the Fresnel zone about the ray between the source S and image receiver R' intersects one or the other surface (see Figure 2). The Fresnel ellipsoid can be defined as the surface generated by the locus of points F (Figure 3) for which the direct path SR' and the broken path SFR' differ by a half wavelength. In addition to changing the effective reflection coefficient, the discontinuity in surface impedance will act as a line source for scattered rays propagating radially in all directions. One of these rays will reach the receiver R, contributing to the field there. Although various solutions to this problem exist, most take a long time to run on a microcomputer, especially at higher frequencies. In consequence, a semi-empirical expression developed by B. A. de Jong and described in detail by Rasmussen (*17*) has been used. The following expressions and discussion from de Jong's work are taken essentially verbatim from Rasmussen's description. This expression can be written as the normalized ratio of the combined field to the free field:

$$\frac{P}{P_f} = 1 + \frac{R_1}{R_2} \exp i\,k\,(R_2 - R_1) \begin{Bmatrix} Q_1 \\ Q_2 \end{Bmatrix} + (Q_2 - Q_1) \frac{\exp(i\,\pi/4)}{\sqrt{\pi}} \frac{R_1}{R_{34}} \times \left[F_{341} + \begin{Bmatrix} + \\ - \end{Bmatrix} F_{342} \exp i\,k(R_2 - R_1) \right] \tag{9}$$

$$F_{341} = F\left[\, |k(R_{34} - R_1)| \,\right] \tag{10}$$

$$F_{342} = F\left[\, |k(R_{34} - R_2)| \,\right] \tag{11}$$

$$R_{34} = R_1 + R_1 \tag{12}$$

$$F(u) = \int_u^\infty \exp(i\,w^2)\, dw \tag{13}$$

$F(u)$ is the Fresnel integral, and the Q are defined by Equation 4. Q_1 and $+1$ are used when the specularly reflected ray path intersects Z1, and Q_2 and -1 are used when the ray intersects Z2 (Figure 3). The equation is valid only when Z1 represents the hard surface. The solution has the right form when Z1 = Z2 and when the specularly reflected ray strikes the discontinuity.

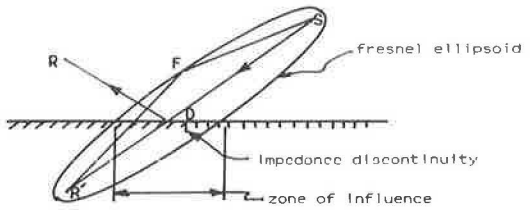

FIGURE 2 Fresnel ellipsoid for reflected path.

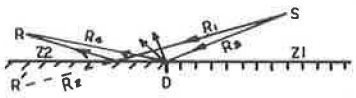

FIGURE 3 Diffraction from pavement-wayside discontinuity.

De Jong used the model in connection with model experiments and with outdoor measurements carried out with a loudspeaker source, with good agreement.

As noted above, there is some concern as to the justification of this approximation at large distances from the discontinuity. Experimental verification is not available for distances greater than 10 m. Until more confidence is established, the diffracted component will be set to zero when the discontinuity-to-receiver distance R_4 exceeds 100 ft (Figure 3).

COMBINED EFFECT OF PARALLEL BARRIERS

When two barriers are present, the ray fields reaching the barrier edge E closest to the receiver may undergo multiple reflections from the barriers and at most one reflection from the pavement. It has been found convenient to classify the rays according to the number of barrier reflections.

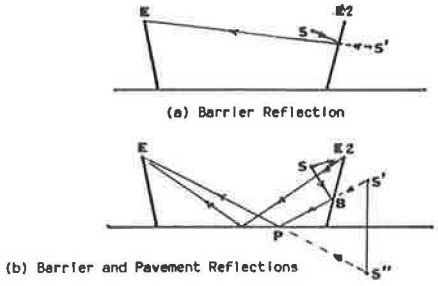

FIGURE 4 Diffracted paths with barrier reflection.

Single Reflection from a Barrier

The case of a single reflection is illustrated in Figure 4. If the ray is not reflected from the pavement, then the field reaching E can be constructed from an image source S', as indicated in Figure 4a, and the reflection coefficient of the barrier. To find the ray field reflected from the pavement, it is necessary to use S'' in Figure 4b, which is the image of S' in the pavement, and the pavement reflection coefficient given by Equation 1.

In addition to the reflected rays reaching E, a ray from S to $E2$ will excite diffracted fields propagating back toward E, either directly or via a pavement reflection. Moreover, if the surface of the reflecting barrier has different impedance in different horizontal bands, then diffracted rays will be excited at the impedance discontinuities. These complications are worsened because the Fresnel zone about the ray from S' to E may include the edge $E2$ or one of the impedance discontinuities (Figure 5). To overcome the difficulties introduced by these diffracted fields, an effective barrier reflection coefficient is used to account for the diffraction and accommodate barriers that have up to three horizontal bands with different surface impedance.

The effective reflection coefficient is obtained by using the physical acoustics approximation. The reflected field at the surface of the barrier is first written as the incident field multiplied by the local reflection coefficient. This field is then used in a Kirchhoff-Huygens integral to give the field at E. Division of this expression by the field for a perfect reflector gives the effective (pressure) reflection coefficient Γ_e. If the standard Fresnel approximations are made in the integral, the result is

$$\Gamma_e = \hat{\Gamma} + \frac{\exp(i\,\Pi/4)}{\sqrt{\Pi}} \operatorname{sgn}(\nu_1 - \hat{\nu})(\Gamma_2 - \Gamma_1)$$

$$\times F(|\nu_1 - \hat{\nu}|) + \operatorname{sgn}(\nu_2 - \hat{\nu})(\Gamma_3 - \Gamma_2)$$

$$\times F(|\nu_2 - \nu|) - \Gamma_3 F(|\nu_3 - \nu|) \qquad (14)$$

Here, Γ_1, Γ_2, and Γ_3 are the plane wave pressure reflection coefficients (Equation 1) of the lower, middle, and upper horizontal bands of the reflecting barrier. The term Γ is the reflection coefficient at the point of specular reflection at the barrier, and the functions $F(u)$ are defined by Equation 13. The quantities ν and ν_i ($i = 1, 2, 3$) are defined by

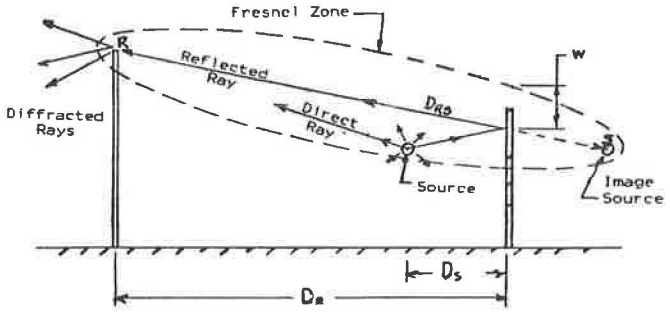

FIGURE 5 Reflection from multiple impedance surface.

$$\hat{\nu} = \hat{Z}\sqrt{k/2}\ \frac{(Dr + Ds)^2}{Drs\sqrt{Dr\ Ds\ Lrs}} \tag{15}$$

$$\nu_i = Z_i\sqrt{k/2}\ \frac{(Dr + Ds)^2}{Drs\sqrt{Dr\ Ds\ Lrs}} \tag{16}$$

$\hat{Z}$ is the height of the Fresnel point on the barrier, and Z_1, Z_2, and Z_3 are the heights of the discontinuities on the barrier. *Dr*, *Ds*, and *Drs* are the distances from the receiver to the reflecting barrier, from the source to the reflecting barrier, and from the receiver to the virtual source, respectively, as projected on the *XZ* plane (Figure 5). *Lrs* is the distance (in *XYZ* space) between the receiver and the virtual source. The half-width of the Fresnel ellipsoid at the barrier intersection is the reciprocal of the coefficient of Z in Equations 15 and 16, so that $(\nu_3 - \nu)$ is the nondimensional distance between the specular ray crossing and the upper edge discontinuity.

Expression 14 gives a continuous variation of the field as the specular point passes from one region of surface impedance to another. Because this expression includes both specularly reflected and diffracted fields, it can give values up to 17 percent higher, or as low as half of Γ_3. It is interesting that the reflection calculated by using Γ_e with the pavement-reflected ray in Figure 4b accounts for the diffracted ray originating at *E*2 that reaches *E* after being reflected by the pavement. Although Equation 14 is derived and is strictly valid only for a single barrier reflection, it is used subsequently for each barrier reflection of multiply reflected rays.

When no barrier is present on the side of the road nearest the receiver, reflections from the opposite barrier can still contribute to the field at the receiver. In this case the image source and appropriate reflection coefficients can be used to compute the reflected field without further introduction of diffraction.

Multiple Barrier Reflection for Zero Tilt

In Figure 6a, the element of multiple reflection for the simplified geometry of zero tilt is introduced. The barriers are numbered from the left (*B*1, *B*2, etc.). *B*3, *B*5, and *B*7 are virtual images of *B*1, and *B*4 and *B*6 are virtual images of *B*2. The zones between the barriers are similarly numbered, so that zone 1 contains real sources and all the subsequent zones contain the virtual sources of increasingly higher order. Virtual ray paths between the diffracting edge *E* of barrier 1 and all of the virtual sources are possible for this geometric configuration (*B*1 of equal or shorter height than *B*2 and its images). However, when *B*1 is taller than *B*2, as in Figure 6b, the higher-order paths fail to intersect *B*2 or its images, the reflections that define the ray do not occur, and then the ray itself cannot exist.

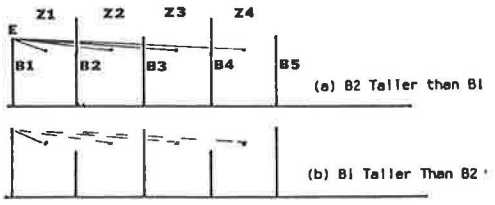

FIGURE 6 Multiple reflection for zero-tilt barrier.

Multiple Barrier Reflection with Tilt

The geometry of multiple reflection between parallel barriers is made more complicated by the presence of barrier tilt. Nevertheless, the construction of Figure 7 can completely rectify the apparently tangled real path (*29*). Because of the equality of angles of incidence and reflection for specular reflection, each ray segment and its virtual reflection are continued across each barrier as a straight line. Because this is true for virtual images of barriers as well as for the real barriers, the final virtual ray path can be displayed as a single straight line, independent of the number of reflections. Figure 8 shows an application of this construction to a more typical example of road geometry. It should be noted that if the ray crossing is above the top or below the bottom of the barrier, it cannot exist (as mentioned previously in the case of vertical barriers). Compatibility tests are therefore required for each ray contribution to locate the position of each assumed barrier crossing and to verify thereby the existence of the assumed reflections. It can be demonstrated that when either or both of the barriers are tilted, the compatibility test will always be violated after a finite number of barrier reflections (the number will depend on the height of the barriers, the width between barriers, and the tilt angles). This important result is the mechanism whereby the acoustically adverse effects of parallel barriers can be (almost) completely suppressed.

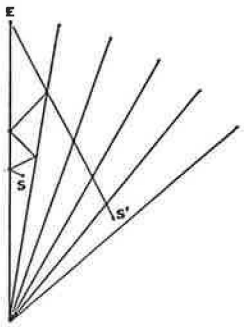

FIGURE 7 Multiple barrier reflection: wedge geometry.

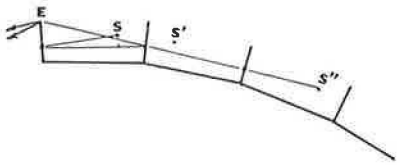

FIGURE 8 Multiple barrier reflection: tilted barriers.

In the present model, a limit of six zones is programmed for vertical barriers, and a limit of four zones is imposed for finite barrier tilt angles. Fewer zones can be specified by the user. It is assumed that four zones will be adequate for finite tilt because practical barrier configurations with tilt angles as small as 2 or 3 degrees show no acoustic contribution beyond the third zone. In general, the tilt angle required for suppression of multiple reflections is less as the ratio of barrier height to road width decreases. Some numerical aspects of this behavior are presented in the section on numerical results.

Multiple Barrier and Pavement Reflection

Another complication is introduced by reflection from the pavement. This effect is somewhat troublesome, as can be observed in Figure 9. This section of a prismatic cylinder shows the real pavement in Zone 1 and its images. The ray path between the virtual source in Zone 3 can reach the diffracting barrier edge E by a path that does not involve pavement reflection (as already considered above), or it can reflect from the pavement or one of its images, or it can do both. To locate the reflection point systematically, the image of the virtual source whereby the path can be rectified must be found. However, because three distinct reflective pavement surfaces exist for this case, three corresponding image locations must be tested for geometric compatibility. In Figure 9, ray SE satisfies the test. Not more than one pavement reflection is possible.

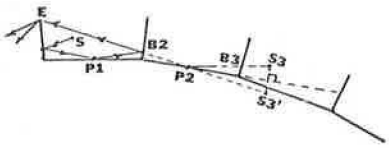

FIGURE 9 Tilted barriers with pavement reflection.

Finite Barrier Length Effects

None of the foregoing configurations takes account of the finite length of the barriers and their images. Figure 10 is a plan view of the base locations of the barrier pair, a single lane, and their images. Four principal cases can be identified:

- Case 1: Line of sight acoustic propagation between the source position and the receiver. This case is applicable only for sources in Zone 1.
- Case 2: Acoustic path with reflection off Barrier 2 but without encounter with Barrier 1. This case is applicable only for sources in Zone 2.
- Case 3: Acoustic path leading to diffraction at the top edge of Barrier 1 with subsequent paths to the receiver. The source can be real (Zone 1) or virtual (all other zones).
- Case 4: None of the above; the path is not viable.

PROGRAM TREATMENT

A critical step in this program is the separation of the speed, volume, and source characteristics from the barrier, highway, terrain, and atmospheric characteristics that could then be lumped into an insertion loss function H. The program is thus able to compute the total acoustic energy at a receiver as a product of the acoustic energy determined as if all the sources were in free space and a term that includes all modifications due to transmission loss from ground and pavement reflection, barrier reflection and diffraction, atmospheric absorption, and so on.

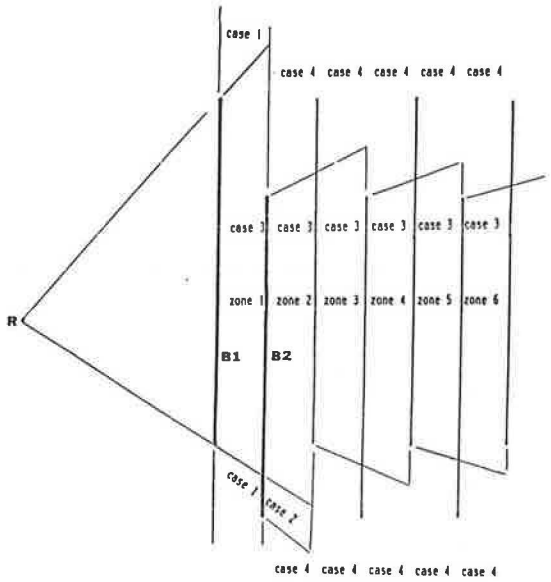

FIGURE 10 Case structure for finite barrier length.

Traffic Flow Integration

To sum the noise contributions of several streams of traffic, each with its own insertion losses due to various diffraction and absorption effect, a single source is considered, moving at constant speed along a representative path. That intensity can be expressed in the form

$$I_n = \frac{Q H_n}{4 \Pi r_n^2} \tag{17}$$

where Q is the strength of the source, r_n is the unobstructed distance from source to receiver, and H_n is the correction factor, without which the expression would represent the free field intensity. Note that 10 log (H_n) is the insertion loss for the path. The source strength can be defined in terms of the free field intensity I_0 and the standard distance r_0 (50 ft):

$$I_0 = \frac{Q}{4 \Pi r_0^2} \tag{18}$$

The total acoustic energy E accumulated at the receiver during a pass by is

$$E = \sum_n I_n \Delta t_n = \frac{1}{S} \sum_n I_n \Delta Y_n \tag{19}$$

where

S = source speed,
Y_n = Y coordinate of source, and
Δn = change in Y coordinate in time Δt_n.

Y_n can be expressed in terms of the X coordinate of the source and the angle θ_n between the X axis and the horizontal projection of the ray path (5), to obtain

$$E = \frac{I_0 r_0^2}{S X_{rs}} \sum H_n \Delta \theta_n \quad (20)$$

It should be noted that the $\Delta\theta$ increments add up to 180 degrees for the case of the infinitely long source path or to any other smaller value for the source path of finite length. Next, the equivalent intensity I_{eq} is obtained by dividing the pass-by energy E by the time between passes by $1/V$, where V is the traffic volume in vehicles per hour:

$$I_{eq} = \frac{I_0 r_0^2 V}{S X_{rs}} \sum H_n \Delta \theta_n \quad (21)$$

This expression must be generalized by incorporating the following extended definitions:

I_0 = I_0 (NV,NST,OCT),
V = VOL(NLAN,NV),
S = SPD(NLAN,NV) * 5280,
NV = vehicle type number (1 to NNV),
NST = source type number (1 to NNST),
NLAN = lane number (1 to NNLAN),
NZ = zone number (1 to NNZ),
OCT = octave band number (1 to 8), and
NR = receiver number (1 to NNR).

The source intensity is redefined in terms of the source strength:

$$I_0 \text{ (NV,NST,OCT)} = 10^{[\text{LS(NST,NV,OCT)}-55)/10]} * I_{REF} \quad (22)$$

where LS is the free field octave band sound pressure level at 50 ft. (The 55-dB term is arbitrary and is used to ease number handling. It is restored at final output.) The equivalent intensity corresponding to all zones, lanes, vehicle types, source types, and stations is found by summing to obtain a result EDEQ(OCT,NR), which depends only on frequency and receiver number. Note that no correction term is included for statistical variation of the source strength LS. The *A*-weighted equivalent intensity EDEQA(OCT,NR) is then obtained by using the AWT(OCT) corrections. EDEQ and EDEQA are printed out as the logarithms LEQ and LEQA. Finally, the LEQA are summed over the octave bands and printed out as the logarithm to obtain the *A*-weighted L_{eq}, LEQAWT(NR).

Program Input Parameters

The user can obtain an overview of the computer programs by examining the input parameters. The user has the option of specifying the following:

- Receiver number (NNR ≤ 20),
- Number of lanes (NNLAN ≤ 10),
- Number of source types (NNST ≤ 3/vehicle type),
- Number of vehicle types (NNV ≤ 5),
- Number of reflection zones (NNZ ≤ 6),
- Shoulder treatment (SHFLAG = 0 or 1; soft or hard),
- Lane dimensions (width of traffic lanes, median, shoulders, terrain strips, and *Y*-coordinates of pavement segment end points),
- Highway surface flow resistances (terrain, shoulders, median, and pavement),
- Barrier endpoints *X*1, *Y*1 to *X*4, *Y*4 (note that *X*1 = *X*2, *X*3 = *X*4),
- Barrier tilt angles (in degrees) and barrier panel widths (by barrier, panel),
- Barrier impedance or reflection coefficient (by barrier, panel, octave),
- Vehicle volume (per hour by lane and vehicle type),
- Vehicle speed (in mph, by lane and vehicle type),
- Source height (by vehicle type and source type),
- Source strength (free field at 50 ft, by vehicle type, source type, and octave band),
- Receiver parameters (coordinates *X*, *Y*, *Z*, ground elevation Z_g, and local ground flow resistance SIGG, for each receiver), and
- Atmospheric absorption (in dB/1,000 ft, each octave).

The parameters are entered by means of a special file that serves as an input template. Details and directions for using the template and the program will be found elsewhere (*30*).

ILLUSTRATIVE NUMERICAL RESULTS

It is interesting to examine the numerical behavior that is the result of the current work. Two kinds of behavior are examined below. The first is the influence of the ground interaction on numerical results without barrier complications, and the second is the behavior with barrier effects.

Figure 11 represents the excess attenuation (the field at the receiver in decibels minus the field that would exist there if the sound propagation were purely spherical, with no reflections, ground interaction or atmospheric attenuation, with sign changed) at various distances from a point source. The point source and the receiver are both at an elevation of 5 ft. The source is located over a hard pavement (flow resistance = 1.0 * 10^{10} N-sec/m^4), and the receiver is over soft soil (flow resistance = 3.0 * 10^5 N-sec/m^4). The strong ground effects are readily apparent and are characteristic of published results. Strong attenuation at grazing incidence can be seen. For example, at 500 Hz the excess attenuation per doubling of distance (dB/dd) varies from 4.4 in the interval 125–250 ft to 6.3 at 800–1600 ft. Note that these figures correspond to total values of 10.4 and 12.4 db/dd when they are combined with

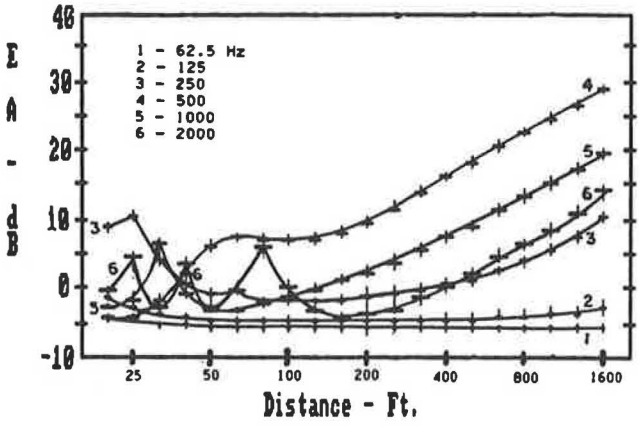

FIGURE 11 Excess attenuation for point source.

spherical spreading. The attenuation at 4 and 8 Khz (not plotted because the resulting figure would be confusing) is found to increase monotonically with distance, primarily because of atmospheric attenuation.

Figure 12 shows the situation for a line source and a receiver, both at elevation of 5 ft, with hard pavement and soft wayside. By comparison with Figure 11, it can be seen that the oscillations are damped by the effect of the line source averaging mechanism, but otherwise the curves have the same form. The excess attenuation per doubling of distance at 500 Hz again increases with distance, averaging 4.2 dB/dd between 125 and 250 ft, and 6.4 dB/dd between 800 and 1,600 ft, in marked contrast with the usual assumption of 1.5 dB/dd for soft ground in the FHWA and STAMINA models.

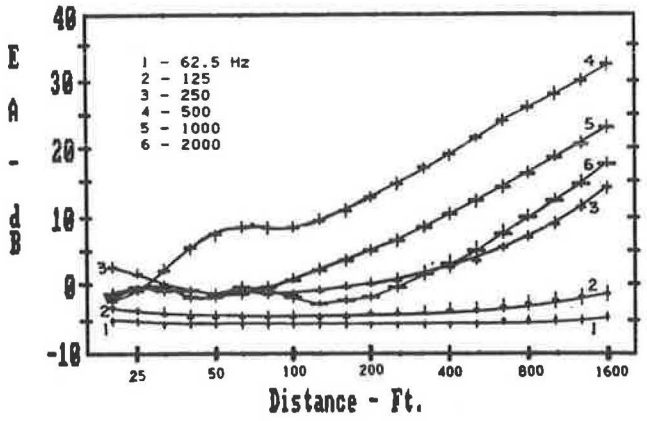

FIGURE 12 Excess attenuation for line source.

The next group of calculations is for the purpose of comparing the *A*-weighted SPL at a receiver caused by a line source in the presence of a single barrier with that due to several different coupled vertical barrier configurations. Figure 13 is for a 150-ft-wide roadway between 15-ft-wide barriers with a line source in the middle. The source heights range from 0.25 to 16 ft above the pavement. Although the tire spectrum that was used is applicable only at 0.25 ft, it was used for all elevations to simplify comparison. The receiver is located over hard terrain at a distance of 150 ft from the barrier base.

The solid curves were generated with program BarrierX (i.e., with Equation 14) for perfectly reflective barriers. The three curves in this group show the cumulative degradation effect of one, two, and five successive barrier reflections (corresponding to the effect of the five image roads) as compared to the case of the single barrier that has no barrier reflection paths. The degradation jumps most markedly as a result of the first barrier reflection, with reduced effect for subsequent reflections. The degradation from elevated sources is small. This is a result of the approach of the specular ray barrier crossing to the barrier edge, the approach of $v_3 - \hat{v}$ to zero in Equation 14, and the consequent decrease of Γ_e to half of Γ_3, with the corresponding reduction of the reflected intensity to 1/4 of what it would be from an infinite wall. Because multiply reflected rays from elevated sources are repeatedly attenuated in this way, they contribute less significantly. This attenuation mechanism also comes into play for some (but not all) of the multiple reflections from less elevated sources as the Fresnel half-width becomes large. This follows from Equation 15 or 16.

The dotted curves were generated by using Barrier for the same geometry and are based on geometric ray optics with local reflection coefficients (equal to unity for perfect reflection) at the specular reflection point. These curves change slowly with source elevation until the barrier height is exceeded, at which point the degradation drops abruptly. It will be noted that the neglect of (reflective) diffraction causes an overly pessimistic prediction of barrier performance.

Figure 14 presents a comparison of several barrier treatments with the single (no reflection) barrier case. The dotted curve labeled "1 - No Treatment" corresponds to the multiple (five) reflection result in Figure 13. The curve labeled "2 - Tilt 1°" displays a benefit of about 1 dB for sources below 5 ft elevation and a loss for elevated sources. A tilt angle of 3 degrees (Curve 3) displays improvement over the whole range of source heights, and a tilt angle of 5 degrees (Curve 4) displays (almost) total recovery for sources under 8 ft. Treatment of all panels with commercial fiberglass facing, with normalized impedance as presented in Table 1, resulted in Curve 5, "Absorption (All Panels)," which is everywhere within 1 dB of the single-barrier (zero-degradation) case.

One of the possible barrier treatments for investigation was that of absorptive treatment of a horizontal strip of the wall instead of the whole surface. Accordingly, in Figure 15 a comparison is made of the baseline (Curve 1, "No Treatment") and Curve 4, "Absorption (All)," both identical with those in

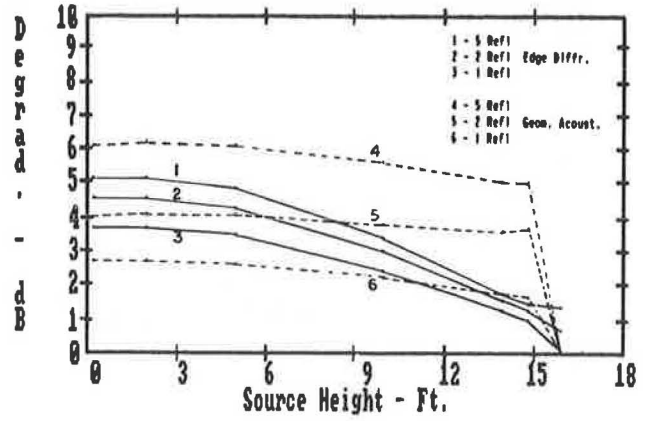

FIGURE 13 Barrier degradation: zone contributions.

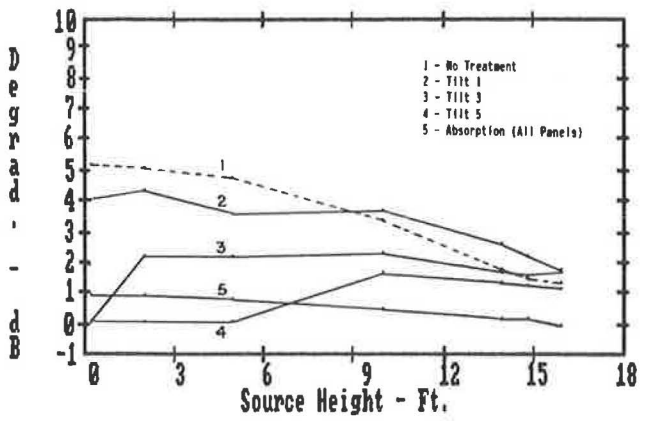

FIGURE 14 Comparison of tilt and absorption.

TABLE 1 NORMALIZED IMPEDANCE OF COMMERCIAL FIBERGLASS FACING

	Frequency							
	62.5	125	250	500	1000	2000	4000	8000
Real	3.51*	3.51	2.01	2.53	2.50	2.77	4.24	4.24*
Imag.	−4.85*	−4.85	−3.09	−0.69	−0.32	0.63	1.45	1.45*
Alpha	0.24	0.33	0.43	0.78	0.83	0.76	0.51	0.30

NOTE: Highway Barrier Test Material 3-in. 733, faced with 1.5 mi poly, hard backing.
*Estimated values.

Figure 14, with cases of partial barrier coverage. Curve 2, "Absorption (Top)," shows improvement over the "No Treatment" case for for elevated source positions, while Curve 3, "Absorption (Bottom)," shows improvement for lower sources. This behavior is physically reasonable but may be inadequate as a practical matter.

As noted, the results described are for a roadway with 150 ft between barriers. In Figure 16, it can be observed that degradation for a narrow road with 60 ft between barriers becomes more severe. Curve 2 is the "No Treatment" case, which compares unfavorably with the corresponding Curve 1 for the 150-ft roadway. A tilt of 5 degrees shows much less improvement than was obtained on the wider roadway and seems rather to have the same general behavior as the 1-degree tilt in Figure 14. A much larger tilt angle would be needed to recover effective barrier performance. Curve 4 is for a vertical wall on the side of the road nearer the receiver and a tilt of 20 degrees for the opposite wall. Full recovery can be observed except for extremely elevated sources, where the loss is less than 1 dB. Finally, a full absorptive treatment (Curve 5) is seen to restore practically full barrier performance.

Comparisons made with some of the Ullrich scale model insertion loss data reproduced by Bowlby et al. (*1*, Figure 3) for a depressed highway were not satisfactory for insertion loss but were good for degradation. The occurrence of Ullrich's barrier degradation of ~8 dB when the single barrier is replaced by the double wall is consistent with Curve 2 of Figure 16. The smaller width (52.5 ft) of the Ullrich model would result in slightly higher degradation than that for the 60-ft road shown in Figure 16. Curve 4 of Figure 16 (20-degree tilt) indicates almost no loss, whereas the scale model (25-degree tilt) shows

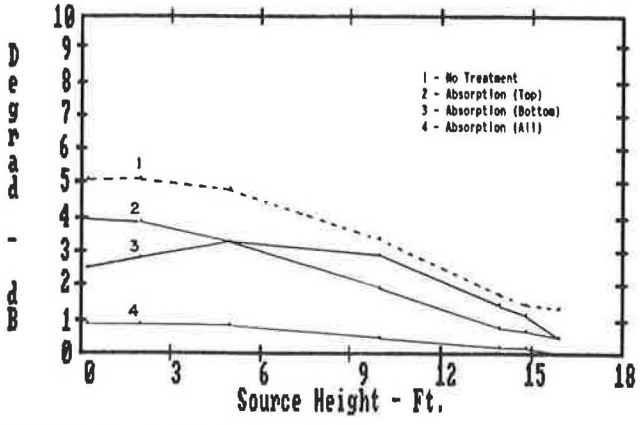

FIGURE 15 Partial absorptive treatment.

1–2-dB losses. Failure to get good agreement for insertion loss may be due to lack of detailed data on acoustic treatment of the (important) edge shoulder region of the depressed highway model.

Comparison with the scale model octave band insertion loss degradation measured by Hutchins (*1*, Table 7) shows that BarrierX loss predictions are generally higher by ~2–4 dB, but no clear trend is noticeable in the comparisons. Further study of these cases and of any other available experimental data would be desirable.

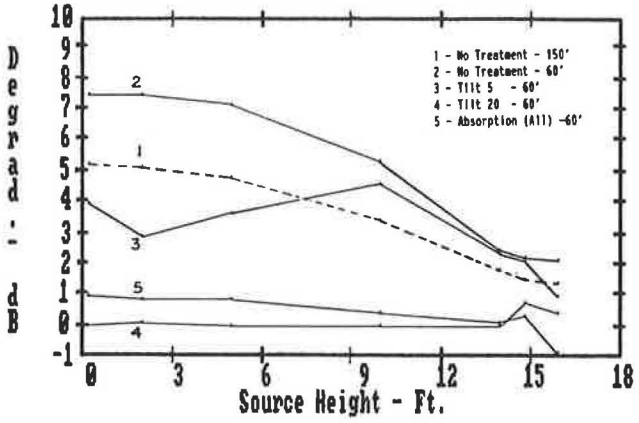

FIGURE 16 Effect of road width.

CONCLUSIONS AND RECOMMENDATIONS

A program has been constructed that can estimate the barrier insertion loss of parallel barriers that are tilted, or coated with acoustically absorbing materials, or both. The program takes into account some of the limitations of ray theory that are relevant when the acoustic wavelength is not small compared to the barrier height or to the width of the absorptive panels. This physical acoustics treatment is strictly valid only for the first barrier reflection and is only a reasonable approximation thereafter.

Predictions for degradation due to multiple reflections made with the physical acoustics program (BarrierX) are not as pessimistic as those made with the geometric acoustics program (Barrier). This decrease in degradation appears to be reasonable if the decreased effective reflectivity of a barrier when the Fresnel half-width becomes small compared to the distance from the specular reflection point to the barrier edge is considered.

Barrier tilt was found to be effective as a method of counteracting the degradation due to multiple reflection. Tilt

angles as small as 3 degrees were found to be effective for wide roadways (150 ft between barriers), and larger values (10 to 15 degrees) are needed for narrow roadways (60 ft between barriers).

Computations made to compare predictions from available scale model experiments reported in the literature show common trends. More experimental data are needed for validation of the program and for testing of confidence.

The program running time is 20 sec on a 6-MHz personal computer (PC) for the baseline case of one receiver, one zone, one lane, one vehicle type, and one source type. Total running time is then roughly proportional to the number of receivers, zones, and so on. Execution on a PC is convenient for exploring trends, but exercise of the program with repeated complex traffic configurations would probably be more convenient on a faster machine.

REFERENCES

1. W. Bowlby, L. F. Cohn, and R. A. Harris. A Review of Studies of Insertion Loss Degradation for Parallel Barriers. *Noise Control Engineering*, Vol. 28, No. 2, March–April 1987, pp. 40–54.
2. W. Bowlby and L. F. Cohn. A Model for Insertion Loss Degradation for Parallel Highway Noise Barriers. *Journal of the Acoustical Society of America*, Vol. 80, Sept. 1986, pp. 855–868.
3. J. J. Hajek. Effects of Parallel Highway Noise Barriers. In *Transportation Research Record 937*, TRB, National Research Council, Washington, D.C., 1983, pp. 45–52.
4. D. A. Hutchins, H. W. Jones, B. Paterson, and L. T. Russell. Studies of Parallel Barrier Performance by Acoustical Modeling. *Journal of the Acoustical Society of America*, Vol. 77, 1985, pp. 536–546.
5. D. R. Pejaver and J. R. Shadley. *A Study of Multiple Reflection in Walled Highways and Tunnels*. Rep. DOT-FH-11-8287. FHWA, U.S. Department of Transportation, 1976.
6. H. Legillon. Les Ecrans Absorbants en Bordure de Routes: Utilité et Caractérisation. *Bulletin de Liaison de la Laboratoire des Ponts et Chaussées*, Vol. 96, 1978, pp. 33–39.
7. W. Bowlby and L. F. Cohn. IMAGE-3: Computer-Aided Design for Parallel Highway Noise Barriers. In *Transportation Research Record 933*, TRB, National Research Council, Washington, D.C., 1983, pp. 52–62.
8. W. Bowlby, J. Higgins, and J. Reagan. *Noise Barrier Cost Reduction Procedure, STAMINA 2.0/OPTIMA: Users Manual*. Rep. FHWA-DP-58-1, April 1982.
9. S. Slutsky and H. L. Bertoni. *Parallel Noise Barrier Prediction Procedure Report 1: Description and Analysis of Tilted Absorptive Barriers*. U.S. Department of Transportation, June 1987.
10. B. B. Baker and E. T.Copson. *The Mathematical Theory of Huygens' Principle*. Oxford at the Clarendon Press, London, 1950, pp. 72–74.
11. A. Sommerfeld. Uber die Ausbreitung der Wellen in der Drahtlosen Telegraphie. *Annalen der Physik*, Vol. 28, 1909, p. 665 and Vol. 81, 1935, p. 1135.
12. H. Weyl. Ausbreitung elektromagnetischer Wellen über einem ebenen Leiter. *Annalen der Physik*, Vol. 62, 1920, p. 482.
13. B. Van Der Pol. *Physica*, Vol. 2, 1935, p. 843.
14. C. F. Chien and W. W. Soroka. Sound Propagation Along an Impedance Plane. *Journal of Sound and Vibration*, Vol. 43, 1975, pp. 9–20.
15. C. F. Chien and W. W. Soroka. A Note on the Calculation of Sound Propagation Along an Impedance Plane. *Journal of Sound and Vibration*, Vol. 69, 1980, pp. 340–343.
16. K. Attenborough, S. I. Hayek, and J. M. Lawther. Propagation Above A Porous Half-Space. *Journal of the Acoustical Society of America*, Vol. 68, 1980, pp. 1493–1501.
17. K. B. Rasmussen. *Sound Propagation Over Level Terrain*. Report 33. Acoustics Laboratory, Technical University of Denmark, 1982.
18. K. B. Rasmussen. Propagation of Road Traffic Noise Over Grass Covered Ground. *Journal of Sound and Vibration*, Vol. 78, 1981, pp. 247–255.
19. D. Habault and G. Corsain. Identification of Acoustical Properties of a Ground Surface. *Journal of Sound and Vibration*, Vol. 100, 1985, pp. 169–180.
20. P. M. Morse. *Vibration and Sound*. McGraw-Hill, New York, 1948, pp. 363–368.
21. M. E. Delaney and E. N. Bazley. Acoustical Properties of Fibrous Absorbent Materials. *Applied Acoustics*, Vol. 3, 1970, p. 1.
22. K. Attenborough. Acoustical Impedance Models for Outdoor Ground Surfaces. *Journal of Sound and Vibration*, Vol. 99, 1985, pp. 521–544.
23. K. Attenborough. Predicted Ground Effect For Highway Noise. *Journal of Sound and Vibration*, Vol. 81, 1982, pp. 413–424.
24. T. F. W. Embleton. Sound Propagation Outdoors. *Noise Control Engineering*, Vol. 18, No. 1, 1982, p. 33.
25. K. B. Rasmussen. Propagation of Road Traffic Noise Over Level Terrain. *Journal of Sound and Vibration*, Vol. 82, 1982, pp. 51–61.
26. *American National Standard Method for the Calculation of the Absorption of Sound by the Atmosphere*. Report ANSI S1.26-1978. Acoustical Society of America, New York, 1978.
27. J. E. Piercy and T. F. W. Embleton. *Handbook of Noise Control* (C. M. Harris, ed.), McGraw-Hill, New York, 1979, pp. 3–10.
28. J. E. Piercy, T. F. W. Embleton, and L. C. Sutherland. Review of Noise Propagation in the Atmosphere. *Journal of the Acoustical Society of America*, Vol. 61, 1977, pp. 1403–1418.
29. L. Cremer and H. A. Muller. *Principles and Applications of Room Acoustics* (T. J. Schultz, transl.), Vol 1, p. 40, Applied Science Publishers, 1982 pp. 105–116.
30. S. Slutsky. *Parallel Noise Barrier Prediction Procedure—Report 2: User's Manual*. U.S. Department of Transportation, June 1987.

Publication of this paper sponsored by Committee on Transportation-Related Noise and Vibration.

Tilted Parallel Barrier Program: Application and Verification

VAN M. LEE, ROBERT A. MICHALOVE, AND SIMON SLUTSKY

In an increasing number of situations on the U.S. urban and suburban highway system, noise barriers are being considered to protect residences on both sides of a roadway. The scheme of two vertical parallel barrier walls forms the parallel barrier problem. In this case, in addition to the sound waves that reach the receiver by diffraction over the near barrier, sound waves caused by complex pavement-barrier-ground reflection and diffraction mechanisms can reach the receiver, thus degrading the effectiveness of the near barrier. In this paper, the results of the first application of the Tilted Parallel Barrier Program to a highway project are presented, along with attempts to verify aspects of the model through comparisons with data that exist in the literature. The model provides excellent agreement in the classical problem of an impedance boundary. It also meets reasonable expectations for parallel vertical, tilted parallel, and parallel absorptive barrier performance when a frequency-dependent optimum design can be selected.

The current version of the FHWA Highway Traffic Noise Prediction Model (STAMINA 2.0) is a single-screen–type barrier diffraction model that is independent of ground impedance. Ground effects are separately handled through site "decay" input parameters (alpha factors) and the use of additional absorbing ground strips representing foliage or shrubbery. Provisions are made in STAMINA 2.0 to ignore the ground effects whenever a barrier is encountered (the alpha value is reset to 0.0). Whenever more than one barrier is encountered, the most significant barrier is retained in lieu of all other barriers, even though the diffracted reflection or reflected diffraction is computed by user-specified reflective barrier computations. The single-image nomogram method outlined in Section 4.3.7 of the FHWA *Noise Barrier Design Handbook* (*1*) includes consideration of the degradation in barrier performance for parallel barriers.

Given that the effective noise insertion loss of many practical barrier schemes is typically of the order of 5–10 dBA for receivers 100–200 ft away from the barriers, degradations of 3 dBA or more, as calculated by using the nomogram method for the first-order reflection diffraction, would significantly counteract the benefits of this abatement measure. It thus becomes essential to have a tool that will act as a better gauge of the degradations due to parallel barriers and explore the effectiveness of treatments such as absorption and tilting to mitigate the degradation.

V. M. Lee, Analysis and Computing, Inc., P.O. Box 234, Hicksville, N.Y. 11802. R. A. Michalove, Frederic R. Harris, Inc., 300 East 42nd St., New York, N.Y., 10017. S. Slutsky, Polytechnic Institute of New York, 333 Jay St., Brooklyn, N.Y. 11201.

The Tilted Parallel Barrier Program (TPBP), developed by Slutsky and Bertoni (*2*) under contracts to FHWA and the Transportation Systems Center (U.S. Department of Transportation), provides an investigative tool to study the complex problem of parallel tilted barriers on segmented impedance boundaries. In addition to accounting for the multiple reflection effect due to parallel barriers, as considered by previous parallel barrier models [e.g., Bowlby and Cohn (*3*), Hajek (*4*)], TPBP considers the effect of tilting on multiple reflections, the effect of ground as an impedance boundary, and the interaction effect of ground reflection and barrier diffraction. Furthermore, TPBP permits the segmentation to represent different types of surfaces, such as pavement, median strips, or grassland. This problem is called wave propagation over segmented impedance surfaces due to the additional complexity of diffraction by impedance discontinuities. Barriers with absorptive or impedance surfaces (up to three segments) can also be accommodated. The problem, which employs powerful mathematical and numerical techniques, has yet to be verified by either theoretical or experimental studies. In this paper, results of the first application of the TPBP to a highway project are presented, along with attempts to verify aspects of the model through comparison with existing data in the literature and with common sense expectations.

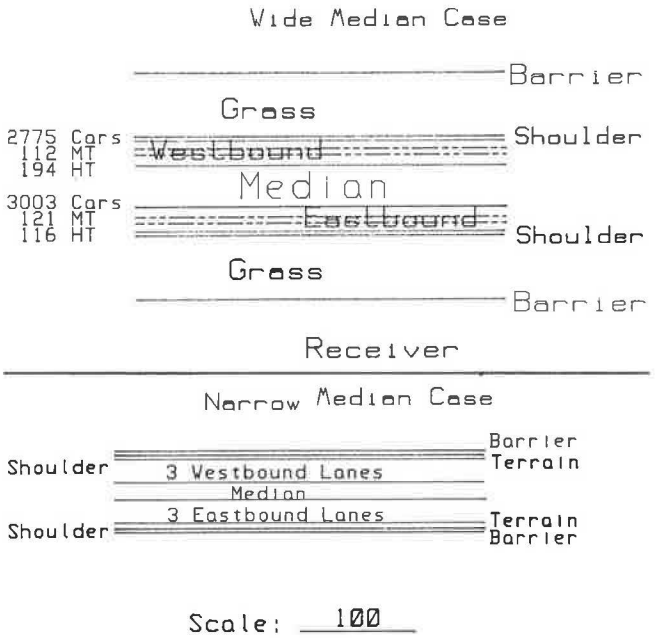

FIGURE 1 Typical roadway configuration.

APPLICATION

TPBP has been applied to a New York State Department of Transportation (NYSDOT) project on a section of the Long Island Expressway (LIE) in Suffolk County where parallel barriers are being considered to reduce the impact of noise on the adjacent residential development. The typical roadway configuration, consisting of six 10-ft lanes, a 60-ft median (including inside shoulders), a 5-ft outside shoulder on each side, and an 85-ft terrain strip between the shoulder and the right of way is shown in Figure 1, top. The barriers are located 150 ft from the roadway centerline. On this roadway, 6,321 vehicles per hour travel at 55 mph, with 3.7 percent medium trucks and 4.9 percent heavy trucks. A STAMINA 2.0/OPTIMA analysis (with alpha = 0.5) indicated that 15-ft barriers would be optimal and would reduce the noise level from ~70 dBA to 63 dBA at the closest residence, which is ~80 ft from the right of way. Use of the nomogram method indicates that a degradation of up to 3 dBA could be expected. This effect would severely reduce the benefits of the proposed noise barriers. It was clear that a more detailed analysis would be required to ascertain the parallel barrier effect and to study the effectiveness of absorptive barriers and tilted barriers.

The mathematical and numerical aspects of TPBP, which involve segmented impedance boundaries and edge diffractions, are new and previously untested. Because no experimen-

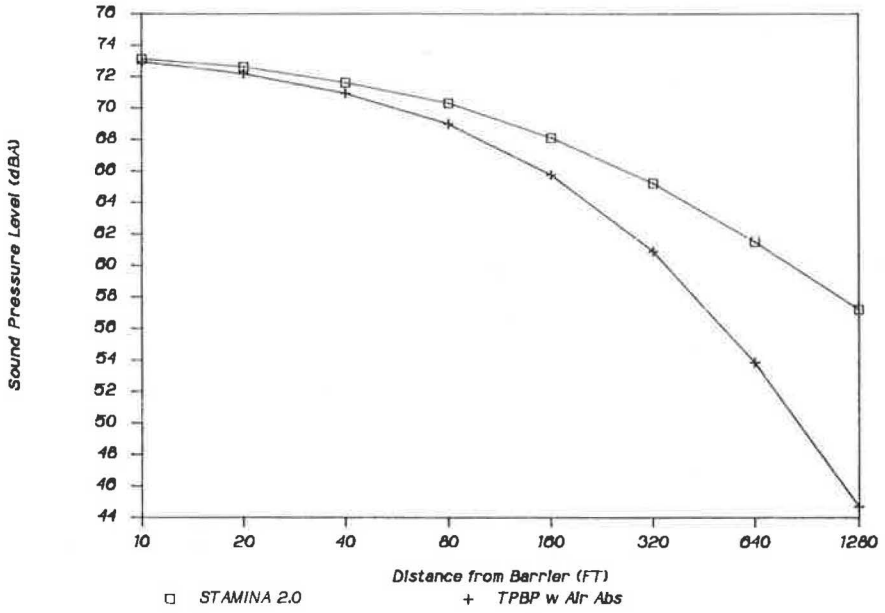

FIGURE 2 Comparison between TPBP and STAMINA 2.0 without barrier.

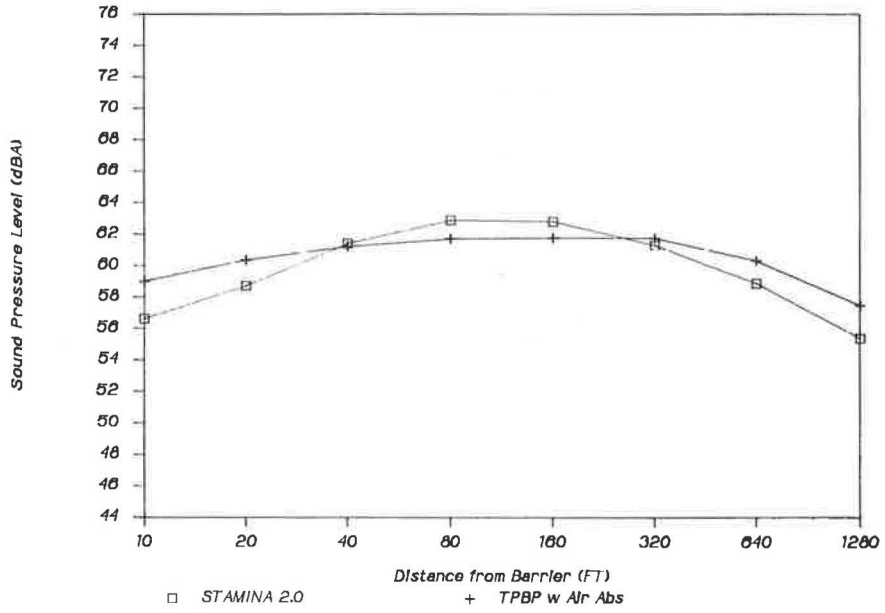

FIGURE 3 Comparison between TPBP and STAMINA 2.0 with a single 15-ft barrier.

tal data are yet available to verify this method, attempts were made to gauge the reasonableness of the model through its results in application. The STAMINA 2.0 model, which has been shown to provide excellent results for receivers in the range 100–250 ft from the edge of the roadway with a 4.5-dB decay rate on flat ground either with or without a single barrier, was used for comparison.

Results of the STAMINA 2.0/TPBP comparisons (with air absorption coefficients corresponding to 20°C and 60 percent relative humidity) are shown in Figures 2 and 3 for the typical LIE configuration, both without a barrier and with a single 15-ft barrier. In Figure 2 it can be seen that the TPBP distance drop-off rate approaches that of STAMINA 2.0 (4.5 dBA per distance doubling) at 100–250 ft away from the edge of the nearest lane (or 10–160 ft from the barrier location), increasing up to 9 dB per distance doubling at distances greater than 1,000 ft. From the literature on source decay characteristics (*5*) and ground effects on sound propagation over large distances (*6*), the TPBP drop-off curve is consistent with the expectation of an increasing ground attenuation rate as the distance increases. In Figure 3 it is shown that the TPBP results for a single barrier agree with the STAMINA 2.0 predictions to within 2 dBA over

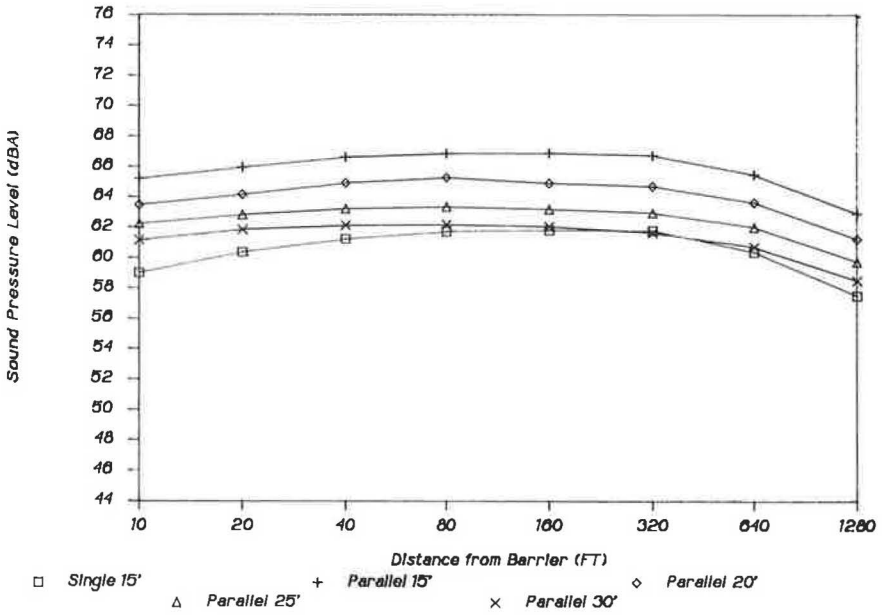

FIGURE 4 Parallel barrier effect including air absorption with increasing heights.

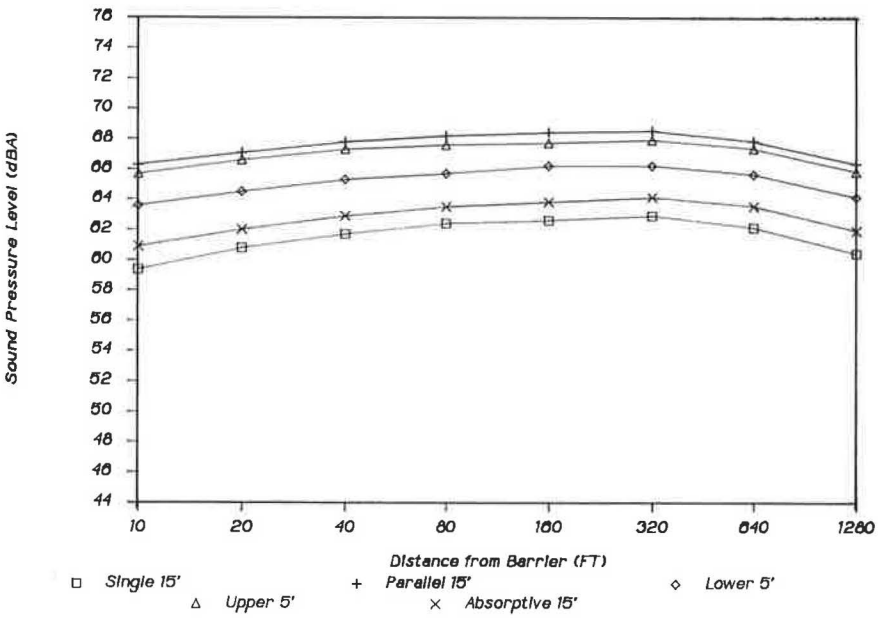

FIGURE 5 Parellel barrier effect not including air absorption with absorptive treatment.

the distance range of 40–320 ft from the barrier. It should be noted that the presence of the barrier raises the effective source height to the top edge of the barrier and thereby drastically diminishes the excess ground attenuation effect of the real source at grazing incidence.

When TPBP was applied to parallel barriers with absorption coefficients corresponding to plywood, the degradation averaged ~6 dB (Figure 4), compared to the nomogram calculation of a 3–4-dB increase for the first-order reflection-diffractions. When the result is compared to measurements reported in the literature [e.g., those by Ullrich (7)], the result was judged to be reasonable.

TPBP may be used as an investigative tool for evaluating various mitigation treatments. Results indicate that increasing the barrier height is not an effective means of compensating for the parallel barrier effect (Figure 4). Results for absorptive barriers (Figure 5) indicate that barriers with very high absorption coefficients (0.9) in the 500–1,000 Hz range could significantly reduce the degrading effect of vertical parallel barriers. Partial absorptive panels were also investigated, but they were found to be less satisfactory. In this particular case, the placement of the absorptive material on the lower third of the barrier was found to be more effective than placement on the upper third because of the large number of automobiles with

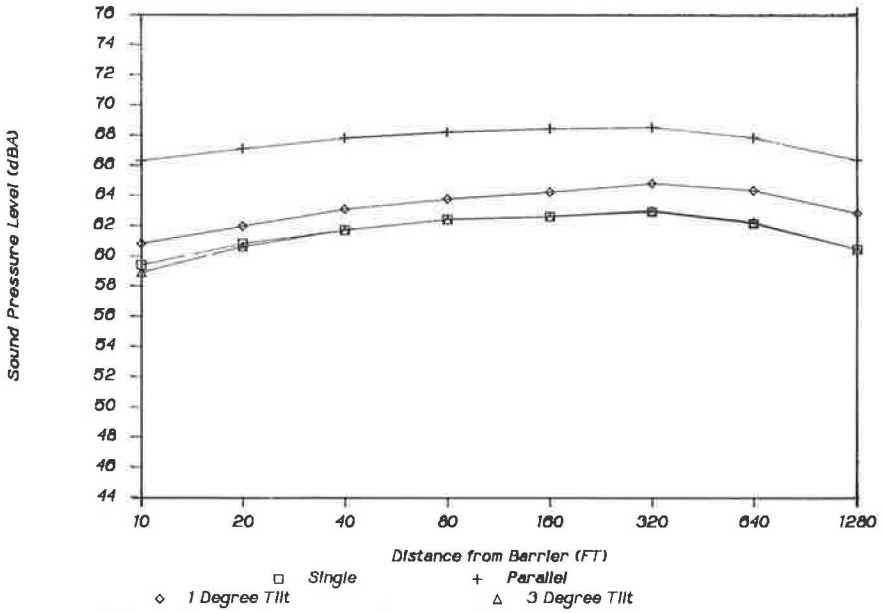

FIGURE 6 Parallel barrier effect not including air absorption with tilting.

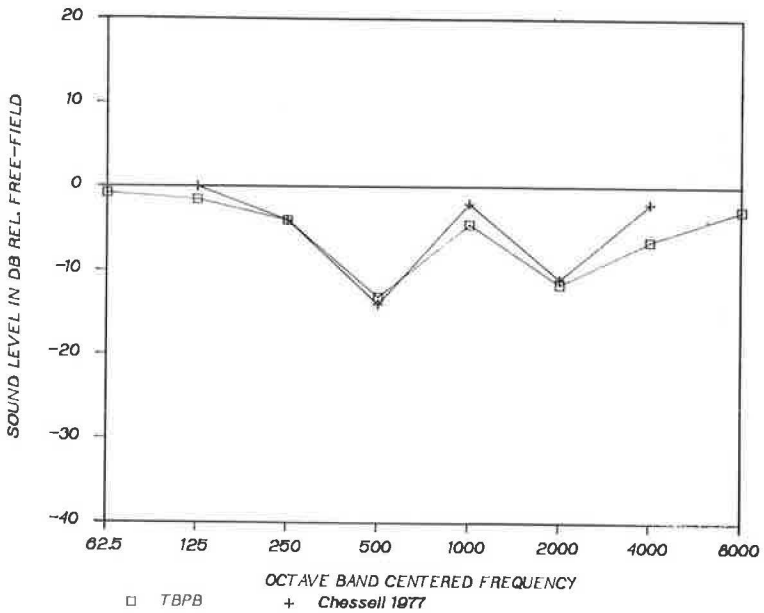

FIGURE 7 Comparison of ground effects.

low source heights. Tilting the barrier, however, is shown to be an extremely effective means of compensating for the parallel barrier degradation (Figure 6) . Results indicate that with a 3-degree tilt (i.e., the top of the barrier tilted away from the roadway), the degradation is totally counteracted. These results reflect the conclusions drawn in a study conducted by Legillon (*8*), who determined that for barrier height/roadway width ratios between 1:20 and 1:10, tilting is favored over absorption, whereas absorption is favored if the ratio is larger than 1:10 and single-barrier attenuation is below 12 dB.

In Figures 2 and 3, it can be seen that at distances greater than 320 ft from the barrier or 410 ft from the edge of the nearest lane, TPBP predicts that noise levels without the barrier will be lower than those with a single 15-ft barrier. This again demonstrates the significant ground attenuation around 500 Hz at grazing incidence, which can be greater than 15 dB at such distances (*6*). The presence of a 15-ft barrier greatly reduces the ground attenuation effect. The ground attenuation effect is greater than the barrier attenuation in this case, resulting in higher noise levels than without the barrier. The effect is accentuated in this particular application by the dominance of

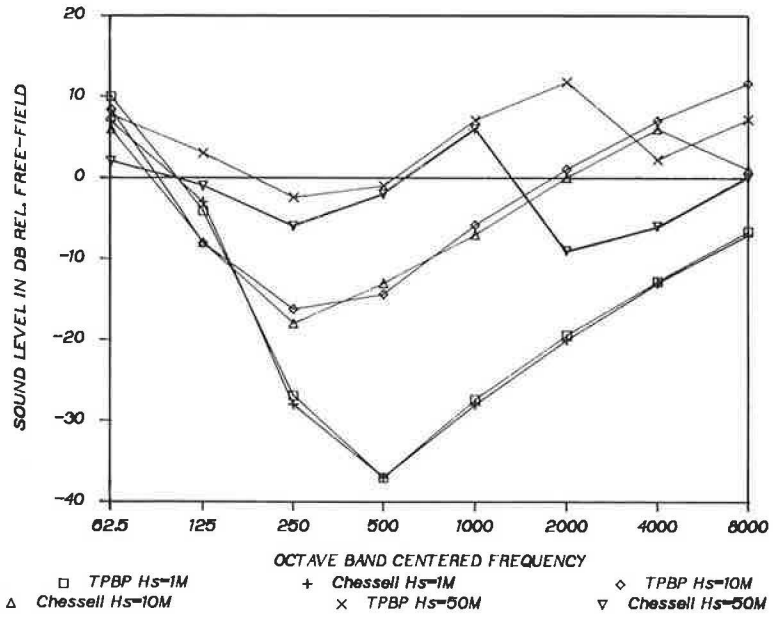

FIGURE 8 Effect of source heights.

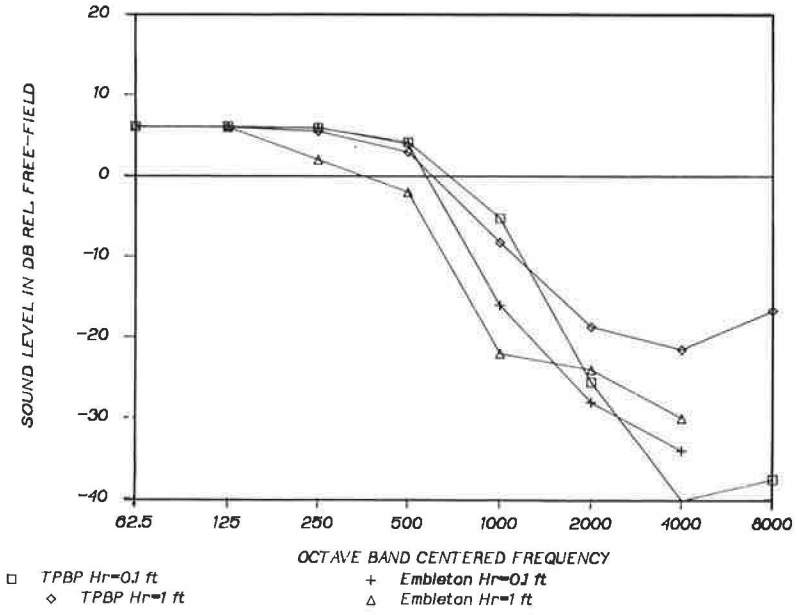

FIGURE 9 Ground effect on receiver heights (Hr=0.1 ft, Hr=1 ft).

automobile traffic with low source heights and the low diffractive loss due to the geometry.

GROUND AS AN IMPEDANCE BOUNDARY

The propagation of sound near the ground is a classic problem, the study of which dates back to Sommerfeld (*9*) in 1909. Even though the solution to this problem is well-known today, the numerical procedures that are applied vary greatly. Furthermore, a common reference describing the surface impedance of the ground is not universally used, making direct comparison with existing data difficult. Figures 7 and 8 present Chessell's data (*10*). Values corresponding to octave band–centered frequencies in Chessell's work are plotted for comparison. It can be seen that the agreement between ground treatment in TPBP and Chessell's work is excellent. In general, grazing incidence would generate much higher attenuations. It can be seen in Figure 8 that with grazing incidence, the ground attenuation at 500 Hz amounts to more than 35 dB. This result explains why it is possible to achieve higher noise levels with the erection of a barrier than without the barrier, if the very large ground attenuation for grazing incidence is lost through the replacement of a barrier.

An attempt was made to compare the TPBP results with work done by Embleton et al. (*11*), as shown in Figures 9 and 10. These figures show only the general agreement of the trend

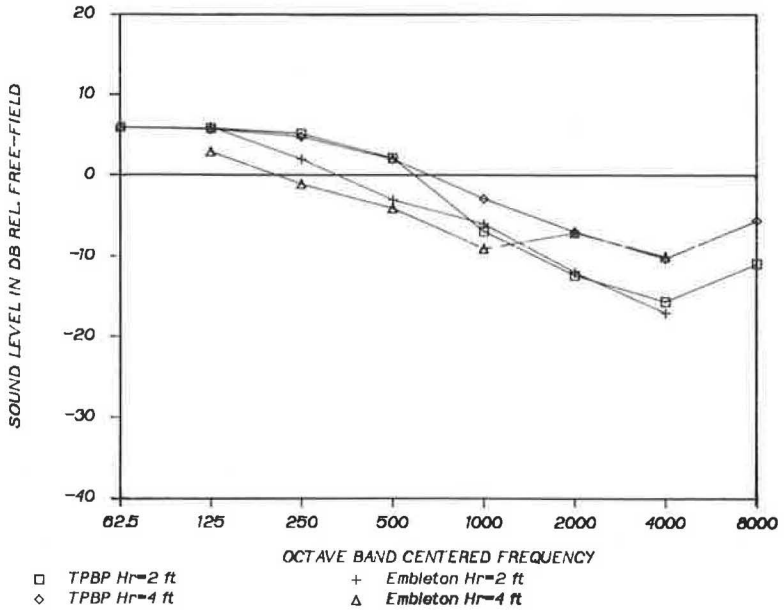

FIGURE 10 Ground effect on receiver heights (Hr=2 ft, Hr=4 ft).

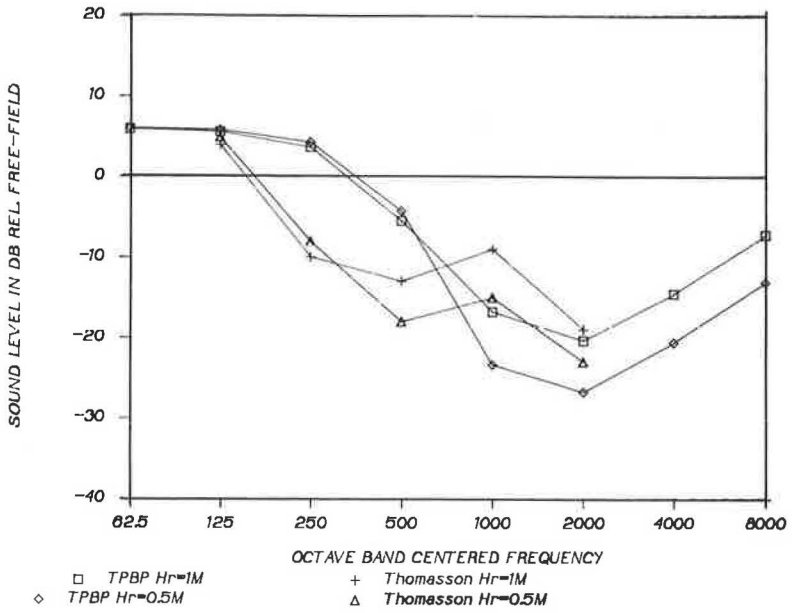

FIGURE 11 Ground effect on receiver heights (Hr=0.5 m, Hr=1 m).

because the surface impedance was assumed to match and because the original graph was highly erratic and difficult to read accurately.

BARRIER-GROUND INTERACTION AND TILTING

A comparison between TPBP and the approach of Thomasson (*12*) was attempted for the case of a simple screen over an impedance ground. Thomasson's technique involved a Kirchhoff-type approximation with a four-parameter model for the ground impedance. The impedance was thus not matched exactly, and the screen surface was assumed to be perfectly reflective. The results are shown in Figure 11. Even though the impedance parameters that Thomasson used were grossly approximated by using the single-parameter flow resistance model, the agreement in frequency of peak attenuation was surprisingly good.

TPBP was tested for reasonableness in handling various tilted barrier configurations. Intuition would indicate that continued tilting should eventually lead to a decrease in barrier effectiveness. TPBP was used to model a second typical section of the LIE project, where the roadway configuration consists of the same six 10-ft traffic lanes, a 20-ft median, a 5-ft outside paved shoulder, and a 5-ft terrain strip (Figure 1, bottom). The 10-ft barriers were located 50 ft from the roadway centerline.

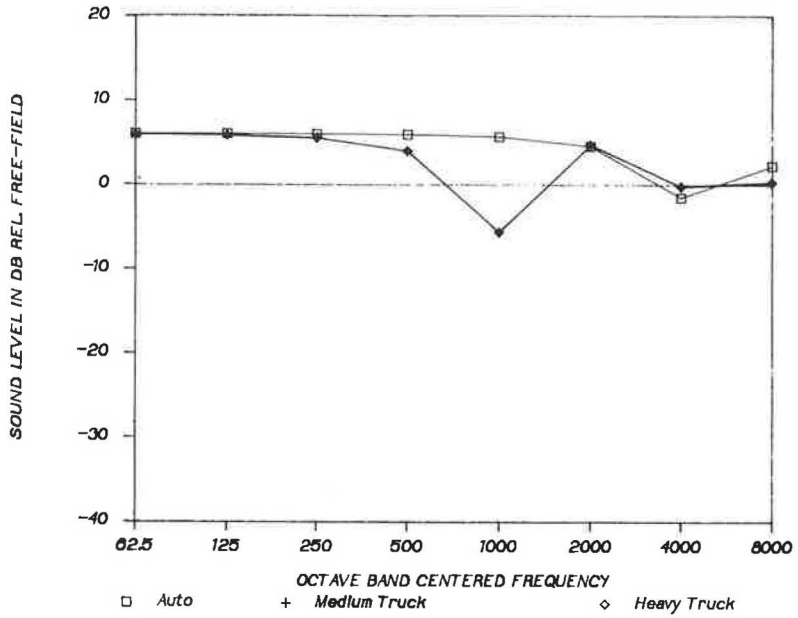

FIGURE 12 Adjustment for ground effect.

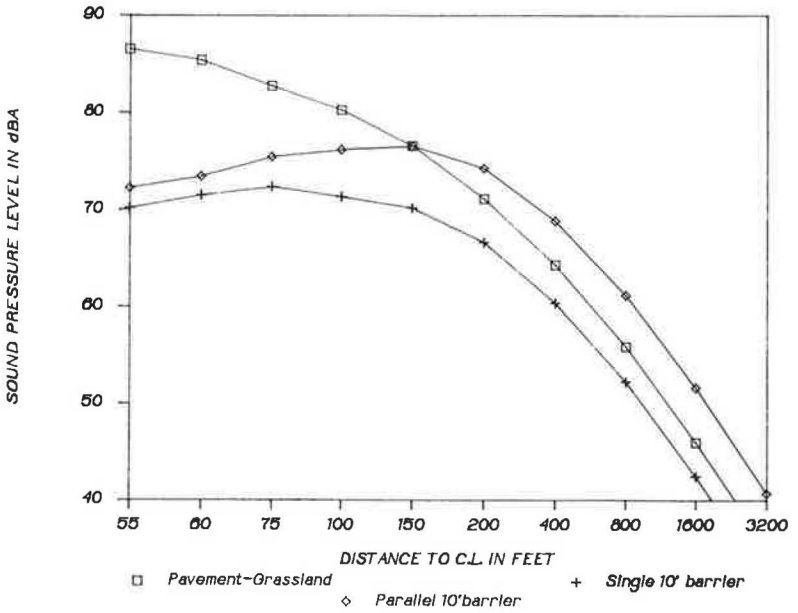

FIGURE 13 Parallel barriers on six-lane highway versus single/no barrier.

The STAMINA 2.0 source emission levels at 50 ft were first adjusted for the ground effect over a hard surface to arrive at the free-field levels for model input. The adjustments for the three vehicle types (automobile, medium trucks, and heavy trucks) are shown in Figure 12. The results of analysis on highway noise for the second roadway configuration are shown in Figures 13–16.

Under this geometry, with a barrier/roadway ratio of 1:10, the parallel barrier degradation is ~9 dBA, as illustrated in Figure 13. At 100 ft from the barrier, the noise level with parallel barriers is higher than without the barriers. Figure 14 shows that for this highway configuration, absorption and tilting are equally as effective in eliminating the parallel barrier effect. Nevertheless, a residual degradation of 2 dBA still remains, unlike the previous case (1:20 barrier/roadway ratio). In the previous case, tilting was more effective and no residual effect remained, as would be expected.

Figure 15 shows the results of tilting the 10-ft barriers further. It can be seen that the effect of tilting a few degrees (5 degrees) results in a drastic improvement in barrier performance and that further tilting quickly reverses the situation. In this case, the optimum tilting could easily be ascertained as being within a degree or two of 5 degrees. Figure 16 presents the same roadway configuration with a 20-ft barrier (barrier/

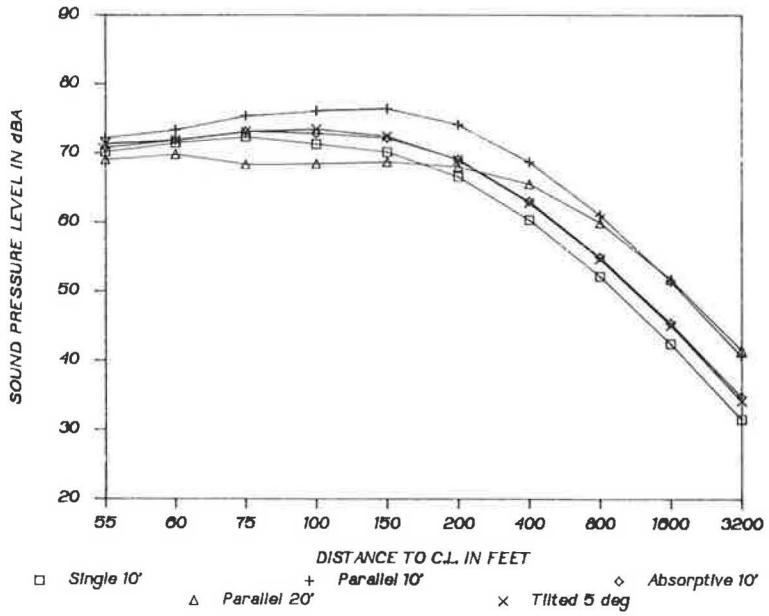

FIGURE 14 Parallel barriers on six-lane highway versus absorptive/tilted barrier.

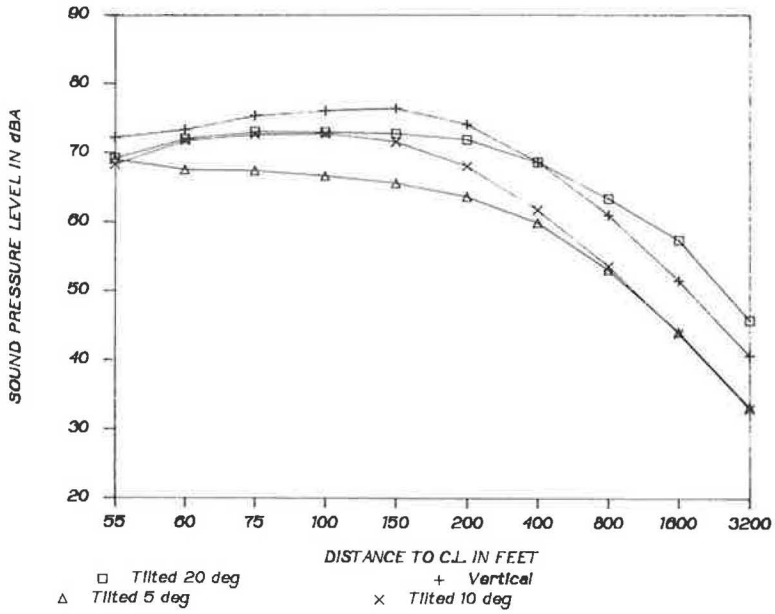

FIGURE 15 Parallel barriers on six-lane highway versus tilting.

roadway ratio of 1:5). It can be seen that for such a configuration, the tilt angles are no longer as critical as would be expected because of the limit of the noise source heights. It is also seen that absorptive treatment is slightly more effective for distances within 25 ft of the barrier, where the barrier insertion loss would be greater than 12 dB. These results are very much in line with Legillon's observations (*8*).

The joint effects of tilting and source height variations within parallel barriers are shown in Figures 17–19 for point source heights of 0.5, 2.3, and 8.0 ft, corresponding to automobiles, medium trucks, and heavy trucks. The barrier/roadway configuration was chosen to accentuate the effect (1:5 ratio, single 30-ft lane, 5-ft shoulders, and 5-ft terrain strips with 10-ft barriers) for a receiver 50 ft away from the roadway centerline and 5 ft above ground. The increase and then decrease in attenuation in the dominant 1-KHz band as the tilt angle increases is evident. These figures demonstrate that there is a frequency-dependent optimum tilt angle for a specific barrier/roadway configuration that can compensate for the parallel barrier degradation.

CONCLUSIONS

By applying the TPBP model to a highway design project and by comparing TPBP results with existing data in the literature for a point source above an impedance boundary and behind a

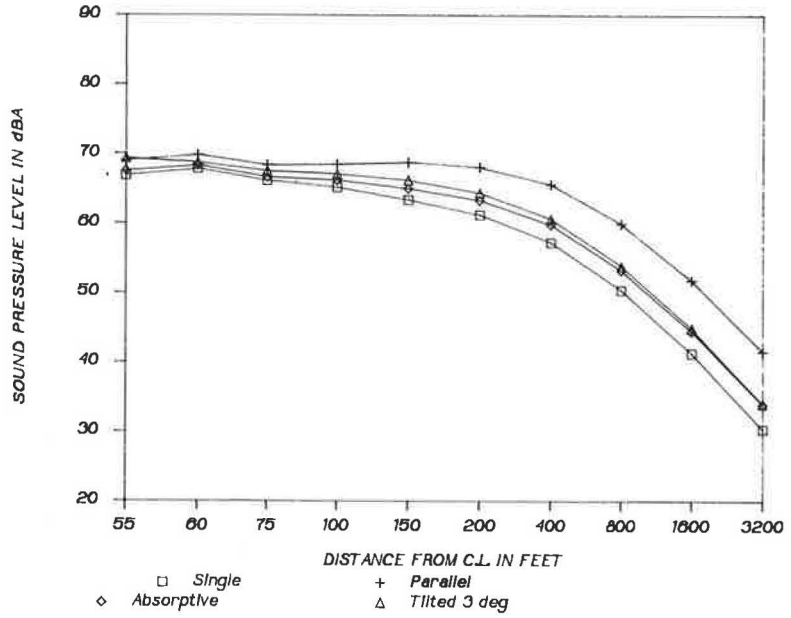

FIGURE 16 Tilted barrier on six-lane highway.

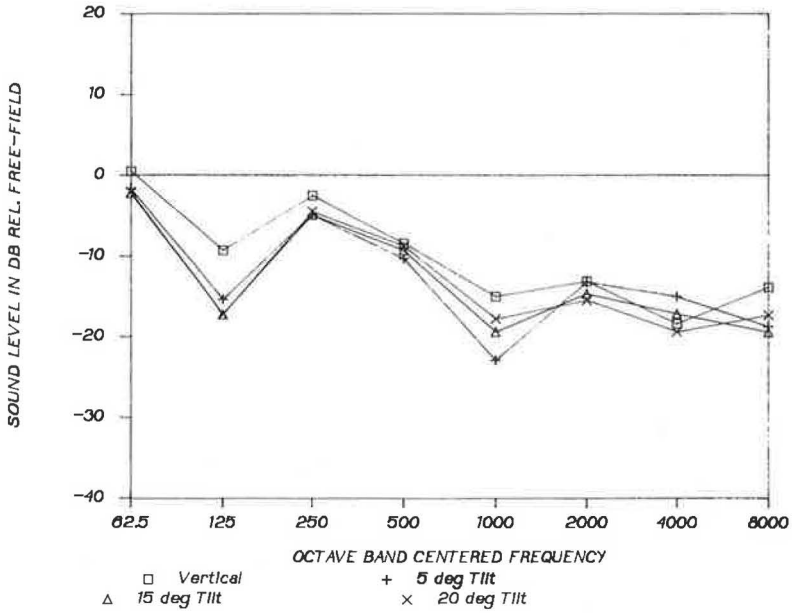

FIGURE 17 Effect of tilting for sources within parallel barriers (Hs=0.5).

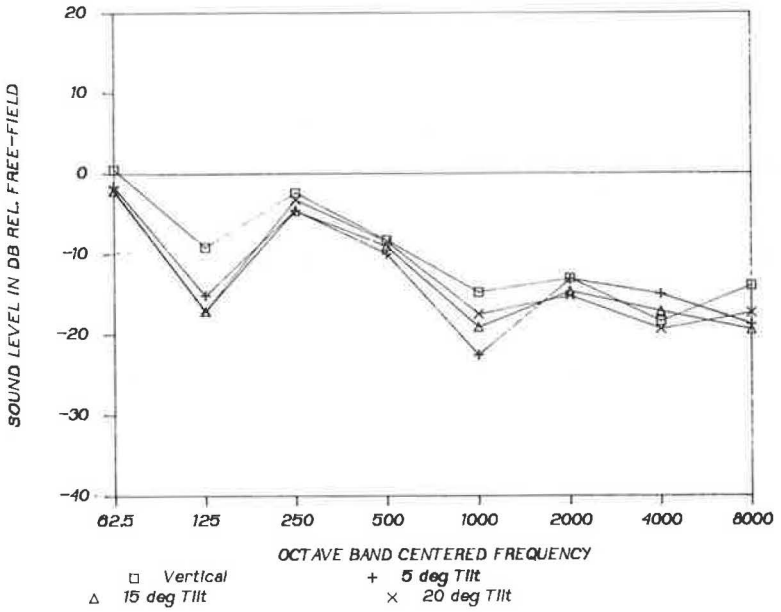

FIGURE 18 Effect of tilting for sources within parallel barriers (Hs=2.3).

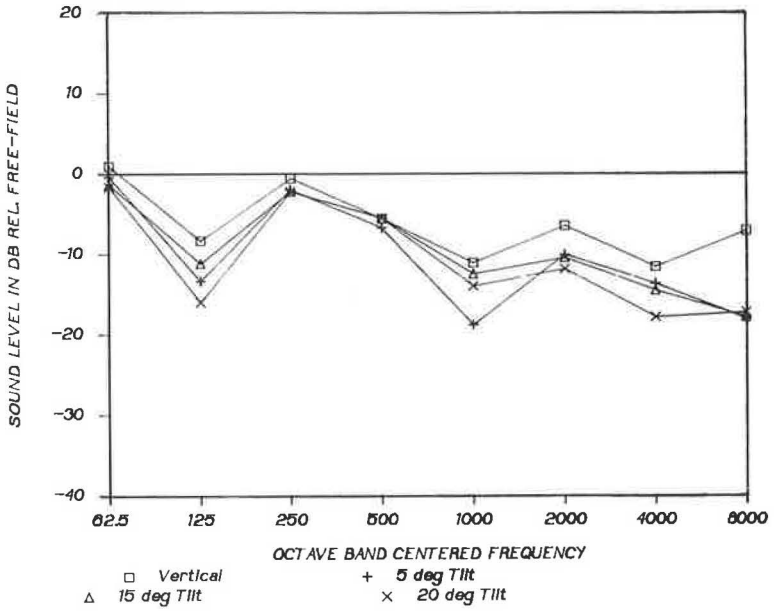

FIGURE 19 Effect of tilting for sources within parallel barriers (Hs=8.0).

screen above an impedance boundary, aspects of the TPBP model were explored and the model's performance was documented. The model provides excellent agreement for the classical problem of an impedance boundary. It also meets reasonable expectations for parallel vertical, tilted parallel, and absorptive parallel barrier performance where a frequency dependent optimum design can be selected for a specific barrier roadway/configuration. Because of the complexity of the problem, however, it must be pointed out that the results presented here, such as the critical tilt angle, must not be generalized to other roadway configurations but must be modeled on a site-specific basis. The TPBP model should be regarded as a useful investigative research tool to be applied meticulously to specific situations until the procedure is experimentally verified and qualified as an operational tool through field tests.

REFERENCES

1. M. A. Simpson. *Noise Barrier Design Handbook*. Report FHWA-RD-76-58. FHWA, U.S. Department of Transportation, 1976.
2. S. Slutsky and H. L. Bertoni. *Parallel Noise Barrier Prediction Procedure*. Transportation Research Center, U.S. Department of Transportation, 1987.

3. W. Bowlby and L. F. Cohn. A Model for Insertion Loss Degradation for Parallel Highway Noise Barriers. *Journal of the Acoustical Society of America,* Vol. 80, 1986, pp. 855–868.
4. J. J. Hajek. *The Effects of Parallel Highway Noise Barriers.* Report AE-82-03. Ontario Ministry of Transportation and Communication, Toronto, Canada, 1983.
5. R. B. Tatge. Noise Radiation by Plane Arrays of Incoherent Sources. *Journal of the Acoustical Society of America,* Vol. 52, 1972, pp. 732–736.
6. J. E. Piercy, T. F. W. Embleton, and L. C. Sutherland. Review of Noise Propagation in the Atmosphere. *Journal of the Acoustical Society of America,* Vol. 61, 1977, pp. 1403–1418.
7. W. Bowlby, L. F. Cohn, and R. A. Harris. A Review of Studies of Insertion Loss Degradation for Parallel Highway Noise Barriers. *Noise Control Engineering Journal,* March-April, 1987.
8. H. Legillon. Les Ecrans Absorbants en Bordure de Routes: Utilité et Caractérisation. *Bulletin de Liaison 96. Laboratoire des Ponts et Chaussées,* France, 1978, pp. 33–39.
9. A. N. Sommerfeld. Propagation of Waves in Wireless Telegraphy (originally in German). *Annals of Physics,* Vol. 28, 1909, p. 665.
10. C. I. Chessell. Propagation of Noise Along a Finite Impedance Boundary, *Journal of the Acoustical Society of America,* Vol. 62, 1977, pp. 825–834.
11. T. F. W. Embleton, J. E. Piercy, and N. Nelson. Outdoor Sound Propagation Over Ground of Finite Impedance. *Journal of the Acoustical Society of America,* Vol. 59, 1976, pp. 267–276.
12. S. V. Thomasson. Diffraction by a Screen Above an Impedance Boundary. *Journal of the Acoustical Society of America,* Vol. 63, 1978, pp. 1768–1781.

Publication of this paper sponsored by Committee on Transportation-Related Noise and Vibration.

Construction Noise: I-78 Through the Watchung Reservation

DENNIS A. DIEHL

The objective of the work described in this paper was to formulate a quantitative assessment of the noise environment adjacent to a segment of I-78 before, during, and after construction of the roadway. Existing noise levels were taken at 10 sites to establish a baseline for comparison with construction noise levels and traffic noise levels. These ambient noise levels ranged into the low 50s for all sites. During construction, four sites experienced no noise impacts, one site was severely affected, and the remaining five sites were intermittently affected by noise during various construction activities. When traffic noise was measured with noise barriers in place, seven sites were not affected, one site was moderately affected, and noise levels at two of the sites increased significantly in comparison to the preconstruction noise levels. At 9 of the 10 sites, the highest single L_{eq} measured was generated during the initial phases of construction. Clearing, cut and fill, and rough grading operations were the major sources of noise at all sites. Drainage installation, bridge work, construction of retaining walls, and rock drilling were secondary sources of noise. The only activity that caused a sustained increase over the existing noise levels was hauling. The noise from this operation dominated other construction noises for the duration of the project.

An assessment was made of the noise environment along the I-78 corridor in the borough of Mountainside, townships of Berkeley Heights and Springfield, and city of Summit in Union County, New Jersey (Figure 1). The evaluation included measurements taken before, during, and after the construction of I-78.

Ambient (existing) equivalent noise levels (L_{eq}) were taken at 10 sites to determine the existing noise environment before the I-78 construction began. Construction noise levels were then monitored at the same 10 locations during all phases of the I-78 project. Noise levels were also monitored with traffic flowing along the completed roadway. The objective was to formulate a quantitative assessment of the noise environment at the areas adjacent to I-78 before, during, and after construction.

Because of the dissimilarities of each site (topography, offset distance from the roadway, shielding effects, etc.), a comparison among sites would be of little use. A site-specific analysis, on the other hand, accomplished the research objective. All the noise levels mentioned in this paper are the L_{eq} for a 15-min period. An impact is defined as either an increase of 10 dBA above the ambient level or an L_{eq} greater than 64 dBA. To save space in publication, bar graphs for the sites show only half of the measurements taken. A full listing of the measurements, with the dates that the measurements were taken and the construction activities that caused the noise levels, is available on request.

Environmental Activity, Bureau of Materials, New Jersey Department of Transportation, 951 Parkway Ave., Trenton, N.J. 08625.

PROJECT SITE DESCRIPTION

This segment of I-78 borders the Watchung Reservation, Hidden Valley Park, and several adjacent communities. Within the project limits, 10 sites were selected as representative noise-sensitive areas: a hospital, a school, and eight private homes. The existing terrain was wooded and mountainous. This segment of I-78 segment was constructed along the face of a mountain range that borders the Watchung Reservation.

NOISE MEASUREMENT INSTRUMENTATION

A Bruel & Kjaer Precision Integrating Sound Level Meter Type 2218 was used to take conventional sound level values, expressed as L_{eq}. All of the measurements reflect the A-weighted L_{eq} value for 15-min periods.

MEASUREMENTS

Summary

Of the 10 sites monitored, 4 experienced no impacts (as defined previously) from construction noise. One site was severely affected, and the remaining five sites were intermittently affected during various construction operations. When traffic noise was measured with noise barriers in place, seven sites experienced no impacts, one site experienced moderate impacts, and the noise levels at the remaining two sites increased significantly in comparison to the preconstruction ambient levels.

At 9 of the 10 sites, the highest single L_{eq} that was measured occurred during the initial phases of construction. Clearing the site, cutting and filling, and rough grading activities all generated noise impacts at all sites for varying periods of time. Drainage installation, bridge work, construction of retaining walls, and rock drilling were secondary sources of construction noise.

The single activity that generated a sustained impact at most sites was hauling. The size and condition of the trucks that were used, in combination with the speed and duration of the operations, created a source of noise that dominated the noise from other construction activities throughout the length and

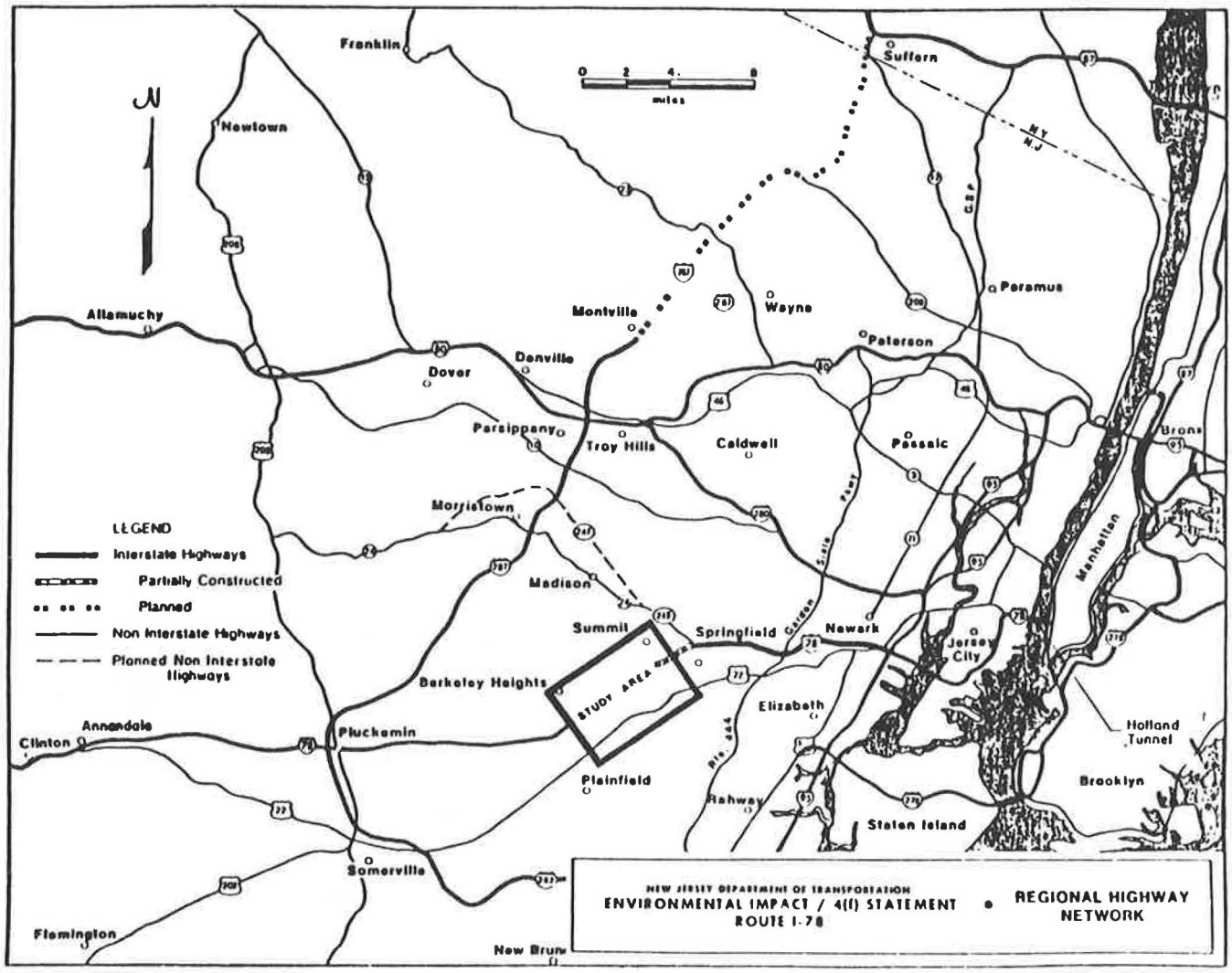

FIGURE 1 Study area.

duration of the I-78 project. Although noise levels for pile driving were the highest of those recorded, the length of time during which pile driving was performed was short enough that this activity did not draw any complaints from the community.

During the time that paving operations were under way, the installation of noise barriers was nearing completion. The noise measurements at the corresponding location varied accordingly. No noise impacts from paving operations were recorded. The noise measurements for the entire project are summarized in Table 1.

Site 1: Sayre House

Although peak L_{eq} construction noise levels were measured at 82 dBA during pile driving along Sayre Pond, this activity was quickly completed. Thus these measurements do not accurately reflect the overall noise levels for all activities at this site. During the first 8 months of construction, noise levels were found to range from the middle to upper 60s (Figure 2).

When the cut and fill operations and the construction of the retaining wall at Sayre Pond were completed, the noise levels generated by subsequent activities (mostly construction vehicles passing by) tapered off somewhat and were found to be less than 60 dBA. Near the final stages of the project, with the noise barriers in place, construction noise levels (exclusively generated by passing vehicles at this point) were consistently in the low 50s. The traffic noise levels at this site generate an L_{eq} of ~60 dBA. It is evident that there was a slight noise impact here from both construction and traffic.

Site 2: Guttman Home

The construction noise at this site was reduced by the shielding effect of the elevated Baltusrol bypass (Figure 3). During the initial phases of construction, noise levels were higher than the overall average at this site. After the cut and fill operations were completed, the noise levels (mainly caused by earthmovers hauling materials along the I-78 main line) caused no impacts.

TABLE 1 L_{eq} NOISE LEVELS

Site	Location	Existing	During Construction		Traffic	Noise Barrier
			Peak	Average		
1	Sayre House	50–52	82	58	59–60	Yes
2	Guttman home, 38 Ascot Way	49–52	75	56	54–55	Yes
3	Engelhardt home, 31 Skylark Drive	53–56	80	63	59–60	Yes
4	Gural home	48–50	82	69	60–61	Yes
5	Swalin home, 264 Oakridge Drive	55–56	62	54	51–53	No
6	Governor Livingston High School	48–52	70	54	56–58	No
7	Chin home, 54 Roland Road	46–50	80	55	55–58	No
8	Schmiedeke home, 69 Ridge Drive	47–50	72	61	65–69	No
9	Cowap home, 47 Twin Falls Road	46–50	64	61	53–56	Yes
10	Runnells Hospital	45–49	53	53	55	Yes

NOTE: All measurements in dBA.

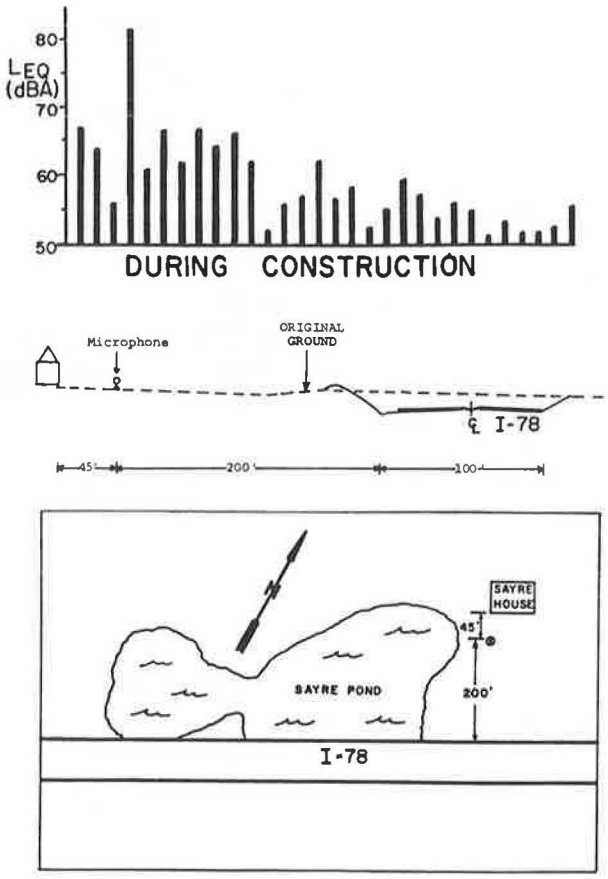

FIGURE 2 Site 1: Sayre House.

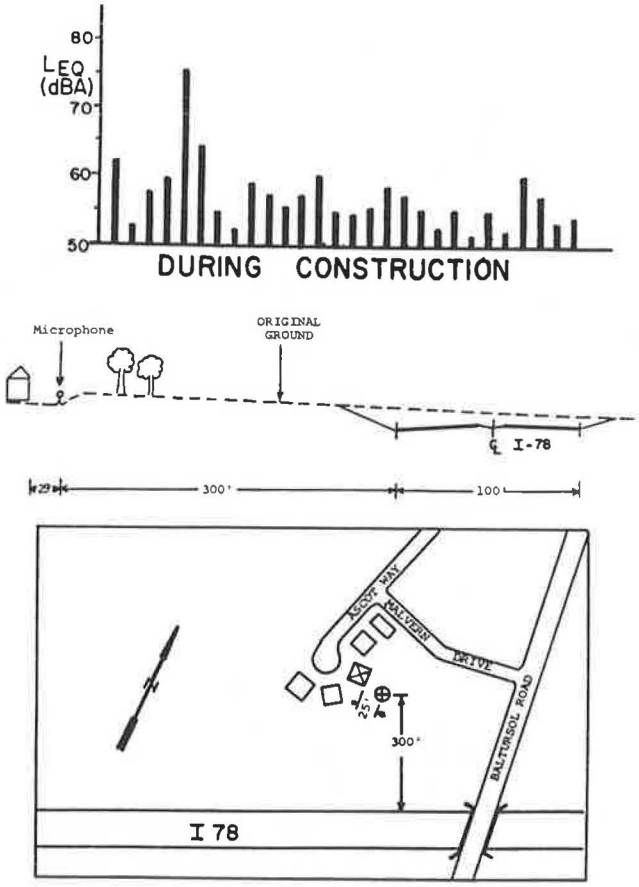

FIGURE 3 Site 2: Guttman home, 38 Ascot Way.

The inclined noise barrier that was used in this area was difficult to install. Currently, the effectiveness of the barrier is being compromised by the gaps that occur where the sections abut. Some differences were apparent when existing levels were compared to construction and traffic noise levels; however, no noise impacts resulted.

Site 3: Engelhardt Home

This site, which was located close to the I-78 main line, was often exposed to noise levels well above 70 dBA. After the cut and fill operations were complete, the noise levels (generated primarily by vehicles passing by) tapered off to the upper 50s (Figure 4).

The postconstruction L_{eq} traffic noise levels, which were in the range 58–60 dBA, verify the effectiveness of the noise barrier at this site. Substantial impacts would have occurred if a noise barrier had not been constructed. Noise during construction did cause slight impacts, but traffic noise did not cause any.

Site 4: Gural Home

The Gural home, located immediately adjacent to the I-78 right-of-way (Figure 5), experienced the most severe impacts

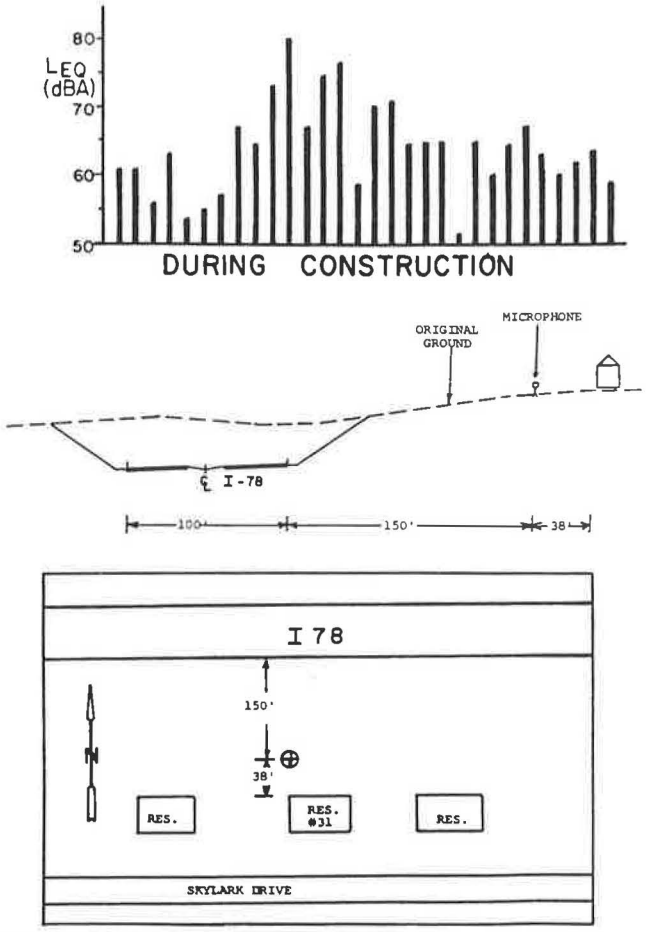

FIGURE 4 Site 3: Engelhardt home, 31 Skylark Drive.

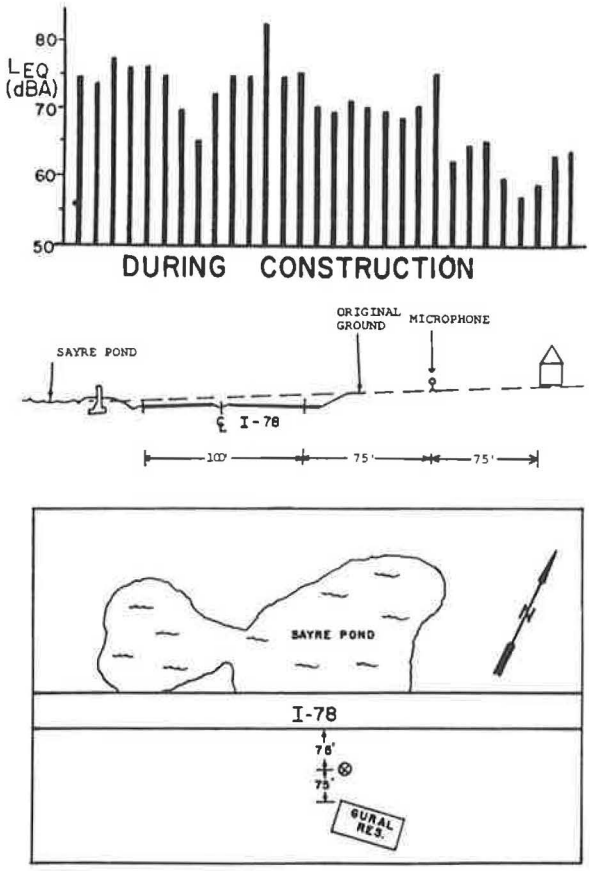

FIGURE 5 Site 4: Gural home.

of any site monitored during the project. L_{eq} levels in excess of 75 dBA were common, and the occupant filed numerous complaints throughout the construction period.

Several changes of plans in the vicinity (the Sayre Pond area) made it necessary to rework many completed parts of the project. The site was near the beginning of the haul road, and accelerating and decelerating trucks generated impacts almost continually during construction.

The noise reduction capabilities of the noise barrier are evident at this site: the traffic noise L_{eq} is only 60–61 dBA. Although there is an obvious noise impact (a 10-dBA increase), traffic noise levels remain well within federal guidelines.

Site 5: Swalin Home

This site, located atop the mountain ridge at a substantial setback from the face of the cut, was exposed to impacts only during activities that occurred immediately near the top of the slope (e.g., clearing, installation of the right-of-way fence). The traffic noise levels are barely audible, with no impacts (Figure 6).

Site 6: Governor Livingston High School

The school is located at a site that has topography similar to that of Site 5 (Figure 7). Noise levels exceeded 70 dBA during only one measurement period, when a bulldozer operation was proceeding along the top of the ridge at the right-of-way. For the most part, construction noise levels were found to be in the low to middle 50s.

Traffic noise levels are slightly greater than both the ambient and construction noise levels. At 56–57 dBA, however, the traffic noise is not an impact and is well within the federal design limits.

Site 7: Chin Home

This home is also located along the ridge, slightly set back and somewhat shielded by trees and heavy vegetation (Figure 8). It was seldom exposed to noise levels in excess of 60 dBA. In addition, this site is located at the western end of the project, at the end of the haul road. Therefore the noise caused by vehicles passing by on the haul road, which affected many of the other sites, was not a factor here. Rock drilling activities, however, did generate an impact for a limited time. Traffic noise levels are greater than the ambient levels, but they are well within design criteria.

Site 8: Schmiedeke Home

The Schmiedeke home is situated directly on the ridge, with no setback (Figure 9). It has an unobstructed view of the roadway and is now subject to major impacts from traffic noise (~20 dBA greater than the ambient noise levels). Construction

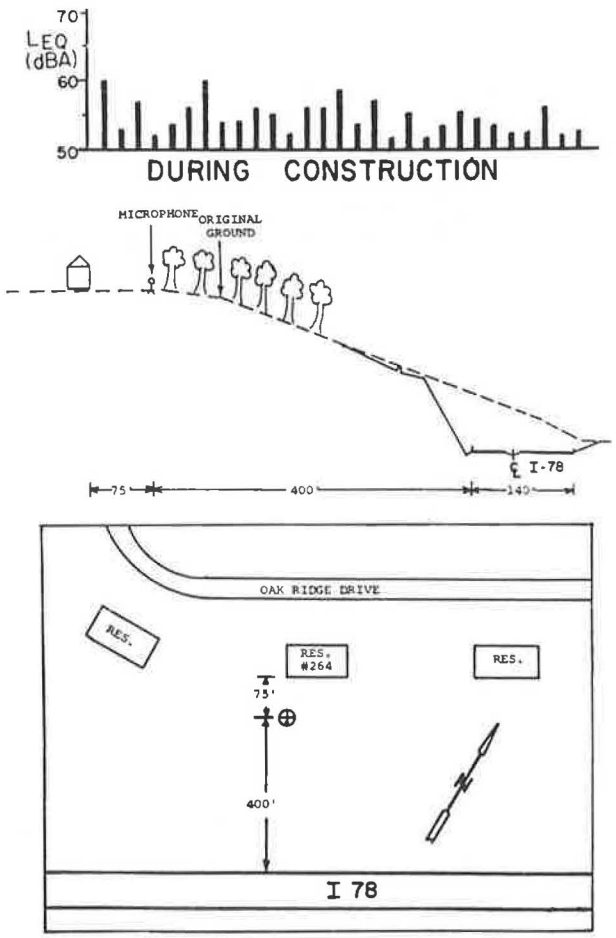

FIGURE 6 Site 5: Swalin home, 264 Oakridge Drive.

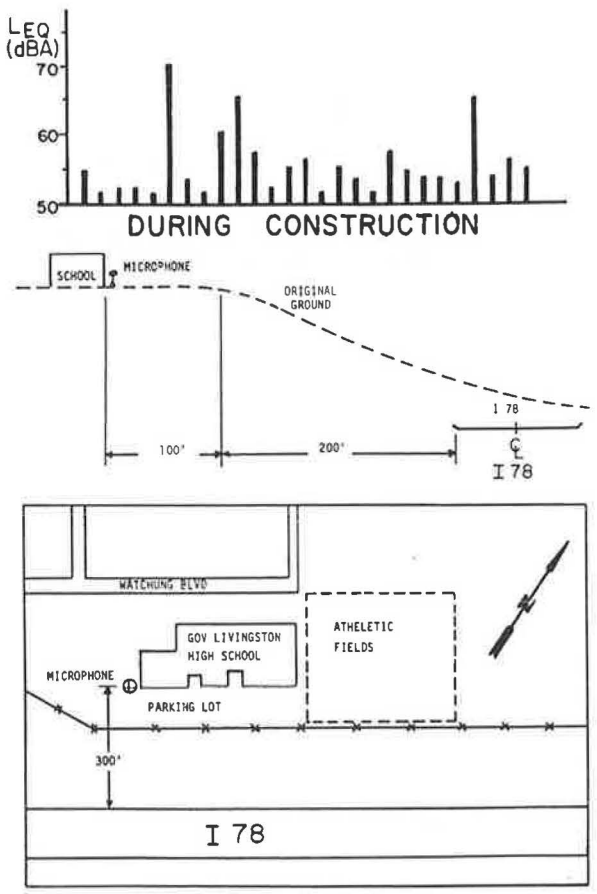

FIGURE 7 Site 6: Governor Livingston High School.

noise impacts, on the other hand, were moderate because this site is also located west of the section of the haul road that carried most of the passing construction vehicles. Some short-term construction noise levels of 65–70 dBA were counteracted in the average by the absence of construction activity during most of the project.

The owner recently complained about traffic noise and inquired about mitigation. Because the home is located directly atop the ridge, noise abatement procedures (namely noise barriers) are not feasible, so the occupant has placed the home on the market.

Site 9: Cowap Home

Construction noise levels generated a slight impact for a short time at this site. After the noise barriers were installed, however, neither the construction noise nor the traffic noise levels generated any impacts (Figure 10). All of these levels were only slightly greater than the ambient and were well within design criteria.

Site 10: Runnels Hospital

Most of the project's construction activities occurred some distance from the hospital (Figure 11). The segment of I-78 that was immediately adjacent to the hospital area had been completed, except for paving, under previous contracts. Because the hospital is considered very sensitive to noise impacts, noise barriers were constructed promptly in this area. The combination of the placement of noise barriers and the distance of the hospital grounds from most of the project's construction activities resulted in no noise impacts at this site. The distant construction activities were barely audible, and their noise levels seldom exceeded 50 dBA.

CONCLUSIONS

It is inevitable that noise impacts will occur during construction. The duration of the impacts is brief, however, in comparison to the overall time frame of an Interstate project of the magnitude of the I-78 construction. Construction noise levels tend to be higher during the initial phases (e.g., clearing, cutting and filling) and then taper off as the project nears completion.

Long-term impacts are generated along haul roads. When there are large amounts of materials to be moved or when the truck speed limits are high, activities on haul roads can generate levels of noise that exceed all guidelines for extended periods. This project required the removal of 3×10^6 yd^3 of material, so the haul road was used continually throughout most phases of construction for about 2 yr.

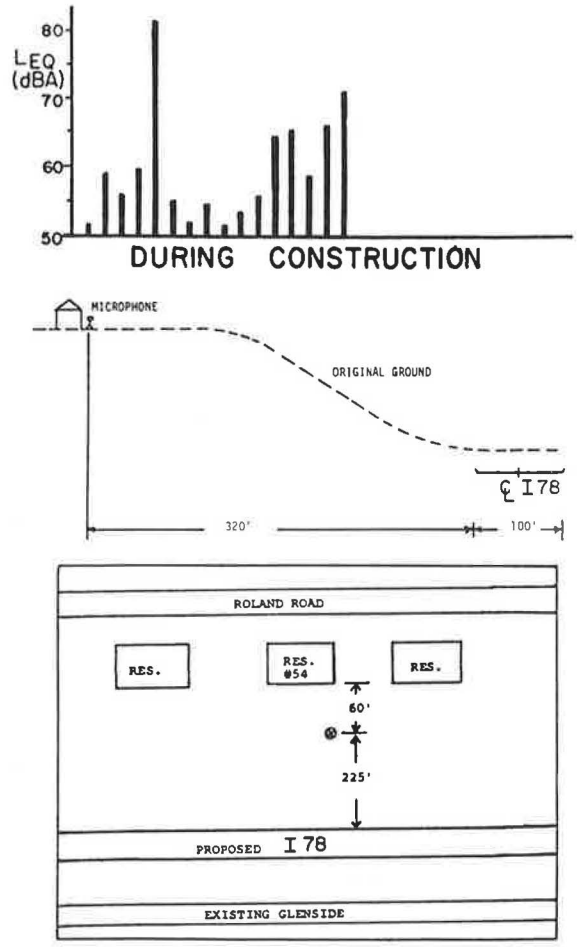

FIGURE 8 Site 7: Chin home, 54 Roland Road.

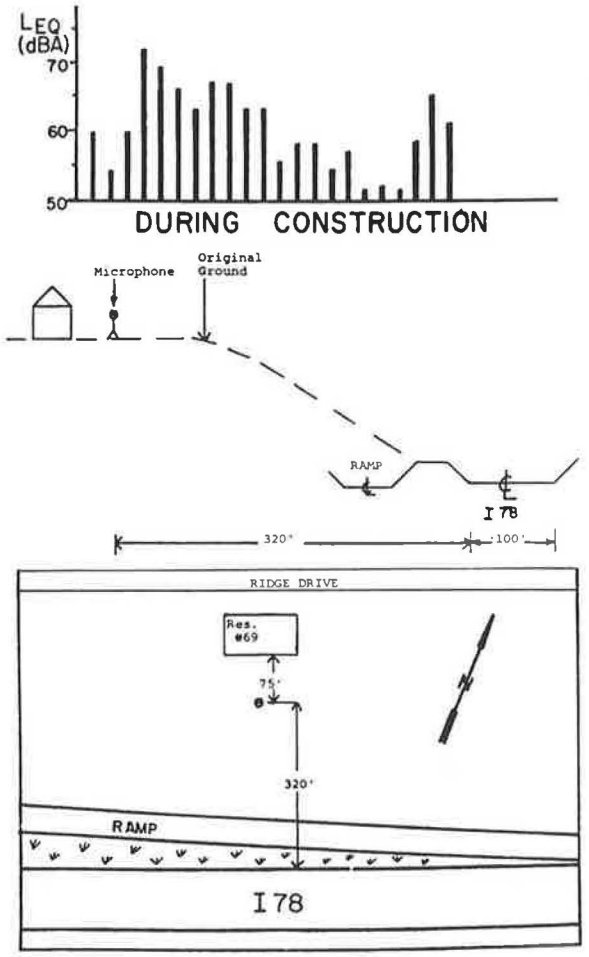

FIGURE 9 Site 8: Schmiedeke home, 69 Ridge Drive.

Involvement in noise impact issues is divided among several parties. The three that are always present during construction are as follows.

Department of Transportation

The responsibilities of this department, or more specifically, its resident engineer, go far beyond the planning stages of the project. Even though numerous commitments are placed in the contract plans and specifications, the resident engineer must ensure that these paper commitments become a reality during construction. For example, working hours (7:00 a.m. to 7:00 p.m.) were incorporated into the I-78 specifications. Contract personnel, however, would routinely start their equipment early to allow warm-up time before 7:00 a.m. Because the equipment was not "operating" (engaging in construction), the contractor did not feel that he was in noncompliance with the working hours.

A compromise was made. The contractor used an area adjacent to the quarry for overnight equipment storage. Because the quarry was far removed from any noise-sensitive areas, the operators could warm up and service the engines and be ready to start work at 7:00 a.m.

Contractor

The contractor is the key to minimizing construction noise impacts. The contractor's willingness to modify certain activities in consideration of noise-sensitive areas supersedes all the recommendations and guidelines that can be established. Prudent location of equipment and materials away from noise-sensitive sites, for example, will lessen the impact of construction.

Another step that the contractor can take to ensure tolerable noise levels is identifying those pieces of equipment that are particularly loud and then providing timely maintenance or replacing the offending equipment to reduce overall noise levels. During the early phases of the I-78 monitoring program, for example, one earth-mover in particular was found to generate noise levels well in excess of 90 dBA. Stack emission was identified as the dominant noise source. The contractor, when advised of the situation, ordered the earth-mover to be removed from operations. This action demonstrated the contractor's good faith in making efforts to address the concerns of this noise-sensitive community.

A final measure that, in particular, can reduce overall noise levels is to limit the speed at which earth-movers and dump trucks can travel the haul roads. This action will lower both peak noise levels and L_{eq}. It will also curtail those overzealous

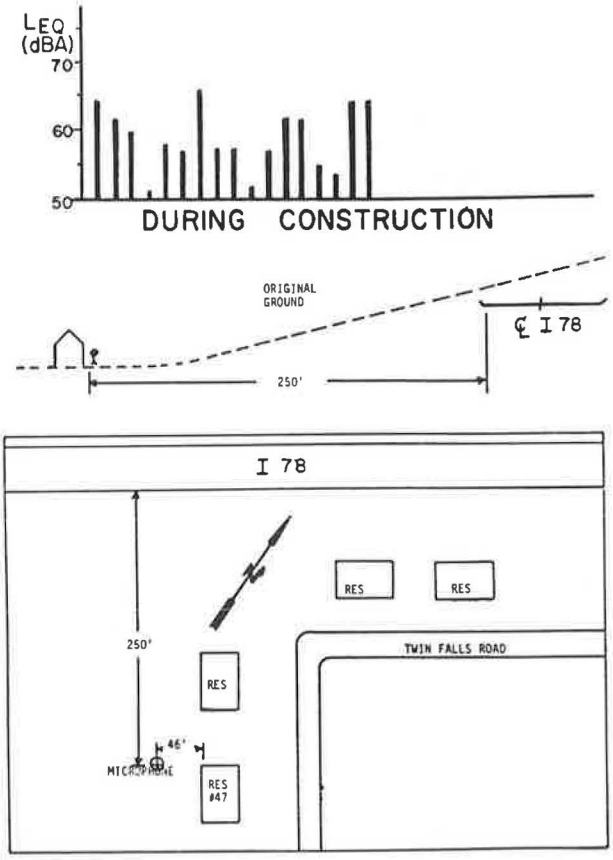

FIGURE 10 Site 9: Cowap home, 47 Twin Falls Road.

drivers who have been observed to operate their vehicles at speeds far exceeding the main flow of traffic.

Community

Community involvement is an integral part of environmental impact statement development. Public meetings, however, are

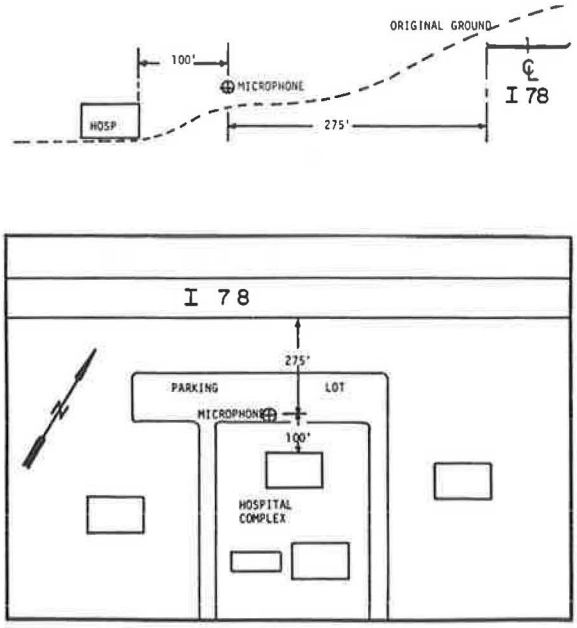

FIGURE 11 Site 10: Runnells Hospital.

conducted a long time before construction actually begins. The efforts of the department of transportation become obscured with time because years may pass between the public meetings and actual construction. A simple letter from the department to those home owners whose property is adjacent to the project site, outlining the anticipated construction schedule and acknowledging that the community will be somewhat inconvenienced, works wonders in maintaining a good working relationship. When this technique was employed on another project, no complaints from the community were received.

Publication of this paper sponsored by Committee on Transportation-Related Noise and Vibration.

Highway Traffic Noise Prediction for Microcomputers: Modeling of Ontario Simplified Program

F. W. JUNG AND C. T. BLANEY

Since its publication in 1977, the FWHA highway traffic noise prediction model, STAMINA, has been used in many manual and computerized forms. In this paper, a streamlined but somewhat limited version of the STAMINA model, written in BASIC for use on personal or pocket computers, is presented. The BASIC version can be used to predict noise from highway traffic for many simple situations. The program predicts noise from three standard classes of vehicle at one receiver location, shielded by a barrier of infinite length. The model includes the free field case and two parallel roadways, and it is consistent with the assumptions made in STAMINA 2.0. The modeling and underlying assumptions are explained in sufficient detail to contribute to a better understanding of the STAMINA 2.0 mainframe program and the mathematical modeling in general. For the applicable situations, the accuracy of computation obtained is virtually the same as with STAMINA.

Several years ago, the method of traffic noise prediction best known as STAMINA was introduced in Ontario, Canada, as a computer program for mainframe computers. In a mainframe computer, the STAMINA program can handle complex cases of noise prediction. The underlying mathematical modeling for the program was first published as a manual method in a 1978 FHWA report (*1*). This document was the basis for several simplified methods designed for getting quick results in the course of planning activities. Among the new methods was a nomographic method developed by the Ontario Ministry of Transportation and Communications (MTC) (*2*).

STAMINA FOR PERSONAL COMPUTERS

The proliferation of personal computers renders all purely manual methods (including the one presented in original report) obsolete. However, the modeling technique presented in the FHWA report is still relevant and valid. It should be noted that the model is analytical, unlike other, earlier models. This means that the STAMINA model is, for example, flexible in changing noise emissions from vehicles.

Various attempts to simplify procedures and improve understanding of the modeling behind the STAMINA program were published in 1981 (*3*). At that time, however, the technical community was not fully geared to using personal computers. Now that personal computers are almost ubiquitous, it is appropriate to present the simplified STAMINA modeling concepts in a form suitable for programming on microcomputers, leaving the mainframe programs for more complicated cases. The following concepts and improvements were developed on the basis of the FHWA method (*1*, *3*).

Research and Development Branch, Ontario Ministry of Transportation, Downsview, Ontario M3M 1J8, Canada.

Modified Subtending Angle

The effect of ground absorption, estimated and expressed by a coefficient, α, in free field segments, can be simply and fairly accurately incorporated by a modification of the subtending angles ϕ_1 and ϕ_2. This downward modification of both angles narrows the field segment and thus compensates for the effect of ground absorption. In calculating a modified subtending angle, $\overline{\phi} = \phi_1' - \phi_2'$, of a segment, the mathematical handling of the coefficient α becomes continuous and very simple (refer to the notation section).

Energy Level Equation

Instead of adding up (logarithmic) decibel values, an equation has been developed to use direct energy levels of (non-logarithmic) sound pressure energy. This not only assists in simplifying computations with α but also allows an additive treatment of vehicle traffic components. This procedure sometimes saves separate calculations for cars and for medium and heavy trucks.

Curve Fitting of Basic Noise Attenuation Tables

The noise attenuation tables in Appendix B of the original FHWA report [(*1*), referred to hereinafter as Original STAMINA] have been curve-fitted for $\phi_R = 90$ degrees and $\phi_L = -90$ degrees, that is, for the infinitely long barrier (minimum values) and for the very short segments (maximum values). Interpolation expressions have been derived to take care of a large range of tabulated Δ values in Appendix B. Barrier segments, which are on one side of the receiver position and do not touch the receiver line perpendicular to the road axis, are not covered by the simplified method presented.

NOTATION

V = total traffic on the road or on the part of the highway being considered, in vehicles per hour.

p = fraction of car traffic (subscript A in Original STAMINA); for instance, p = 0.85 means that cars represent 85 percent of V (P = 85).
q = fraction of medium truck traffic (originally, subscript MT).
r = fraction of heavy truck traffic (originally, subscript HT).
P, Q, R = percentage of car, medium truck, and heavy truck traffic, respectively.
S = average traffic speed, assumed to be uniform (km/hr).
D_0 = reference distance from centerline of traffic (D_0 = 15 m is the standard value).
D_N = horizontal distance from the noise source to the center of the nearest lane (m).
D_F = horizontal distance from the noise source to the center of the farthest lane (m).
D_E = equivalent lane distance, equal to $\sqrt{D_N D_F}$, for free field only (m).
L = hourly reference energy emission level (dBA).
L_{eq} = equivalent sound level (dBA).
α = ground cover coefficient, according to Original STAMINA (*1*): α = 0 for hard, reflective surfaces and α = 0.5 for soft, absorptive surfaces.
ϕ = subtending segment angle in degrees, viewed from the point of the receiver toward the road.
ϕ_1, ϕ_2 = subtending angles for a segment (see Figure 1) (*1*).
ϕ_1', ϕ_2' = modified angles for a segment.
$\bar{\phi}$ = equivalent subtending angle ($\bar{\phi}$ is reduced because of soft ground cover, as discussed later in the paper).
Δ = noise attenuation for a segment from a sound barrier parallel to the highway (dBA).
N_0 = Fresnel number for path length difference δ.
δ = path length difference perpendicular to the road axis (see Figure 6).
I = sound barrier insertion loss (dBA).

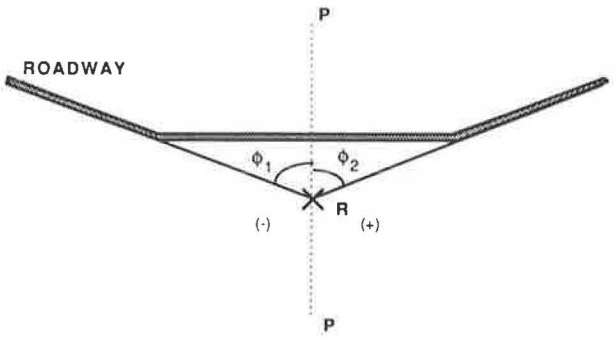

FIGURE 1 Subtending angle for "turning away" roadway.

For free field conditions, ground cover coefficients can be estimated in accordance with the list in the following section.

GROUND COVER COEFFICIENTS, α

These values are proposed by the authors:

- α = 0 for reflective ground cover, such as paved parking lots, ice-covered ground, or collector and residential streets;
- α = 0.25 for moderately reflective ground cover, such as bare soil, minor patches of grass, partially paved backyards, or parking lots interspersed with lawns;
- α = 0.5 for absorptive ground cover, such as lawns and soft soil fields or backyards with plants, flowers, and small shrubs; and
- α = 0.75 for very absorptive ground cover, such as backyards with trees and shrubs, cornfields, or similar surfaces.

MODIFIED SUBTENDING ANGLE

The concept can be easily recognized from Equation A-64 of Original STAMINA (*1*, p. A-29). Looking from the receiver toward the roadway, the segment of investigation is enclosed by the angle ϕ_1 to the left and ϕ_2 to the right, as shown in Figure 1 for a special case of a roadway that curves away. The angles enclose the subtending angle, ϕ.

The subtending angle is always calculated as follows:

$$\phi = \phi_1 - \phi_2 \tag{1}$$

where ϕ_1 and ϕ_2 are measured from line P-P perpendicular to the road, at the receiver position R, positive in the clockwise direction. Note that the angle ϕ_1 in Figure 1 is negative.

In the case of soft, absorptive ground cover, the angles ϕ_1 and ϕ_2 should be modified, and a modified or equivalent subtending angle is calculated as follows:

$$\bar{\phi} = \phi_1' - \phi_2' \tag{2}$$

The modified angles ϕ_1' and ϕ_2' have the same signs as the actual angles ϕ_1 and ϕ_2, respectively. The absolute values of ϕ_1 and ϕ_2 can be determined from Table 1, which is the solution of the following integral:

$$\phi_1' = \frac{180}{\pi} \int_0^{\phi_i} (\cos \phi)^{\alpha} \, d\phi \tag{3}$$

Substitution of Equation 3 into Equation 2 leads to Equation A-64 of Original STAMINA, except for a factor of 180 degrees.

In the computer program, the angles ϕ_1, ϕ_2, ϕ_1', ϕ_2', and the rest are calculated from input values of distances and lengths of segments. In accordance with the convention for the sign of those angles, the lengths of segments, or parts thereof, can be positive (to the right) or negative (to the left; refer to Figures 1 and 2). For algebraic expressions of $\phi' = f(\alpha)$, refer to the section on curve fitting, later in this paper. Values for the

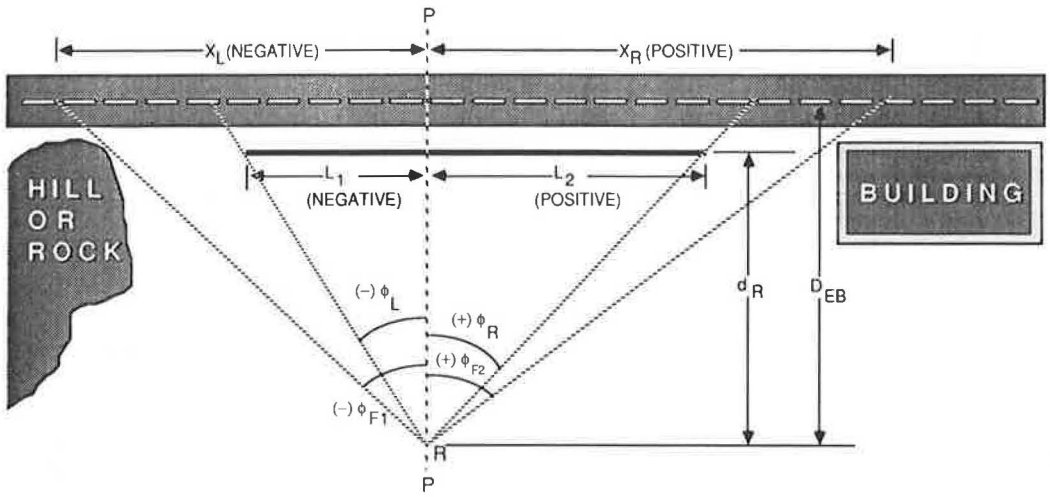

FIGURE 2 Subtending angles for barrier and roadway.

TABLE 1 ABSOLUTE VALUES OF ϕ'

ϕ	$\alpha = 0$	$\alpha = 0.25$	$\alpha = 0.5$	$\alpha = 0.75$
0°	0	5.000	5.000	5.000
5°	5	4.998	4.997	4.995
10°	10	9.987	9.975	9.962
15°	15	14.957	14.914	14.872
20°	20	19.898	19.796	19.696
25°	25	24.799	24.601	24.406
30°	30	29.651	29.309	8.975
35°	35	34.442	33.901	33.374
40°	40	39.161	38.353	37.576
45°	45	43.793	42.645	41.554
50°	50	48.325	46.754	45.278
55°	55	52.741	50.654	48.723
60°	60	57.021	54.318	51.860
65°	65	61.141	57.714	54.659
70°	70	65.072	60.805	57.091
75°	75	68.772	63.544	59.119
80°	80	72.178	65.866	60.703
85°	85	75.173	67.664	61.785
90°	90	77.150	68.606	62.237

Note: For $\alpha = 1$ $\phi' = \frac{180}{\pi} \sin \phi$

NOTE: Algebraic expressions for $\phi' = f(\alpha)$ may be found in the section on curve fitting. Values for the modified subtending angle ϕ' can be taken from this table for manual calculations.

modified subtending angle, ϕ', can be taken from Table 1 for manual calculations.

ENERGY LEVEL EQUATION

The *A*-weighted reference energy mean emission levels for cars, medium trucks, and heavy trucks can be transformed into direct energy expressions. The equations used in Original STAMINA are given in the FHWA report (*1*, pp. 4–5). The transformed or delogarithmized equations are, for cars, medium trucks, and heavy trucks, respectively,

$$C = 0.57544 \cdot S_A^{3.81} \tag{4}$$

$$M = 43.6516 \cdot S_{MT}^{3.39} \tag{5}$$

$$H = 7079.4578 \cdot S_{HT}^{2.46} \tag{6}$$

This leads to a simple equation for the total hourly equivalent sound level, L_{eq} (h) in dBA:

$$L_{eq}(h) = 10 \log \left[\frac{\bar{\phi}}{15} \bar{VK} \left(\frac{15}{D_E} \right)^{1+\alpha} \right] \tag{7}$$

where

$$\bar{K} = K_A + K_{MT} + K_{HT} \tag{8}$$

$$K_A = (P/44253)\, S_A^{2.81} \tag{9}$$

$$K_{MT} = (Q/583.36)\, S_{MT}^{2.39} \tag{10}$$

$$K_{HT} = 0.27801 \cdot R \cdot S_{HT}^{1.46} \tag{11}$$

Equations 9–11 (or A-3, A-4, and A-5) are derived from Original STAMINA (*1*). They represent U.S. national averages for vehicle types. It is recommended that these equations be modified if vehicle noise emission levels differ from those established in the United States in 1977, although there is no reason to change the equations if differences are smaller than the statistical variations in the noise emission data. The ground cover coefficient, α, was discussed earlier in this paper.

Data collected in Ontario during 1984 and 1985 resulted in a different set of equations:

$$K_A = (P/1114.14)\, S_A^{2.041} \tag{9'}$$

$$K_{MT} = (Q/8.2402)\, S_{MT}^{1.406} \tag{10'}$$

$$K_{HT} = 45.5051 \cdot R \cdot S_{HT}^{0.259} \tag{11'}$$

These equations, labeled B-1, B-2, and B-3 in Original STAMINA, would replace original Equations A-3, A-4, and A-5 (9–11 in this paper). The underlying emission level equations can be found elsewhere (*4*).

CURVE FITTING OF TABLE 1 (EQUATION 3 RESULTS)

A closed solution of the integral expression of Equation 3 is not possible. Table 1 was established by numerical integration. The columns can be curve fitted approximately by the following equations (A-6 to A-9 in Original STAMINA). In this way, a solution that is suitable for small computers can be achieved, and calculations will be fast and direct.

$$\phi_i' = \phi_i \left[1 - \frac{M}{|\phi_i|} \left(\frac{|\phi_i|}{90} \right)^n \right] \tag{12}$$

$$M = (90) \left(\frac{0.58\ \alpha^{0.9}}{0.58\ \alpha^{0.9} + 1} \right) \tag{13}$$

$$N = \frac{1}{0.134\ \alpha + 0.225} \tag{14}$$

For $\alpha = 1$, the accurate solution is

$$\bar{\phi} = \frac{180}{\pi} (\sin \phi_2 - \sin \phi_1) \tag{15}$$

The special case of $\phi_2 = 90$ degrees and $\phi_1 = -90$ degrees has been approximated by a different equation. For $0 \le \alpha \le 0.75$,

$$\bar{\phi} = \frac{180}{1 + 0.58\ \alpha^{0.9}} \tag{16}$$

and for $\alpha = 1$, the accurate solution in this case is

$$\bar{\phi} = \frac{180}{\pi/2} \tag{17}$$

The ground cover coefficient is treated as a continuous variable. The approximation of the integral Equation 3, represented by Equations 12–17, is accurate enough for all practical purposes.

BARRIER INSERTION

When free field noise is intolerably high, the insertion of a sound barrier wall may help. Figure 2 shows a typical case of a barrier that is shorter than the visible part of the roadway. There are three segments that contribute to traffic noise at point R, namely, left of the barrier, over the barrier, and right of the barrier. Their subtending angles are $\phi_L - \phi_{F1}$, $\phi_R - \phi_L$, and $\phi_{F2} - \phi_R$, respectively. These angles can be calculated from length and distance dimensions, which are also given in Figure 2 (X_L and X_R are the left and right road distances, or visible road length, and L_1 and L_2 are the left and right barrier length). It should be noted that angles and corresponding barrier or roadway distances can be negative when they point left from the perpendicular receiver line through R. The three segments must be treated separately and their noise contributions added. The procedure is explained thoroughly in Original STAMINA (*1*), and some of the explanation is repeated here to establish references for programming.

The basic barrier attenuation, Δ, is a function of ϕ_L and ϕ_R, as defined in Figure 2, and of the Fresnel number, N_0. The insertion of a barrier has an effect on sound absorption by a soft ground. For high barriers (4 to 5 m), the benefit of soft ground absorption can be assumed to be eliminated completely so that such barrier sections must also be calculated for $\alpha = 0$. For barriers of low height (less than or equal to 3 m) the absorption of a soft ground cover is still effective, but the coefficient α may be reduced considerably from its maximum value for the free field condition (*5, 6*).

To establish reference equations for the PC program, a discussion of the Fresnel number calculation and path length difference is included here. In the usual, well-known way, the Fresnel number is calculated as follows:

$$N_0 = 2\left(\frac{f\,\delta}{c}\right) = 2\left(\frac{550\ \delta}{343}\right) = 3.207\ \delta \approx 3.21\ \delta \tag{18}$$

where

- f = frequency of sound waves, with $f = 550$ Hz selected as a representative frequency for noise (Hz);
- c = velocity of sound in air, equal to 343 m/s; and
- δ = path length difference between noise source and receiver, perpendicular to the road axis, comparing a direct path line C with an indirect path line over top of the barrier ($A + B$; see Figure 3); $\delta = A + B - C$ (m).

To calculate the path length difference, the calculations must be organized in terms of horizontal distances and heights above the road surface. Denotation should be in accordance with Figure 4:

- h_S = level of noise source above the road surface (m),
- h_R = level of receiver of noise above the road surface (m),
- h_T = level of barrier top above the road surface (m),
- d_S = horizontal distance of noise source from a vertical plane through the barrier top (m), and
- d_R = horizontal distance of noise receiver from a vertical plane through the barrier top (m).

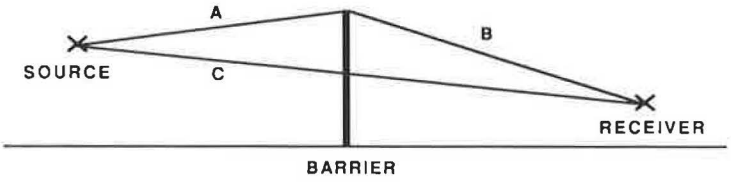

FIGURE 3 Path length difference, δ.

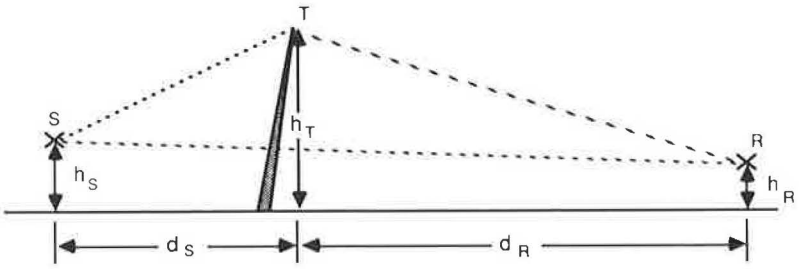

FIGURE 4 Organizing the calculation of δ.

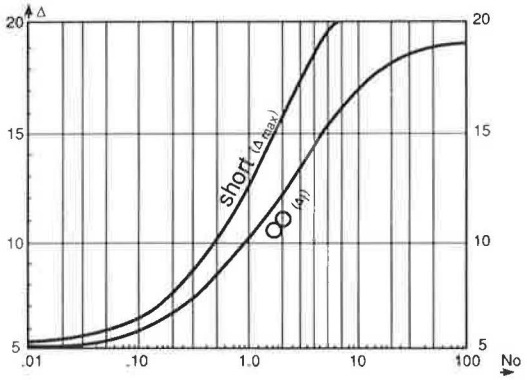

FIGURE 5 Characteristics of Equations 15 and 16.

Then

$$\delta = A + B - C$$

$$\delta = \sqrt{(h_T - h_s)^2 + d_s^2} + \sqrt{(h_T - h_R)^2 + d_R^2} - \sqrt{(h_S - h_R)^2 + (d_S + d_R)^2} \quad (19)$$

The following assumptions are made for receiver and source heights above ground or road surfaces, respectively:

- Noise from cars: $h_{SA} = 0$;
- Noise from medium trucks: $h_{SMT} = 0.7$ m;
- Noise from heavy trucks: $h_{SHT} = 2.44$ m; and
- Height of receiver above ground: $h_R = 1.5$ m (may be lower or higher than 1.5 m above the road surface).

Once a barrier is in place, the equivalent lane distance from the source to the receiver is different. The distance of the near lane from the barrier is denoted dN (m) and the distance of the far lane from the barrier is denoted dF (m). Then

$$D_{EB} = d_R + \sqrt{d_N \times d_F} \quad (20)$$

CALCULATING BARRIER ATTENUATION

Basic Equations

Original STAMINA presents the solution of a complex integral in the form of tables for the value Δ, the noise attenuation in dBA, representing a function of N_0, ϕ_L, and ϕ_R (*1*, pp. B-11–B-71). The important range begins at $N_0 = 0.05$ for $N = 3$. Beyond this range, the barrier either would not be warranted or would be too high (5 m or higher), heavy, and ugly. High barriers with $N_0 > 3$ are still included, and low barriers (below $N_0 = 0.05$) approach a value of $\Delta = 5$ dB without much error or deviation.

A portion of the previously mentioned tabulated function has been curve fitted (see Figure 5). The basis of this approach was established by finding an equation to fit the values of Δ for $\phi_L = -90$ degrees and $\phi_R = +90$ degrees (i.e., for an infinitely long barrier). This equation is a function of N_0 only:

$$\Delta_I = 5 + 14.4 \cdot e^{-0.175(2 - \log N_0)^{2.5}} \quad (21)$$

The equation is accurate within ±0.04 dB; that is, it is as accurate as the table values.

Equation 21 is only valid for barriers that intercept the line of sight between source and receiver. For barriers with a top lower than this line of sight, the following equation is assumed, using positive values of N_0 as input:

$$\Delta = 5 - 25\, N_0 \geq 0 \quad (22)$$

Equation 22 is an assumed approximate model for this range of low barrier heights, for which accuracy is of lesser importance. Because of the limitations in the calculation of barrier attenuation values, cases in which the barrier height above the roadway surface is less than 0.6 m should be declared invalid. (Cases below 2 m height should be approached with some caution when the ground cover is soft.)

The maximum values of Δ for short segments of barriers at the source-receiver line (*1*, pp. B-11–B-71) have also been curve fitted, as follows:

$$\Delta_{max} = 5.15 + 14.4\, e^{-0.59(1 - \log N_0)^2} \quad (23)$$

Between these Δ values, for infinitely long and very short barriers (Δ_I and Δ_{max}), a complex interpolation formula has been derived, as follows:

$$\Delta = \Delta_{max} - (\Delta_{max} - \Delta_I)\,(\phi_E/90)\eta \quad (24)$$

where

$$\phi_E = \frac{\phi_R - \phi_L}{2} \quad \text{(average of } |\phi_R| \text{ and } |\phi_L|\text{)} \quad (25)$$

$$\eta = 1 + \left(1.25 + \frac{N_0}{2}\right)\left[1 - 3.24\left(\frac{|\phi_L + \phi_R|}{90}\right)^2\right] \quad (26)$$

This interpolation is valid for a certain limit of the difference between $|\phi_R|$ and $|\phi_L|$, namely, for

$$\phi_R + \phi_L \leq 45 \text{ degrees} \quad \text{(note: } \phi_L \text{ is negative)} \quad (27)$$

For differences outside this domain, $\phi_R + \phi_L > 45$ degrees, the following approximation is more accurate than Equations 25 and 26:

$$\eta = 1 + \left(1.25 + \frac{N_0}{2}\right) \quad (28)$$

$$\phi_E = \phi_R + \frac{\phi_L}{5} \quad |\phi_R| > |\phi_L| \quad (29)$$

$$\dot{\psi}_E = -\dot{\psi}_L - \frac{\phi_R}{5} \quad |\dot{\psi}_L| > |\dot{\psi}_R| \quad (30)$$

Normally, ϕ_R is always positive and ϕ_L is always negative, according to definitions given in Figures 1 and 2 and earlier in the text. However, small angles of opposite sign (up to 10 degrees) can be accepted. Thus the following condition was introduced: if $\phi_R < -10$ degrees or $\phi_L > +10$ degrees, the barrier insertion loss is declared invalid.

Ground Absorption

In the selection of a ground absorption coefficient, α, the following factors should be noted. When the ground cover coefficient α_F for free field sound absorption is selected in accordance with the list presented in the earlier section on coefficient α, the program user should understand that the recommended values are only for normal, fairly even terrain. It should be noted that the beneficial effect of ground absorption (i.e., the coefficient α) deteriorates when the height of the sound propagation paths between source and receiver above the absorptive ground increases beyond the normal average height of source and receiver. This condition occurs with high noise barriers, but it also occurs also when the ground between source and receiver is significantly depressed.

In the STAMINA 2.0 mainframe computer program the value α_B (for barrier present) is therefore set to zero in any segment at which a barrier is present before the attenuation, Δ, is deducted (refer to the terms LB and Δ in Equation 26). Generally, this results in a much reduced or decreased net insertion loss (compared to Δ). For very low barrier heights this could even lead to negative values for this net insertion loss, which would actually be an apparent gain in noise level above the free field condition level, in spite of the presence of a barrier. The program avoids such embarrassing contradictions by internal controls (IF LL < LF THEN LL = LF), without having a true solution.

When a valley or a ground depression of some kind is located between the source and receiver, the coefficient α_F should be selected accordingly, that is, below the pertinent value indicated in the list presented earlier. A further reduction from α_F to α_B is then less severe.

For barriers of low and moderate heights (below 3 m) there is a transition problem with the value α_F and zero. Further guidance on this issue can be found in the work of Jung (*6*). Without this precaution, both the PC versions presented here and the mainframe STAMINA would underestimate the effect of low barriers in a terrain of absorptive ground. The problem of ground absorption, however, has not yet been sufficiently clarified that a definite procedure can be recommended as a solution.

CALCULATION PROCEDURES

Calculations are carried out for the three vehicle types (cars, medium trucks, and heavy trucks) and for a maximum of two parallel roadways separately, and the results are then combined or added at a later stage. The program consists of one basic subroutine to calculate the free field noise for any segment, using dummy variables for D_E, α, and ϕ_1 and ϕ_2 (the angles left and right of the segment, measured clockwise from the perpendicular line through point *R*, i.e., the line *P-P* in Figures 1 and 2). By using this subroutine, free field noise levels are calculated from the total roadway section (LF) from ϕ_{F1} to ϕ_{F2}, the barrier section (LB) from ϕ_L to ϕ_R, the segment left of the barrier (LX) from ϕ_{F1} to ϕ_L, and the segment right of the barrier (LY) from ϕ_R to ϕ_{F2} (see Figure 2).

Another major part of the program consists of calculating barrier attenuation, denoted as Δ, for each vehicle type and for the segment with barrier, from ϕ_L to ϕ_R, adjusted in accordance with the method shown above. The barrier net insertion loss (IL) for each vehicle type and roadway is then calculated as

$$IL = LF - (LB - \Delta + LX + LY) \quad (31)$$

where the terms in parentheses represent the noise level after barrier construction (LL).

At the end, the two kinds of noise levels, LF and LL, for each roadway are then added the LF and LL totals. A new, final net insertion loss is then calculated: I = LF – LL.

The sound absorption coefficient α_F for ground cover, as listed earlier, is only valid for free field conditions (LF, LX, LY). The term LB must be calculated with a reduced α, and the STAMINA mainframe computer program assumes a value of $\alpha_B = 0$, which may be too low for very low barrier heights

(*6*). To be consistent with STAMINA, the program here assumes that $\alpha_B = 0$ unless another option is chosen.

PROGRAM COMPARISONS

The proposed new program for microcomputers was compared with the mainframe STAMINA program. In most instances there were virtually no differences in the results. This was to be expected because the basic assumptions in modeling the programs were identical. However, inexplicable small differences of about 0.5 dBA were found at low barrier heights (less than or equal to 2.5 m) (see Figure 6).

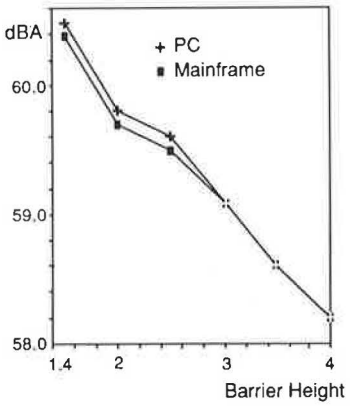

FIGURE 6 Comparison with the mainframe program STAMINA (variable barrier height).

BASIC PROGRAM

Program Listing

```
10  REM BARRIER NOISE PREDICTION PROGRAM
15  DIM LU(4), LV(4) : OPEN 4, 4, 0
20  READ V, Q, R, S1, S2, S3
25  READ NR, X1, X2, DN, DF, AF
30  LET P = 100-R-Q : DO = SQR(DN*DF)
40  LET PI = 3.14159265 : X = 180/PI
45  F1 = X*ATN(X1/DO) : F2 = X*ATN(X2/DO)
50  D1 = DN-DR : D2 = DR-DR
55  DS = SQR(D1*D2) : DB = DR + DS
60  FL = X*ATN(L1/DR) : FR = X*ATN(L2/DR)
65  IF FL < F1 THEN FL = F1
70  IF FR > F2 THEN FR = F2
75  DEF FN F(XX) = INT(1000*XX +.5)/1000
80  INPUT "ALPHA FOR BARRIER FIELD = "
85  GOTO 350
90  REM FREE FIELD NOISE SUBROUTINE
100  IF AL=0 THEN PH=P2-P1 : GOTO 230
110  IF ALL=1 THEN PH = (SIN(P2/X)-SIN(P1/X)*X :
     GOTO 230
130  N = 1/(0.1334*AL + 0.225)
140  M = (90)*(0.58*AL ↑ 0.9 + 1)
150  Y1 = ABS(P1) : Y2 = ABS(P2)
160  IF P1 = 0 THEN GOTO 180
170  PA = P1*(1-(M/Y1)*(Y1/90.) ↑ N)
180  IF P2 = 0 THEN GOTO 200
190  PB = P2*(1 -(M/Y2)*(Y2/90.) ↑ N)
200  IF P1 = 0 THEN LET PA = 0
210  IF P2 = 0 THEN LET PB = 0
220  PH = PB - PA
230  K(1) = (P/44253)*S1 ↑ 2.81
240  K(2) = (Q/583.36)*S2 ↑ 2.39
250  K(3) = 0.27801*R*S3 ↑ 1.46
260  K(4) = K(1) + K(2) + K(3)
270  FOR J = 1 TO 4 STEP 1
280  IF PH < 0.001 THEN L(J) = 0
290  IF PH < 0.001 GOTO 330
300  IF K(J) = 0  THEN L(J) = 0
310  IF K(J) = 0 GOTO 330
320  L(J) = (10/LOG(10))*LOG((PH/15)*V*K(J)*(15/DE)
     ↑ (1+AL))
330  NEXT J
340  RETURN
350  REM FREE FIELD NOISE FOR C, MT, HT
360  P1 = F1 : P2 = F2 : AL=AF : DE=D0
370  GOSUB 100
380  FOR J = 1 TO 4 STEP 1
390  LF(J) = L(J)
400  U(J) = FN F(LF(J))
410  NEXT J
420  PRINT U(1), U(2), U(3), U(4)
440  IF A=1 GOTO 810
450  REM FR. FIELD NOISE OF BARRIER SEC.
460  P1 = FL : P2 = AL = AB : DE = DB
470  GOSUB 100
480  FOR J = 1 TO 4 STEP 1
490  LB(J) = L(J) : NEXT J
500  REM CALCULATE DELTAS OF BARRIER
510  LET H(1) = 0.0
520  LET H(2) = 0.7
530  LET H(3) = 2.44
540  FOR J = 1 TO 3 STEP 1
550  AA = SQR((HB-H(J))*(HB-H(J)) + DS*DS)
560  BB = SQR((HB-HR)*(HB-HR + DR*DR)
570  CC = SQR ((H(J)-HR)*(H(J)-HR) + DB*DB)
580  PD(J) = AA + BB - CC
590  T(J) = 3.207*PD(J)
600  NEXT J
610  GOSUB 1000
615  IF A = 1 GOTO 810
620  FOR J = 1 TO 3 STEP 1
630  LG = LOG(T(J))/LOG(10)
640  DY = 5 + 14.4*EXP(-.175*(2-LG) ↑ 2.5)
650  DX = 5.15 + 14.4*EXP(-.59*(1-LG ↑ 2)
660  IF NN > 1.0 THEN NN = 1
670  IF NN < 6.0 THEN NN = 6.0
720  D(J) = DX-(DX-D6)*(FI/90) ↑ NN
730  IF D(J) > 19.5 THEN D(J) = 19.5
740  IF HB-HR ≤ (H(J) -HR)*(DR/DB) THEN D(J) = 5 -
     25*T(J)
745  IF D(J) 0 THEN D(J) = 0
750  V(J) = FN F(D(J))
755  NEXT J : AR = 0
760  PRINT V(1), V(2), V(3)
770  FOR J = 1 TO 3 STEP 1
```

```
780  LL(J) = LB(J)-D(J)
785  W(J) = FN F(LL(J))
790  AR = AR + 10 ↑ (LL(J)/10) : NEXT J
800  LL(4) = 10*(LOG(AR))/LOG(10)
802  W(4) = FN F(LL(4))
805  PRINT W(1), W(2), W(3), W(4)
810  REM FREE F. NOISE & DELTA OUTPUT
820  PRINT#4, " FREE FIELD NOISE LEVEL AND
     DELTA VALUES"
830  PRINT#4
840  PRINT#4, "CARS:   ", U(1), V(1)
850  PRINT#4, "MEDIUM TRUCKS:   ", U(2), V(2)
860  PRINT#4, "HEAVY TRUCKS:   ", U(3), V(3)
870  PRINT#4, "TOTAL, ALL VH.:   ", U(4)
875  IF A = 1 THEN PRINT#4, "INVALID BARRIER
     CASE"
876  IF A=1 THEN PRINT "INVALID BARRIER CASE"
877  IF A=1 GOTO 2200
880  PRINT#4 : PRINT#4
885  IF FI > 89 GOTO 1890
890  IF FL < = -88 GOTO 915
895  P1 = F1 : P2 = FL : AL = AF : DE = D0
900  GOSUB 100
905  FOR J = 1 TO 4
910  LX(J) = L(J) : NEXT J
915  IF FR > = 88 GOTO 940
920  P1 = FR : P2 = F2 : AL = AF : DE = DO
925  GOSUB 100
930  FOR J = 1 TO 4
935  LY(J) = L(J) : NEXT J
940  FOR J = 1 TO 4
945  KK = 10 ↑ ((LL(J))/10 + 10 ↑ ((LX(J))/10) + 10 ↑
     ((LY(J))/10)
950  LL(J) = 10*LOG(KK)/(LOG(10))
955  IF LL(J) LF(J) THEN LL(J) = LF(J)
960  W(J) = FN F(LL(J))
965  NEXT J
970  PRINT W(1), W(2), W(3), W(4)
975  GOTO 1800
1000  REM SUBROUTINE DETERMINING FI & NN
1005  LET QQ = 0.20
1010  IF FR < -10 GOTO 1060
1015  IF FL > +10 GOTO 1060
1020  IF ABS(FR+FL) ≤ 45 GOTO 1100
1030  IF ABS(FR) > ABS(FL) GOTO 1120
1040  IF ABS(FR) < ABS(FL) GOTO 1130
1060  A = 1 : GOTO 1150
1100  NN = 1+(1.25+ T(J)/2)*(1-3.24*(ABS(FR+FL)/90 ↑
      2)
1110  FI = (FR - FL)/2 : GOTO 1150
1120  FI = FR + QQ*FL
1125  NN = 2.25 + T(J)/2 : GOTO 1150
1130  FI = -QQ*FR - FL
1135  NN = 2.25 + T(J)/2
1150  RETURN
1890  FOR J = 1 TO 4 STEP 1
1900  IL(J) = LF(J) - LL(J)
1905  Z(J) = FN F(IL(J)) : NEXT J
1910  REM FINAL OUTPUT FOR ONE ROADWAY
1915  PRINT Z(1), Z(2) , Z(3), Z(4)
1920  PRINT#4, " NOISE AFTER BARRIER AND NET
      INSERTION LOSS:"
1930  PRINT#4
1940  PRINT#4, "CARS:   ", W(1), Z(1)
1950  PRINT#4, "MEDIUM TRUCKS:   ", W(2), Z(2)
1960  PRINT#4, "HEAVY TRUCKS:   ", W(3), Z(3)
1970  PRINT#4, "TOTAL, ALL VH.:   ", W(4), Z(4)
1980  PRINT#4 : PRINT#4
1985  IF LU(4) <<x 0 GOTO 2060
1990  ON NR GOTO 2200, 2000
2000  REM STORE IMPORTANT RESULTS
2010  FOR J = 1 TO 4
2020  LU(J) = LF(J) : LV(J) = LL(J)
2030  NEXT J
2040  GOSUB 2210
2045  GOTO 35
2060  FOR J = 1 TO 4
2070  SS = 10   ↑ (LU(J)/10)+10 ↑ (LF(J)/10)
2080  FF(J) = (10/LOG(10))*LOG(SS)
2085  XU(J) = FN F(FF(J))
2090  RR = 10 ↑ (LLV(J)/10) +10   ↑ (LL(J)/10)
2100  YY(J) = (10/LOG(10))*LOG(RR)
2105  YV(J) = FN F(YY(J))
2110  II(J) = FF(J) - YY(J)
2115  IW(J) = FN F(II(J))
2130  NEXT J : PRINT#4 : PRINT#4
2140  PRINT#4, "TOTALS FROM TWO ROADWAYS:"
2150  PRINT#4 : PRINT
2155  PRINT#4, "NO." , " BEFORE", " AFTER", "
      INS.LOSS"
2160  FOR J = 1 TO 4
2170  PRINT XU(J), YV(J), IW(J)
2180  PRINT#4, J, XU(J), YV(J), IW(J)
2190  NEXT J : PRINT#4
2200  CLOSE 4: END
2210  REM READING NEW DATA FOR SECOND
      ROADWAY
2220  READJ V, Q, R, S1, S2, S3
2230  READ X1, X2, DN, DF, AF
2240  RETURN
3000  REM
3010  REM V, Q, R, S1, S2, S3
3020  DATA 363, 6.612, 6.061, 75, 75, 75
3030  REM
3040  REM NR, X1, X2, DN, DF, AF
3050  DATA 2, -10000, 10000, 60, 60, .50
3060  REM
3070  REM HB, L1, L2, DR, HR, RS
3080  DATA 1.5, -500.0, 500.0, 48.17, 1.5, 1.5
3090  REM
3100  REM
3110  REM V, Q, R, S1, S2, S3
3120  DATA 318, 3.774, 7.862, 75, 75, 75
3130  REM
3140  REM X1, X2, DN, DF, AF
3150  DATA -100000, 10000, 63.66, 63.66, .5
```

Appendix D of Original STAMINA provides an example with similar input, except that HB = 4.0 m, L1 = 17.532 m, and L2 = 132.346 m (*1*).

Notation: Input Terms

NR = Number of roadways: one (1) or two (2).
X1 = Length of visible roadway to the left of the perpendicular receiver line; must be a negative value when measured to the left of that line (exception: skew to the right) (m).
X2 = Length of visible roadway to the right of the perpendicular receiver line; must be a positive value when measured to the right of the line (exception: skew to the left) (m).
DN = Distance of near lane from receiver (m).
DF = Distance of far lane from receiver (m).
AF = Ground absorption coefficient α for free field, to be chosen according to ground cover conditions.
AB = Modified ground absorption coefficient for a field after barrier insertion; for a barrier of normal height, AB = 0.
HB = Barrier height measured from roadway surface level (m).
L1 = Length of the barrier left of the perpendicular receiver line; must be negative when measured to the left of that line (m).
L2 = Length of the barrier right of the perpendicular receiver line; must be positive when measured to the right of that line (m).
DR = Distance between receiver and barrier measured perpendicular to the road axis (m).
HR = Receiver height above the road surface level; can be positive or negative, depending on the ground level at the receiver (standard assumption is 1.5 m above ground level, then add the difference between ground and roadway level) (m).
RS = Standard receiver height above ground level (1.2 m or 1.5 m) (m).
V = Hourly volume of total traffic (number of vehicles per hour, or vph).
P = Percentage of cars and small trucks.
Q = Percentage of medium trucks.
R = Percentage of heavy trucks.

Notation: Calculated Terms

F1, F2 = Subtending angles calculated from X1 and X2.
FL, FR = Subtending angles calculated from L1 and L2 (note that F1 and FL are usually negative values, and all angles are in degrees).
DO = Equivalent lane distance for free field condition (m).
DB = Equivalent lane distance for field with barrier insertion (m).
P1 = Left subtending angle.
P2 = Right subtending angle for a section or segment (note that these are dummy variables).
AL = Ground cover coefficient α.
DE = Equivalent lane distance (m).
PA = Modified subtending angle to the left of the segment (ϕ_1') (in degrees).
PB = Modified subtending angle to the right of the segment (ϕ_2') (in degrees).
PH = PB – PA = $\bar{\phi}$
L(J) = Noise level; output dummy variable (dBA).
LF(J) = Noise level for free field, before barrier (dBA).
LB(J) = Noise level for barrier field or segment (dBA).
LL(J) = Noise level after barrier construction (dBA).
H(J) = Source heights for cars and for medium and heavy trucks (m).
PD(J) = Path length differences (m).
T(J) = Fresnel number (N_0).
D(J) = Noise attenuation (Δ), basic values (dB).
FI, FF = Entrance angle for modifying the noise attenuation value, D(J) (in degrees).
LX(J) = Leakage of noise left of the barrier (dBA).
LY(J) = Leakage of noise right of the barrier (dBA).
IL(J) = Net insertion loss for one roadway (dBA).
FF(J) = Free field noise level from two roadways (dBA).
YY(J) = Noise level from two roadways, after barrier installation.
II(J) = Final net insertion loss for two roadways.

The arrays defined above have different names for the values rounded to three decimal places. For practical application a further rounding to one decimal place is recommended.

Deviations from STAMINA are predominantly conservative, ranging from 0.1 to 0.3 dBA, approximately. The larger errors occur for larger values of D(J). Deviations for free field noise calculations are less than 0.1 dBA.

EXAMPLE AND USER GUIDE

To provide an example and user's guide to using the (low-level) BASIC program, a problem has been chosen that is in manual form in Original STAMINA: Problem 10 (*1*, pp. 39–53). The following values are given:

- Average speed of all vehicles: 75 km/hr in all lanes;
- Vehicles per hour, for eastbound (EB) and westbound (WB) lanes:
  - Cars: EB 317, WB 281;
  - Medium Trucks: EB 24, WB 12;
  - Heavy Trucks: EB 22, WB 25;
  - ΣEB = 363, ΣWB = 318.

These data lead to the following input values:
EB, first roadway:

V = 363 vehicles/hr $S_1 = S_2 = S_3$ = 75 km/hr

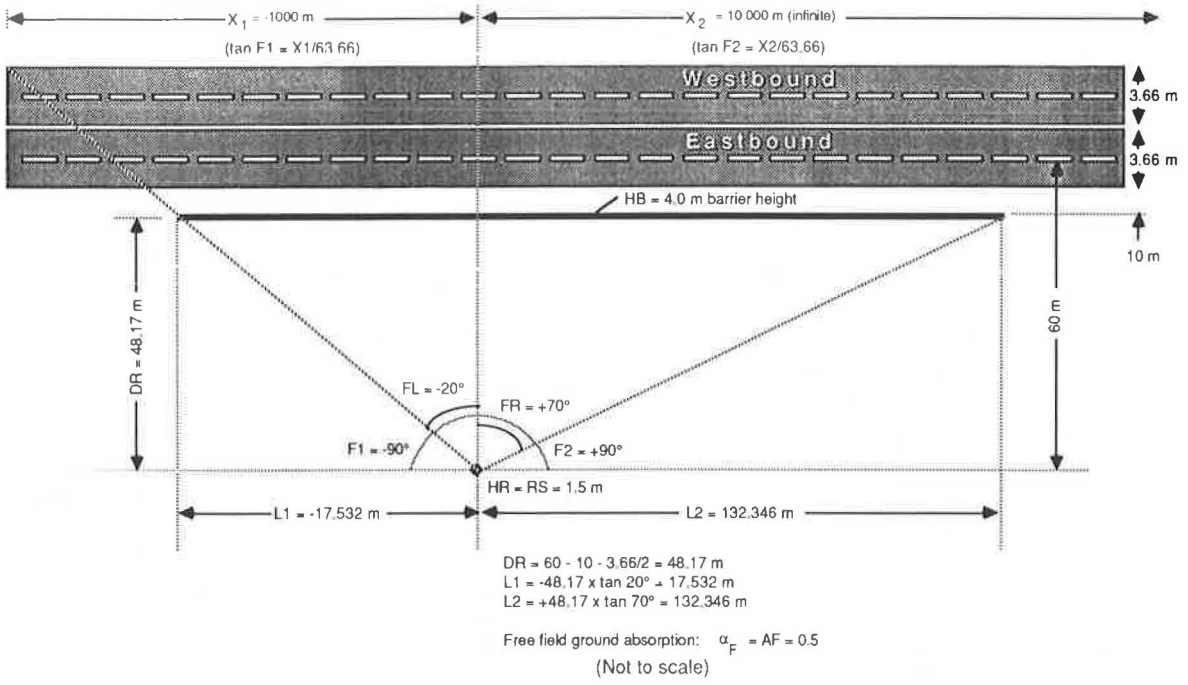

FIGURE 7 Geometric data (not to scale).

$$Q = \frac{24 \times 100}{363} = 6.612 \text{ percent}$$

$$R = \frac{22 \times 100}{363} = 6.061 \text{ percent}$$

WB, second roadway:

V = 318 vehicles/hr $S_1 = S_2 = S_3 = 75$ km/hr

$$Q = \frac{12 \times 100}{318} = 3.774 \text{ percent}$$

$$R = \frac{25 \times 100}{318} = 7.862 \text{ percent}$$

It should be noted that the program will also accept different speeds for the three classes of vehicles and for the two roadways or lanes. In this example the two lanes, EB and WB, are treated as two different roadways because of the difference in traffic volumes. If volumes (and speeds) were identical, the two lanes could be combined on a roadway with different values of D_F and D_N.

A ground cover coefficient is chosen to handle absorption: $\alpha_F = 0.5$. Figure 7 shows the geometric data of the example. For each of the two roadways, EB and WB, the values presented in Table 2 must be obtained from drawings, maps, and other materials (see Figure 7). Input data are listed at the end of the program, using a convenient batch input:

```
3000 REM
3010 REM V, Q, R, S1, S2, S3
3020 DATA 363, 6.612, 6.061, 75, 75, 75
3030 REM
```

TABLE 2 VALUES OF GEOMETRIC DATA FOR THE EXAMPLE

	Value (m)	
	Eastbound	Westbound
Left length of roadway, X1 (negative)	−10 000	−10 000
Left length of barrier, L1 (negative)	−17.532	(−17.532)
Right length of roadway, X2 (positive)	−10 000	10 000
Right length of barrier, L2 (positive)	132.346	(132.346)
Near lane distance, DN	60	63.66
Far lane distance, DF	60	63.66
Receiver distance from barrier, DR	48.17	(48.17)
Barrier height above roadway, HB	4.0	(4.0)
Receiver height above roadway, HR	1.5	(1.5)
Receiver height above ground level, RS	1.5	(1.5)

NOTES: Because there is only one lane per roadway, DN = DF. 10,000 and −10 000 m stand for a practically infinite length of roadway. Values in parentheses need not be repeated because they remain the same for both westbound and eastbound lanes.

```
3040 REM NR, X1, X2, DN, DF, AF
3050 DATA 2, 10000, 10000, 60, 60, .5
3060 REM
3070 REM HB L1, L2, DR, HR, RS (EB & WB)
3080 DATA 4.0, 17.532, 132.346, 48, 17, 1.5, 1.5
3090 REM
3100 REM
3110 REM V, Q, R, S1, S2, S3
3120 DATA 318, 3.774, 7.862, 75, 75, 75
3130 REM
3140 REM X1, X2, DN, DF, AF
3150 DATA 10000, 10000, 63.66, 63.66, .5
3160 REM
```

FREE FIELD NOISE LEVEL AND DELTA VALUES (EB)

CARS:	51.822	15.157
MEDIUM TRUCKS:	51.538	13.878
HEAVY TRUCKS:	55.822	9.649
TOTAL, ALL VEHICLES:	58.304	

NOISE AFTER BARRIER AND NET INSERTION LOSS, ALPHAB = 0

CARS:	48.360	3.461
MEDIUM TRUCKS:	48.204	3.331
HEAVY TRUCKS:	53.249	2.574
TOTAL, ALL VEHICLES:	55.391	2.913

FREE FIELD NOISE LEVEL AND DELTA VALUES (WB)

CARS:	50.912	14.210
MEDIUM TRUCKS:	48.142	12.979
HEAVY TRUCKS:	55.991	9.171
TOTAL, ALL VEHICLES:	57.678	

NOISE AFTER BARRIER AND NET INSERTION LOSS, ALPHAB = 0

CARS:	47.557	3.355
MEDIUM TRUCKS:	44.943	3.200
HEAVY TRUCKS:	53.582	2.409
TOTAL, ALL VEHICLES:	55.002	2.677

TOTAL NOISE BEFORE AND AFTER BARRIER, AND NET INSERTION LOSS

NUMBER	BEFORE	AFTER	INSERTION LOSS
1 CARS	54.401	50.988	3.413
2 MEDIUM TRUCKS	53.174	49.885	3.290
3 HEAVY TRUCKS	58.918	56.429	2.489
4 TOTAL	61.013	58.211	2.802
	L_{eq} (BEFORE)	L_{eq} (AFTER)	I (FOR BOTH, EB & WB)

COMPARISON OF THE TOTAL WITH REFERENCE 1, TABLE 4

BEFORE	AFTER	NET INSERTION LOSS
61.1	58.2	2.9

FIGURE 8 Sample output (Ontario program).

An example of the output produced by the program is presented in Figure 8.

CONCLUSIONS AND RECOMMENDATIONS

The Ontario simplified BASIC program for traffic noise prediction is built on the same first principles of acoustics and uses the same assumptions as STAMINA. With the simplified program, it is possible to use small PCs or pocket calculators in a large range of simple cases to predict traffic noise without loss of accuracy. For suitable cases, there is practically no difference between results obtained with the mainframe STAMINA program and those acquired with the proposed simple method.

The Ontario program, which was presented herein, is eminently suitable for modification by adding or replacing functions of emission levels of vehicle types. Substitute equations for the 1985 research on emission levels are given in the section on the energy level equation. The method of deriving these equations is not shown; however, it can be inferred.

Although vehicle emission levels are a matter of statistics and can be treated accordingly by periodic research efforts, it appears inevitable that there will be uncertainty about the influence of ground absorption. Even more uncertain is the influence of wind and temperature gradients on propagation rates. Could these aspects be researched to a level that would result in improved methods and standards of traffic noise prediction, measurements, or both? Observed changes in the source heights of noise emitted by trucks are another problem. Further research on these issues may be warranted.

Researchers interested obtaining copies of the Ontario program on IBM-compatible diskette should contact author C. T. Blaney. Information on updated versions of the program is also available.

REFERENCES

1. T. M. Barry and J. A. Reagan. *FHWA Highway Traffic Noise Prediction Model.* Report FHWA-RD-77-108. FHWA, U.S. Department of Transportation, 1977.
2. J. J. Hajek and F. W. Jung. *Simplified FHWA Noise Prediction Method.* Report AE-82-05. Ontario Ministry of Transportation and Communications, Downsview, Canada, 1982.
3. F. W. Jung. *Manual Method of Prediction Highway Traffic Noise and Sound Barrier Performance.* Report AE-81-07. Ontario Ministry of Transportation and Communications, Downsview, Canada, 1981.
4. F. W. Jung, C. T. Blaney, and A. L. Kazakov. *Noise Emission Levels for Vehicles in Ontario.* Report HOS-85-02. Ontario Ministry of Transportation and Communications, Downsview, Canada, 1985.
5. R. W. Krawczyniuk and J. J. Hajek. *Guidelines for Noise Barrier Cost Reduction Procedure, STAMINA 2.0 and OPTIMA.* Report AE-83-01. Research and Development Branch, Ontario Ministry of Transportation and Communications, Downsview, Canada, May 1983.
6. F. W. Jung. *Ground Attenuation Effect of Highway Traffic Noise for Height and Distance.* Report AE-83-02. Research and Development Branch, Ontario Ministry of Transportation and Communications, Downsview, Canada, May 1983.

Publication of this paper sponsored by Committee on Transportation-Related Noise and Vibration.

Noise Barriers and the Community Involvement Process

DIANE SELVAGGI SEIGEL

In this paper, the community involvement process used in the New Jersey Department of Transportation (NJDOT) noise program is examined. The procedure for carrying out the community involvement process is discussed, and the results of a case study project are presented. On those highway projects for which construction of noise abatement devices is recommended, NJDOT requires the approval of the mayor and council of the municipality in which the abatement will be built before construction may begin. The mayor and council also have the power to oppose the recommended noise abatement, in which case the noise mitigation structures will not be constructed. The decision of the mayor and council is obtained through the NJDOT community involvement process, which includes meetings with the mayor and council as well as public information centers for the affected residents. NJDOT has found this method to be successful and will continue its use on future projects for which noise abatement is an issue.

The New Jersey Department of Transportation (NJDOT) conducts noise studies on both new alignment projects and improvement projects (e.g., widening, vertical or horizontal alignment changes, safety upgrades, or resurfacing). If noise impacts are identified, mitigation measures are investigated for feasibility and effectiveness in addressing the noise abatement provisions of FHWA's *Federal Highway Program Manual,* Volume 7, Chapter 7, Section 3 (or FHPM 7-7-3) (*1*). On projects for which noise abatement has been recommended, NJDOT requires the approval of the mayor and council of the municipality in which the abatement structure will be built before construction may begin. The mayor and council also have the power to oppose the recommended noise abatement, in which case the noise mitigation structures will not be constructed. The decision of the mayor and council is obtained through the NJDOT community involvement process, which includes meetings with the mayor and council and conferences called "public information centers" for the affected residents.

In the first part of this paper, a detailed discussion of the steps of the NJDOT community involvement process is provided. This is followed by a case study of a construction project in which the NJDOT community involvement process played a major role in the outcome of noise abatement construction.

Bureau of Environmental Analysis, New Jersey Department of Transportation, 1035 Parkway Avenue, CN 600, Trenton, N.J. 08625.

NJDOT COMMUNITY INVOLVEMENT PROCESS STUDY METHOD

The NJDOT community involvement process for noise studies consists of four basic steps:

1. The noise study is conducted.
2. The meeting with the mayor and council is held.
3. The public information center is held.
4. The noise study is completed.

It is important that each of these four steps be included in the process to ensure that all of the involved individuals are properly informed of NJDOT's recommendations and that the correct procedure is followed for incorporating any changes to the recommendation as a result of public opinion.

Noise Study Conducted

Before the completion of the environmental document (Environmental Assessment, EA, or Environmental Impact Statement, EIS), a Technical Environmental Noise Study (TES) of the project area is conducted to identify existing and predicted noise impacts and preliminary areas for noise abatement. While the predicted noise impacts are being determined, all roadway design alternatives are considered, along with the "no-build" or "do-nothing" case (*2*). The criteria used to gauge the effect of the traffic-generated noise levels on the study area are the Noise Abatement Criteria (NAC) given in the *Federal Highway Program Manual* (FHPM). According to the guidance available from the FHWA New Jersey Divisional Office, a project is defined as having noise impacts should either of the following conditions occur:

- Predicted L_{eq} noise levels approach or exceed the NAC given in Table 1. According to the New Jersey FHWA District Office, a 3-dBA change in noise levels is the threshold of perception. Therefore noise levels that approach the criteria are defined as occurring at 3 dBA less than these criteria (*2*).
- A substantial increase in predicted noise levels over existing noise levels occurs, even though the impact criteria level is not reached. This increase is considered to be 10 dBA or greater, which is roughly a doubling or more of the perceived noise levels. Increases in noise levels that approach 10 dBA may be evaluated and discussed as circumstances dictate (*2*).

When estimated noise levels are projected to approach or exceed the NAC, or when there are substantial increases in predicted noise levels over existing noise levels, an evaluation

TABLE 1 NOISE ABATEMENT CRITERIA (*1*)

Activity Category	Noise Abatement Criteria (dBA) L_{10}	L_{eq}	Description of Activity Category
A (Exterior)	60	57	Tracts of land for which serenity and quiet are of extraordinary significance and serve an important public need and where the preservation of those qualities is essential if the area is to continue to serve its intended purpose. Such areas could include amphitheaters, particular parks, or portions of parks, open spaces, or historic districts that are dedicated or recognized by appropriate local officials for activities requiring special qualities of serenity and quiet.
B (Exterior)	70	67	Picnic areas, recreation areas, playgrounds, active sports areas, and parks that are not included in Category A, and residences, motels, hotels, public meeting rooms, schools, churches, libraries, and hospitals.
C (Exterior)	75	72	Developed lands, properties, or activities not included in Category A or B above.
D	–	–	For requirements on undeveloped lands, see paragraphs 11*a* and *c* of *Federal Aid Highway Program Manual*, Volume 7, Chapter 7, Section 3.
E (Interior)	55	52	Residences, motels, hotels, public meeting rooms, schools, churches, libraries, hospitals, and auditoriums.

of noise mitigation measures is made to address the noise abatement provisions of FHPM 7-7-3 (*2*). Calculations to determine impacts are performed with the FHWA Noise Model (*3*) and the noise barrier cost reduction procedure STAMINA 2.0/OPTIMA (*4*).

After the approval of the EA or EIS, a Final Noise Study (FNS) is conducted to finalize the number of noise impacts for the chosen roadway design alternative and determine details of noise barrier design, such as lengths, heights, and location, and the number of noise impacts mitigated. NJDOT considers three factors in justifying the recommendation and construction of noise abatement: adequate attenuation, engineering and design feasibility, and cost effectiveness (*2*). These three factors are considered as follows:

- *Does the mitigation measure provide adequate attenuation?* NJDOT's initial goal in designing a barrier is to reduce the noise by at least 10 dBA, which will be perceived as a halving of the noise level. However, the 10-dBA goal is not an absolute value, and reductions that approach or exceed 10 dBA will be considered on the basis of the barrier's cost effectiveness.
- *Is the mitigation measure feasible from an engineering and design standpoint?* Physical features of the project area are studied to determine what types of mitigation devices, if any, may be constructed. For example, if available state-owned right-of-way (ROW) is limited, construction of an earthen berm may not be possible without extensive easements or parcel purchases. Therefore a freestanding noise barrier may be the only option for abatement. Other points to consider include topography, access areas to the roadway, and utilities.
- *Is the mitigation measure cost effective for the number of impacts mitigated?* NJDOT determines cost effectiveness on a case by case basis by comparing the "cost per residence mitigated" figures of all mitigation measures on a single project. There are no established state or federal standards for this figure. If abatement is recommended on a particular project for only one area, cost figures are compared to a similar project to determine cost effectiveness.

If the noise mitigation measure meets all three criteria, then it is recommended for construction. NJDOT's Bureau of Environmental Analysis coordinates with the bureaus of Landscape, Design, and Structures to decide on a barrier material and any aesthetic finishes to the barrier faces. NJDOT generally selects either concrete or wood for the noise barriers on the basis of the nature of the surrounding area (urban, suburban, or rural), favorable past experiences with construction ease, and public responses to barriers that have already been constructed. Before construction and preferably before final design, however, NJDOT requires approval from the municipality in which the abatement is to be constructed. This leads to direct involvement with the community.

Meeting with Mayor and Council

Representatives from NJDOT meet with the local mayors and councils of the municipalities for which the noise abatement is recommended. The purpose of this meeting is to present the recommended noise abatement to the mayor and council and request any necessary easements. The mayor and council are also informed of the date that the public information center meeting will be held. NJDOT then requests a resolution that states whether the mayor and council are in favor of or opposed to the recommended noise abatement scheme. Receipt of the resolution is requested in 30 days' time from the date of the public information center.

It is recommended that the borough or township engineer review NJDOT's recommendation for abatement. As a result, the mayor and council will occasionally ask for specific changes to the noise abatement presented by NJDOT, such as barrier alignment shifts or additional landscaping. NJDOT

always considers the input from the mayor and council and makes every effort to incorporate these changes into the project, if they are feasible and requested for valid reasons.

Public Information Center

After the meeting with the mayor and council, NJDOT representatives hold a public information center at a convenient local site within or near the borough. The residents who will be affected by the recommended noise abatement are invited to attend. The purpose of this meeting is to inform the residents of NJDOT's proposal for noise mitigation measures. General location and abatement specifics are presented, followed by a question-and-answer session. It is suggested that the residents contact their mayor and council to voice their concerns about and opinions of the noise abatement.

The NJDOT representatives informally present the recommended abatement scheme, using project displays and aerial photography. The locations of the noise abatement are noted, along with the noise level contours for the "existing," "predicted," and "predicted-with-abatement" conditions. The existing noise levels are determined by random monitoring of Category A or B areas near the project corridor (see Table 1). The predicted and predicted-with-abatement noise levels are calculated for a design year of the roadway roughly 20 years after the outset of the project. These predicted values are determined by using the STAMINA 2.0/OPTIMA computer models (*4*) and future traffic projections.

Photomontages or artist's renderings are also used to give the homeowners an idea of the appearance of the abatement measure after it has been constructed. The perspective used on the montages and renderings is usually from the resident's viewpoint; that is, the view is from the yard of a home that has been predicted to have a future noise impact, looking toward the roadway. It is useful to provide before and after montages or renderings to help the residents visualize the noise abatement and the effects that it may have on their property. If possible, samples of the barrier material are also provided, complete with color and aesthetic treatment.

NJDOT has produced an educational videotape, "A Community Primer," that is shown at the public information center. The videotape explains the basic concept of decibels and shows existing noise barriers throughout the state of New Jersey. After the community members have seen the primer, a videotape of the project area is shown that contains footage of noise-sensitive areas for which abatement has been recommended. Noise levels of the existing, predicted, and predicted-with-abatement conditions are dubbed in and played for the residents so that they can hear what the difference will be in their noise environment as a result of the construction project.

Finally, taped testimony of individual residents' opinions on the recommended abatement is taken, if this material has been requested by the municipal mayor and council. This tape is then submitted to the mayor and council to help them in their decisions on the resolution of the noise abatement issue.

Noise Study Completed

After public opinions have been heard and any requested changes to the noise abatement are studied, NJDOT receives the resolution from the mayor and council. If the resolution is in favor of the recommended abatement, then final design will proceed, followed by eventual construction. The NJDOT noise report is finalized by stating that noise abatement will be constructed as presented in the report because the municipality passed a resolution declaring approval of the abatement as a result of the community involvement process.

If the resolution is in opposition to NJDOT's recommendation, then this opposition is incorporated into the noise report by discussing the community involvement process and the steps that led to the rejection of the abatement by the community. It is also stated that although noise abatement measures were warranted and offered by NJDOT, they will not be constructed, in accordance with the resolution passed by the municipality, who opposed the abatement through the community involvement process. The finalized noise study report is then submitted to FHWA for their concurrence (*2*).

After FHWA issues approval, the noise study is also given to the local governments and planning agencies for their review. Local governments, as well as local and regional planning boards, may be interested in the effect of traffic noise and may use the information provided in the noise study report to help establish ordinances and zoning and to implement planning so that the community as a whole could benefit by a quieter environment.

CASE STUDY: NJ-17, BERGEN COUNTY, NEW JERSEY

Project Description

Description of the Proposed Action

New Jersey Route 17 is located within the New Jersey portion of the Metropolitan Area of Greater New York and functions as a major through route between the highly populated northeast region of New Jersey and New York State (Figure 1). NJ-17, for most of its length, also functions as an urban arterial roadway, carrying local traffic that is heading toward the commercial strip located along most of the highway's length. NJ-17 also functions as a secondary Central Business District for many of the towns through which it passes.

The Route 17 Widening Project involved the improvement and upgrading of 7.4 mi of the roadway. The project limits extended from south of Linwood Avenue, in Ridgewood, to the Franklin Turnpike, in Ramsey. Between these limits, the project also crossed portions of the municipalities of Ho-Ho-Kus, Waldwick, Saddle River, Allendale, and Upper Saddle River (Figure 2). As a result of the environmental studies and the community involvement process, nine noise barriers were constructed to mitigate noise impacts on the residential areas through which NJ-17 passes.

Project Need

The Route 17 Widening Project had been developed in response to the increase in traffic volumes and accident rates in Bergen County within the previous decade. For example, the average daily traffic (ADT) for NJ-17 in 1971 was 49,848; it increased to 60,524 in 1981. NJDOT technical studies have shown that NJ-17 operates at levels of service D and E.

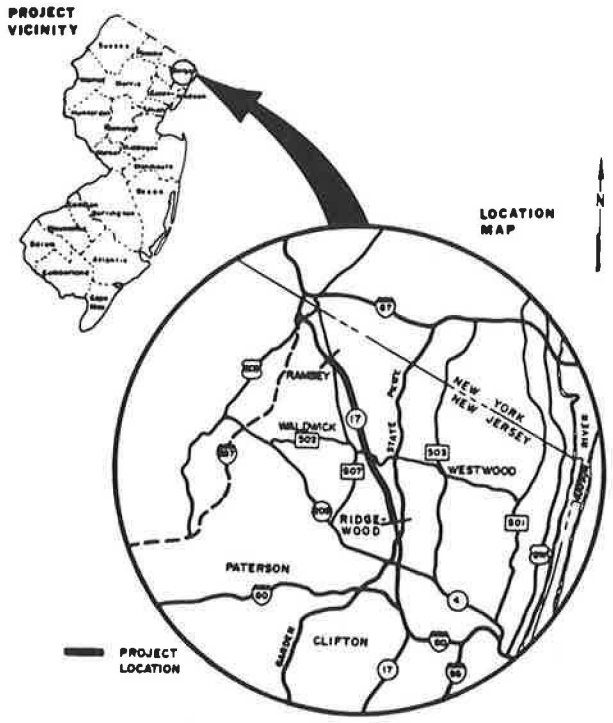

FIGURE 1 NJ-17 project vicinity and location map.

The accident rate increased from 3.46 per million vehicle miles in 1971 to 3.81 in 1981. In 1982, the total number of accidents was 557, with 311 people injured and 5 fatalities on this section of NJ-17. In 1983 there were also 5 fatalities. For 1983, 12.5 percent of the fatal accidents in Bergen County occurred on this route. In March 1983, the Center for Auto Safety included NJ-17 on the list of the 10 most dangerous roads in the United States.

Except for the construction of grade-separated interchanges, major improvements to the roadway have not occurred since the mid-1950s, when the highway was dualized. Safety improvements were needed, especially in the center median, where crossover accidents had occurred (3 percent of the total accidents). A permanent center concrete median barrier curb was required as a safety measure to prevent this type of accident. Resurfacing was also necessary because of the deterioration of parts of the roadway.

NJDOT had also received a large amount of correspondence from local residents and municipalities, expressing concern about the existing conditions on NJ-17 and showing support for the proposed improvements. Comments included opposition to the acquisition of private land for the project, support for mitigation of possible noise impacts with noise barriers, and concern for safety problems because of the lack of a center median barrier curb (*5*).

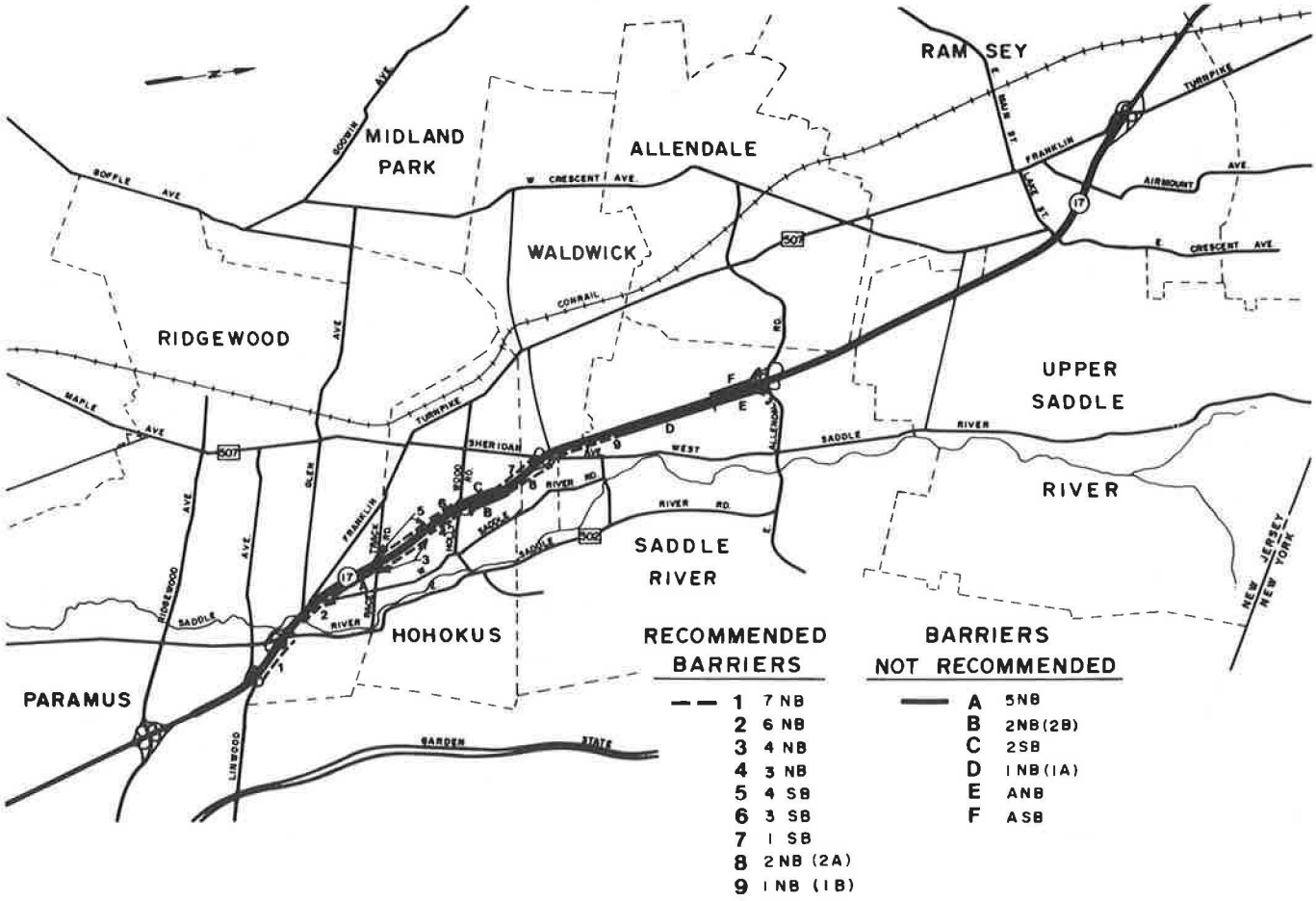

FIGURE 2 Project limits and barrier locations.

Alternatives Considered

NJDOT considered various alternatives to improve the NJ-17 roadway. These alternatives were developed in an attempt to minimize the environmental impact on the local residents and businesses, to minimize the ROW acquisition that would be required because the corridor is heavily developed, and to improve safety for the motoring public. Alternatives considered included widening and safety improvements (the chosen alternative), mass transit, and no-build.

Widening and Safety Improvements (Build Alternative) This alternative was chosen because it met transportation objectives established for the NJ-17 corridor, including increased safety for motorists as well as pedestrians, relief of extreme congestion on NJ-17 and connecting arteries, repair of severely deteriorated sections of the roadway, and lessened environmental impacts, such as air and noise pollution. Along with the build improvements, transportation system management improvements will also be enacted, as discussed next.

Mass Transit The existing mass transit system in Bergen County consists of bus and rail facilities. The mass transit alternative alone is not a practical solution to the problems of NJ-17 because the route is a land service roadway that primarily functions as a means of access to local commercial establishments from local residential areas. Congestion will not be alleviated by mass transit improvements alone. The most reasonable solution is to combine the widening and safety improvements of this project with improvements to the mass transit system and encouragement of ridesharing.

No-Build The no-build alternative was rejected because of the necessity of the improvements on NJ-17. The objectives of improving traffic flow and safety would not be realized without changes. The problems associated with the roadway would continue, and the safety of the motoring public would deteriorate. Selection of the no-build alternative could also eventually have had a negative effect on the economy of the area because as congestion increased, customers would have avoided commercial establishments located on NJ-17.

Noise Abatement Summary

The Route 17 Widening Project in Bergen County, New Jersey, crosses residential portions of four municipalities, namely

- Borough of Ridgewood,
- Borough of Ho-Ho-Kus,
- Borough of Waldwick, and
- Borough of Saddle River.

The portions of other municipalities through which the NJ-17 contract passes are primarily commercial areas adjacent to the highway.

A noise study was conducted for the project area to identify the number of noise impacts for the existing, predicted, and predicted-with-abatement conditions. Within the four municipalities mentioned, the number of receptors predicted to have noise impacts is 357. As a result of the noise study, NJDOT recommended the construction of 11 noise barriers, totaling 2.9 mi in length, to mitigate the noise impact at 283 of these receptors. However, the community involvement process resulted in the approval for construction of only nine noise barriers, with a total length of 2.1 mi. Therefore the total number of impacts mitigated will be reduced by 108, for a total of 175 (Tables 2 and 3).

TABLE 2 PREDICTED NOISE IMPACTS ALONG THE NJ-17 WIDENING PROJECT (DESIGN YEAR 2004)(*6, 7*)

Municipality	Predicted	Predicted, with Recommended Abatement	Predicted, with Constructed Abatement
Ridgewood	79	40	50
Ho-Ho-Kus	116	5	5
Waldwick	137	5	102
Saddle River	25	24	25
Total impacts	357	74	182
Impacts mitigated	n/a	283	175

TABLE 3 RECOMMENDED AND CONSTRUCTED NOISE BARRIERS ALONG THE NJ-17 WIDENING PROJECT (*6, 7*)

	Recommended		Constructed	
Municipality	Abatement (Barriers)	Impacts Mitigated	Abatement (Barriers)	Impacts Mitigated
Ridgewood	2	39	2	29[a]
Ho-Ho-Kus	5	111	5	111
Waldwick	4	132	2	35
Saddle River	0	1	0	0

[a]The reduction in impacts mitigated is due to the shortening of one barrier by 600 ft in length.

The existing noise levels along the project corridor range from 59 to 77 dBA L_{eq}. The predicted levels were only slightly higher, ranging from 63 to 77 dBA after the additional lane was constructed. The average insertion loss of the barriers is 10 dBA, which is the "goal noise reduction" for noise barriers in New Jersey. As determined from the accepted bid prices, the noise barriers that were constructed cost approximately $2.8 million in 1985 dollars (*5, 6*). The following material provides profiles of the individual municipalities and descriptions of how the community involvement process affected the outcome of the construction of noise abatement.

Residential Municipalities: Profiles and Results

Borough of Ridgewood

The first residential municipality through which NJ-17 passes is the established upper–middle class Borough of Ridgewood. In this location, 79 residential noise impacts were identified. The residents and borough council were receptive to the construction of barriers, and the council voted favorably on the barriers recommended by NJDOT. The result was the construction of two noise barriers to mitigate 29 noise impacts.

For the most part, the community was in favor of the barriers. However, one of the barriers was shortened by 600 linear feet because of residential opposition. The noise levels at the 10 homes protected by this 600-ft section of barrier were projected to approach the NAC, and the residents felt that the

noise would not be enough of a problem to warrant the construction of the entire barrier. The barrier ended in the middle of a bermed area, and the end of the barrier was gradually stepped down to avoid an abrupt appearance.

The barriers were constructed in a post and panel style, with 8-in. concrete stacked panels. The concrete is tinted a blend of Sequoia Sand and Salmon, and both sides of the barriers have a Midland Staggered form-lined aesthetic treatment. While the barriers were under construction, every effort was made to preserve the existing mature vegetation on the residential side. Because of these efforts, the tinted barrier blends well with the surroundings. The barriers in Ridgewood range in height from 14 to 16 ft and have a total length of 0.4 mi.

Borough of Ho-Ho-Kus

The Borough of Ho-Ho-Kus, like Ridgewood, is an established middle-class community. In Ho-Ho-Kus, 116 residential impacts were identified.

The Ho-Ho-Kus residents were the first to request construction of noise barriers on a land service road in New Jersey. One very concerned resident educated himself on state and federal noise policies and then organized a community coalition to support the installation of noise barriers. After numerous noise complaints, many meetings, and reams of correspondence, the coordination between the community and NJDOT resulted in the construction of five noise barriers to mitigate 111 residential noise impacts. The community was overwhelmingly in favor of the barrier recommendation. They also wanted an additional barrier to be constructed in an area that had been studied, but the barrier had already been deemed not cost effective by NJDOT.

Again, existing mature vegetation was preserved on the residential side of the barrier, and the barriers blend well with the environment. The five barriers constructed in Ho-Ho-Kus range in height from 12 to 18 ft and have a total length of 1.3 mi. The Ho-Ho-Kus barriers created a parallel situation and were tilted 6 degrees away from the highway to reduce multiple noise reflections, which might have degraded the barriers' attenuating performance.

Borough of Waldwick

The Borough of Waldwick is also an upper–middle class community of established homes. Waldwick is unique in that its homes are the closest to the NJ-17 alignment in the entire project. Many are within 30 ft of the closest traveled lane. As a result, the existing noise levels measured at the homes in Waldwick are the highest in the project: noise levels as high as 77 dBA L_{eq} were measured.

On the northbound side of NJ-17 as it passes through Waldwick, all of the side streets have been closed to access to and from NJ-17. On the opposite, southbound side, the streets remain open to NJ-17 access.

In Waldwick, 137 noise impacts were identified. NJDOT's original barrier recommendation did not include abatement for the residences on the southbound side of the highway because the side streets retained access. The mayor and council requested that a barrier be studied for this side of NJ-17 and that if it were found feasible, they would close the side streets off to allow the barrier to be continuous.

NJDOT deemed an additional barrier feasible on the southbound side and recommended it for construction. However, after numerous meetings with the mayor, council, and residents, the two barriers that had been recommended for both sides of the highway were rejected for a number of reasons, including the following:

- The barriers would cause unmanageable traffic patterns on the local roads.
- The resulting traffic patterns would, in turn, cause a safety problem for pedestrians.
- If a single barrier were constructed, perceivable levels of noise would reflect off the barrier to the residences on the other side of the highway, making an already unfavorable noise environment much worse.

NJDOT had recommended four noise barriers to mitigate 132 impacts, but as a result of the community involvement process, only two barriers were constructed to mitigate 35 residential impacts.

As in the other municipalities, mature vegetation was restored on the residential side of the barrier to blend the barrier in with the surrounding area. The two barriers built in Waldwick range in height from 12 to 18 ft and have a total length of 0.4 mi. They are also parallel and so were tilted 6 degrees to reduce noise reflections. The barriers rejected by the borough council would have totaled 0.8 mi along the most densely populated area of the project.

Borough of Saddle River

The Borough of Saddle River is a growing, elite upper-class community with specific designs for future development. The borough has 2-acre zoning for single family residences.

In Saddle River, only 25 residential noise impacts were identified, all of which would have had noise levels approaching the NAC. This total included vacant lots that already had approved building permits for homes. The homes are located, on the average, 200 ft from the traveled way.

No noise barriers were recommended by NJDOT because these abatements would not be cost effective if the number of impacts that would be mitigated by the barrier were considered. An effective noise barrier would have to be ~0.9 mi long to mitigate 19 impacts. In comparison with the other abatements constructed on the project, the Saddle River noise abatement was unreasonably expensive and therefore not recommended.

The residents of Saddle River are strongly in favor of noise abatement, and they formed a community coalition for the construction of barriers. After numerous meetings and correspondence, the coalition sued the state of New Jersey in an attempt to direct the state to build their barriers. The suit was dismissed on premature grounds. At the time of writing, settlement was in progress, including discussions on alternatives. One possibility was a berm/wall proposal that had originally been rejected by the residents but was now being reconsidered.

CONCLUSIONS

The community involvement process has proved to be a valuable decision-making tool in the noise abatement process in New Jersey. Because the municipalities have the chance to voice the concerns of the public and because NJDOT considers their input, the final noise barriers may be more satisfactory to those who live in the area. Also, if the noise abatement recommended by NJDOT is rejected by the municipality, money is saved for the state and federal governments, and the municipality is saved from being burdened with a structure that is not favored by its residents. By dealing with the local municipal governments instead of directly with each affected resident, NJDOT receives organized input from the public in less time than a survey of the entire population would take. This time savings allows room in the project schedule for minor design or landscaping changes as a result of public opinion. NJDOT will continue to use the community involvement process on all projects for which noise abatement is recommended.

REFERENCES

1. *Federal Aid Highway Program Manual.* FHWA, U.S. Department of Transportation, Washington, D.C. August 9, 1982.
2. J. J. Kessler, L. J. Jacobs, and F. H. Zahn. *Noise Policy and Procedure.* New Jersey Divisional Office, FHWA/Division of Project Development, New Jersey Department of Transportation, Trenton, August 23, 1984.
3. *Federal Highway Administration Highway Traffic Noise Prediction Model: Guidance on Use.* Technical Advisory, FHWA, U.S. Department of Transportation, Washington, D.C. August 22, 1980.
4. W. Bowlby, J. Higgins, and J. Reagan. *Noise Barrier Cost Reduction Procedure, STAMINA 2.0/OPTIMA: User's Manual.* Report FHWA-DP-58-1. FHWA, U.S. Department of Transportation, April 1982.
5. L. J. Jacobs, E. J. Wisniewski, K. Hart, and B. J. Hawkinson. *Environmental Assessment, Route 17 Widening Project.* Report FHWA-NJ-EA-85-02. FHWA, U.S. Department of Transportation/ New Jersey Department of Transportation. Trenton, February 1985.
6. D. N. Selvaggi. *Final Noise Study, Route NJ 17, Sections 5AA and 6J, 5AC.* Bureau of Environmental Analysis, New Jersey Department of Transportation, Trenton, June 1985.
7. D. Selvaggi Seigel. *Final Noise Study: Route NJ 17, Section 6J, 5AC.* Bureau of Environmental Analysis, New Jersey Department of Transportation, Trenton, June 1987.

Publication of this paper sponsored by Committee on Transportation-Related Noise and Vibration.

Overview of NJDOT's Noise Mitigation Program

ROBERT C. CEBRICK

In this paper, the specific noise procedures by which the New Jersey Department of Transportation (NJDOT) studies and constructs noise mitigation measures are discussed. Details on NJDOT's noise impact definition and environmental process are provided, along with a summary of NJDOT's noise mitigation program that highlights the type and cost of such measures. In addition, specific mitigation projects are presented as examples of concrete, wood, and metal freestanding walls. Two environmentally sensitive projects, I-78 Watchung and I-295/I-195, are discussed in depth. Finally, NJDOT's standardized designs for concrete and wooden walls are described.

The purpose of this paper is to present an overview of the noise mitigation process in New Jersey by providing some background on New Jersey Department of Transportation (NJDOT) procedures and a composite view of the state's noise mitigation projects. The report begins with a brief outline of the policies that define a noise impact and the criteria for recommending noise barriers, and ends with a presentation of the results of the noise mitigation program and preferred barrier types.

FEDERAL PROCEDURES

The Federal Highway Procedures for Abatement of Highway Traffic Noise (FHPM 7.7.3) provide a listing of various land uses and define their noise sensitivity. These categories are presented in Table 1. Although Category A and Category E areas are occasionally evaluated, Category B areas are the primary concern. Category B areas include residences, exterior school areas, and parks, whereas Category A contains lands for which serenity is of special significance and Category E areas are the interiors of public schools, libraries, and hospitals.

As written, the procedures provide considerable latitude for interpretation on the part of the FHWA division office and the state transportation agency. The definition of a noise impact that is used in this paper was developed from these procedures in conjunction with the FHWA division office.

NOISE IMPACT CRITERIA

The first definition of a noise impact is "predicted L_{eq} noise levels that approach or exceed the Noise Abatement Criteria," as given in Table 1. Because a 3-dBA change in noise levels approximates the threshold of perception, noise levels that approach the criteria are defined as occurring at 3 dBA less than this criterion.

The second definition is "a substantial increase in predicted noise levels over existing noise levels, even though the impact criteria level is not reached." The increase is considered to be 10 dBA or greater, which is a doubling or more of the perceived noise level. This criterion is not considered to be an absolute; increases in noise levels approaching 10 dBA may be evaluated and discussed as circumstances dictate.

When noise impacts are identified on a federally funded project that involves new alignment, lane addition, or horizontal or vertical modifications, FHWA regulations require an evaluation of noise mitigation measures. The lead NJDOT unit responsible for evaluating the need for noise mitigation and recommending such measures is the Bureau of Environmental Analysis (BEA). BEA was established as a unit within NJDOT to assess social, economic, and environmental factors in the development of highway projects. The multidisciplinary staff is capable of assessing such factors as water quality, ecology, socioeconomics, archaeology, historic architecture, air quality, aesthetics, hazardous waste, and noise. As highway projects are developed, they are given a Level of Action classification by BEA. As a result, the projects are then processed with one of the following procedures:

- Environmental Impact Statement (EIS),
- Environmental Assessment (EA), or
- Categorical exclusion.

A noise study, known as a Technical Environmental Study (TES), is generally performed only for EIS and EA documents. These environmental documents are compiled during the early stages of project development. If noise mitigation measures are recommended at this stage, then a Final Noise Study (FNS) is conducted as part of the final design of the project.

RECOMMENDED MITIGATION GUIDELINES

During the final design of a project, NJDOT will recommend the incorporation of noise barriers into a project if the following criteria are satisfied:

- The barriers are effective in providing a significant reduction in noise levels while also eliminating the majority of noise impacts identified. The initial goal used in designing a barrier is to reduce noise levels by at least 10 dBA. However, the 10-dBA goal is not an absolute value, and reductions approaching

New Jersey Department of Transportation, Bureau of Environmental Analysis, 1035 Parkway Avenue, Trenton, N.J. 08625

TABLE 1 FEDERAL HIGHWAY ADMINISTRATION NOISE ABATEMENT CRITERIA

Activity Category	Noise Abatement Criteria (dBA) L_{10}	L_{eq}	Description of Activity Category
A (Exterior)	60	57	Tracts of land for which serenity and quiet are of extraordinary significance and serve an important public need and where the preservation of those qualities is essential if the area is to continue to serve its intended purpose. Such areas could include amphitheaters, particular parks or portions of parks, open spaces, or historic districts that are dedicated or recognized by appropriate local officials for activities requiring special qualities of serenity and quiet.
B (Exterior)	70	67	Picnic areas, recreation areas, playgrounds, active sports areas, and parks that are not included in Category A, and residences, motels, hotels, public meeting rooms, schools, churches, libraries, and hospitals.
C (Exterior)	75	72	Developed lands, properties, or activities not included in Category A or B above.
D	–	–	For requirements for undeveloped lands, see paragraphs 11*a* and *c* of the *Federal Aid Highway Program Manual*, Volume 7, Chapter 7, Section 3.
E (Interior)	55	52	Residences, motels, hotels, public meeting rooms, schools, churches, libraries, hospitals, and auditoriums.

or exceeding 10 dBA will be considered on the basis of reasonable cost.

- The barriers are reasonable in cost, considering the number of impacts mitigated.
- The barriers are feasible from a design perspective. For this criterion, the barriers are reviewed to evaluate any potential drainage problems, structural problems, or other design constraints.
- There is favorable community input.

NOISE PROGRAM BACKGROUND AND RESULTS

Since 1979, more than 19 mi of noise barriers have been constructed in New Jersey at a cost of more than $20 million. If those projects currently in final design are considered, an additional 22 mi of barriers will be constructed in the next 2 yr (Figure 1).

The vast majority of noise mitigation devices used in New Jersey have been free-standing walls. As can be observed in Table 2, concrete and wood are the primary types. Metal walls are restricted to those areas where dead load restrictions prohibit the use of wood or concrete (i.e., on bridges and retaining walls).

From an aesthetic viewpoint, earth berms would be the first choice for noise barriers. Because of a lack of the necessary right-of-way (ROW) in most projects, however, the use of this measure has been limited. Favorable noise mitigation results have been achieved with gabion walls on several recent projects, but because of ROW limitations, the use of such walls on future projects will be restricted. Design modifications have been incorporated into several projects and include such measures as a depressed roadway profile and the construction of ramps on fill instead of on structure.

Insulation of school buildings has been used at a number of projects to either mitigate construction noise or eliminate the impact of future traffic noise. These measures included the use of central air conditioning, unit air conditioning, and building modifications such as window replacements.

TABLE 2 NOISE BARRIER MATERIALS USED IN NEW JERSEY

Type	Constructed Length (mi)	Constructed Cost ($)	To Be Constructed Length (mi)	To Be Constructed Cost ($)
Concrete	15.40	16,302,000	15.41	23,878,600
Wood	3.06	3,495,000	2.24	2,322,000
Metal	0.78	462,000	0.63	822,000
Gabions or berms	0.51	(no cost)	4.10	4,869,000
School insulation	NA	611,000	NA	815,100
Total	19.75	20,260,000	22.38	32,706,000

MITIGATION PROJECTS

It is useful at this point to examine two projects that are significant examples of noise mitigation in New Jersey. These projects provide examples of two types of freestanding walls. Examples of other types of walls are also briefly considered.

Concrete Barriers on I-78

This project was considered to be very sensitive because it skirted the 2,000-acre Watchung Reservation. The plan involved the construction of a 5.5-mi, six-lane section of I-78. In conjunction with this project, an adjacent section of existing I-78 was upgraded (Figure 2).

Highway noise was a major consideration during the environmental analysis of I-78, in addition to concerns about parkland displacement and the effects on wildlife. After the noise study was conducted during the EIS phase, numerous final noise studies were undertaken during the highway's design phase. In all, seven final noise studies were completed, corresponding to each of the construction contracts.

Because of the project's sensitive nature, NJDOT took care to use mitigation treatments that were compatible with the environment. During the final noise study process, an aesthetics committee was formed to review and select the material type, color, and architectural treatments for the walls. The committee included representatives from the BEA; the

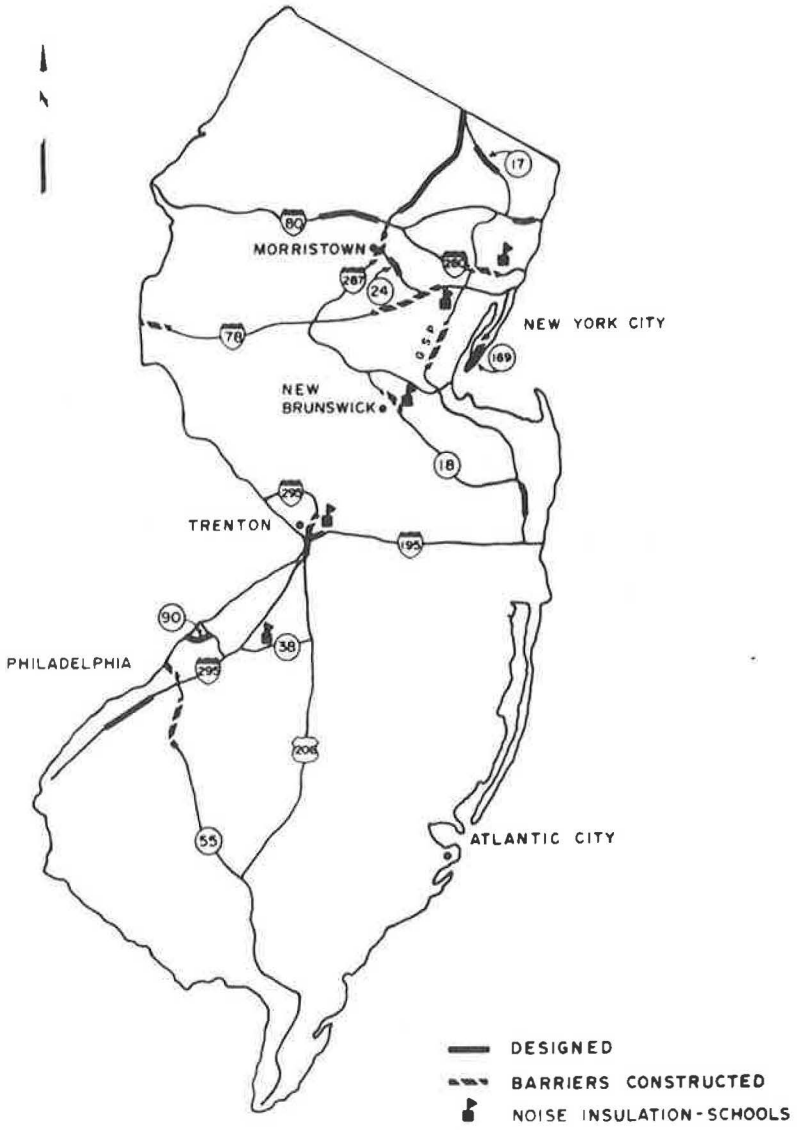

FIGURE 1 Location of noise mitigation measures designed or constructed in New Jersey.

NJDOT design, structures, and landscape divisions; and FHWA. The Watchung Park Commission was opposed to the construction of wooden walls, mainly because of their fire potential. For this reason, the committee selected concrete walls as the barrier type for this project.

To provide texture on the highway side of the concrete walls, a grape stake form liner was used. All noise barriers within the reservation were integrally tinted with an earth tone color (Pueblo Brown) that was selected to blend with the surrounding rock formations. The residential (nonhighway) sides of the walls have a "fuzzy finish" treatment (Figure 3). This finish is made by texturing the wet concrete surface to a rough finish with an asphalt rake in such a manner that tine marks do not remain. The fuzzy effect is a result of the contrast produced on the rough surface by reflection of light.

The final noise studies, under the direction of FHWA, proposed nearly 9 mi of noise barriers at a cost of $8.5 million. Construction of the project began in October 1982 and was completed in August 1986.

Basically, three types of barriers were used along this project. An integral panel and post barrier system, known as a "Sierra Wall," was the first barrier constructed along the site. The panel of the noise barrier is cast with one post, and the post is bolted to a footing that interlocks with an adjoining post and panel. As with all the barriers within the Watchung project, the posts and panels are integrally tinted Pueblo Brown and have a grape stake finish on the highway side. These barriers are 14 ft high.

The majority of barriers in the I-78 project are a separate post and panel design. The posts are first installed in the ground, and then the panels are positioned between the posts. In one section of the project, through the park, a parallel barrier situation occurred. Detailed analysis during the design stage noted that multiple reflections between the parallel barriers would degrade barrier performance. Because this area was Category A parkland (i.e., lands for which serenity and quiet are of extraordinary significance), measures to minimize this situation were studied. Incorporating absorptive

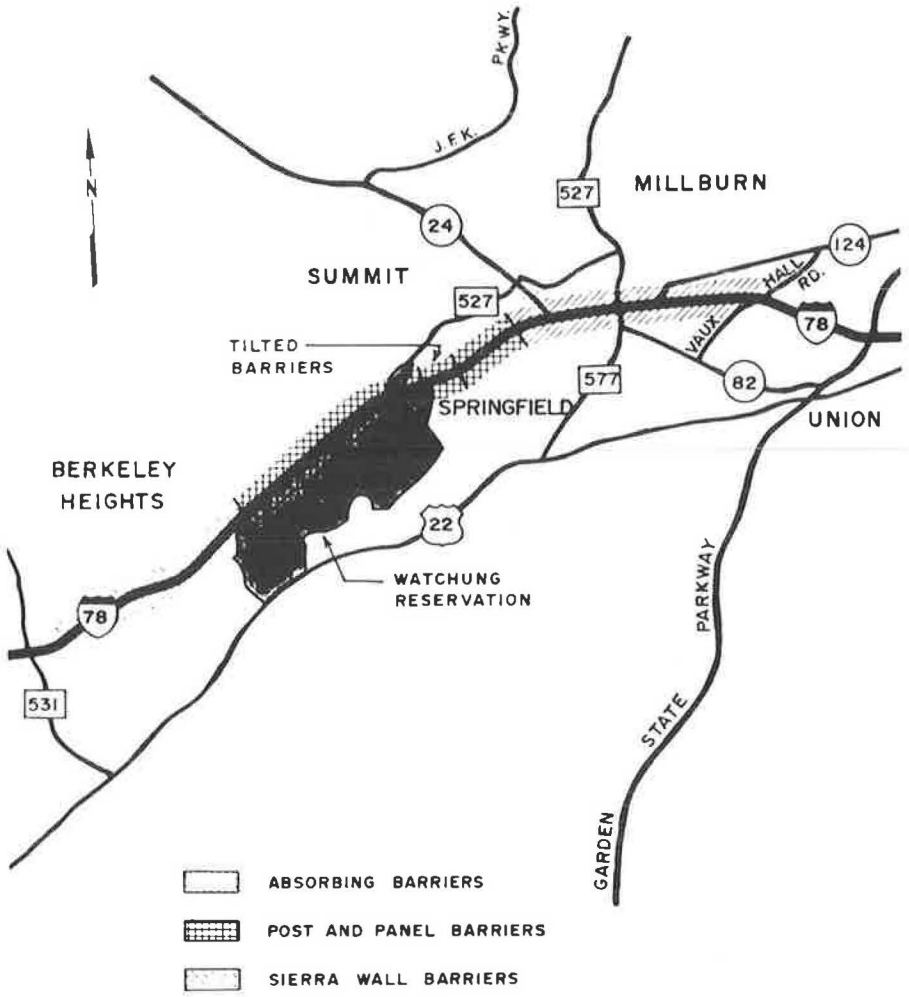

FIGURE 2 Location of barrier by type along I-78.

material into the exterior barrier surface, raising the barrier heights, and tilting the barrier were all investigated. Tilting the barrier was the most cost-effective alternative. The barriers are now tilted 10 degrees and are ~18 ft high (Figure 4).

The last area of special interest was to the east of the Watchung project on the existing section of I-78 that was upgraded during the project construction. The barriers are of a post and panel design, but they have an absorptive treatment known as "Sound Lok" to minimize barrier reflections. Tilting the barriers and raising their height were not considered practical alternatives because sections of this system were up to 24 ft high. Originally, the Sound Lok treatment was to be applied to the noise wall as a smooth 2-in. finish. Inspection of test sample barriers revealed that Sound Lok treatment fissured when it was applied as a smooth finish. A number of surface texturing methods were tried, and it was found that if a vertically ribbed form liner pattern was used on the Sound Lok surface (Figure 5), the fissuring was eliminated and the coefficient of absorption was increased.

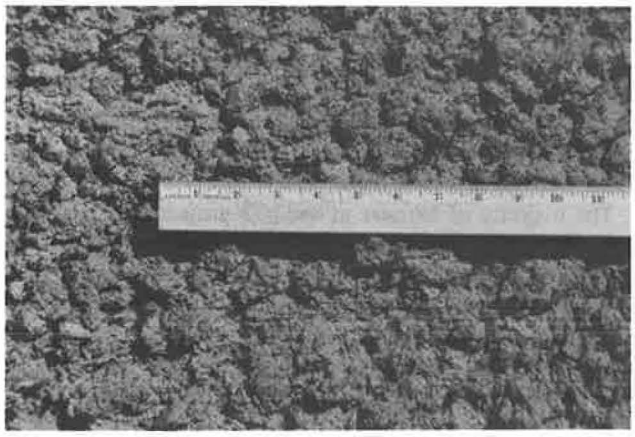

FIGURE 3 Fuzzy finish surface on nonhighway side of concrete barrier.

The surface architectural treatment is not the only difference between these walls and the majority of barriers along I-78: the walls in this section are also of a slightly lighter color (Sequoia Sand). The color was chosen to blend with existing natural concrete roadway structures in this section (e.g., barrier curbs and bridge parapets).

Wooden Barriers on I-295/195

Wooden noise barriers have been incorporated into several highway projects within New Jersey. They were recently used on the I-295/195 (Trenton Complex) project.

FIGURE 4 Separate post and panel barrier, tilted 10 degrees.

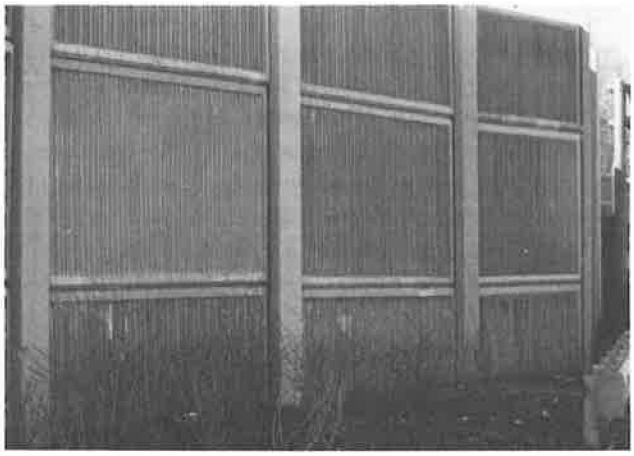

FIGURE 5 Concrete barrier with Sound Lok absorptive treatment.

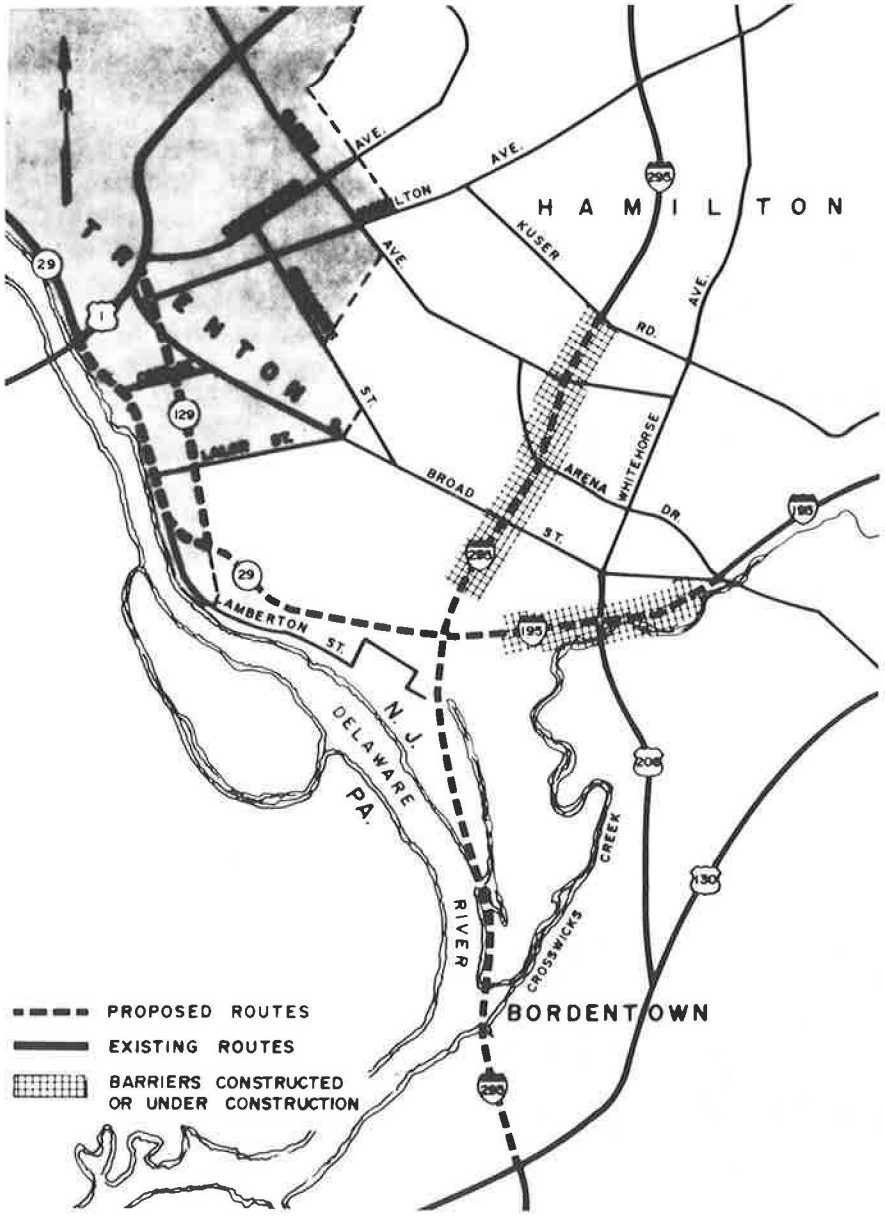

FIGURE 6 Barrier locations along I-295/195.

The Trenton Complex project will connect the present terminals of NJ-29 and Interstates 195 and 295 in and around Trenton. The project consists of 7.6 mi of Interstate routes and 5.9 mi of state highways for a total length of 13.5 mi. The construction of the first segment of the Trenton Complex began in 1983, and the last section is expected to be completed in 1993. Segments of the project are still in the design process.

Three FNSs have been completed to date, and several more will be completed in the next 2 years. As part of the three noise studies, 3.7 mi of noise barriers, ranging in height from 10 to 25 ft, were recommended and constructed (Figure 6). The major environmental issues for this project were wetlands, recreational lands, and cultural resources (archaeological and historic sites). Noise is a sensitive issue because the project will traverse a number of park and residential areas.

The post and panel noise walls were constructed of glue-laminated wood. Standard post spacing is 9 ft on center. Between each post are four individual panel sections, 22 in. wide, that interlock by the attachment of a batten. Purlins (horizontal structural supports) are placed at the top and bottom of the panels. The glue-laminated barrier is the standard design for wooden walls in New Jersey (Figures 7 and 8).

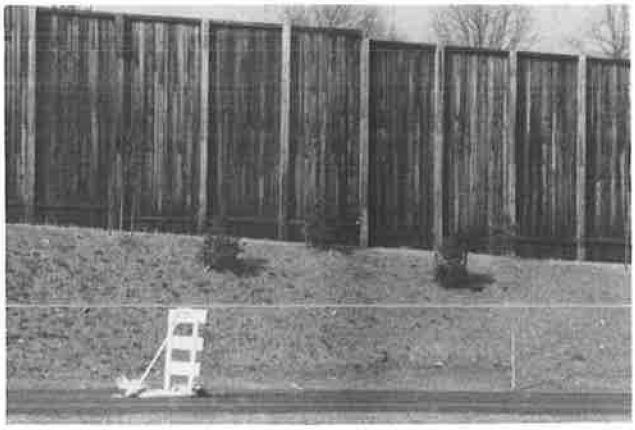

FIGURE 7 Standard wooden barrier located along I-295/195.

FIGURE 8 Wooden barrier supported by double wall along I-295/195.

Metal Barriers

Although more than 1 mi of these barriers have been constructed in New Jersey, their use has been limited to bridges and retaining walls, where they are used to minimize dead load on the structures. Only two types of free-standing metal barriers have been used: ARMCO type steel, a single-thickness barrier, and CAMEO, a double-layered aluminum barrier with a honeycomb-type material sandwiched between the metal sleeves (Figure 9). The metal panel thickness varies from 22 gauge (single layer) to 2.25 in. (double layer). Generally, there are 10-ft spaces between posts on this type of barrier.

FIGURE 9 Cameo double-layered aluminum barrier along I-280 in Harrison, New Jersey.

Earthen Berms and Gabions

During the study process, consideration is always given to the use of natural barriers. However, ROW limitations and material limitations often restrict the use of such barriers. Natural barriers have the least installation problems and are usually the most aesthetically pleasing.

To date, earthen berms in conjunction with free-standing walls have been used on a number of projects, including I-78. Gabions are being used on a section of I-78 that is under construction in Alpha, New Jersey. The standard size of the gabion cages is 3 ft × 3 ft × 6 ft.

Special Cases

There were several New Jersey cases in which noise mitigation involved the noise insulation of public schools. This was done in situations where barriers were found to be either ineffective or not feasible. The noise insulation primarily involved air conditioning of school buildings, such as Our Lady of Czestachowa along I-280 in Harrison, N.J., where noise barriers alone were not effective in reducing interior noise levels.

In conjunction with the NJ-18 freeway project in New Brunswick, a deck was placed over the highway to provide noise mitigation for three Rutgers University dormitories. The bottom two floors of these buildings contained classrooms. The deck also provided parkland replacement because the roadway had occupied recreational land in the construction of

the freeway over the bed of the Delaware and Raritan Canal. To mitigate noise in the classrooms during construction, a modular, vented sound-absorbing wall system was affixed to the exterior bottom two floors of the buildings (Figure 10). This was so effective in reducing noise levels that the university requested that it remain in place after the highway was completed.

NJDOT also has depressed the profile of a number of projects during the early stages of design. This modification has been incorporated into the design of such projects as I-287 and I-78.

FIGURE 10 Modular sound wall affixed to exterior of Rutgers University building.

CONCLUSIONS

In conjunction with New Jersey's transportation program, NJDOT has succeeded in providing effective noise mitigation measures as part of its highway projects. The goal for such projects is to provide the driving public and the residents of New Jersey with an effective, aesthetically pleasing noise mitigation system.

The primary method of noise mitigation employed by NJDOT has been free-standing walls constructed of either wood or concrete. NJDOT has been satisfied with the results of these efforts and will continue to use these two materials.

ACKNOWLEDGMENTS

The author would like to thank the staff of the Bureau of Environmental Analysis, particularly the Technical Section Noise Staff. The assistance of Domenick Billera is gratefully acknowledged.

Publication of this paper sponsored by Committee on Transportation-Related Noise and Vibration.

Acoustical Insulation Design for Existing Schools and Residences Near San Francisco International Airport

MICHAEL HOGAN AND BALLARD W. GEORGE

The environs of the San Francisco International Airport include a large number of residences and other examples of sensitive land use that are acoustically incompatible with California state requirements for the noise levels found near the airport. In this study, a sample of 12 residences and 2 schools in the area was examined. Retrofit designs were developed for each structure to reduce interior sound levels, using simultaneous indoor-outdoor sound level measurements and architectural acoustical analysis of the structures. Follow-up sound level measurements were conducted to confirm the original acoustical predictions for interior sound levels.

South San Francisco (population ~50,000) is one of the suburban communities that has grown up in San Mateo County, California, around San Francisco International Airport. When commercial aviation began, the city of San Francisco lacked suitable land within its own boundaries for airport development, so the city government purchased land in San Mateo County to build what eventually became San Francisco International Airport. Thus the acoustical impact of the airport primarily affects areas other than the city of San Francisco. The airport is now among the most important and most active in the world. More than 24 million passengers use the airport every year. If general aviation and military flights are both included, there are ~380,000 takeoffs and landings per year.

To characterize community responses to noise, the government of the state of California has devised the community noise equivalent level (CNEL), which is a measurement in decibels of the total daily noise dosage, adjusted to account for the frequency response of the human ear, the number of individual noise events, and the heightened sensitivity of human communities to noise during evening and nighttime. For this study, the boundaries of the noise compatibility planning area approximately followed the 65-CNEL contour. The structures in the project area are in the 65–70 exterior CNEL exposure zones. These CNEL levels are generally considered to be a significant noise impact.

A substantial body of scientific evidence documents the effects of very high levels of noise on human health and well being, both physical and psychological. There is also documentation on the effects of noise on the level of annoyance in subjects and interference with their daily living. The problem is particularly serious in urban areas surrounding major metropolitan airports, such as the San Francisco International Airport, where the arrivals and departures of jet aircraft create a great deal of noise in the areas surrounding the airport.

The response to the problem of airport-related noise in general can be twofold: (a) reducing noise at its source and (b) resolving or preventing land use incompatibilities around the airport. It is the latter approach that is addressed in the study described in this paper.

The choice of 65 CNEL as the boundary for the study area was based primarily on the provisions of the California Airport Noise Standard. This noise standard required that by January 1, 1986, all land uses around airports that are subject to noise levels of 65 CNEL or above should be compatible with the noise environment generated by airport operations. Schools and residences are land uses that are usually defined as incompatible with airport noise above 65 CNEL. However, these uses are compatible under the following circumstances:

- There is an avigation easement for noise,
- The structures are high-rise apartments with acoustical treatment to achieve maximum interior noise level of 45 CNEL, and
- Any existing residential unit subject to noise levels of 65 to 80 CNEL has acoustical treatment of the structure to provide an interior noise level that does not exceed 45 CNEL.

Commercial, industrial, agricultural, and other open space uses are deemed compatible with airport noise under this California law.

DEFINITION OF RESIDENCES AND SCHOOLS ANALYZED

The selections of residences for the study were based on the following factors:

- The need for a reasonable sampling of residential types,
- The ability to produce successful insulation results,
- The desire for a strong numerical representation of dwelling units near and within the 70-CNEL zone, and
- Input from the city of South San Francisco and from interested volunteers.

The project created strong community interest, and there were far more interested volunteers than could be accommodated in the first phase. Home owners who expressed interest were placed on a list of prospective volunteers, and 12 residences were selected from the targeted structures for study by the authors.

Earth Metrics, 859 Cowan Rd., Burlingame, Calif. 94010.

The residences selected were typically of wood frame construction, with stucco or wood siding and peaked roofs. The roofing was of reasonably airtight materials, such as tar and gravel, bitumen, or composition shingles. The attics were not utilized as living space. Ceilings consisted of gypsum board or similar relatively high-density material, and there were no exposed beams. The attics were not insulated in some cases. The windows were single paned.

Two schools were also included in the first-phase insulation study. Saint Veronica's School is a single-story wood frame structure with exterior stucco and relatively large windows that face the playground and parking lot. A flat roof with numerous skylights created special insulation problems. The Ponderosa Elementary School is a flat-roofed single-story wood frame structure with a stucco exterior and large windows facing north.

SOUND REDUCTION MEASUREMENTS

Sound level readings were conducted simultaneously inside and outside each of the 12 residences and 2 schools. The results were reported in CNEL units and were based on a minimum reading of 1 hr at each structure. Readings in each dwelling unit were taken in the geometric center of the main bedroom at the same height (4 ft) above floor level. Readings were also taken outside of the same bedroom at a distance of 10–20 ft from the exterior wall, as far as feasible from other walls or obstructions, at a height of 4 ft. At each school, four different interior measurement locations were selected in representative classrooms. The exterior measurement site was selected so that it was exposed to the predominant aircraft flight pattern nearest the subject school.

The results of the premodification monitoring are presented in Table 1, along with the results of the postmodification monitoring (discussed later). As can be observed, the premodification monitoring in the residences yielded outdoor-to-indoor sound level differences that ranged from 18 to 24 dBA. The outdoor CNELs were determined to be 46–50 dBA. In the schoolrooms, the outdoor-to-indoor differences before retrofitting were measured at 18 dBA, and the CNEL was determined to be 47 dBA in each case.

RECOMMENDATION OF SOUNDPROOFING MEASURES

Each structure was inventoried for physical characteristics, and a spectral analysis was conducted to determine the exterior and interior insertion losses by 1/3-octave frequency. A mathematical analysis was carried out to simulate the acoustical response of each structure to a variety of retrofit strategies. The simulation methodology was one that was used previously at San Jose International Airport (*1*). In essence, the computer model that is used is responsive to hypothetical structure modifications and permits an accurate forecast of interior sound levels for a known exterior noise environment. Use of the model allows exploration and costing for a wide variety of retrofitting strategies.

Residential Soundproofing

The customized solution for one of the residences, 125 Rockwood Drive, that resulted from the computer model is typical. It was decided to install weatherstripping around the front and kitchen-garage doors. The kitchen-garage door was replaced with a solid core door. The windows in the living room, dining room, and bedrooms and the sliding glass door were replaced with tight-fitting, thoroughly caulked, double-glazed window assemblies with total glass thicknesses of 3/8 in. The greenhouse window in the kitchen was replaced with a double-glazed, tight-fitting greenhouse window with total glass thickness of 3/8 in. The bathroom window was also replaced with a tight-fitting, thoroughly caulked, double-glazed assembly with total glass thickness 3/8 in., frosted. Insulation was installed in the attic, which had no existing insulation, and the attic trap door was replaced with a perimeter-sealed heavy door (a minimum of 2-in.-thick solid core) to reduce sound transmis-

TABLE 1 RESULTS OF PREMODIFICATION AND POSTMODIFICATION SOUND MONITORING AT RESIDENCES

Residence Address	Exterior CNEL	Premodification Monitoring Sound Level: Outdoor/Indoor Attenuation (dB)	Postmodification Monitoring Sound Level: Outdoor/Indoor Attenuation (dB)	Premodification Monitoring: Interior Level (CNEL)	Postmodification Monitoring: Interior Level (CNEL)
101 Manor	70	20	26	50	44
102 Manor	70	21	25	49	45
111 Manor	70	24	31	46	39
125 Rockwood	70	24	28	46	42
127 Rockwood	70	24	30	46	40
129 Rockwood	70	20	26	50	44
203 Rockwood	65	19	29	46	36
223 Rockwood	65	18	23	47	42
315 Rockwood	65	19	29	46	36
343 Rockwood	65	19	22	46	43
112 Sherwood	65	19	28	46	37
107 Rosewood	65	18	25	47	40

NOTE: There is actually a range of values within a given residence because the acoustical response varies from room to room and may even vary within a given room. The lowest or most conservative value is used here and for ensuing calculations.

TABLE 2 RESULTS OF PREMODIFICATION AND POSTMODIFICATION SOUND MONITORING AT PONDEROSA AND SAINT VERONICA'S SCHOOLS

Exterior CNEL	Room	Premodification Monitoring: Outdoor/Indoor dB Reduction	Postmodification Monitoring: Outdoor/Indoor dB Reduction	Premodification Monitoring: Interior Level (CNEL)	Postmodification Monitoring: Interior Level (CNEL)
Ponderosa School					
65	1	18	23	47	42
65	11	18	23	47	42
Saint Veronica's School					
65	3	—[a]	37	—[a]	28
65	8	18	36	47	29

[a]Room 3 was unavailable for premodification monitoring.

sion from the attic to the main residence. The new living room windows were supposed to have wood frames, in keeping with the existing decor. The cracks at the top and bottom of the existing wood paneling were sealed to reduce potential noise transmission pathways.

Ponderosa School

The existing windows were replaced with double-glazed windows, and the existing exit doors were replaced with solid core doors. The existing ceiling was removed, a new ceiling was installed, and the existing light fixtures were readjusted. Baffles were installed around the gravity roof vents and around the furnace flue at the roof. Trim was installed at the ceiling along the windows.

Saint Veronica's School

Double-glazed windows were installed at all existing classroom skylights and at all existing clerestory windows in the library. All existing metal doors were replaced with new solid core doors with double-glazed openings. All existing acoustical tile was removed to allow installation of new gypsum board in all classrooms. The existing metal grid systems in the ceilings were removed and the existing acoustical tiles were replaced with new supporting systems in all classrooms. The existing light fixtures were then relocated. New exterior vent enclosures were installed at all existing furnaces and painted. A new roof ventilation fan for the library and classrooms was installed. New gypsum board was placed over existing plywood at the clerestory ceiling. Insulation was installed around the existing furnace flue at the roof, and the existing caps were replaced with new caps at all classrooms.

SOUND LEVEL MEASUREMENTS AFTER RETROFITTING

Monitoring was performed again after insulation was installed. Tables 1 and 2 present the results obtained and the conversion to indoor CNEL. The goal of 45 CNEL was met in all structures and exceeded in many. The data validate the computer model's ability to predict the changes in sound levels for a given retrofit strategy. Saint Veronica's School showed the greatest improvement as well as the lowest postmodification interior CNEL measurement. The test data for the school were subjectively confirmed by the favorable opinions expressed by the principal, teachers, and students.

CONCLUSION

The results provide additional evidence that soundproofing of existing structures in sensitive areas affected by airport noise is a viable method for noise reduction. The most important technical finding of the present study is that use of a detailed mathematical model to evaluate proposed retrofitting strategies is a must. For example, a variety of the insulation strategies analyzed for a given building turned out to be virtually without effect, even though these same strategies had been applied effectively in apparently similar situations elsewhere. In other words, each structure is unique and must be treated as an individual case in soundproofing design. The costs for retrofitting each residence were $7,000–$9,000 per single-family dwelling.

ACKNOWLEDGMENTS

The authors would like to acknowledge the pioneering efforts of Mayor Robert Teglia and the South San Francisco City Council, as well as those of Bob Yee, Director of Public Works, in facilitating the grant program under which this work was conducted. The staff of the San Francisco International Airport and the FAA are also commended for their efforts.

REFERENCE

1. C. M. Hogan and J. Ravnkilde. Design of Acoustical Insulation for Existing Residences in the Vicinity of San Jose Municipal Airport. In *Transportation Research Record 1033*, TRB, National Research Council, Washington, D.C., 1985, pp. 54–59.

Publication of this paper sponsored by Committee on Transportation-Related Noise and Vibration.

Development and Verification of the California Line Source Dispersion Model

PAUL E. BENSON

A description of the California Line Source Dispersion Model, CALINE4, is given, along with a brief history of the model's development. CALINE4 is based on the Gaussian plume methodology and is used to predict air pollutant concentrations near roadways. Predictions can be made for carbon monoxide, nitrogen dioxide, and suspended particulates. An option for modeling air quality near intersections is described. CALINE4 represents an updated and expanded version of CALINE3. The newer model can handle a greater variety of problems and has improved input/output flexibility. Estimates of vertical and horizontal dispersion are enhanced by accounting for vehicle-induced thermal turbulence and wind direction variability. CALINE4 is verified by using results from five separate field studies. Comparisons to CALINE3 indicate modest improvements in the accuracy of the newer version.

The California Department of Transportation (Caltrans) published its first line source dispersion model for predicting carbon monoxide (CO) concentrations in 1972 (*1*). Model verification using preliminary field observations was inconclusive. In 1975, the original model was replaced by a revised version, CALINE2 (*2*). The new model was able to compute concentrations for depressed sections and for winds parallel to the roadway. Subsequent studies indicated that CALINE2 seriously overpredicted concentrations for stable, parallel wind conditions (*3, 4*).

In 1979, a third version of the model was developed (*5, 6*). This version, CALINE3, retained the basic Gaussian dispersion methodology but used new vertical and horizontal dispersion curves modified for the effects of surface roughness, averaging time and vehicle-induced turbulence. It also replaced the virtual point source model used in CALINE2 with an equivalent finite line source and added multiple link capabilities to the model format. The changes helped reduce the magnitude and frequency of overpredictions for stable, parallel wind conditions. The performance of CALINE3 was evaluated by several independent investigators and found to be comparable to other published line source models (*7, 8*). In 1980, the Environmental Protection Agency (EPA) authorized CALINE3 for use in estimating concentrations of nonreactive pollutants near highways (*9*).

California Department of Transportation, Transportation Laboratory, 5900 Folsom Blvd., Sacramento, Calif. 95819.

CALINE4 is the most recent version of the CALINE series (*10*). It represents a refinement and extension of the capabilities contained in CALINE3. Concentrations of CO, nitrogen dioxide (NO_2), and aerosols can be predicted by the model. An option for modeling intersections has been added. The model employs a modified Gaussian plume approach similar to the one used in CALINE3 but with new provisions for lateral plume spread and vehicle-induced thermal turbulence. Submodels for CO modal emissions and reactive plume chemistry are included.

MODEL DESCRIPTION

CALINE4 divides individual highway links into a series of elements from which incremental concentrations are computed and summed. As shown in Figure 1, each element is modeled as an "equivalent" finite line source (FLS) positioned normal to the wind direction and centered at the element midpoint. Element size increases with distance from the receptor to improve computational efficiency. The emissions from an element are released uniformly along the FLS and dispersed in a Gaussian manner by the model. Incremental downwind concentrations are computed by using the crosswind Gaussian formulation for a line source of finite length:

$$C(x, y) = \frac{q}{\pi \sigma_z u} \int_{y_1 - y}^{y_2 - y} \exp\left(\frac{-y^2}{2\sigma_y^2}\right) dy \qquad (1)$$

where q is the lineal source strength, u is the wind speed, σ_y and σ_z are the horizontal and vertical Gaussian dispersion parameters, and y_1 and y_2 are the FLS endpoint y coordinates.

The model permits the specification of up to 20 links and 20 receptors. Each link defines a relatively straight segment of roadway with a constant width, height, traffic volume, and vehicle emission factor. The location of the link is specified by the endpoint coordinates of its centerline. The locations of receptors are similarly defined in terms of a uniform coordinate system.

CALINE4 treats the region directly above the highway as a zone of uniform emissions and turbulence. This "mixing zone" is defined as the region over the traveled way plus 3 m (about two vehicle widths) on either side. The additional width

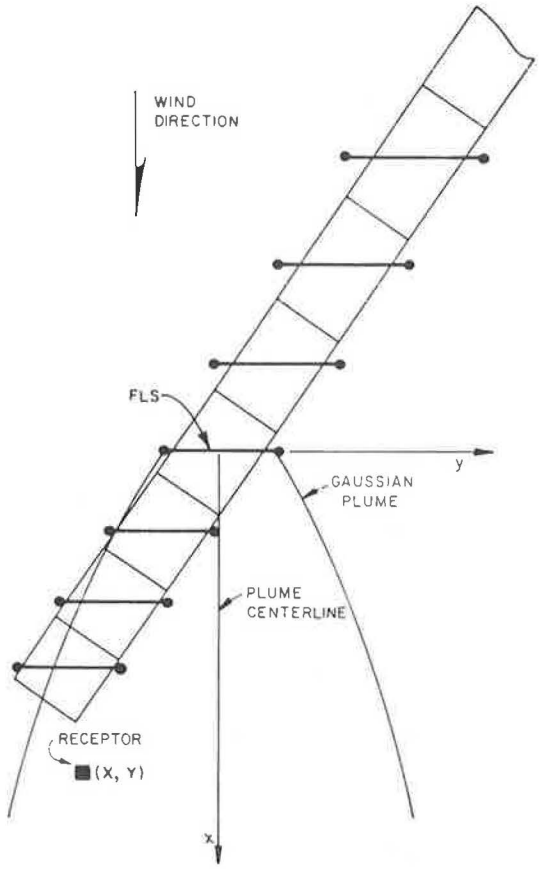

FIGURE 1 CALINE4 link representation as a series of elements with equivalent finite line sources superimposed.

accounts for the initial horizontal dispersion imparted to pollutants by the vehicle wake. Within the mixing zone, the mechanical turbulence created by moving vehicles and the thermal turbulence created by hot vehicle exhaust are treated as significant dispersive mechanisms (*11, 12*).

A number of studies have noted a correlation between crossroad wind speed and initial vertical dispersion (*3, 12–14*). Each of these studies has concluded that lower wind speeds result in greater initial vertical dispersion. In CALINE4, it is assumed that initial vertical dispersion at the edge of the mixing zone, $\sigma_{z(i)}$, is determined by the length of time air resides in the mixing zone, t_r. An empirically derived equation,

$$\sigma_{z(i)} = 1.5 + (t_r/10) \quad (2)$$

relates $\sigma_{z(i)}$ in meters to t_r in seconds (*10*).

The Pasquill-Smith vertical dispersion curves (*15*) are modified by CALINE4 to incorporate the effects of vehicle-induced thermal turbulence. A composite heat release rate of 24.6 J/cm per vehicle (based on an assumed average fuel economy of 8.5 km/l, 0.6 heat loss factor, and specific energy of 3.48×10^7 J/l) is used in conjunction with Smith's stability nomograph (*16*) to predict a modified stability class over the mixing zone. The rate of vertical plume spread is assumed to follow the modified stability curve until either the plume centerline or more than 50 percent of the plume mass falls outside of the mixing zone. The model does not incorporate a modification to the heat release rate for vehicle speed or percent cold starts. Additional research and improved accuracy of model inputs are needed to justify such refinements.

Horizontal dispersion is estimated directly from the wind direction standard deviation, σ_θ, using a method developed by Draxler (*17*). This approach is preferred to the stability classification scheme used in CALINE3 because it can address site-specific conditions and unique meteorological regimes (e.g., directional meander caused by low wind speed). An adjustment is included to account for the effect of wind shear on lateral plume spread. Values for σ_θ may be obtained by direct measurement or estimated by various methods (*18, 19*).

An algorithm suggested by Turner (*20*) has been incorporated into the model to handle bluff and canyon situations. The algorithm computes the effect of single or multiple horizontal reflections for each FLS plume in much the same way that mixing height reflections are handled. The model also includes a method to account for surface deposition of gases and gravitational settling of aerosols (*21*).

Intersection Link Option

CALINE4 normally requires that the user assign a composite emission factor for each link. At controlled intersections, however, the operational modes of deceleration, idle, acceleration, and cruise have a significant effect on the rate of vehicle emissions. Traffic parameters such as queue length and average vehicle delay define the location and duration of these emissions. The net result is a concentration of emissions near the intersection that cannot be modeled adequately by using a single, composite emission factor. For this reason, a specialized intersection link option has been added to CALINE4.

A CALINE4 intersection link encompasses the acceleration and deceleration zones created by the presence of the intersection for one direction of traffic flow. A stop line distance is referenced to the link endpoints, and approach (vph_i) and depart (vph_o) traffic volumes are assigned. A full intersection can be modeled by using four of these links.

Cumulative modal emissions profiles representing the average deceleration, idle, acceleration, and cruise emissions per signal cycle per lane are constructed for each intersection link. These profiles are determined by using the following input variables:

- v = Cruise speed,
- t_a = Acceleration time,
- t_d = Deceleration time,
- t_1 = Maximum idle time,
- t_2 = Minimum idle time,
- n_c = Number of vehicles per signal cycle per lane, and
- n_d = Number of vehicles delayed per signal cycle per lane.

The traffic parameters, n_c and n_d, are chosen to represent the dominant movement for the link. The model assumes a uniform vehicle arrival rate, constant acceleration and deceleration rates, full stops for all delayed vehicles, and an "at rest" vehicle spacing (d_0) of 7 m. The time rate modal emission factor, $\dot{e}$, is computed for each mode from composite

emission rates for average route speeds of 0 (idle) and 26 km/hr. This method employs the acceleration-speed product as a measure of power per unit mass expended during acceleration modes (*22*) and the proportionality of drag force to v^2 for cruise modes. Deceleration emissions are assumed to be 1.5 times the idle emission rate.

A cumulative emissions profile for a given mode is developed by determining the time that vehicles are in the mode as a function of their location on the link, multiplying by the appropriate $\dot{e}$, and summing the results over the number of vehicles per cycle per lane. The elementary equations of motion are used to relate time in mode to location. The assumed value of d_0 is used to specify the positional distribution of the vehicles. Individual profiles are based on the assumption that $\dot{e}$ is constant throughout the modal event. This means that the cumulative modal emissions from a vehicle are directly proportional to the time that the vehicle has spent in the mode.

In the case of an acceleration starting from an "at rest" position, the cumulative emissions for the ith vehicle are given as

$$\text{ECUM}_i = \dot{e}_a \, (2t_a d/v)^{1/2} \tag{3}$$

where d equals the distance from the start of the acceleration. The total cumulative acceleration emissions per cycle per lane is obtained by summing Equation 3 over the number of vehicles delayed, as follows:

$$\text{ECUM}(d) = \dot{e}_a \, (2t_a/v)^{1/2} \sum_{i=1}^{n_d} [d - d_0 \, (i - 1)]^{1/2} \tag{4}$$

where d is now defined as the distance from the end of the vehicle queue to the point where the cumulative emissions are being calculated. Similar reasoning is used for developing the other modal profiles.

To obtain the average lineal emission rate over an element, CALINE4 computes the total cumulative emissions for the four modes at each end of an element. The difference between these amounts represents the emissions released over the element per cycle per lane. This quantity is multiplied by either vph_i/n_c or vph_o/n_c, depending on whether the element is before or after the stop line, respectively, and divided by the element length to yield a lineal emission rate.

Turn movements are not handled explicitly by CALINE4. Instead, the cumulative emissions profile per cycle per lane for the dominant approach movement is prorated by the approach or departure volume, depending on the relative location of the stop line. This method implicitly assigns a turning vehicle's deceleration, idle, and part of its acceleration emissions to its approach link. The remainder of its modal emissions are assigned to its departure link. The method assumes that the acceleration patterns for turning and through vehicles are roughly similar.

NO_2 Option

A number of methods have been developed to expand the use of the Gaussian plume formulation to reactive species such as NO_2 (*23*). These include the exponential decay, ozone limiting, and photostationary state methods. An unfortunate weakness of these methods is their assumption that reactants mix instantaneously as they disperse and that the resulting time-averaged concentrations determine the reaction rates (*24, 25*). Because the component reactants, nitrogen oxide (NO) and ambient ozone (O_3), are not mixed instantaneously by the relatively large-scale dispersive processes of the atmosphere, the assumption leads to overestimates of NO_2 production (*26, 27*).

In CALINE4 a computational scheme that models the dispersion of reactants separately from the plume chemistry is used to predict NO_2 concentrations. As with the preceding methods, a simplified set of controlling reactions is assumed:

$$NO_2 + h_\nu \rightarrow NO + O \tag{5}$$

$$O + O_2 + M \rightarrow O_3 + M \tag{6}$$

$$NO + O_3 \rightarrow NO_2 + O_2 \tag{7}$$

where h_ν represents an interacting photon of sunlight and M is an unspecified catalytic agent.

Because of the relatively high concentration of O_2, the reaction given in Equation 6 is assumed to occur instantaneously. It is further assumed that emissions and ambient reactants are fully mixed over the roadway, that initial tailpipe NO_x emissions are 92.5 percent NO and 7.5 percent NO_2 by mass, and that parcels of the mixed reactants retain their identity relative to molecular scales of motion for distances of ~300 m downwind.

The initial mixing zone concentrations of the reactants are determined on the basis of upwind concentrations of NO, NO_2, and O_3 and vehicular contributions of NO_x. The dispersion of this initial mix is characterized as a scattering of discrete parcels, with reactions proceeding as isolated processes within each parcel. The initial concentrations and time of travel from element to receptor govern the final concentration of NO_2 within the discrete parcels. The reactions proceed independently of the dispersion process because the reaction rates are controlled by the reactant concentrations within a small neighborhood (of the scale of the mean free path of the molecules), whereas the dispersion process acts on a much larger scale. The reactions can therefore be modeled in accordance with the first-order rates for the reactions presented as Equations 5 and 7 on the basis of the photolysis rate constant and temperature input by the user, until concentration gradients are reduced to the extent that molecular diffusion becomes significant. For microscale modeling applications, travel times are usually not long enough for this to occur.

Discrete parcel NO_2 concentrations are computed by CALINE4 for each element-receptor combination because of the variable travel times involved. These concentrations are not, of course, the same as time-averaged NO_2 concentrations. To arrive at time-averaged values, the link source strength is adjusted by element to yield an initial NO_2 mixing zone concentration equal to the discrete parcel concentration at the receptor. The model then proceeds to compute the time-averaged concentration exactly as the concentration for a nonreactive species such as CO would be computed.

The discrete parcel approach is appropriate only when the assumptions of fully mixed initial reactants and short travel times are reasonably met. Use of the NO_2 option under parallel

wind conditions or strongly convective regimes is not recommended. However, the approach appears to be well suited for stable, crosswind conditions.

FIELD STUDIES

The CALINE4 model was verified by using data from several independent field studies. These studies represent a variety of possible model applications, including the intersection link and NO_2 options.

General Motors Sulfate Dispersion Experiment

The General Motors (GM) Sulfate Experiment was conducted at GM's Michigan test track in October 1975 (*28*). The track is 5 km long and is surrounded by lightly wooded, rolling hills. A total of 352 cars, including 8 vehicles emitting SF_6 tracer gas, were driven at a constant speed of 80 km/hr around the track. Monitoring probes were stationed at 6 upwind and 11 downwind locations located out to a distance of 113 m from the track centerline. Wind speed and direction measurements were made at various locations by using Gill UVW anemometers. Data for 66 half-hour sampling periods were compiled. Most of these tests were conducted during the early morning hours.

Illinois EPA Freeway/Intersection Study

This 1978 study involved the measurement of CO concentrations near two urban sites located just outside of Chicago, Illinois (*29*). SF_6 tracer releases were made as part of the study, but these results were not used for CALINE4 verification because only a single release vehicle was used.

A section of the Eisenhower Expressway (I-90) between Des Plaines and First Avenue was chosen by the Illinois Environmental Protection Agency (EPA) as a representative freeway site. This is a heavily traveled six-lane freeway with average daily traffic in excess of 100,000 vehicles. The test section traverses terrain covered with grass and scattered trees. Air samples were collected for 1-hr averaging periods during June–August at eight locations near the test section. Distances ranged from 3 to 192 m from the roadway edge.

A second site was monitored during October and November at the intersection of two six-lane arterials, North and First Avenues. The site is typical of a high-volume urban intersection. It is surrounded by a mix of single-story buildings, parking lots, and forest preserve. Eight bag sampling locations were established near the intersection. A ninth background sampler monitored concentrations 100–150 m upwind of the intersection. Meteorological data were collected at a tower located in the southeast quadrant.

EPA NO_2/O_3 Sampler Siting Study

In August 1978 a study was conducted by EPA along a section of the San Diego Freeway (I-405) in Los Angeles, California, to quantify the effect of mobile source NO_x emissions on ambient O_3 concentrations immediately downwind of a heavily traveled freeway (*30*). The test took place 0.8 km north of Wilshire Boulevard in relatively flat terrain. I-405 carries approximately 200,000 vehicles per day at this location. Six monitoring sites were spaced from 8 to 400 m downwind of the roadway. Continuous sampling was conducted at a height of 3 m, with results averaged over 1 hr. A 10-m-tall meteorological tower measured wind speed and direction immediately upwind of the freeway.

Caltrans Intersection Study

From January through March of 1980, the California Department of Transportation (Caltrans) performed a detailed study of air quality at the intersection of Florin Road and Freeport Boulevard in Sacramento, Calif. (*6*). At the time of the study, the intersection was surrounded by bare ground for a distance of at least 50 m in all directions. The nearby terrain was level and occupied by scattered single-story residential developments.

Fifteen sampling locations were established in the northwest and southwest quadrants of the intersection. A 10-m-tall meteorological tower was located in each of these quadrants, at least 15 m back from the traveled ways. CO concentrations averaged over 1 hr were recorded concurrently with pertinent traffic and meteorological parameters.

Caltrans Highway 99 Tracer Experiment

A series of SF_6 tracer experiments was conducted by Caltrans during winter 1981–1982 along a 4-km section of US-99 in Sacramento (*10*). The four-lane divided highway carries more than 35,000 vehicles daily, with a peak hourly volume of 3,450 vehicles. The nearby terrain consists of open fields, parks, and scattered residential developments. The sampling site was located 1 km from the south end of the test section. Three locations were sampled on each side of the highway at 50, 100, and 200 m from the highway centerline and a height of 1 m. A 12-m-tall meteorological tower was located near the south end of the test section, in an open, plowed field.

The SF_6 was released from eight specially equipped sedans. The distribution of the tracer vehicles was controlled at a staging area by spacing departures at 90-sec intervals. In all, 14 tracer release tests were made. Most of these were morning tests with half-hour samples taken from 6:30 to 8:30 a.m.

MODEL VERIFICATION

A statistical method involving the computation of an overall figure of merit (FOM) on the basis of six component statistics (*31*) was used to evaluate CALINE4's performance in comparison to that of CALINE3. These statistics are defined as follows:

- S_1: The ratio of the largest 5 percent of the measured concentrations to the largest 5 percent of the predicted concentrations,
- S_2: The difference between the predicted and measured proportion of exceedances of a concentration threshold or air quality standard,
- S_3: Pearson's correlation coefficient for the paired measured and predicted concentrations,
- S_4: The temporal component of Pearson's correlation coefficient,

- S_5: The spatial component of Pearson's correlation coefficient, and
- S_6: The root mean square (rms) of the difference between the paired measured and predicted concentrations.

The six component statistics are transformed into individual figures of merit (F_1, F_2, etc.) on a common scale from 0 to 10. They are then weighted and summed as follows:

$$\text{FOM} = \frac{F_1 + F_2}{6} + \frac{F_3 + F_4 + F_5}{9} + \frac{F_6}{3} \quad (8)$$

Scatter plots and relative error plots were also used to evaluate model performance.

Highway Sites

A direct comparison between CALINE3 and CALINE4 on the basis of FOM values was made for the three highway sites for which measured concentrations of SF_6 or CO were available. A summary of the individual and overall FOMs is presented in Table 1. The results were based on measured (M) and predicted (P) concentrations at downwind locations only. For the Illinois EPA study, the sample locations north of I-90 did not match the locations to the south, making it necessary to compute separate statistics for each. The threshold values used for computing F_2 were 1.0 parts per billion (ppb) SF_6 for the two tracer studies and 10 parts per million (ppm) CO for the Illinois EPA study. These values were selected to yield statistically significant measures of F_2.

For both the GM and Caltrans studies, the individual and overall FOMs clearly indicate improved performance by CALINE4. However, the results for the Illinois EPA study are inconclusive. Although CALINE4 displays slight improvements in temporal correlation and residual error, it does not perform as well in predicting high concentrations.

The higher values of F_1 obtained for CALINE3 by using the Illinois EPA data could have been the result of bias in the emission factor calculations. Emission factors were computed by using the MOBILEI emission factor model (*32*). An examination of the actual values of the statistic S_1 demonstrated that CALINE4 was overpredicting the high concentrations to a slightly greater degree than CALINE3. The uncertainty of the modeled emission factors make it difficult to attach any significance to this, especially when results from the two independent tracer studies indicate, overall, an improved performance by CALINE4.

A comparison between F_4 and F_5 in Table 1 indicates that both models predicted spatial patterns of observed concentrations better than they do temporal sequences. The result is not surprising, given the consistent spatial pattern of downwind concentrations apparent in the data. Virtually all ground-level concentrations decreased with distance from the roadway in both tracer studies. Similarly, elevated sampling sites in the GM study followed repeatable patterns. The models had little

TABLE 1 COMPARISON OF CALINE3 AND CALINE4 FIGURES OF MERIT

Study	Number of Locations	Number of Periods	Model	F_1	F_2	F_3	F_4	F_5	F_6	FOM
Highway Sites										
GM	11	62	C3	6.5	10.0	7.8	7.1	9.7	2.0	6.2
			C4	8.5	10.0	8.3	7.2	9.7	2.8	6.8
Caltrans	3	56	C3	5.7	9.9	5.6	3.5	10.0	2.5	5.6
			C4	8.6	10.0	5.9	4.2	10.0	3.2	6.4
Illinois EPA (North)	4	249	C3	9.7	10.0	7.3	4.3	9.9	3.6	6.9
			C4	8.8	10.0	7.5	4.6	9.9	3.7	6.8
Illinois EPA (South)	4	49	C3	9.9	10.0	7.2	2.4	9.9	3.4	6.6
			C4	8.6	10.0	8.0	3.1	9.9	3.6	6.6
Intersection Sites										
Caltrans	15	38	C4	8.2	10.0	8.8	8.8	9.4	2.6	6.9
Illinois EPA	8	39	C4	8.5	9.9	8.1	6.7	9.2	3.7	7.0
NO_2 Site										
US SPA	6	30	C4	8.4	9.9	7.7	7.9	6.9	5.7	7.5

NOTE: C3 = CALINE3 and C4 = CALINE4.

difficulty in predicting these trends. However, prediction of temporal variations at a given site was much more difficult. Temporal changes are influenced by more variables, some of which may interact in ways that are not clearly understood.

The values of F_6 are, in most cases, the lowest of the individual figures of merit. F_6 is a function of the ratio between rms paired differences, S_6, and the average measured concentration. As this ratio increases, F_6 decreases. Paired differences for low measured concentrations usually decrease S_6 less than they decrease the average concentration, disproportionately influencing the statistic. The result is a much lower value of F_6 for the combined data reported in Table 1 than for most values computed individually by location. For example, F_6 values of 5.4 and 4.5 for the GM and Caltrans studies, respectively, are obtained for CALINE4 by averaging individual values of F_6 computed by location.

Scatter plots of the CALINE4 results, displaying predicted versus measured SF_6 concentrations for the GM and Caltrans studies, are presented in Figure 2. A line of perfect agreement and factor of 2 envelope defined by $P = 2M$ and $P = M/2$ are superimposed to assist in interpreting the results. The number of observations (n) and the least squares linear regression intercept (a), slope (b), and correlation coefficient (r) are also given.

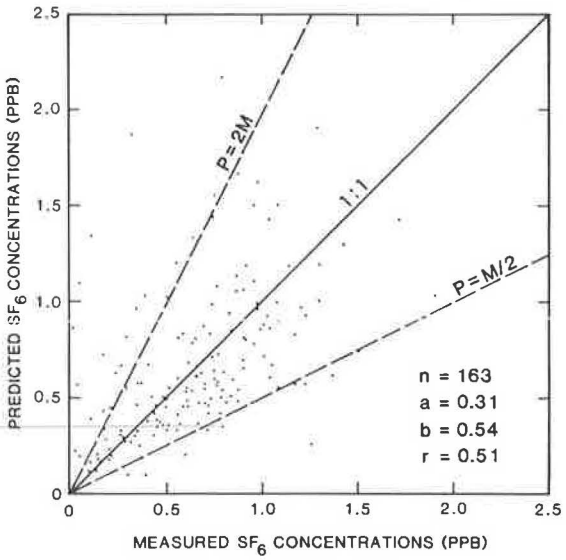

FIGURE 2 Scatter plot showing CALINE4 predictions and measured results for the Caltrans U.S.-99 study.

Less than 15 percent of the combined results fall outside of the factor of 2 envelope. Of these, 85 percent are overpredictions. For the more significant high concentrations (above 1 ppb), only one serious underprediction occurs for the 762 combined measurements. This particular measurement was made 200 m from the roadway under low wind speed and parallel wind conditions. For the last 10 min of the sampling period, the wind speed dropped to 0.14 m/sec, far below the lower limit for a Gaussian model and the threshold of the meteorological instruments.

The overall scatter of the results is significantly greater for the Caltrans study, as indicated by the lower value of r. Of all the Caltrans results outside of the factor of 2 envelope, more than 90 percent occurred during sampling periods when either u was less than 1 m/sec or the roadway-wind angle, ϕ, did not exceed 15 degrees. All of the extreme overpredictions ($P/M >$ 4) occurred during three sampling periods during which both these conditions existed. The single unusual overprediction for the GM study ($M = 0.17$, $P = 2.13$ ppb) involved an anomalous measurement that was nearly an order of magnitude lower than all concurrent measurements made nearby.

Gaussian model performance deteriorates as wind speed approaches zero because along-wind diffusion, σ_x, is assumed to be negligible when compared to advective dilution. The result is unrealistically high predicted concentrations, typified by the extreme overpredictions presented in Figure 2. Fewer overpredictions occur in Figure 3 because only 10 percent of the GM measurements (versus 40 percent of the Caltrans measurements) were made at wind speeds below 1 m/sec.

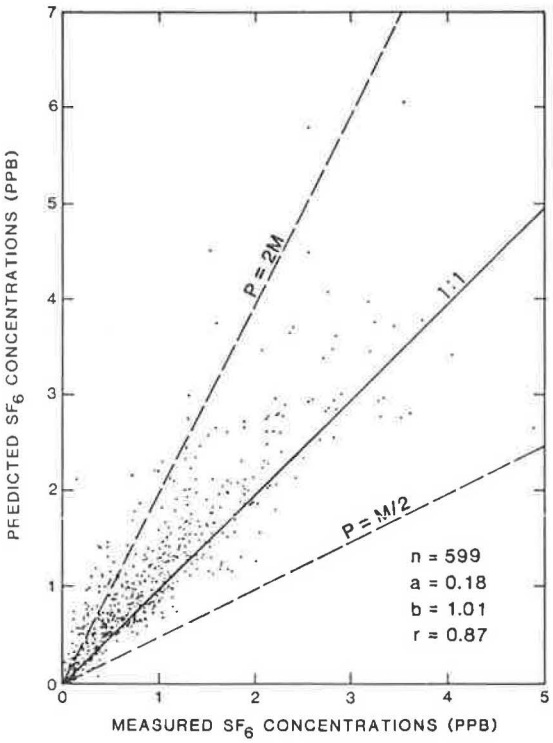

FIGURE 3 Scatter plot showing CALINE4 predictions and measured results for the GM study.

Parallel wind conditions make Gaussian line source models much more sensitive to the assumption of steady state, homogeneous wind flow. Field data invariably contain sampling periods during which horizontal plume meander is a significant dispersive mechanism. When the wind direction is parallel or nearly parallel to the roadway, meander can lead to extreme differences between measured and predicted results. This is exacerbated at low wind speeds by the failure of instrumentation to accurately record conditions.

Unfortunately, low wind speeds and horizontal meander often occur together during stable or transitional meteorological regimes. The use of a horizontal dispersion algorithm, such as the one in CALINE4, can help cope with these conditions.

However, the model must still assume that concentrations are normally distributed about a single mean wind direction. If the computed wind direction actually represents two or more distinct distributions, inaccurate predictions can result.

Plots of relative error versus ϕ for four of the GM ground-level sampling locations are given in Figure 4. Relative error, defined as

$$E_r = (P - M)/(P + M) \quad (9)$$

offers a convenient way to plot widely differing residual errors on a single scale. For each of the plots, E_r becomes more erratic as ϕ approaches zero. A general tendency toward overprediction by the model and increased data scatter at more distant locations is also evident. Similar results were obtained for CALINE4 when Caltrans data were used.

A systematic trend toward overpredicting median concentrations during parallel wind conditions can be observed in Figure 4*a*. In all, 95 percent of the GM and Caltrans median measurements made under parallel wind conditions (ϕ less than 10 degrees) were overpredicted by CALINE4. This is not surprising, given the empirical nature of the mixing zone model. The model does not attempt to resolve the complex processes of the dispersion within the mixing zone. Instead, it focuses on the net results downwind of the roadway. Assumptions of constants for σ_z and q over the mixing zone and the lack of a mechanism for modeling shear between opposing flows of traffic are probably the reasons for the inaccuracies. Still, 80 percent of the median overpredictions were within the factor of 2 envelope.

Relative error for both the GM and Caltrans tracer data was also studied as a function of u. In general, model performance deteriorated as u decreased. When u was below 1 m/sec, predicted results fell outside the factor of 2 envelope ~25 percent of the time. When u exceeded 1 m/sec, only 10 percent of the predictions were outside.

CALINE4 performed significantly better than CALINE3 at speeds below 1 m/sec, achieving a 66 percent reduction in rms error. An examination of the data revealed that virtually all of this improvement occurred for near-parallel winds with significant horizontal meander. Because CALINE4 was better able to cope with these conditions, the allowable lower limit

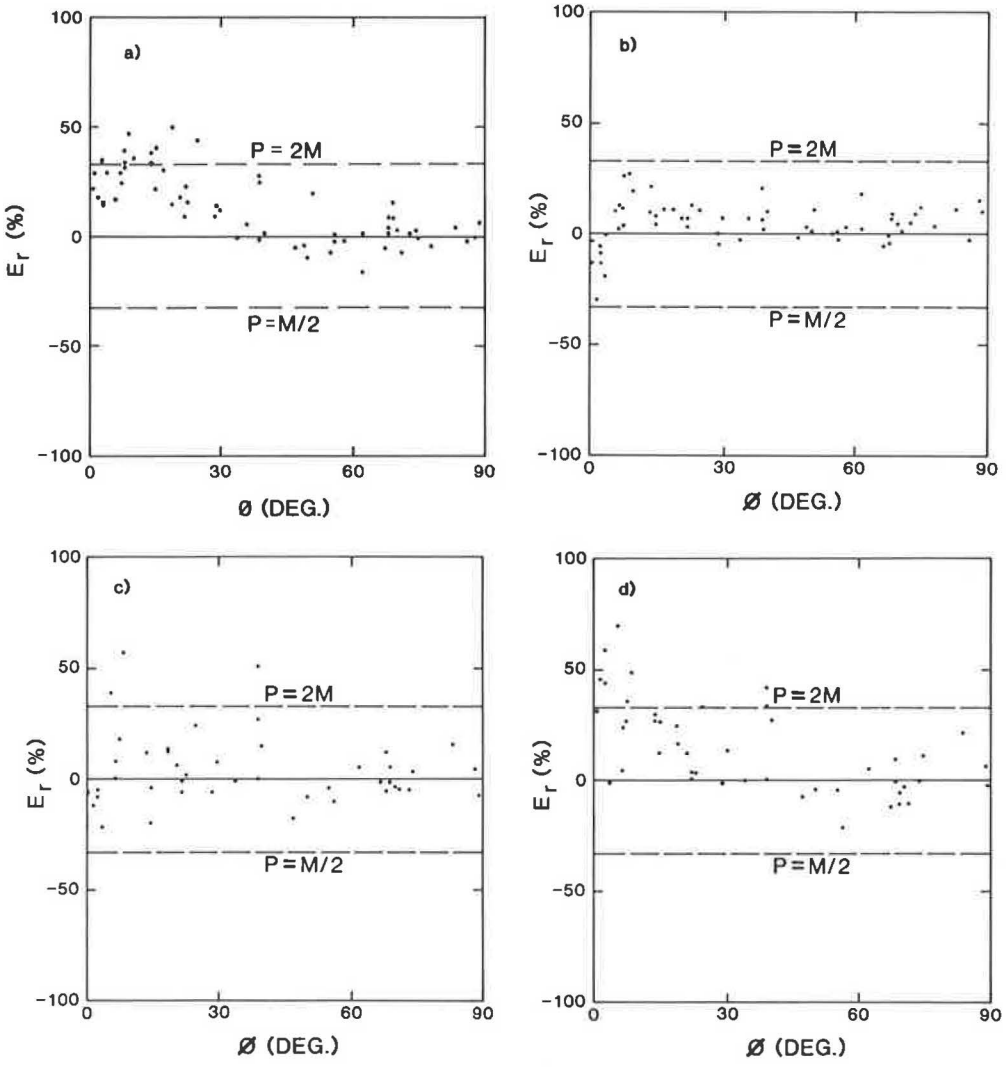

FIGURE 4 Relative error E_r versus roadway-wind angle ϕ for GM ground-level sampling locations at four distances from the roadway centerline: (a) 0 m (at median); (b) 15 m, (c) 43 m, and (d) 113 m.

for u has been reduced from the 1 m/sec value used by CALINE3 to 0.5 m/sec.

Intersection Sites

Emission factors and traffic parameters for the two intersection sites were estimated by using the best available information for each site. The distribution of vehicles by operating mode was assumed to follow the national average (21 percent cold start, 27 percent hot start). The percentages of vehicle types were based on vehicle classification counts. Acceleration rates, vehicle delay, turn movements, and other needed traffic parameters were estimated from floating car surveys and representative traffic counts.

Because of the difficulty in accumulating the input data needed to run the intersection link option, only a fraction of the intersection data was used in the verification analysis. For each data base, ~30 randomly selected hours were combined with the 10 hours of highest concentration to form a verification data set. The CALINE3 model was not run on the intersection or NO_2 data bases because it was not designed for those kinds of applications.

Model performance for intersection sites actually exceeded the performance for highway sites on the basis of the FOMs in Table 1. Two possible reasons for this are the higher wind speeds that were experienced during the intersection sampling and the elimination of parallel winds as a critical condition.

NO_2 Option

The verification analysis for the CALINE4 NO_2 option was performed by using the EPA NO_2/O_3 sampler siting study data base. From the data base, 30 time periods were chosen to represent a variety of traffic and meteorological conditions. Photolysis rate constants were determined by using a method that incorporated the effects of cloud cover (*33*). Emission factors were determined by using a California emission factor model (*34*) and assuming representative distributions of vehicle type and operating mode. The resulting individual and overall FOMs are given in Table 1.

The model performance is actually better than the results presented for the relatively inert species, SF_6 and CO. However, the improvement is due to the nature of the site, not the use of the NO_2 option. Prevailing winds were perpendicular to the highway alignment and were steady in speed and direction. For the 30 time periods studied, the roadway-wind angle was never less than 60 degrees, and the average wind speed never dropped below 1.4 m/sec. Under these conditions, the CALINE4 model gives its best performance. Because of the assumptions involved, application of the NO_2 option is not recommended for parallel winds unless measured results are available for calibrating the model.

CONCLUSIONS

The comparisons between CALINE3 and CALINE4, summarized in this paper, indicate that modest improvements in accuracy can be expected from the newer version of the model. It is assumed that these improvements are attributable to the use of σ_θ in CALINE4 to estimate horizontal dispersion, a method recommended by others as the best practical solution for near-field dispersion in flat terrain (*35–37*), and the addition of a vehicle-induced heat flux algorithm. No other significant differences in dispersion mechanisms exist between the models.

The problem of accurately predicting pollutant concentrations near line sources during conditions of low wind speed and parallel wind is not, however, fully solved by σ_θ methodology. Shifts in wind direction over time or distance make the parallel wind case the most difficult to model successfully with a Gaussian plume approach, especially at low wind speeds. Fortunately, model predictions are usually conservative under such conditions. Because measured results are usually integrated over an arbitrary time interval, during which adverse meteorological conditions might not persist, the conservative model prediction may actually be a better estimate of the true maximum concentration.

The ability of CALINE4 to handle a greater variety of problems in a more flexible manner is just as important as its enhanced accuracy. This is particularly true with regard to the intersection link option. Accurate predictions of microscale air quality effects near intersections can only be obtained by a realistic spatial allocation of the modal emissions. This is exactly what CALINE4 is designed to do.

Verification analyses for both the intersection link and NO_2 options were based on limited field data and multiple assumptions about emissions. Additional laboratory work on modal emissions and field studies, incorporating either better documentation of pertinent traffic parameters or tracer gas controls, is needed. As better estimates of modal emission rates become available, they can easily be incorporated into the CALINE4 intersection link option.

Modifications of the NO_2 option for parallel wind conditions (not tested in this analysis) would be much more difficult because of the restrictive assumptions employed. It is quite possible, however, that crosswind conditions cause higher NO_2 concentrations near the roadway than do parallel winds. The abundant supply of upwind O_3 available to react with roadway-generated NO during crosswind conditions may raise the NO-to-NO_2 conversion rate to much higher levels than occur under parallel winds, leading to higher downwind NO_2 concentrations.

ACKNOWLEDGMENTS

The development of both the CALINE3 and CALINE4 models was sponsored by FHWA, U.S. Department of Transportation, and carried out by Caltrans staff. The author wishes to acknowledge the work of the following individuals: Jim Quittmeyer, Dick Wood, and Greg Brown, who programmed CALINE4; Pat Connally and Bill Nokes, who performed the verification analysis; and Ken Pinkerman, Greg Edwards, Bob Cramer, and Ken Robertson, who were responsible for the two Caltrans field studies.

REFERENCES

1. J. L. Beaton et al. *Mathematical Approach to Estimating Highway Impact on Air Quality*. Report FHWA-RD-72-36. California Department of Transportation, Sacramento, April 1972.

2. C. E. Ward et al. *CALINE2: An Improved Microscale Model for the Diffusion of Air Pollutants from a Line Source.* Report CA-DOT-TL-7218-1-76-23. California Department of Transportation, Sacramento, Nov. 1976.
3. P. E. Benson and B. T. Squires. *Validation of the CALINE2 Model Using Other Data Bases.* Report FHWA-CA-TL-79-09. California Department of Transportation, Sacramento, May 1979.
4. K. E. Noll et al. A Comparison of Three Highway Line Source Dispersion Models. *Atmospheric Environment,* Vol. 12, 1978, pp. 1323–1329.
5. P. E. Benson. *CALINE3: A Versatile Dispersion Model for Predicting Air Pollutant Levels Near Highways and Arterial Streets.* Report FHWA-CA-TL-79-23. California Department of Transportation, Sacramento, Nov. 1979.
6. P. E. Benson. *Background and Development of the CALINE3 Line Source Dispersion Model.* Report FHWA-CA-TL-80-31. California Department of Transportation, Sacramento, Nov. 1980.
7. S. Trivikrama Rao and J. R. Visalli. On the Comparative Assessment of the Performance of Air Quality Models. *Journal of the Air Pollution Control Association,* Vol. 31, 1981, pp. 851–860.
8. J. B. Rodden et al. Comparison of Roadway Pollutant Dispersion Models Using the Texas Data. *Journal of the Air Pollution Control Association,* Vol. 32, 1982, pp. 1226–1228.
9. EPA Announces Proposed Revisions to Air Quality Modeling Guidelines. *Journal of the Air Pollution Control Association,* Vol. 31, 1981, p. 76.
10. P. E. Benson. *CALINE4: A Dispersion Model for Predicting Air Pollutant Concentrations near Roadways.* Report FHWA-CA-TL-84-15. California Department of Transportation, Sacramento, Nov. 1984.
11. R. E. Eskridge and S. Trivikrama Rao. Measurement and Prediction of Traffic-Induced Turbulence and Velocity Fields near Roadways. *Journal of Climatology and Applied Meteorology,* Vol. 22, 1983, pp. 1431–1443.
12. W. F. Dabberdt et al. *Experimental Studies and Evaluations of Control Measures for Air Flow and Air Quality on and near Highways.* Report FHWA-RD-81-051. FHWA, U.S. Department of Transportation, March 1981.
13. D. P. Chock. General Motors Sulfate Dispersion Experiment: An Overview of the Wind, Temperature and Concentration Fields. *Atmospheric Environment,* Vol. 11, 1977, pp. 553–559.
14. S. Trivikrama Rao and M. T. Keenan. Suggestions for Improvement of the EPA-HIWAY Model. *Journal of the Air Pollution Control Association,* Vol. 30, 1980, pp. 247–256.
15. F. Pasquill. *Atmospheric Diffusion.* 2nd edition. John Wiley, New York, 1974.
16. F. B. Smith. *A Scheme for Estimating the Vertical Dispersion of a Plume from a Source near Ground Level.* Air Pollution Modeling 14. Committee on the Challenges of Modern Society, North Atlantic Treaty Organization, Brussels, 1972.
17. R. R. Draxler. Determination of Atmospheric Diffusion Parameters. *Atmospheric Environment,* Vol. 10, 1976, pp. 99–105.
18. R. J. Yamartino. A Comparison of Several "Single-Pass" Estimates of the Standard Deviation of Wind Direction. *Journal of Climatology and Applied Meteorology,* Vol. 23, 1984, pp. 1362–1366.
19. S. R. Hanna. Lateral Turbulence Intensity and Plume Meandering During Stable Conditions. *Journal of Climatology and Applied Meteorology,* Vol. 22, 1983, pp. 1424–1430.
20. D. B. Turner. *Workbook of Atmospheric Dispersion Estimates.* Publication AP-26. Environmental Protection Agency, Research Triangle Park, N.C., 1970.
21. D. L. Ermak. An Analytical Model for Air Pollutant Transport and Deposition from a Point Source. *Atmospheric Environment,* Vol. 11, 1977, pp. 231–237.
22. R. G. Griffin. *Air Quality Impact of Signaling Decisions.* Report FHWA-CO-RD-80-12. Colorado Department of Highways, Denver, Oct. 1980,
23. H. S. Cole and J. E. Summerhays. A Review of Techniques Available for Estimating Short-Term NO2 Concentrations. *Journal of the Air Pollution Control Association,* Vol. 29, 1979, pp. 812–817.
24. C. D. Donaldson and G. R. Hilst. Effect of Inhomogenous Mixing on Atmospheric Photochemical Reactions. *Environmental Science and Technology,* Vol. 6, 1972, pp. 812–816.
25. R. W. Bilger. The Effect of Admixing Fresh Emissions on the Photostationary State Relationship in Photochemical Smog. *Atmospheric Environment,* Vol. 12, 1978, pp. 1109–1118.
26. R. P. Angle et al. Observed and Predicted Values of NO2/NOx in the Exhaust Plume from a Compressor Installation. *Journal of the Air Pollution Control Association,* Vol. 29, 1979, pp. 253–255.
27. J. P. Blanks et al. *Investigation of NO2/NOx Ratios in Point Source Plumes.* Report EPA-600/7-80-036. Environmental Protection Agency, Research Triangle Park, N.C., Feb. 1980.
28. S. H. Cadle et al. General Motors Sulfate Dispersion Experiment: Experimental Procedures and Results. *Journal of the Air Pollution Control Association,* Vol. 27, 1977, pp. 33–38.
29. M. Claggett and T. L. Miller. *Final Report: Carbon Monoxide Monitoring and Line Source Model Evaluation Study for an Urban Freeway and Urban Intersection.* Illinois Environmental Protection Agency, Springfield, Nov. 1979.
30. C. E. Rodes and D. M. Holland. *NO2/O3 Sampler Siting Study.* Contract 68-02-2292. Environmental Protection Agency, Research Triangle Park, N.C., Aug. 1979.
31. J. R. Martinez et al. *NCHRP Report 245: Methodology for Evaluating Highway Air Pollution Dispersion Models.* TRB, National Research Council, Washington, D.C., Dec. 1981, 85 pp.
32. *Mobile Source Emission Factors: Final Document.* Report EPA-400/9-78-006. Environmental Protection Agency, Research Triangle Park, N.C., March 1978.
33. F. L. Jones et al. A Simple Method for Estimating the Influence of Cloud Cover on the NO2 Photolysis Rate Constant. *Journal of the Air Pollution Control Association,* Vol. 31, 1981, pp. 42–45.
34. D. M. Coats et al. *Mobile Source Emission Factors.* California Department of Transportation, Sacramento, May 1980.
35. S. R. Hanna et al. AMS Workshop on Stability Classification Schemes and Sigma Curves: Summary of Recommendations. *Bulletin of the American Meteorological Society,* Vol. 58, 1977, pp. 1305–1309.
36. F. Pasquill. *Atmospheric Dispersion Parameters in Plume Modeling.* Report EPA-600/4-78-021. Environmental Protection Agency, Research Triangle Park, N.C., May 1978.
37. J. S. Irwin. Estimating Plume Dispersion: A Comparison of Several Sigma Schemes. *Journal of Climatology and Applied Meteorology,* Vol. 22, 1983, pp. 92–114.

Publication of this paper sponsored by Committee on Transportation and Air Quality.

Dispersion Characteristics of Flows in Asymmetric Street Canyons and Sensitivity to Block Shape

WALTER G. HOYDYSH AND WALTER F. DABBERDT

Flow visualization and tracer concentration measurements were made in rectangular and square (plan view) street canyon models in which the ratio of street width to the height of the upwind building was held constant at 0.83. The ratio of the heights of the upwind and downwind buildings was varied among 2.0, 1.0, and 0.67 for the rectangular block and was held constant at 1.0 for the square block. Tracer measurements were obtained across the faces of both the leeward and windward buildings for emissions in the local street canyon. Orientation of the canyon axis with respect to the free stream flow was varied from 0 to ±90 degrees in 10-degree increments. The structure of the dispersion patterns is strongly dependent on the canyon's asymmetry and is less dependent on the canyon's orientation to the prevailing flow. The patterns are also sensitive to the shape of the block: the rectangular block has a concentration maximum in midblock and the square block has maxima near the ends of the block. Concentrations are also significantly greater for the rectangular block than for the square block. Comparisons among vertical concentration profiles observed on the two canyon faces and among estimates from several commonly applied models for the rectangular block configuration are presented.

A fluid modeling and analytical study of flows in street canyons was made, using the Environmental Science and Services Corporation's atmospheric boundary layer wind tunnel (ABLWT) (Figure 1). Dispersion characteristics were investigated for three types of canyons: a step-up notch with the upwind building shorter than the downwind building, a step-down notch with the upwind building taller than the downwind building, and an even notch with upwind and downwind buildings of equal height. Normalized concentrations for various wind angles were determined at receptors mounted on the upwind and downwind building faces. Two shapes or configurations for the city block were studied, namely, rectangular and square (as observed in plan view). Vertical concentration profiles measured at midblock were compared with the predictions of several empirical and analytical models for those cases in which the free stream flow is normal to the axis of the rectangular street canyons.

W. G. Hoydysh, Environmental Science and Services Corp., Long Island City, N.Y. 11101. W. F. Dabberdt, National Center for Atmospheric Research, P.O. Box 3000, Boulder, Colo. 80307.

EXPERIMENTAL PROCEDURE

The boundary layer simulation was accomplished by using a 0.29-m-high castellated barrier and vortex generators placed at the test section entrance. The test section floor was covered with gravel roughness panels. Wind tunnel calibration and test procedures were in accordance with those outlined by the Environmental Protection Agency (*1*, *2*).

Wind tunnel calibration consisted of an atmospheric dispersion comparability test (ADCT) to demonstrate that the fluid model dispersion was comparable to the predictions of the Gaussian plume distribution. Flow visualization and tracer concentration measurements were conducted with a scale model of an urban street grid mounted on a turntable that was inserted into the ABLWT test section. During these tests, the wind tunnel speed at a height of 1 m above the ABLWT floor was a constant 2 m/sec. Hoydysh et al. (*3*) have shown that for urban street grid models of the type studied here, the flow field and concentration patterns are independent of wind speed if the Reynolds number, based on building height and the free stream velocity, exceeds 3,400. For the present experiments, the Reynolds number was 10,000.

Two scale models of urban street grids were alternately tested in the ABLWT by mounting them on the turntable. The first model consisted of a central portion that had 12 city blocks, of which 10 had actual dimensions of 60 cm (length) × 20 cm (width) × 7.5 cm (height). The "street" width was 6.25 cm, and the "avenue" width was 10 cm. A second series of tests was conducted with a second urban model in which the city blocks were of the same height (7.5 cm) as in the first series, but their width and length were both set to 20 cm. In essence, the first series investigated rectangular city blocks, whereas the second series investigated square city blocks.

The street-level emission source used in both configurations consisted of two linear point source arrays separated by 2.5 cm. Adjacent point sources in the linear arrays were separated by 1.5 cm, and the source length was 90 cm. The emission source was nonbuoyant, zero exit momentum ethane trace gas with an emission rate of 200 cm^3/sec.

Tracer gas concentrations were measured at receptors mounted on the upwind (leeward) and downwind (windward) faces of the buildings that made up the street canyon. A maximum of 30 and 56 active receptors were used in rectangular and square block tests, respectively. In all tests, an additional receptor was located upwind of the model to monitor background concentrations in the wind tunnel approach flow.

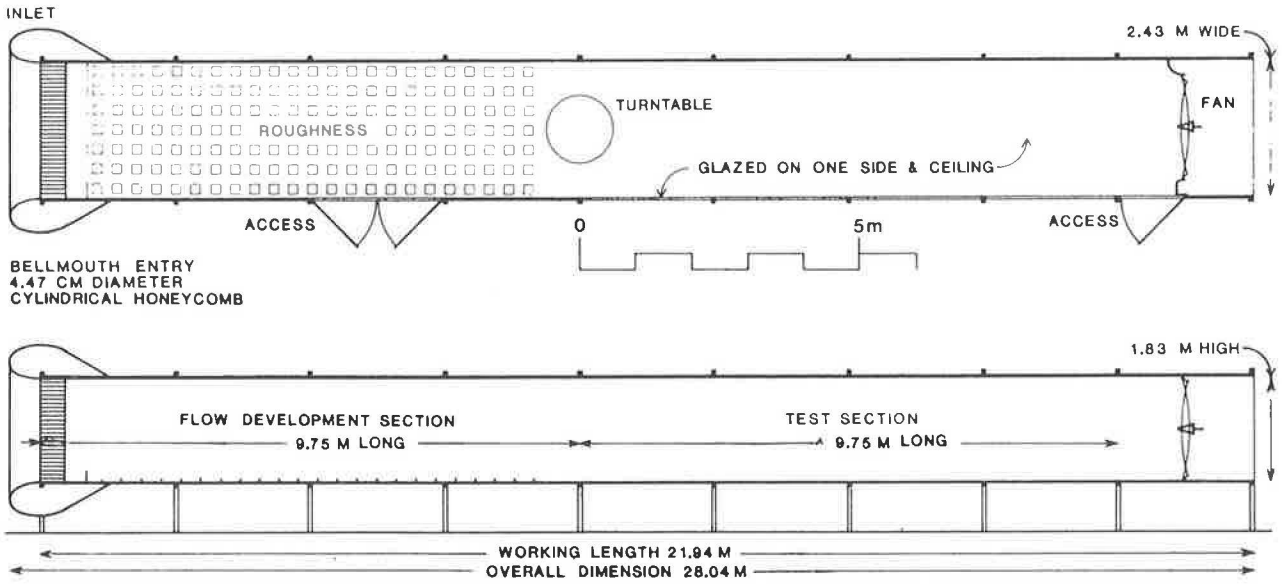

PERFORMANCE & POTENTIAL

MEAN VELOCITY RANGE	0.3 - 4.6 M/SEC FOR DIFFUSION STUDIES, UP TO 18.2 M/SEC FOR WIND LOAD STUDIES
CONFIGURATION	HYBRID - OPEN OR CLOSED CIRCUIT
STRATIFICATION CONTROL	GROUND LEVEL SURFACE HEATING & COOLING NEUTRAL, STABLE, UNSTABLE, & INVERSION CONDITIONS
BOUNDARY LAYER THICKNESS	0.6 M TO 0.91 M IN TEST SECTION
MODEL SCALING	UP TO 1000:1

FIGURE 1 ESSCO Atmospheric Boundary Layer Wind Tunnel.

Concentrations were obtained by collecting simultaneous 1-liter samples over 5 minutes at each receptor. Samples were transferred to sample bags and analyzed off line by a Beckman Model 400 Hydrocarbon Analyzer (a flame ionization detector).

In the rectangular block tests, the height of the upwind block face was 7.5 cm. Receptors on the upwind face were arranged in five vertical arrays, three receptors were in each of the noncentral arrays, and the central array contained five receptors. The downwind block face was also equipped with five vertical receptor arrays. The number of receptors in each array varied with the height of the block: 3.75, 7.5, and 11.25 cm, respectively, for the step-down, even, and step-up notches. In the square block tests, receptors were mounted in vertical arrays on both block faces. Seven equally spaced arrays of four uniformly spaced receptors were arranged on each block face.

CONCENTRATION PATTERNS: RECTANGULAR BLOCK

Figure 2 illustrates contour patterns of the normalized concentration C^* (CU/Q) on the face of the upwind and downwind buildings for wind directions that are perpendicular to the notch axis (i.e., $\theta = 0$ degrees). The patterns for the step-down notch (upwind building twice the height of downwind building) are given in Figure 2. Several significant features can be observed. The contour pattern on the upwind building face displays a street-level gradient directed from the corners to midblock, and the vertical concentration gradient is similar at the corners and midblock. These patterns reflect horizontal transport into the notch from the corners (and their intersecting notches or streets) and significant upward transport along the entire face of the upwind building (i.e., the leeward face). Although there are few sampling points on the face of the downwind building (i.e., the windward face), a similar contour pattern is visible. One notable feature is the maximum concentration value on the short windward face, which exceeds the maximum on the taller leeward face by nearly 25 percent. This feature is present for wind angles through 30 degrees. For wind angles of 50–90 degrees, the more common situation of larger leeward face concentration is observed.

Concentration contours for the "even notch" (equal building heights) are similar on the upwind face and different on the downwind face. The pattern on the leeward face is virtually identical to that of the step-down configuration. The pattern on the windward (downwind) face is similar to the leeward face except that the concentrations and the gradients are less. The pattern of street-level concentrations on the leeward (upwind) face is very similar to the pattern on the windward face. However, the magnitude of the concentrations is about a factor of two larger than on the windward face. This is the more common cross-street gradient and has been observed in a large number of ambient observational studies (*4–8*) and fluid modeling studies (*9–15*). The mechanism for the advection from the building corners to midblock is presumably the intermittent vortices that are shed on the building corners. The

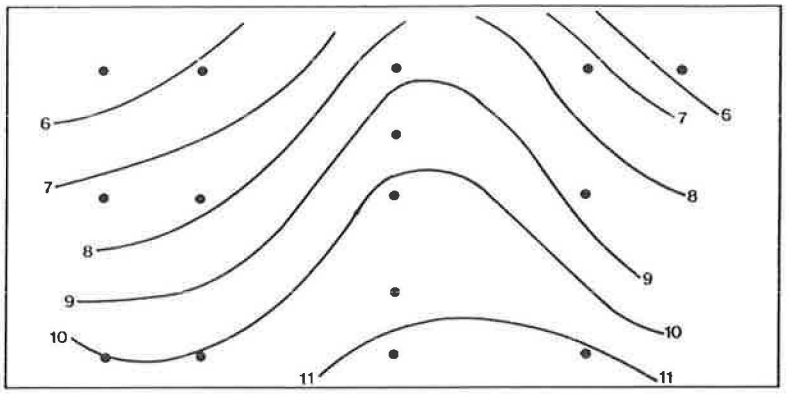

(a)

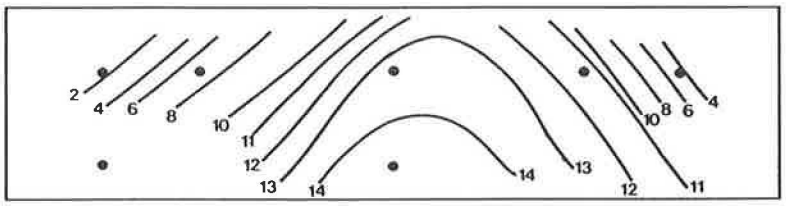

(b)

Street-Level Source, $\theta = 0^{O}$ and $H_{up} = 2H_{dn}$

FIGURE 2 Contours of normalized concentration ($C^* \times 10^{-3}$ CU/Q).

two vortices create a convergence zone in the midblock region, resulting in larger concentrations there, both at street level and aloft.

Concentration patterns for the "step-up notch" (upwind building height 0.67 of the downwind building height) exhibit both similarities and differences from those observed for the step-down and equal notches. Contours on the leeward face are nearly horizontal and do not show the upward midblock bulge characteristic of the step-down and even notches. The magnitude of the street-level concentrations on the leeward face is 50 percent that observed with the other two configurations, and the cross-street gradient is consistent with that of the even notch (i.e. about 2.5:1). The smaller concentrations indicate either more rapid flushing of the notch or enhanced entrainment of ambient air into the notch. However, the latter supposition is not supported by the concentrations associated with emissions from roof level (not shown), which are only slightly greater than for the other two notch configurations. If entrainment is a significant factor, it is probably the result of horizontal advection of clean air.

Figures 3 and 4 illustrate the dependence of the concentration due to street emissions on the angle of the wind relative to the notch. By convention, $\theta = 0$ degrees indicates a wind that is perpendicular to the notch axis, and $\theta = 90$ degrees is a wind parallel to the notch axis. The concentrations shown are those at midblock.

Figures 3 and 4 illustrate contour patterns as a function of height and wind angle for the equal notch for the leeward and windward faces, respectively. On the leeward face (Figure 3), street level concentrations vary only about ±10 percent over the range of θ values. The pattern is more varied at roof level, where C^* decreases monotonically from a maximum at $\theta = 0$ degrees to a minimum at about 30 degrees; between 40 degrees and 90 degrees there is little variation. As a consequence, the vertical gradient is a minimum at 0 degrees and a maximum from 30 degrees through 90 degrees. On the windward side (Figure 4), the street-level concentration is a maximum at $\theta = 90$ degrees, with a secondary maximum at 0 degrees and a broad minimum between 20 degrees and 70 degrees. Near roof level, the concentration decreases steadily from its maximum value at 0 degrees to a minimum around 40 degrees and then varies little through 90 degrees. The variation with θ of both the leeward and windward patterns differs significantly from the common assumptions for street canyons (*4*) in that the pattern is invariant in each of two flow regimes, namely, the cross-street region (θ = 0–60 degrees) and the along-street region (θ = 60–90 degrees). Also, the concentration maxima near 90 degrees at street level and the cross-street gradient at 90 degrees are anomalies not described by earlier studies.

Concentrations on the leeward face of the step-down notch increase slightly at all heights between $\theta = 0$ and $\theta = 20$ and then fall off with increasing values of θ, decreasing slowly near street level and rapidly at roof level. At $\theta = 90$ degrees, the C^* value at street level is two-thirds that at $\theta = 0$ degrees, whereas near roof level the ratio is one-fifth.

The patterns for the step-up notch are again different from those of the other two configurations. Little horizontal (i.e., θ) structure is observed for the windward face for all θ values available (i.e., $\theta \leq 60$ degrees; no data were available for 60–90 degrees). The leeward face also shows little structure

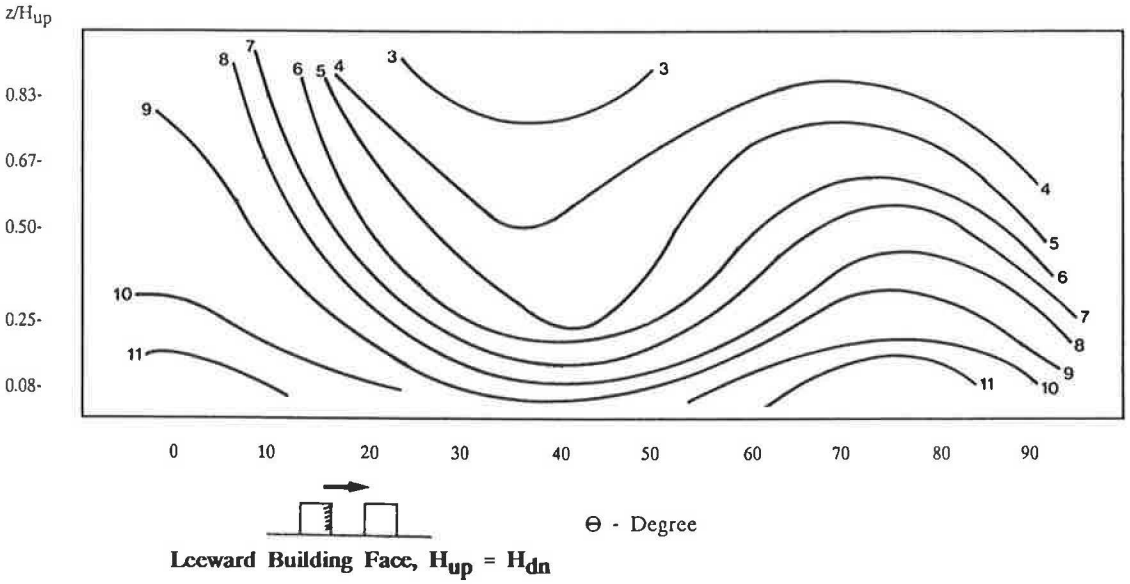

FIGURE 3 Midblock concentration ($C^* \times 10^{-3}$ CU/Q) contour diagram (height vs. wind angle), leeward.

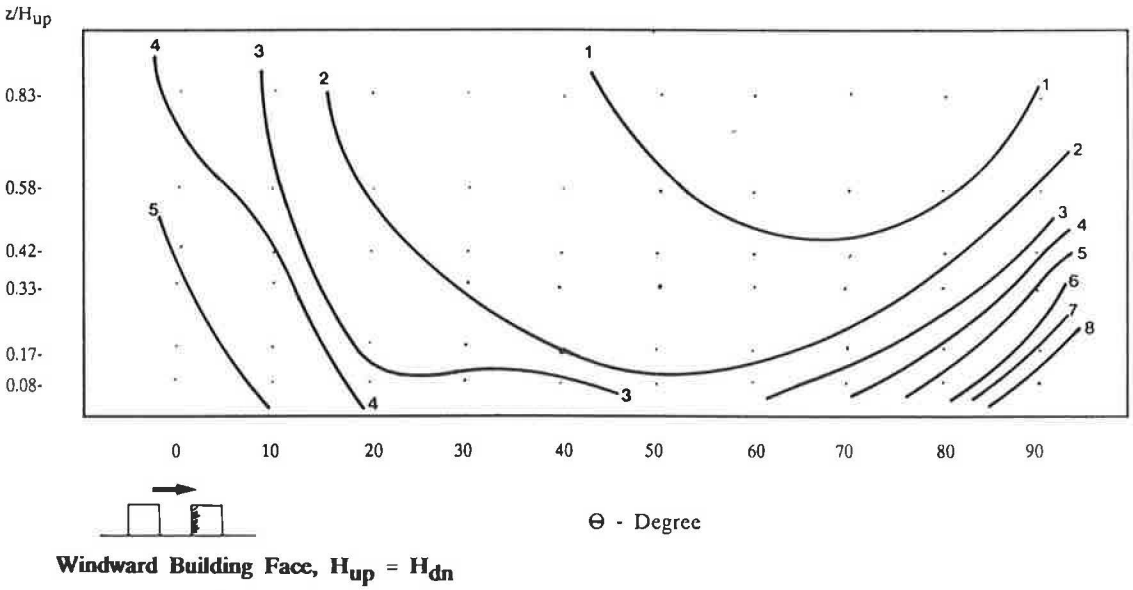

FIGURE 4 Midblock concentration ($C^* \times 10^{-3}$ CU/Q) contour diagram (height vs. wind angle), windward.

with θ through 40 degrees and then reflects a significant increase at all heights in concentration through θ = 50 degrees and 60 degrees.

CONCENTRATION PROFILES: RECTANGULAR BLOCK

The quantitative nature of the vertical profiles of concentration at the middle of the block were examined for all three notch configurations and then compared with empirical and analytical street canyon models for the even notch configuration. The observed vertical concentration profile on the leeward face of the step-down notch configuration is shown in Figure 5 for wind angles of 0, 30, 60, and 90 degrees. The street-level concentration first increases slightly with increasing θ (0–30 degrees) and then decreases markedly as θ increases further. Near-roof concentrations are a maximum at θ = 0 degrees, and they first decrease slightly, then sharply decrease with θ. As a consequence, the curvature of the vertical profile increases systematically as θ increases from 0 degrees to 90 degrees. The height variation of the concentration is seen to be well approximated by a simple exponential profile of the form

$$C^* = a \exp bz/H_{up} \quad (1)$$

where a and b are regression coefficients, z is height, and H_{up} is the height of the upwind building. In Figure 5, the observed concentrations are indicated by different symbols and the regression curve is given by the solid line. Both a and b vary with θ in a complex manner: the value of a ranges from 8.55 to

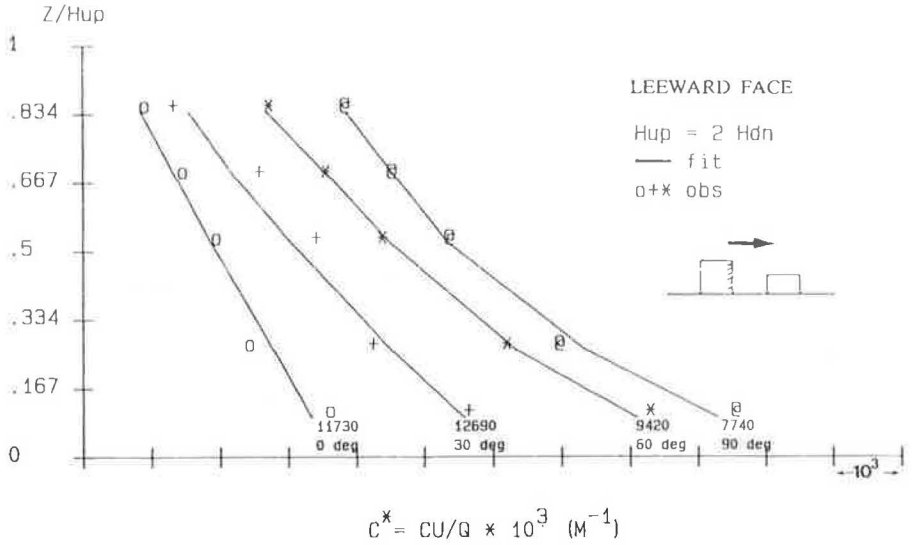

FIGURE 5 Midblock vertical concentration profiles for step-down notch configuration.

13.82×10^3, whereas b varies from a maximum of -0.33 to a minimum of -1.86. However, the exponential regression provides a consistently good fit to the data, with the explained variance (given by r^2) ranging from 0.95 to 1.00.

Street-level concentrations on the leeward face of the even-notch configuration are nearly invariant for θ values from 0 to 90 degrees. Near roof level, concentrations are a maximum at 0 degrees and decrease with increasing θ. The curvature of the vertical concentration profile again increases with θ. The pattern on the windward face reflects a fairly uniform slope from 0 degrees through 60 degrees. At larger values of θ, the curvature increases markedly, primarily in response to a large increase in the street-level concentration. The r^2 values range from 0.93 to 0.99 (with an average of 0.97 ±0.02) on the leeward face and from 0.81 to 0.99 (0.92 ±0.06) on the windward face. The empirical exponential curve again provides a consistently good fit to the observations. As before, both a and b vary widely with wind angle (θ).

The curvature of the profile for the step-up notch increases significantly with increasing θ on the leeward face, as did those of the other two configurations, but (unlike the case of the even notch) the curvature changes little on the windward face. The change in curvature on the leeward face is primarily due to an increase in the street-level concentration rather than the slope of the curve. The regression curves again fit the observations well: r^2 values range from 0.91 to 0.96 (average of 0.93 ±0.02) on the leeward face and from 0.87 to 0.99 (average of 0.93 ±0.05) on the windward face. The individual coefficients (a and b) vary less with θ, but the observed data are limited to a θ range of 0–60 degrees.

A number of empirical and analytical street canyon models have been developed over the past two decades for determining the height and cross-street variation of the pollutant mixing ratio (or concentration) from street-level vehicular emissions as a function of wind speed and direction, emission flux, and street canyon geometry. Two empirical models and one analytical diffusion model are evaluated here by using the concentration data from the even notch.

One of the earliest street canyon models was the empirical predecessor to the well-known APRAC model (named for the Air Pollution Research Advisory Committee) developed by Johnson et al. (*16*) from the observations of Georgii et al. (*4*) in Frankfurt am Main, West Germany. With street-perpendicular flow (θ = 0 degrees), Johnson and colleagues proposed that the streetside concentration on the windward (C_W) and leeward (C_L) sides is given by expressions of the form

$$C_W = C_b \exp\,[29\,Q(1 - z/z_r)] \tag{2}$$

$$C_L = C_b \exp\,[(45.6 + 4.68\,u)\,Q(1 - z/z_r)] \tag{3}$$

where Q is the emission flux, z/z_r is the ratio of the receptor height to building roof height, u is the wind speed, and C_b is the urban background concentration. Street-parallel flows were the average of the two equations. Although Georgii's data were all represented by Equations 2 and 3, other data were not well described. Subsequently, Johnson et al. identified several reasons:

- C_b should be an additive contribution rather than a determinant value;
- No separation of road and receptor was considered; and
- C at z_r did not necessarily equal C_b.

Some of these limitations are considered here by replacing the term C_b with the street-level concentration ($C_{W,0}$ or $C_{L,0}$), solving for the effective emission flux in Equation 3, and then evaluating the shape of the predicted windward concentration profile from Equation 2. If linearly extrapolated values of the leeward concentration at street and roof level for the even notch and a vortex radial velocity equal to 0.5 m s^{-1} (as determined from the flow visualization analysis) are used, the results presented in Table 1 are obtained for the observed and modeled concentrations on the leeward face. With both street-level and roof-level values of C_L^* prescribed, it is not

surprising that the "model" (Equation 3) explains 94 percent of the variance of the intermediate five data points.

Next, the windward concentrations were determined from Equation 2 and the observed street-level windward concentration, yielding the results presented in Table 2. Clearly, the model (Equation 2) underpredicts the decrease in windward concentration with height; the corresponding value of r^2 is only 0.34. From the earlier analysis it was observed that the concentration decrease with height on both windward and leeward faces is well represented by a simple exponential function. The present analysis merely illustrates that the relative profile curvature on the two building faces is not described well by the modified form of the Johnson et al. model (*16*).

TABLE 1 OBSERVED AND MODELED (Equation 3) CONCENTRATIONS ON THE LEEWARD FACE

z/z_r	C_L^*(obs.)	C_L^*(3)	C_L^*(obs.)/C_L^*(3)
0.000	11,800	11,800	1.000
0.083	11,400	11,470	0.994
0.250	10,200	10,835	0.941
0.500	9,460	9,950	0.951
0.667	9,210	9,399	0.980
0.833	8,800	8,882	0.991
1.000	8,390	8,390	1.000

TABLE 2 OBSERVED AND MODELED (Equation 2) CONCENTRATIONS ON THE WINDWARD FACE

z/z_r	C_W^*(obs.)	C_W^*(2)	C_W^*(obs.)/C_L^*(2)
0.000	5,480	5,480	1.000
0.083	5,390	5,471	0.985
0.167	5,300	5,461	0.971
0.333	5,320	5,444	0.977
0.417	5,020	5,434	0.924
0.583	4,290	5,416	0.792
0.833	3,610	5,389	0.670
1.000	3,160	5,371	0.588

Johnson et al. (*4*) used new field data from San Jose, California, to develop a revised street canyon algorithm. If ΔC is the increment to the concentration that is attributable to street canyon emissions, then

$$\Delta C_L = Q/U_s\, Y \tag{4}$$

where Y is the vertical extent of the mixing volume and is assumed to be proportional to the sum of the diagonal traffic receptor separation plus a vehicle induced mixing length [$Y = k_1\,(L + L_0)$]. The effective street-level wind U_s is taken to be proportional to the roof-level wind U_r and a vehicle drag flow (0.5 m s^{-1}), such that $U_s = k_2\,(U_r + 0.5)$. When L_0 is assumed to be of the order of one vehicle dimension (about 2 m), then

$$\Delta C_L = Q/k_1\, k_2\, W\,(U_r + 0.5)\,(L + 2) \tag{5}$$

Johnson et al. (*5*) and Ludwig and Dabberdt (*17*) have determined experimentally that $k_1 k_2 = 1/7$ in independent field studies. The windward face concentration (ΔC_W) was first modified by Johnson et al., who reasoned that it should be height independent because of the thorough mixing and considerable transport from the emission source by the street canyon vortex:

$$\Delta C_W = Q/k_1\, k_2\, W\,(U_r + 0.5) \tag{6}$$

(where W is the street width). Ludwig and Dabberdt (*17*), however, reexamined Equation 6 and noted a decrease with height from entrainment. This observation resulted in the present form of the APRAC street canyon model, where

$$\Delta C_W = Q\,(H - z)/k_1\, k_2\, W\,(U_r + 0.5)H \tag{7}$$

Ludwig and Dabberdt stated that Equations 5 and 7 hold for values of θ from 0 to ±60 degrees.

In the absence of vehicle-induced turbulence in the notch, Equations 5 and 7 are revised slightly in the present application:

$$\Delta C_L = Q/k_1\, k_2\, LU_r \tag{8}$$

$$\Delta C_W = Q\,(H - z)/k_1\, k_2\, WHU_r \tag{9}$$

The distance L is taken to be the diagonal from the center of the street to the receptor; therefore Equation 8 can be rewritten for the even notch as

$$C_L^* = 7N^*/[(z/H)^2 + 1/4]^{1/2} \tag{10}$$

where $N^* = C_L^*\,(z = 0)/[7/0.4]$. If the observed C_L^* are used to normalize at street level, the values presented in Table 3 are the result. The corresponding value of $r^2 = 0.94$ indicates the observed profile is well represented by the APRAC model on the leeward face. However, it should be noted that the model systematically underpredicts at the upper receptor heights.

TABLE 3 OBSERVED AND MODELED (Equation 8) CONCENTRATIONS ON THE LEEWARD FACE

z/z_r	C_L^*(obs.)	C_L^*(8)	C_L^*(obs.)/C_L^*(8)
0.000	11,800	11,800	1.000
0.083	11,400	11,640	0.979
0.250	10,200	10,544	0.967
0.500	9,460	8,344	1.134
0.667	9,210	7,080	1.301
0.833	8,800	6,077	1.448
1.000	8,390	5,276	1.590

By using the normalizing factor for C_L^* and Equation 9, absolute values of C_W^* can be determined, as presented in Table 4. Again, the model systematically underpredicts at the upper levels: r^2 is very large at 0.93. Another measure of the performance of the APRAC street canyon model is its representation of the street-level cross-street concentration gradient.

The observed data indicate a ratio of C_L^* (observed)/C_W^* (observed) of 2.115 at the lowest measurement height (z/H = 0.083), while the APRAC model indicates a ratio of 1.794.

Hotchkiss and Harlowe (*18*) undertook both numerical and analytical solutions of the two-dimensional equations of motion and diffusion for unsteady flow in an open infinite notch. For the analytical solution evaluated here, the momentum equations were linearized and the diffusion equation was solved by a power series expansion of the velocity field. The geometry of the notch was very similar to the even notch reported here. The concentrations determined by Hotchkiss and Harlowe have been normalized as before, according to the observed value of C_L^* near street level, with the following results for both the leeward and windward faces. The ratio of observations to simulations varies on the leeward face from 1.0 at street level (by definition) to 1.832 near roof level and on the windward face from 0.667 at street level to 1.203 near roof level.

TABLE 4 OBSERVED AND MODELED (Equation 9) CONCENTRATION ON THE WINDWARD FACE

z/z_r	C_W^*(obs.)	C_W^*(9)	C_W^*(obs.)/C_W^*(9)
0.000	5.480	7.080	0.774
0.083	5.390	6.490	0.831
0.250	5.300	5.310	0.998
0.333	5.320	4.720	1.127
0.417	5.020	4.130	1.215
0.583	4.290	2.950	1.454
0.833	3.610	1.180	3.059
1.000	3.160	0	∞

These comparisons of observations with predictions by Hotchkiss and Harlow (H & H) indicate generally good agreement. On the leeward face, r^2 is 0.96, but the H & H model increasingly underpredicts with increasing height (as does the APRAC model). On the windward face, the model overpredicts substantially (by about 50 percent) near street level and underpredicts moderately near roof level. Overall, the modeled vertical gradients are significantly greater than the observed vertical gradients on both faces of the notch. At street level, the horizontal gradient from the H & H predictions is less than that observed. This was also the case with the APRAC model.

CONCENTRATION PATTERNS: SQUARE BLOCK

As summarized in the preceding sections, a major finding of the dispersion tests with the rectangular block configuration was the position of the concentration maxima in the middle of the street canyon with a perpendicular wind (i.e., θ = 0 degrees). Earlier fluid modeling tests in which Hoydysh and Ogawa (*12*) and Wedding et al. (*13*) used square blocks yielded different results: the concentration maxima were located at the ends of the street canyon near the intersections. Figure 6 illustrates representative concentration isopleth patterns from Hoydysh and Ogawa. To establish the sensitivity of the concentration pattern to block configuration, additional tests were conducted in the ABLWT.

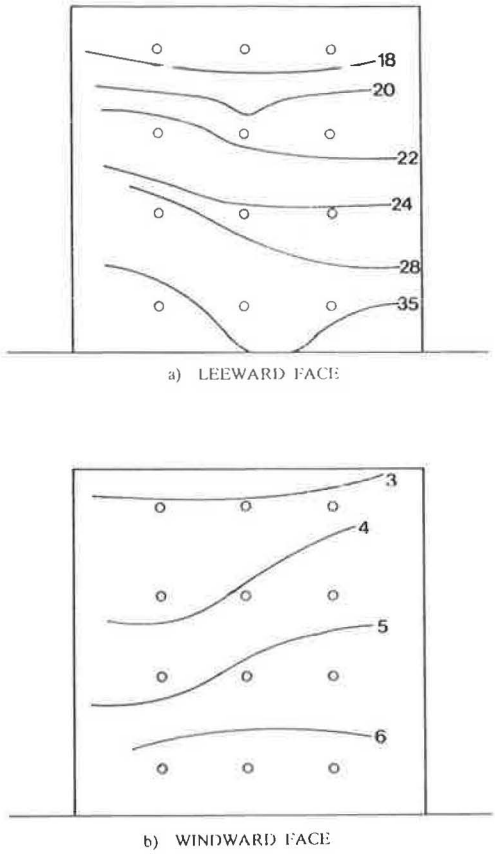

FIGURE 6 Concentration patterns in a square block grid (*12*).

The urban street model was changed from a rectangular block configuration to a square block configuration, but the length and intensity of the line source remained unchanged. Similarly, the building height and street and avenue widths were also kept fixed. The resulting street canyon concentration pattern for the even notch is shown in Figures 7 and 8 for the upwind (a) and downwind (b) building faces. Figure 7 has an upwind fetch over a smooth surface, and Figure 8 corresponds to a rough upwind fetch. Upwind roughness has an insignificant effect on the magnitude or distribution of the concentration isopleths in the street canyon. This insensitivity is probably due to the very large roughness of the urban core, which dominates the roughness of the upwind fetch.

In a manner similar to that observed in the two earlier square block studies, the concentrations increased from the center of the street canyon outward to the edges or ends of the block. The leeward (i.e., upwind) concentrations continue to be significantly greater than the concentrations on the downwind (windward) building face. If the magnitude of the concentrations for the square (Figure 7) and rectangular blocks are compared, it can be observed that concentrations are more than a factor of two greater for the rectangular block. The reduction in the square block configuration is a consequence of the increased ventilation that corresponds to the shorter length of the street canyon. For the

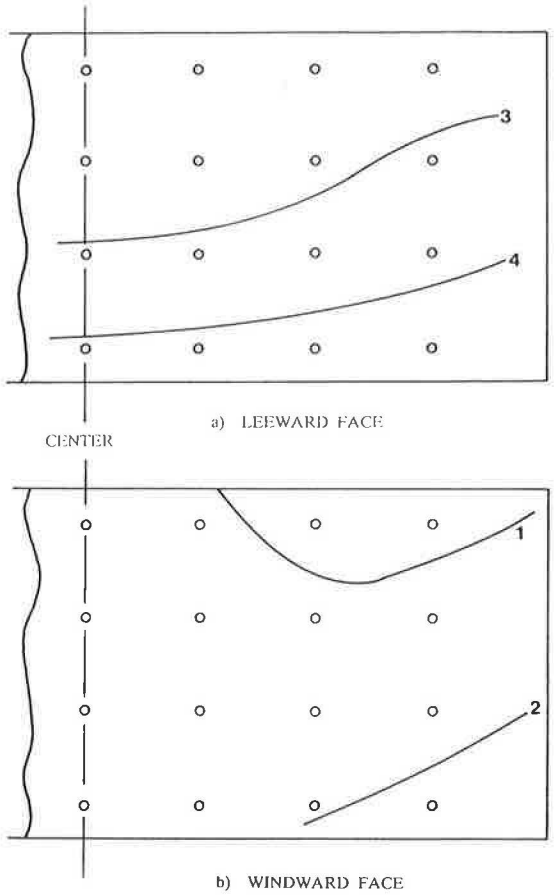

FIGURE 7 Concentration ($C^* \times 10^{-3}$) contours for square block and smooth upwind fetch; θ = 0 degrees.

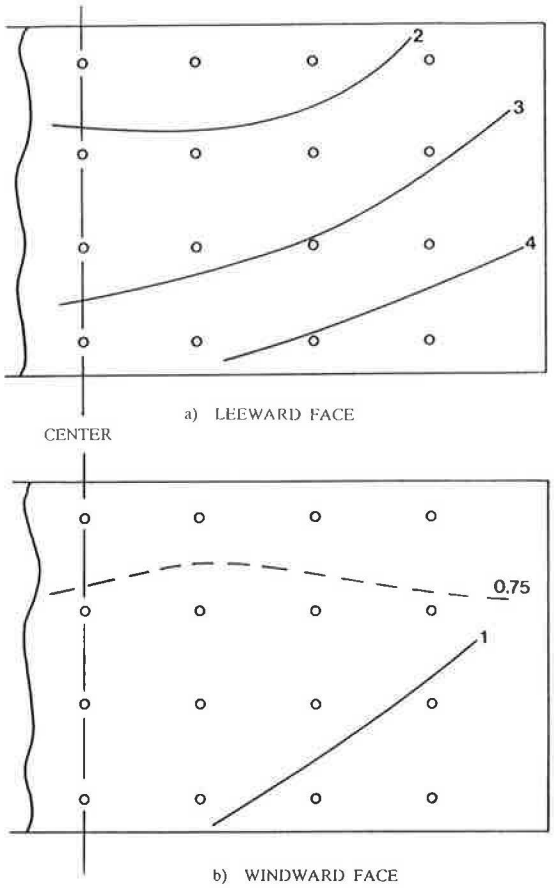

FIGURE 8 Concentration ($C^* \times 10^{-3}$) contours for square block and rough upwind fetch; θ = 0 degrees.

rectangular configuration the ratio of street length (along the line source) to open space corresponding to the intervening avenues is 6:1, whereas for the square configuration the ratio is 2.0:1. A secondary effect may also be the result of the size of the corner vortices compared to the length of the block. For the shorter square block, it can be assumed that the turbulent mixing caused by the two corner vortices affects the entire length of the block.

CONCLUSIONS

The dispersion characteristics of flow in three notch configurations on a rectangular block were examined by using tracer gas techniques. The notches are representative of the broad types of street canyons found in urban areas. In addition, the differences between rectangular and square blocks for the street canyon distribution of concentrations were investigated. The results of these investigations have confirmed some previous research findings and provided several new insights as well.

From the rectangular block configuration, it can be concluded that

- Entrainment into the street canyon appears to be primarily the result of horizontal advection caused by vertical axis corner vortices.
- The distribution of trace gas concentration contours is nearly identical on the leeward faces of the even and step-down notch configurations and is characterized by higher concentrations at midblock. Leeward contours for the step-up notch are horizontally stratified throughout the notch, suggesting the absence of convergence (in comparison to the other configurations).
- Street-level cross-notch gradients indicate that concentrations are generally a factor of two or more greater for the leeward than for the windward face. The exception is for the step-down notch, where windward concentrations are slightly greater than those to leeward for free stream wind directions nearly perpendicular (θ ≤ 30 degrees) to the longitudinal notch axis.
- Concentrations are generally a factor of two lower in the step-up notch than in either the step-down or even notches.
- The vertical concentration profile is a simple exponential function for both notch faces and all three notch configurations in the case of the rectangular block, but the scale and shape coefficients vary widely.
- Evaluation of one analytical and two empirical models of concentration profile showed mixed results on the basis of data for the even notch and perpendicular flow in the rectangular block. The general features are represented, but the magnitude of the cross-street gradient is underestimated and the vertical gradient is both under- and overestimated by the various

models. None of the models is structured to represent the observed contour patterns as functions of wind angle and notch configuration.

When the concentration pattern in the even notch of the rectangular block is compared with that in the square block, it can be observed that

- Concentration maxima occur in the middle of the rectangular block but near the edges of the square block.
- With equivalent line source emission rates, concentration magnitudes are more than a factor of two greater for the rectangular block than for the square block.

The effect of block configuration on the shape and magnitude of the concentration field is a major new finding from this study.

REFERENCES

1. *Research and Development: Guideline for Fluid Modeling of Atmospheric Diffusion.* Report EPA 600/8-81-009. Office of Air Quality Planning and Standards, Environmental Protection Agency/Environmental Sciences Research Laboratory, Research Triangle Park, N.C., April 1981.
2. *Guideline for Use of Fluid Modeling to Determine Good Engineering Practice Stack Height.* Report 450/4-81-003. Office of Air Quality Planning and Standards, Environmental Protection Agency, Research Triangle Park, N.C., July 1981.
3. W. G. Hoydysh, Y. Ogawa, and R. A. Griffiths. A Scale Model of Dispersion of Pollutants in Street Canyons. APCA Paper 74-157. Presented at the 67th Annual Meeting of the Air Pollution Control Association, Denver, Colo., June 1974.
4. H. W. Georgii, E. Busch, and E. Weber. *Investigation of the Temporal and Spatial Distribution of the Emission Concentration of Carbon Monoxide* (in German). Report 11. Institute for Meteorology and Geophysics, University of Frankfurt, Frankfurt, Germany, 1967.
5. W. B. Johnson, W. Dabberdt, F. Ludwig, and R. Allen. *Field Study for Initial Evaluation of an Urban Diffusion Model for Carbon Monoxide.* Contract CAPA-3-68 (1-69)/SRI Project 8563, Stanford Research Institute, Menlo Park, Calif., 1971.
6. W. F. Dabberdt, F. L. Ludwig, and W. B. Johnson. Validation and Applications of an Urban Diffusion Model for Vehicular Emissions. *Atmospheric Environment,* Vol. 7, 1973, pp. 603–618.
7. H. Waldeyer, P. Leisen, and W. R. Mueller. Die Abhängigkeit der Immissionsbelastung in Strassenschluchten von meteorologischen und verkehrsbedingten Einflussgrossen. In *Proceedings, Abgasbelastungen durch den Kraftfahrzeugverkehr,* Technischer Ueberwachungs-Verein Rheinland, Köln, Germany, 1981, pp. 85–114.
8. R. Joumard. Ausbreitungsmodelle für Verkehrs-Immissionen in Strassenschluchten und Vergleich zu französischen Messungen. In *Proceedings, Abgasbelastungen durch den Kraftfahrzeugverkehr,* Technischer Ueberwachungs-Verein Rheinland, Köln, Germany, 1981, pp. 187–206.
9. W. G. Hoydysh. *An Experimental Investigation of the Dispersion of Carbon Monoxide in the Urban Complex.* AIAA Paper 71-523. Presented at the Urban Technology Conference, New York, N.Y., May 1971.
10. R. B. Jacko. *A Wind Tunnel Parametric Study to Determine the Air Pollution Dispersion Characteristics in an Urban Center.* Ph.D. thesis. Purdue University, West Lafayette, Ind., 1972.
11. T. Odaira et al. *Using Wind Tunnel Experiments to Forecast Automobile Exhaust Gas Concentrations Along Streets.* Department of Sanitary Engineering, Kyoto University, Kyoto, Japan, 1972.
12. W. G. Hoydysh and Y. Ogawa. *Characteristics of Wind, Turbulence, and Pollutant Concentration in and above a Model City.* Report ERL TR110/NASA Grant N6R 33-016-149. Center for Interdisciplinary Studies, New York University, New York, N.Y., 1972.
13. J. B. Wedding, D. J. Lombardi, and J. E. Cermak. A Wind Tunnel Study of Gaseous Pollutants in City Street Canyons. *Journal of the Air Pollution Control Society,* Vol. 27, No. 6, 1977, pp. 557–566.
14. W. Dabberdt, E. Shelar, D. Marimont, and G. Skinner. *Analysis, Experimental Studies, and Evaluations of Control Measures for Air Flow and Air Quality on and near Highways.* Final Report FHWA/RD-81/051. SRI International, Menlo Park, Calif., 1981.
15. P. Leisen, P. Jost, and K. S. Sonnborn. Modellierung der Schadstoffausbreitung in Strassenschluchten Vergleich von Aussenmessungen mit Rechnerischer und Windkanal-simulation. In *Proceedings, Abgasbelastungen durch den Kraftfahrzeugverkehr,* Technischer Ueberwachungs-Verein Rheinland, Köln, Germany, 1981, pp. 207–234.
16. W. B. Johnson, F. L. Ludwig, and A. E. Moon. Development of a Practical, Multi-Purpose Urban Diffusion Model for Carbon Monoxide. Presented at the Symposium on Multiple-Source Urban Diffusion Models, Chapel Hill, N.C., October 1969.
17. F. L. Ludwig and W. F. Dabberdt. *Evaluations of the APRAC 1A Urban Diffusion Model for Carbon Monoxide.* Stanford Research Institute, Menlo Park, Calif., 1972.
18. R. S. Hotchkiss and F. H. Harlow. *Air Pollution in Street Canyons.* Report EPA-R4-73-029. Meteorology Laboratory, Environmental Protection Agency, Research Triangle Park, N.C.; Los Alamos National Laboratory, Los Alamos, N. Mex. 1973.

Publication of this paper sponsored by Committee on Transportation and Air Quality.

Corrections to Hot and Cold Start Vehicle Fractions for Microscale Air Quality Modeling

PAUL E. BENSON

A model is developed to correct hot and cold start vehicle fractions for input to conventional emission factor models. The method is appropriate for microscale air quality analyses of urban freeways and arterials. It is based on the propositions that hot and cold start transient emissions are highest at engine start-up and gradually diminish to zero as engine and catalyst reach a stable operating temperature and that the distribution of vehicles on urban freeways and arterials in the warm-up phase of operation is skewed such that more vehicles are near the end of the phase than the beginning. Use of the FTP-75 split 27 percent hot and 21 percent cold starts may result in significant overpredictions of air quality impacts for urban freeways. Corrected values of 1 and 5 percent, respectively, are predicted by the model.

Estimates of vehicle emission factors play a key role in evaluating microscale air quality impacts of proposed highway facilities. An important component of this estimation process is the determination of the fraction of vehicles in the warm-up phase of operation. During this phase, vehicles release excess quantities of carbon monoxide (CO) and hydrocarbons. These are referred to as transient emissions because their release occurs only during warm-up. After the engine and exhaust system reach a stable running temperature, called the hot stabilized mode, average CO and hydrocarbon emissions drop to much lower levels. Because the amounts of transient emissions are often quite large in comparison to those of hot stabilized emissions, their estimation is an important part of the overall emissions modeling process.

If the modeling of transient emissions is to be better understood, the operation of the internal combustion engine during warm-up must be considered. When an engine is cold, fuel fed to its cylinders is not readily vaporized. To achieve the ratio of air to fuel vapor needed for combustion, a fuel-rich mixture is used. The colder the air temperature, the more excess fuel needed. Much of this fuel leaves in the exhaust stream as unburned or partially burned carbon compounds. The suppression of combustion in the vicinity of the relatively cold cylinder walls further contributes to elevated levels of CO and hydrocarbons. For catalyst-equipped vehicles, the ability to deal with excess emissions during warm-up is controlled by the temperature of the catalyst.

The length of time required for warm-up of both engine and catalyst depends primarily on initial temperature of the components, engine size, and vehicle speed (*1*). A start is categorized as either hot or cold, depending on the length of time the engine has been off and whether or not the vehicle has a catalyst. For purposes of vehicle certification, the warm-up phase is defined by a standard driving cycle that is part of the 1975 Federal Test Procedure (FTP-75) (*2*). This cycle represents the first 3.59 mi of a typical urban trip, lasting 505 s at an average speed of 25.6 mph.

The MOBILE3 computer program (*3*) is used in most states to estimate vehicle emissions for proposed highway facilities. MOBILE3 was derived primarily from emissions data that were collected in accordance with FTP-75. Composite emission factors are reported by the program in grams per vehicle mile (g/vmi) as a function of ambient temperature, average vehicle speed, vehicle type distribution, calendar year, operating mode distribution, and several other variables. The model is extremely sensitive to the cold start portion of the operating mode distribution, especially at low temperatures.

Figure 1 shows MOBILE3 cold start and hot stabilized emission factors as a function of ambient temperature for a 1990 mix of light-duty gas vehicles (LDGVs) operating at an average speed of 20 mph. The cold start results represent the sum of both transient and hot stabilized emissions, and the difference between the curves represents the transient contribution. At 750°F, the average CO emissions of vehicles in cold start mode is three times that of hot stabilized vehicles. This increases to nearly six times at 0°. Hot start emission factors (not plotted) are similar to the hot stabilized factors. The figure shows that accurate estimation of the cold start vehicle fraction is critical to the accuracy of the overall composite emission factor estimate, especially at low temperatures. Estimation of the hot start fraction is much less important.

Because combustion efficiency increases with engine temperature (*4*), transient emissions from hot and cold starts will begin high and then gradually decrease to zero as the engine and catalyst approach stable operating temperatures. If the distribution of travel distances for vehicles in the warm-up phase is such that more vehicles are in the later stages of warm-up, the overall transient emissions on a particular highway segment may be lower than expected. This is frequently the case in urban corridors, where vehicles that have traveled longer distances are drawn from a larger area of potential trip origins. Previous efforts at characterizing the fractions of vehicles in hot and cold start operation make no correction for this factor (*5*, *6*).

California Department of Transportation, Transportation Laboratory, 5900 Folsom Blvd., Sacramento, Calif. 95819.

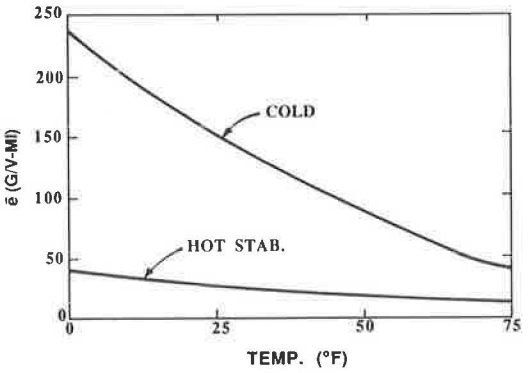

FIGURE 1 MOBILE3 composite emission factors for cold transient and hot stabilized operation (1990 LDGV mix at 20 mph).

TRANSIENT EMISSIONS MODEL

The conventional method of modeling transient emissions for microscale applications is to add an average transient emission rate, $\bar{e}_t$, to the baseline hot stabilized rate for the fraction of vehicles in the warm-up phase. This approach is applied to both hot and cold start fractions. The value of $\bar{e}_t$ is defined as

$$\bar{e}_t = \frac{E_t}{R} \tag{1}$$

where E_t equals the average transient emissions per vehicle trip and R equals the total distance traveled during warm-up (3.59 mi). A more comprehensive model for describing the distribution of transient emissions can be fashioned by establishing a set of boundary conditions consistent with the smooth, continuous nature of the warm-up process. A representation of this model is given in Figure 2. Note that either time or distance could be used as the abscissa in this model. Distance was chosen so that the model would be compatible with the travel distribution model discussed in the next section.

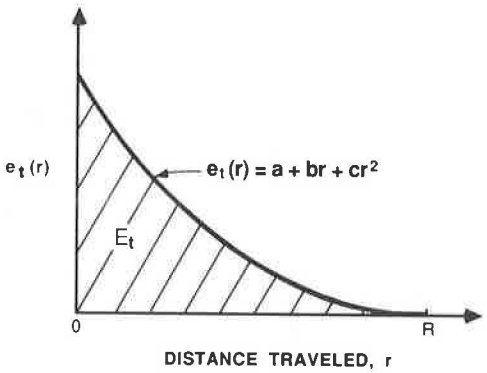

FIGURE 2 Transient emissions model.

By definition, transient emissions will dissipate to zero by the end of the warm-up phase so that

$$e_t(r)\Big|^R = 0 \tag{2}$$

where $e_t(r)$ represents the rate of excess emissions (g/vmi) as a function of distance traveled, r. Furthermore, it is reasonable to assume that the rate of change of $e_t(r)$ will decrease during warm-up and will approach zero as a smooth function so that

$$\frac{de_t(r)}{dr}\Big|^R = 0 \tag{3}$$

The quadratic equation

$$e_t(r) = a + br + cr^2 \tag{4}$$

is the simplest functional form that will satisfy the boundary conditions of Equations 2 and 3. The final boundary condition needed to evaluate the coefficients in Equation 4 is

$$E_t = \int_0^R e_t(r)\, dr \tag{5}$$

Simultaneous solution of Equations 2, 3, and 5, with substitution into Equation 4, yields

$$e_t(r) = 3\bar{e}_t\left[1 - 2\frac{r}{R} + \left(\frac{r}{R}\right)^2\right] \tag{6}$$

Equation 6 may also be cast as a function of the fraction of the warm-up phase completed, $f_r = r/R$. This form of the equation leads to a generalized relation between the fraction of transient emissions released, f_e, and f_r:

$$f_e = 3\int_0^{f_r}(1 - 2f_r + f_r^2)\, df_r \tag{7}$$

Performing the indicated integration and then simplifying gives

$$f_e = f_r^3 - 3f_r^2 + 3f_r \tag{8}$$

Equation 8 provides a simple way to calculate the cumulative amount of transient hot or cold start emissions up to any point in the 3.59-mi warm-up phase. Measured results of f_e, based on cold start CO emissions at 200°F for twenty-five 1967 to 1974 LDGVs (*7*), are compared to Equation 8 in Figure 3. The measurements were made at 137 and 343 s into the cold start portion of the FTP-75 test cycle. In terms of distance traveled, these times are equivalent to $f_r = 0.19$ and 0.73, respectively. The hot stabilized component was deducted so that the measurements could be compared directly to the transient emissions model. The mean and 95 percent confidence limits of the mean for the 25 vehicles are also plotted in Figure 3.

Clearly, the model falls short of accurately predicting f_e during the early phase of warm-up. The vehicles are emitting a greater proportion of their transient cold start emissions in the first 137 s than was predicted. Addition of a cubic term to Equation 4 would provide a better fit of the data but would require a fourth, somewhat arbitrary boundary condition. Because Equation 8 provides a conservative estimate of fe that is superior to the straight line estimate, $f_e = f_r$, and because it is based on acceptable boundary conditions, it will be used.

TRAVEL DISTRIBUTION MODEL

As long as vehicles operating in the warm-up phase are distributed equally by distance traveled, $\bar{e}_t$ adequately describes

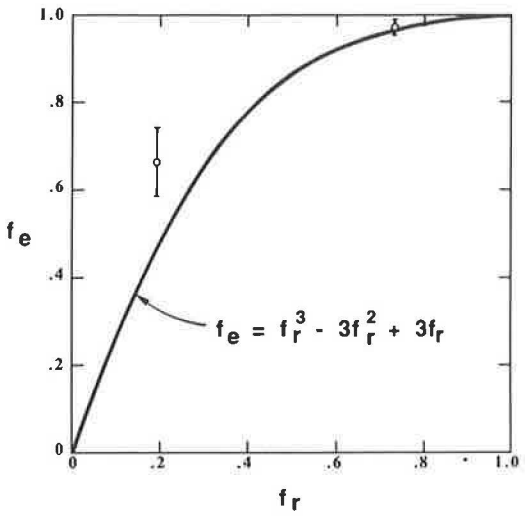

FIGURE 3 Verification of transient emissions model, illustrating the mean and 95-percent confidence limits for measured results from 25 LDGVs.

the transient emission rate. However, urban freeways and many urban arterials will attract vehicle trips at a more or less constant rate over distances approaching R. If evenly distributed trip generation can be assumed, vehicles that travel a longer distance will be drawn from a larger area of potential trip origins and will therefore be more numerous. Applying $\bar{e}_t$ to the overall fraction of vehicles in either hot or cold start mode without a correction for this factor will result in overestimates of the actual emissions.

To illustrate this point, consider the highway segment of length R presented in Figure 4*a*, with travel in one direction only, carrying an average traffic volume of V in vehicles per hour (vph) and drawing traffic from a corridor half-width W at a uniform rate v (vph/mi). Let the fraction of vehicles entering the highway in the warm-up phase be denoted as f_t, and let the travel distance from coordinates x, y to point P via the most direct route over a rectangular street grid be represented by r, such that

$$r = |x| + |y| \tag{9}$$

To model the number of vehicles at P in the warm-up phase that have traveled a distance r, three assumptions must be made. First, assume that the production of trips passing point P is constant over the corridor half-width. Second, assume that V is constant over the highway segment. Third, assume that all vehicles exiting the highway are in hot stabilized mode. For major urban corridors in which microscale modeling results are most critical, these assumptions approximate actual conditions during peak commute hours.

All vehicles entering the highway upstream of the segment will be in the warm-up phase at P because their travel distance will exceed R. Similarly, vehicles beginning trips in the shaded area may enter the segment after traveling less than R, but they will have exceeded this travel distance by the time they reach P. Although these vehicles are included in the estimate of f_t, they will not be emitting transient emissions at P. Only

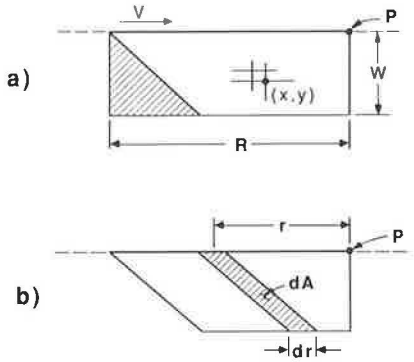

FIGURE 4 Illustration of the travel distribution model.

vehicles that started trips within the unshaded area will be in the warm-up phase at P. The total vph passing P in the warm-up phase is given by

$$N_t = f_t v \left(R - \frac{W}{2} \right) \quad W \leq R \tag{10}$$

The distribution of hot or cold start vehicles by travel distance can be determined by applying the proportion of an infinitesimal element area, dA, shown in Figure 4*b*, to the total area from which the trips derive, $WR - (W^2/2)$. The resulting equation for the differential of n trips of distance r is

$$dn = \frac{f_t v}{W} r\, dr \quad 0 < r \leq W$$
$$dn = f_t v\, dr \quad W < r \leq R \tag{11}$$

By integrating Equation 11, the fraction of vehicles that have traveled r or less at P, n_r/N_t, can be constructed. The resulting curves for $W = R/4$ and $W \geq R$ are presented in Figure 5. The greater fraction of trips in the later stages of warm-up is exhibited by the increasing slope of the curves as f_r

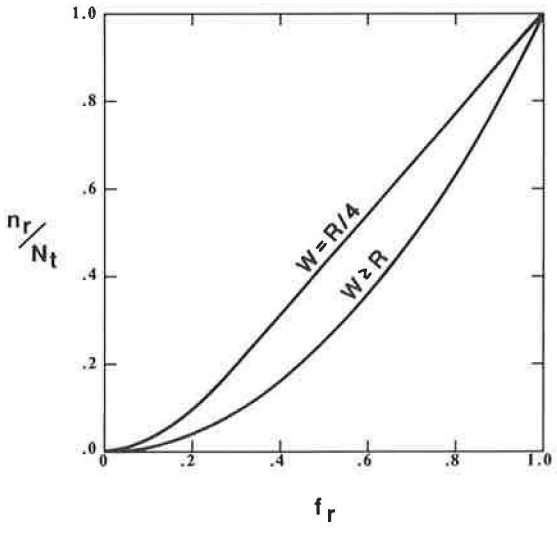

FIGURE 5 Fraction of vehicles that have traveled a distance r or less for two corridor half-widths.

approaches W/R. This effect is considerably more important as W becomes larger.

COMBINED MODEL

Gaussian line source dispersion models such as HIWAY2 (*8*) and CALINE4 (*9*) use a composite emission factor from MOBILE3 together with traffic volume to compute a lineal source strength term, q, in units of pollutant mass per length-time. The transient emissions and travel distribution models described in this paper can be combined to correct the transient component of q, q_t. Strictly speaking, the correction should be applied directly to q_t. However, the same result can be achieved by correcting the fraction of vehicles in hot or cold start mode. The corrected fraction can then be input directly to the MOBILE3 program without the need to isolate the transient emissions.

The correction must account for both the skewed distribution of travel distances for hot and cold start vehicles at P and the number of vehicles passing P in the hot stabilized mode. If it is assumed that the traffic volume and rate of entering vehicles are relatively constant over the section of highway being studied, the solution at P will be valid for all points. Even if this assumption is not entirely true, the solution will provide a good average value to use if it is calculated from average values of V, v, and f_t.

If the corrected fraction of vehicles in the warm-up phase at P is defined as ${}_cf_t$, q_t can be written as

$$q_t = {}_cf_t V \bar{e}_t \tag{12}$$

Another way of expressing q_t is as a summation of transient contributions from all vehicles passing P:

$$q_t = \int_0^{N_t} e_t(r)\, dn \tag{13}$$

Before this expression is evaluated, one further refinement needs to be made. For major arterials such as freeways, a minimum distance must be traveled by all vehicles before gaining access. In the model, this is represented as a trip length augmentation, r_a. Only vehicles that have traveled r_a or greater can be on the highway segment. Therefore, Equation 13 must be restated as

$$q_t = \int_0^{N_t} e_t(r + r_a)\, dn \tag{13'}$$

This modification will mean that the area from which N_t is drawn will be smaller, with the highway segment reduced in length to $R-r_a$ and a further restriction, that $W \le R-r_a$. However, the modification does not alter the travel distribution model described by Equation 11.

By including r_a in the model, the final solution will be applicable to a wider range of conditions. The inclusion of the factor not only adjusts for highway access but also can be used to account for inefficiencies in local street collector systems. In residential areas, most trips will start on local streets, not collectors or arterials. During travel to the nearest collector or arterial, it is not likely that a vehicle will always be able to travel directly toward P. An average value can be assigned to r_a to account for these detours.

Substitution of Equations 6 and 11 into Equation 13′ and assignment of the proper limits of integration gives

$$q_t = \bar{e}_t f_t v \left\{ \frac{3}{W} \int_0^W r \left[1 - \frac{2(r + r_a)}{R} + \frac{(r + r_a)^2}{R^2} \right] dr + 3 \int_W^{R-r_a} \left[1 - \frac{2(r + r_a)}{R} + \frac{(r + r_a)^2}{R^2} \right] dr \right\} \tag{14}$$

The final model is determined by integrating Equation 14, combining the result with Equation 12, and solving for ${}_cf_t$:

$${}_cf_t = \frac{f_t v}{V} \left[R - W\left(\frac{3}{2} - \frac{W}{R} + \frac{W^2}{4R^2}\right) - 3r_a\left(1 - \frac{W}{R} + \frac{W^2}{3R^2}\right) + 3r_a^2\left(\frac{1}{R} - \frac{W}{2R^2}\right) - \frac{r_a^3}{R^2} \right] \tag{15}$$

If we assume that $r_a = 0$ and $W = R$, Equation 15 simplifies to

$${}_cf_t = \frac{f_t v R}{4V} \tag{16}$$

The combined model assumes that the warm-up portion of FTP-75 typifies the actual driving pattern of all vehicles in the travel distribution model. This assumption is not true in all cases. The FTP-75 cycle, which has as its genesis a 12-mi test loop in downtown Los Angeles (*10*), represents both city street and freeway driving conditions. Vehicles entering a free-flowing freeway shortly after start-up will operate at higher average speeds than the FTP-75 average of 25.6 mph. Higher speeds favor a quicker warm-up of the engine and catalyst so that hot stabilized conditions may be achieved in less than 3.59 mi (*1*). Conversely, vehicles traveling on stop-and-go city streets exclusively may require more or less than 3.59 mi to reach hot stabilized operation. The exact distance will depend on the amount of time spent idling and the overall average speed.

To account for these differences, a further disaggregation of the travel distribution model might be possible on the basis of average speed or a breakdown of idle, acceleration, deceleration, and cruise modes. Such a refinement is worthwhile, however, only if the composite emission factors generated by MOBILE3 contain sufficient detail to make use of the disaggregation. This is not currently the case. MOBILE3's idle emission rates and speed correction coefficients are both derived from data that are valid only for hot stabilized vehicles (*11, 12*).

MODEL SENSITIVITY

To evaluate the sensitivity of the model described by Equation 15, realistic values for v/V and f_t were used. A recent study by the New Jersey Department of Transportation recommended values of f_t for a variety of facility types in both urban and rural settings (*13*). In that comprehensive study, vehicles in

cold start mode were identified by using a relationship between oil temperature and elapsed time from start-up derived for 32 representative test vehicles. A driver survey was used to identify vehicles in hot start mode. Vehicles were sampled randomly during peak (7 to 9 a.m.) and off-peak (9 a.m. to noon) periods. More than 7,500 vehicles were tested at 49 sites. The summary of the percentages of vehicles in hot and cold start operation presented in Table 1 provides a basis for estimating f_t.

TABLE 1 SUMMARY OF COMBINED RESULTS FOR HOT AND COLD START PERCENTAGES (*13*)

Roadway Classification	Hot Transient Fraction (%)		Cold Transient Fraction (%)	
	Peak	Off-Peak	Peak	Off-Peak
Urban principal	6.5	21.1	46.8	29.9
Urban minor arterial and collector	10.6	29.1	46.4	29.7
Urban local	8.3	30.8	64.0	30.7
Rural principal arterial	3.0	8.6	36.9	23.2
Rural minor arterial and collector	5.6	14.3	44.8	27.8
Rural local	4.9	20.8	45.2	34.2

To quantify v/V for typical urban freeways, 10 representative sections were chosen from urban areas in California. For each section, the average daily traffic (ADT) and entering volumes in ADT per mile were obtained (*14, 15*). The ratios of these averaged daily results were used as an approximation of peak hour v/V. As can be observed in Table 2, the results were reasonably consistent from section to section.

Figure 6 shows values of ${}_cf_t/f_t$ as a function of corridor half-width for r_a equal to 0 and 0.25 mi. The curves were generated by using Equation 15 and assuming a value of 0.1 for v/V. The importance of W to the travel distribution and resulting correction to f_t is clearly illustrated. As W decreases, a smaller correction is necessary for f_t. As W approaches zero,

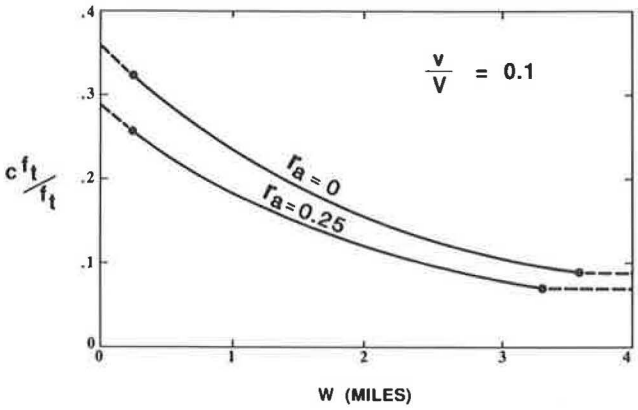

FIGURE 6 Sensitivity of the combined model to the corridor half-width and trip length augmentation variables.

the correction becomes a simple function of the dilution effect of hot stabilized through traffic characterized by v/V. Figure 6 also indicates that r_a assumes greater importance as W approaches zero, but that overall this factor appears to be less critical than either W or v/V.

As a realistic example, the information in Tables 1 and 2 can be combined with the simplified form of the model (Equation 16) to determine the corrected percentage of hot and cold start operation for a typical urban freeway. Because this example will be based on representative data, the results will demonstrate the importance of correcting hot and cold start fractions for travel distance distribution. Because freeway access is typically limited to arterials, approximate values for f_t from Table 1 of 10 percent hot and 50 percent cold starts will be used. When Equation 16 is applied and $v/V = 0.1$ (approximated from Table 2) is assumed, corrected fractions of 1 percent and 5 percent, respectively, are obtained.

The importance of this correction is best illustrated by comparing composite emission factors for the uncorrected values from Table 1, the hot/cold start split defined by FTP-75 (27/21 percent, respectively), and the corrected values of 1 and 5 percent from Equation 16. In Figure 7, MOBILE3 composite emission factors at 55 mph for each of these scenarios is

TABLE 2 RATIOS OF ON-RAMP VOLUMES TO ADT FOR URBAN CALIFORNIA FREEWAYS, 1982–1983

County	Route	Post Miles	ADT/Mile (v)	ADT (V)	v/V
Sacramento	US-50	1–16	8,900	83,000	0.11
Alameda	I-880	22–30	16,800	189,000	0.09
San Mateo	US-101	12–20	16,900	199,000	0.08
Santa Clara	I-280	4–10	25,400	154,000	0.16
Los Angeles	I-10	32–42	13,800	136,000	0.10
Los Angeles	I-110	10–20	20,300	212,000	0.10
Orange	I-405	11–20	21,500	192,000	0.11
Riverside	SH-91	9–22	9,900	98,000	0.10
San Diego	SH-94	5–10	10,700	93,000	0.12
San Diego	I-805	3–13	13,700	92,000	0.15
Average					0.11

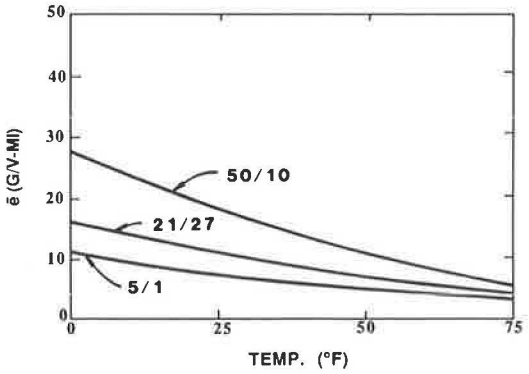

FIGURE 7 MOBILE3 composite emission factors as a fraction of ambient temperature for three cold/hot start fractions (1990 LDGV mix at 55 mph).

plotted against ambient temperature for a 1990 LDGV mix. The results indicate that using the 21/27 percent split can result in overpredictions of freeway emissions of 25 to 50 percent. Use of the uncorrected Table 1 values leads to even higher overpredictions.

SUMMARY AND CONCLUSIONS

The model described by Equation 15 provides a method to correct the fraction of vehicles in either hot or cold start operating mode for the type of travel distance distribution that is likely to be found on urban freeways and arterials. Reliance on the model is based on the acceptance of two concepts. First, transient emissions are high at the beginning of the FTP-75 hot and cold start cycles and gradually diminish to zero by the end of the cycles. Second, more vehicles on urban freeways and arterials in hot or cold start mode are likely to be near the end of the warm-up phase than the beginning.

The first of these concepts was tested against measured results from 25 LDGVs. The measured transient emissions dropped off even faster than the model predicted. The form of the model was retained, however, because it is conservative and avoids arbitrary boundary conditions. The second concept remains untested.

Measured traffic volumes and cold start percentages were used to develop a corrected cold start fraction of 5 percent for typical urban freeways during morning commute. This calculation assumed trip attraction at a uniform rate to a distance of at least 3.59 mi. In cases for which this assumption is valid, use of 21 percent cold start vehicles or higher will result in significant overpredictions of vehicle emissions.

More accurate estimates of cold start percentages can be obtained by using project-specific values for the variables in Equation 15 and applying the resulting correction factor to the cold start fractions given in Table 1 or derived from other sources. Although this approach is less important to the overall result, it can be applied to the fraction of vehicles in hot start mode.

Further work is certainly needed before the model can be used with complete confidence. However, all other methods for estimating microscale transient emissions are equally untested, and many lack coherent rationale. The method presented in this paper is based on well-defined concepts and is adaptable to unique situations. By specifying a corridor halfwidth, the model may be adjusted for parallel commute corridors or natural restrictions to development, such as coastlines or canyons. The trip length augmentation may be used to accommodate minimum access distances, detouring, or even ramp metering. Such flexibility offers a distinct improvement over the use of "average" values or tabulated ranges of values. More important, the model addresses the nonlinear nature of transient emissions release during warm-up, an aspect that was not considered by other published methods.

ACKNOWLEDGMENTS

This work was sponsored by the California Department of Transportation (Caltrans). Assistance was provided by Caltrans staff members Dick Wood and Bill Nokes.

REFERENCES

1. T. A. Fuca and O. J. Senyk. *Determination of Hot and Cold Starts in New Jersey: Phase I, Task 2—Vehicle Operating Experiment.* Division of Research and Development, New Jersey Department of Transportation, Trenton, 1978.
2. *Federal Register,* Vol. 42, No. 124, Part III, 1977.
3. *Compilation of Air Pollutant Emission Factors: Highway Mobile Sources.* Report EPA-460/3-84-005. Environmental Protection Agency, Ann Arbor, Mich., 1984.
4. T. C. Pearce and M. H. L. Waters. *Cold Start Fuel Consumption of a Diesel and a Petrol Car.* Supplementary Report 636. Transport and Road Research Laboratory, British Department of the Environment Department of Transport, Crowthorne, England, 1980.
5. T. P. Midurski and A. H. Castaline. *Determination of Percentages of Vehicles Operating in the Cold Start Mode.* Report EPA-450/3-77-023. Environmental Protection Agency, Research Triangle Park, N.C., 1977.
6. G. W. Ellis, W. T. Camps, and A. Treadway. *The Determination of Vehicular Cold and Hot Operating Fractions for Estimating Highway Emissions.* Report DOT-FH-11-9207. Alabama Highway Department, Montgomery, 1978.
7. B. H. Eccleston and R. W. Hurn. *Ambient Temperature and Vehicle Emissions.* Report EPA-460/3-74-028. Environmental Protection Agency, Ann Arbor, Mich., 1974.
8. W. B. Peterson. *User's Guide for HIWAY-2: A Highway Air Pollution Model.* Report EPA-600/8-80-018. Environmental Protection Agency, Research Triangle Park, N.C., 1980.
9. P. E. Benson. *CALINE4: A Dispersion Model for Predicting Air Pollutant Concentrations near Roadways.* Report FIIWA/CA/TL-84/15. California Department of Transportation, Sacramento, 1984.
10. D. J. Simanaitis. Emission Test Cycles Around the World. *Automotive Engineering,* Vol. 85, No. 8, 1977.
11. P. Kunselman et al. *Automobile Exhaust Emission Modal Analysis Model.* Report EPA-460/3-74-005. Environmental Protection Agency, Ann Arbor, Mich., 1974.
12. M. Smith et al. *Development of Revised Light-Duty-Vehicle Emission—Average Speed Relationships.* Report EPA/460/3-77/011. Environmental Protection Agency, Ann Arbor, Mich., 1977.
13. K. J. Brodtman and T. A. Fuca. *Determination of Hot and Cold Start Percentages in New Jersey.* Report FHWA/NJ-84/001. New Jersey Department of Transportation, Trenton, 1984.
14. *Traffic Volumes on California State Highways.* California Department of Transportation, Sacramento, 1984.
15. *Ramp Volumes on the California State Freeway System.* California Department of Transportation, Sacramento, 1984.

Publication of this paper sponsored by Committee on Transportation and Air Quality.